# The Petrology, Petrogenesis, and Metallogeny of the South Kawishiwi Intrusion in the Nokomis Deposit Area, Duluth Complex, Northeastern Minnesota

A THESIS
SUBMITTED TO THE FACULTY OF THE GRADUATE SCHOOL
OF THE UNIVERSITY OF MINNESOTA
BY

Christopher Reed White

IN PARTIAL FULFILLMENT OF THE REQUIREMENTS
FOR THE DEGREE OF
MASTER OF SCIENCE

Advisor: James D. Miller; Co-advisor: John W. Goodge.

August 2010

## Acknowledgements

I would like to thank my advisor Jim Miller for his unwavering support and dedication to me through the entirety of this project. Jim is a tireless mentor, and I am grateful for everything that he has taught me. I thank co-advisor John Goodge for bringing me to Duluth, taking an early interest in my studies, and helping to point my ambitions in the right direction. I thank Dean Peterson for all of the one-on-one time in the field, and for all of the insightful conversations that we have had on magmatic processes. I thank Paul Siders for faithfully serving on my committee, and for helping me to make it through Physical Chemistry in one piece. I thank Mark Severson for his early guidance with core logging.

This work was supported in large part by Duluth Metals, both financially and logistically. I thank Rick Sandri, Dave Oliver, and everyone at Duluth Metals past and present for their continuous support throughout this project. I thank the Precambrian Research Center for supporting me through a Research Assistantship, for providing me with field gear, and for supporting this study both financially and intellectually. I thank the Department of Geological Sciences – University of Minnesota Duluth for awarding me with a Teaching Assistantship, and for providing funds for this project.

Lastly, I thank my lovely wife Ann, my dog Scout, and my family and friends for patiently allowing me the time to conduct and complete my studies at Duluth.

## Dedication

I dedicate this work to all of the scientists who have studied the Midcontinent rift, past and present. Your work has facilitated a tremendous knowledge base to work from, and provides the inspiration to continue developing new ideas about the rift and the rocks that it produced.

## ABSTRACT

A recent flurry of minerals exploration in northeastern Minnesota has legitimized the Duluth Complex as one of the largest deposits of base and precious metals in the world. These activities have facilitated both the need and the means for academic studies geared toward developing and defining the numerous Cu-Ni-PGE resources in the Duluth Complex. This study focuses on Duluth Metals' Nokomis deposit, taking advantage of huge volumes of new drilling and associated data to examine previous work conducted by Severson (1994), and Peterson (2001) with regard toward the petrology, stratigraphy, and genesis of the South Kawishiwi intrusion in the Nokomis deposit (formerly known as Maturi Extension) area.

Through the examination of recently drilled core, and bedrock mapping in the study area Severson's (1994) igneous stratigraphy was evaluated and largely adopted with several additions and minor modifications. Analyses of geochemistry allowed for confirmation of several stratigraphic attributes alluded to by Severson (1994). Whole-rock, major-element geochemistry showed progressive re-charge trends through the upper parts of the intrusion, while whole-rock, major-element geochemistry and mineral chemistry data seemed to show order through chaos in the basal contact area of the intrusion. Major-element, whole-rock geochemistry also confirmed a large block of exotic rocks within the intrusion. As such, the intrusion has been broken into several major zones (basal contact zone, and upper zone) with a third zone consisting of a large block of remnant anorthositic series rocks (anorthositic inclusion block).

Testing Peterson's (2001) open versus confined style mineralization model for the South Kawishiwi intrusion was the prime objective of this study. Petrographic and chemical analysis of samples collected from recently drilled core, as well as the analysis of available whole-rock and assay geochemical data led to the exploration and development of answers to several questions related to Peterson's (2001) model. Analyses geared toward testing for lateral flow in the basal contact area of the intrusion ultimately led to the determination that magma flow was likely prominent in the basal contact area of the South Kawishiwi intrusion, and that channelized flow may have resulted in significant upgrading of metals. This study ultimately results in the presentation of several petrogenesis and metallogenesis models for the South Kawishiwi intrusion in the Nokomis deposit area, which are largely founded on Peterson's (2001) mineralization model, and Severson's (1994) ideas regarding petrogenesis of the South Kawishiwi intrusion.

# TABLE OF CONTENTS

## List of Tables

## List of Figures

## List of Plates

# CHAPTER ONE: INTRODUCTION

Mafic intrusions throughout the world are renowned for hosting Cu-Ni sulfide and PGM deposits, including major occurrences in Skaergaard, Noril'sk-Talnakh, Voisey's Bay, Jinchuan, and the Duluth Complex (Naldrett, 2004). Cu-Ni-PGE deposits of the 1.1 Ga Duluth Complex, the subject of this study, have sparked continued geologic and prospecting interest since they were first discovered in the early 1950's (Severson and Miller, 2002). Currently, five companies are actively conducting exploration drilling on the dozen or so deposits historically identified in the Duluth Complex. Recent estimates of copper and nickel reserves among magmatic Cu-Ni deposits rank the Duluth Complex second and third in global copper and nickel tonnage, respectively (Eckstrand and Hulbert, 2007). The United States is a net importer of copper and nickel, relying on 37% copper, and 17% nickel to come from foreign sources (U.S. Geological Survey, 2008). The Duluth Complex hosts an estimated 37% of the United States' copper resources, an estimated 95% of the United States' nickel resources, and an estimated 75% of the United States' total precious metals resources (Peterson, 2009). With roughly 19 billion tons of ore containing average grades of 0.266% copper, 0.091% nickel, and 10 ppm total precious metals (Peterson, 2007), the Duluth Complex remains an untapped resource that could help relieve the United States of its reliance on foreign base and precious metals.

The South Kawishiwi intrusion (SKI), along with the Partridge River intrusion (PRI), forms the mineralized northwestern margin of the Duluth Complex and hosts at least six Cu-Ni-PGE deposits. This study focuses on an area in the northern part of the SKI that contains the Maturi deposit and its down-dip projection, the Maturi Extension.

An aggressive drilling program by Duluth Metals Corp (DM), which began in 2006, has greatly expanded the defined resource of the Maturi Extension deposit such that DM renamed it the Nokomis deposit in early 2008. Currently, the Nokomis deposit hosts an estimated 808 million tons of ore with at least 0.624% copper, 0.194% nickel, and 0.600 grams per tonne total precious metals (Duluth Metals press release, 2008).

Various studies of the Cu-Ni-PGE mineralization in the Duluth Complex provide good documentation of their mineralogic, textural and geochemical characteristics (e.g., Bonnichsen, 1972; Weiblen and Morey, 1976; Severson 1994; Lee and Ripley 1996; Theriault et al., 1997; Peterson, 2001; Ripley et al., 2007). The mineralization models proposed from these studies generally follow that conceived by Naldrett (1997, 2004) for magmatic sulfide deposits. However, only a few models have attempted to explain the stratigraphic and lateral variations in metal grade and tenor commonly observed within and between the various Duluth Complex deposits. In the South Kawishiwi Intrusion, for example, Severson (1994) documented intrusion-wide lateral and vertical lithologic and textural variations, while Peterson (1996) documented lateral and vertical variations in base and precious metals grades and tenors. Subsequently, Peterson (2001) defined two main styles of mineralization, which he termed open and confined, and proposed a dynamic flow model of sulfide-bearing magma emplacement. In this model, constricted turbulent flow is postulated to result in higher grades and metal tenors of entrained sulfide that is typical of confined-style mineralization.

Naldrett (1997) stated that sulfide saturation of magma alone will not produce a massive concentration of metal-sulfides, but that an appropriate physical environment is

also required, not only to produce sulfide over-saturation at an appropriate time and location, but also to concentrate metal-sulfides from a large volume of magma at an accessible location. Duluth Complex deposits illustrate this point by having formed in a plume-influenced crustal rift environment. Metal-rich mantle melts were emplaced into sulfide-bearing crustal rocks which produced extensive sulfide contamination and gave rise to both massive and disseminated deposits. The Nokomis deposit is a disseminated ore body with small, localized massive sulfide occurrences. It occurs at the basal contact of the South Kawishiwi intrusion and is rather uniquely situated between a footwall of Archean granite and a hanging wall of earlier form gabbroic anorthositic rocks of the Duluth Complex's anorthositic series. It displays relatively high grades (~0.6% Cu, ~0.2% Ni, and ~0.6 grams per ton total precious metals) over a 50-150 meter-thick stratigraphic interval, making it typical of Peterson's (2001) confined-style mineralization. This study focuses on documenting the geologic setting, petrology, and metallogeny of the Nokomis Cu-Ni-PGE deposit in order to better understand the salient magmatic and mineralization processes that created this deposit. One of the primary goals of this investigation is to test Peterson's (2001) open vs. confined mineralization model. This study also hopes to provide valuable information with which to guide future exploration of Duluth Complex Cu-Ni-PGE deposits.

## 1.1 REGIONAL GEOLOGY

The South Kawishiwi Intrusion (SKI) occurs in northeastern Minnesota, southeast of the town of Ely. It forms the western margin of the Duluth Complex, which is a

multiply-intruded mafic igneous complex comprising the largest exposed plutonic component of the 1.1 Ga Midcontinent Rift (Fig. 1). The basal contact of the SKI

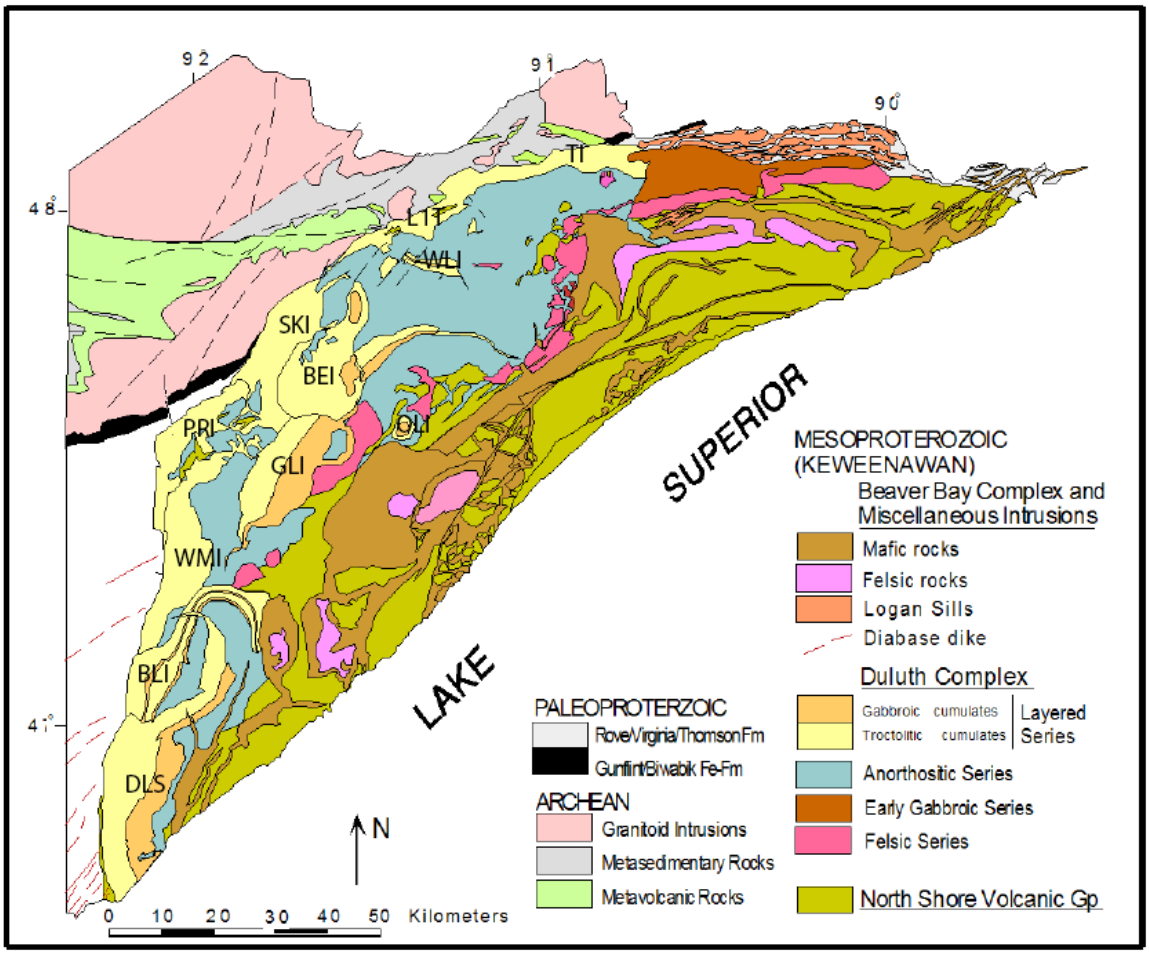


Figure 1: Locations of layered series intrusions in the Duluth Complex. BEI-Bald Eagle intrusion, BLI-Boulder Lake intrusion, DLS-Layered series at Duluth, GLI-Greenwood Lake intrusion, L1T-Lake One troctolite, OLI-Osier Lake intrusion, PRI-Partridge River intrusion, SKI-South Kawishiwi intrusion, TI-Tuscarora intrusion, WLI-Wilder Lake intrusion, WMI-Western Margin intrusion. Modified from Miller and Severson (2002).

overlies granitic rocks of the Archean Giants Range batholith along its northeastern margin, and sedimentary rocks of the Paleoproterozoic Animikie Group to the southwest. Described below is a brief summary of the general geologic features of these two older

Precambrian units, and the igneous components of the Midcontinent Rift in northeastern Minnesota, especially the Duluth Complex.

### 1.1.1. Giants Range Batholith

The Archean Giants Range batholith consists of granite, granodiorite, tonalite, and monzodiorite emplaced into supracrustal metasedimentary and metavolcanic rocks of the western part of the Wawa Subprovince of the Superior Province roughly 2.7 billion years ago (Boerboom and Zartman, 1993). A porphyritic hornblende monzodiorite, the Farm Lake pluton of Green (1970), comprises the eastern part of the batholith and forms the northwestern footwall of the SKI in the study area. The monzodiorite locally contains hornblendite, syenite, and aplite and foliated biotite-rich zones. Adjacent to the Duluth Complex, the monzodiorite shows effects of high-grade contact metamorphism, including partial melting, metasomatization, and recrystallization textures, creating hybrid-like dioritic and noritic rocks to depths of 61 meters below the contact (Peterson and Severson, 2002).

### 1.1.2. Animikie Group

Paleoproterozoic Animikie Group sedimentary rocks extend from east-central to northeastern Minnesota. These sediments were deposited about 1.85 Ga in a tectonic foreland basin along the southern continental margin of the Superior Province during the Penokean orogeny (Southwick, 1996). In the study area, the deformational and metamorphic effects of Penokean tectonism are minimal. Here, the Pokegama Quartzite,

Biwabik Iron Formation, and Virginia Formation are the main stratigraphic units and form the SKI's footwall in the southwest half of the intrusion (Fig. 1). Animikie Group sedimentary rocks overlie the Giants Range batholith in the southwestern footwall area of the SKI. They are locally present in the northeast half of the intrusion, occurring exclusively as rare inclusions. This implies that at one time Animikie Group rocks may have entirely covered the Giant's Range in this area, but were assimilated or delaminated from the Archean basement by emplacement of the SKI.

The Pokegama Quartzite forms the base of the Animikie Group and unconformably overlies the Giants Range granitic rocks. It consists of a lower shale facies and an upper sandstone facies deposited in subtidal, high-energy environments (Ojakangas, 1983). The formation thickens to the west from several meters thick at the eastern end of the Mesabi Range to as much as 61 meters at the western end, and it is only locally present in the Duluth Complex area (Peterson and Severson, 2002). The Pokegama Quartzite is conformably overlain by the Biwabik Iron Formation.

The Biwabik Iron Formation consists of four lithostratigraphic members, each dominated by either cherty iron-formation or slaty iron-formation (Peterson and Severson, 2002). Gunderson and Schwartz (1962) further divided these members into 22 submembers. In the vicinity of the Duluth Complex, contact metamorphism of the Biwabik Iron Formation progresses to pyroxene hornfels facies. Inclusions of Biwabik Iron Formation within the SKI exhibit several morphologies, including: well-bedded type, magnetite-rich iron-formation, banded varieties with alternations of orthopyroxene, plagioclase, and magnetite, and massive oxide pods lacking preserved bedding (French,

1968; Peterson and Severson, 2002). The wide variety of textural variations of inclusions may be due to a combination of partial melting, assimilation, and metasomatic processes (Severson, 1994).

The Virginia Formation conformably overlies the Biwabik Iron Formation and consists of two members: a lower argillaceous lithosome and an upper silty and sandy lithosome (Lucente and Morey, 1983). The lower member consists mostly of carbonaceous argillite, argillaceous siltstone, silty argillite, and local chert, and it is locally pyritic. The upper member is dominated by interbedded siltstone and sandstone (Lucente and Morey, 1983). In the vicinity of the Duluth Complex, Virginia Formation sediments are strongly metamorphosed with several metamorphic packages superimposed on the sedimentary rocks (Severson et al., 1996). Severson et al. (1996) described these metasediments as consisting of five main groups: cordieritic metasediments, recrystallized units, disrupted units, graphitic argillite with bedded pyrrhotite (formerly pyrite), and chert/calc-silicate horizons. The sulfidic component of the Virginia Formation is commonly cited as the contamination source of sulfide mineralization for Duluth Complex Cu-Ni sulfide deposits (Ripley, 1986).

The Virginia and Biwabik Iron formations also locally contain several mafic sills. Based on their geochemistry, it is thought that they may correlate with early Duluth Complex intrusions (Peterson and Severson, 2002).

### 1.1.3. Midcontinent Rift

The Midcontinent Rift (MCR) was first delineated as the Midcontinent geophysical anomaly in the 1940's when its prominent curvilinear gravity and magnetic signatures were first recognized (Woollard, 1943). These anomalies extend southwest from the Lake Superior area (Fig. 2), where the exposed geology consists of mafic igneous rocks and red-bed sediments. With the general acceptance of plate tectonic theory in the late 1960's, these mafic rocks and their associated geophysical anomaly came to be recognized as representing an intracontinental rift (Chase and Gilmer, 1973) and the term Midcontinent Rift System, or simply the Midcontinent Rift (MCR), was adopted (Wold and Hinze, 1982; Hinze et al., 1997). Due to a strong well-defined geophysical anomaly, the MCR is now known to extend in an arcuate path for more than 2,000 kilometers across North America (Fig. 2).

Midcontinent Rift bedrock is exposed in the Lake Superior region, but remains buried beneath Paleozoic strata south of the Lake Superior region. Where exposed, the rift consists largely of volcanic and intrusive rocks overlain by siliciclastic rocks with considerable inter-layering of volcanic and sedimentary rocks that display progressive waning of volcanism and an increase in sediment deposition during subsequent thermal subsidence. However, this simple picture is complicated by late reverse faults that locally cross-cut the volcanic and sedimentary fill (Fig. 3). Flows and sedimentary units generally dip toward the long axis of Lake Superior, defining a synformal structure called the Lake Superior Syncline (White, 1966). This syncline is

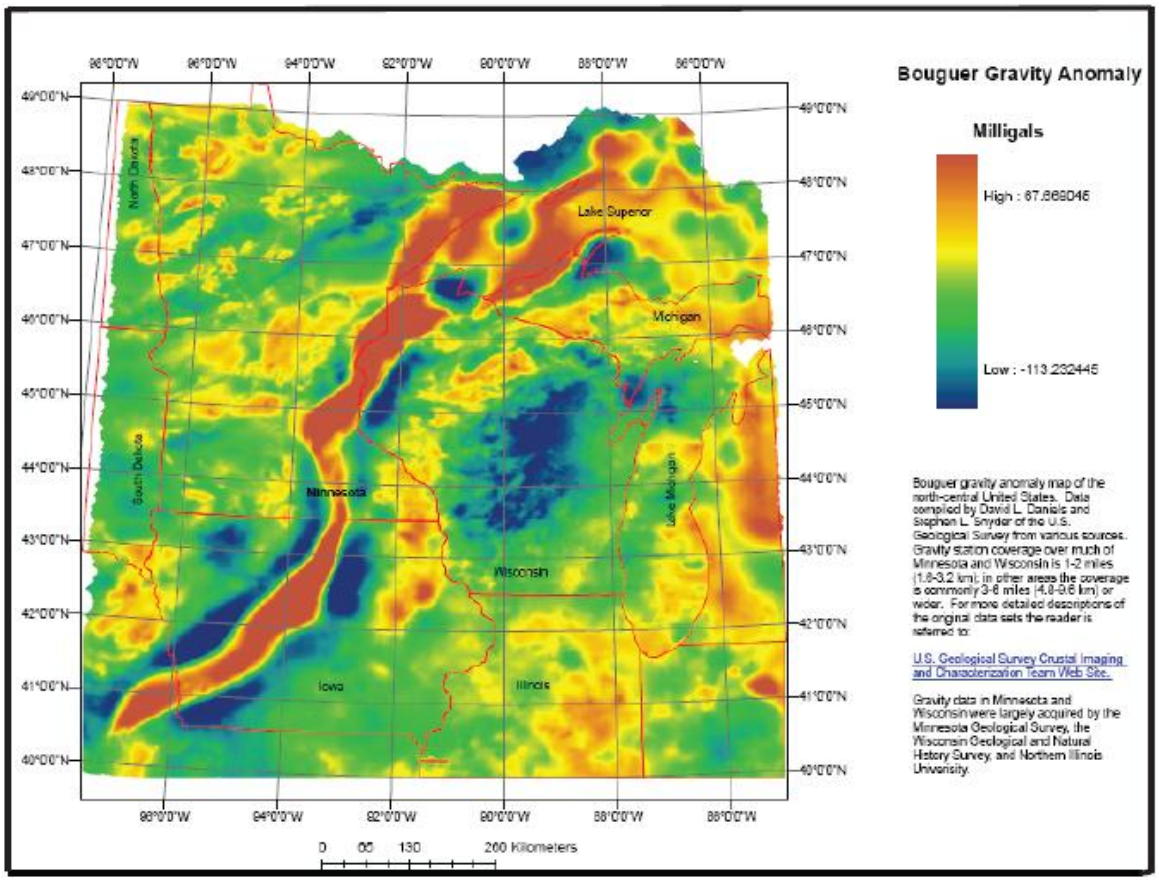


Figure 2: Bouger gravity anomaly map of the upper Midwest, showing the occurrence of the Midcontinent gravity high (from geo.umn.edu/mgs/nicegeo/pdfs/boug_grav.pdf) [isn't there a set of authors on this compilation map?]. This anomaly marks the extent of mafic igneous rocks related to Midcontinent Rift. Data compiled by David L. Daniels and Stephen L. Snyder, United States Geological Survey.

commonly segmented and asymmetric, with the deepest parts of the rift graben commonly alternating across accommodation zones (Dickas and Mudrey, 1997). Seismic reflection profiles and modeling of gravity and magnetic data in the western Lake Superior basin (e.g., Fig. 3B) indicate that volcanic and sedimentary rocks fill the axis of the rift to a thickness of up to 30 kilometers (Cannon et al., 1989; Allen et al., 1997). These units gradually decrease in thickness away from the rift axis and are locally

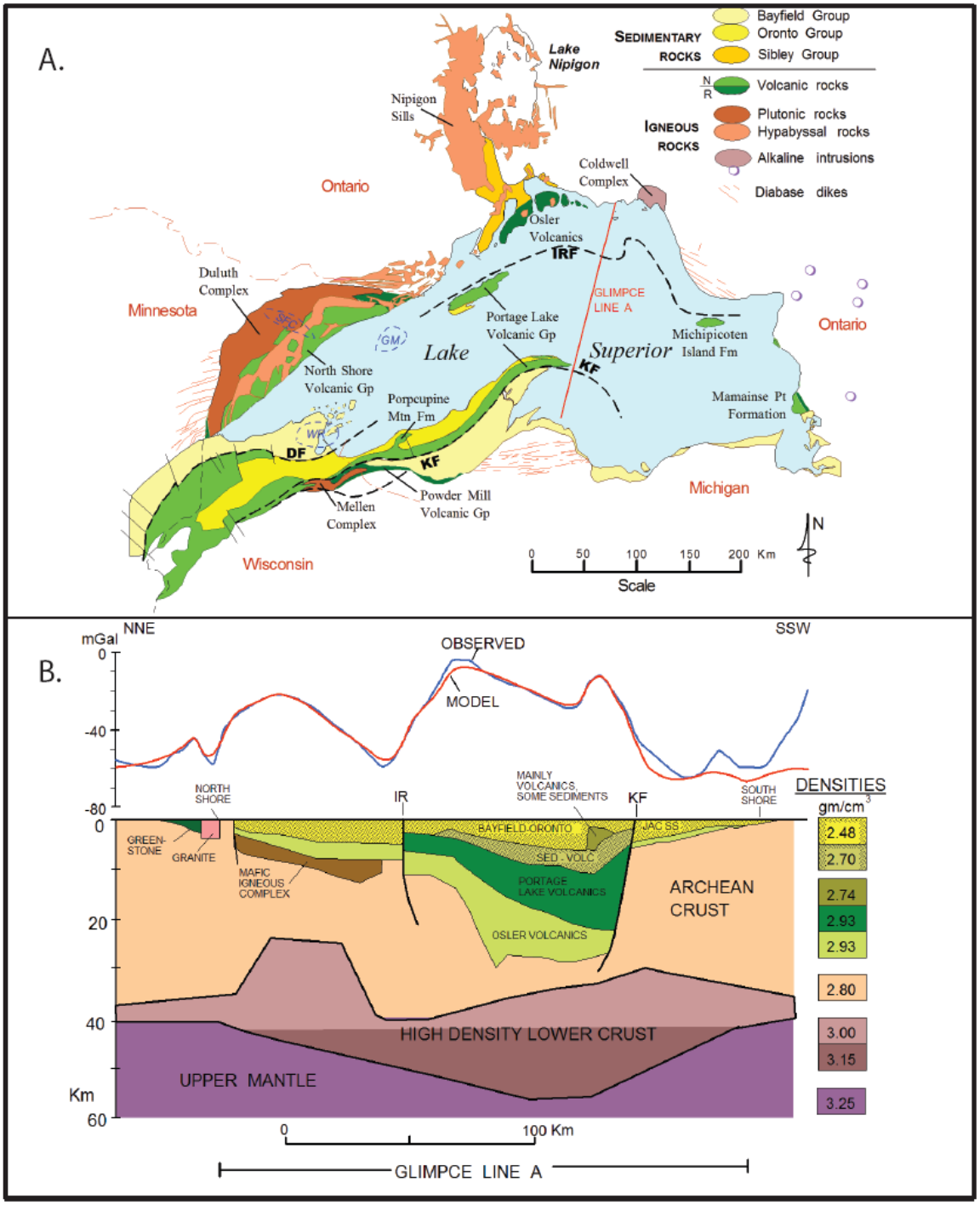


Figure 3: A. Geology and structure of the Midcontinent rift in the Lake Superior region (from Miller et al., 1995). Large-scale lithostratigraphic and lithodemic features are noted, including major reverse faults: DF-Douglas fault, KF-Keweenawan fault, and IRF-Isle Royal fault. B. Gravity model along GLIMPCE seismic profile line A (from Thomas and Teskey, 1994).

truncated by large-scale reverse faults (Fig. 3). Outboard of these faults, the volcanics abruptly thin by several orders of magnitude implying that the reverse faults initially served as graben-bounding, growth-type normal faults during volcanism (Fig. 3B). Gravity data over the rift further imply that a significant volume of mafic and ultramafic rock forms a thick underplated mass at the base of the crust (Fig. 3B). Along Minnesota's north shore of Lake Superior, the volcanic and minor sedimentary fill thins to a maximum thickness of 10 kilometers (Green, 1972). Extending inland from the shoreline these basaltic flows and minor interflow sediments give way to intrusive rocks of the Beaver Bay Complex and Duluth Complex (Figs. 1 & 3).

Isotopic studies of basalts in the Lake Superior region indicate that most mafic magmas were derived from an undepleted primitive mantle source (Nicholson and Shirey, 1990; Nicholson et al., 1997; Shirey et al., 1997). This, along with a calculation of total volcanic fill exceeding $1.5x10^6$ $km^3$ (Cannon, 1992) and evidence of extensive crustal underplating (Fig. 3B) have led to the general agreement that the MCR was influenced, if not generated, by a mantle plume (Nicholson and Shirey, 1990; Hutchinson et al., 1990; Cannon, 1992; Nicholson et al., 1997; Vervoort et al., 2007). Rhyolites and granophyres, which can locally comprise 25% of the magmatic fill of the rift, have isotopic signatures indicating an origin by partial melting of lower continental crust of Paleoproterozoic to Archean age (Vervoort and Green, 1997; Vervoort et al., 2007).

Several authors (Miller and Vervoort, 1996; Nicholson et al., 1997; Miller and Severson, 2002; Vervoort et al., 2007) have interpreted geologic, geochemical and geochronologic data from volcanic and intrusive rocks of the MCR in the western Lake

Superior basin to indicate that the rift evolved in several tectonomagmatic stages. Miller and Vervoort (1996) proposed four main stages, which they termed early, latent, main, and late (Fig. 4).

The early magmatic stage (1109-1107 Ma) represents the initial impact of a mantle plume into the base of the lithosphere (Fig. 4A). This stage is initially characterized by rapid emplacement of a large volume of plume-generated magmas directly into the upper crust. Soon after this initial burst, however, magmas evidently began staging in the lower crust, which resulted in the eruption of more evolved, crustally contaminated mafic and felsic melts. This early stage occurred during a period of reversed magnetic polarity. More recent U-Pb dating of intrusions in northwestern Ontario (Heaman et al., 2007) suggest that the early stage of magmatism may have begun around 1112 Ma.

The latent magmatic stage (1107-1102 Ma) represents a period of continued plume upwelling and melting, extensive crustal underplating, and lower crustal melting (Fig 4B). Evidently, the only magmas to reach the upper crust were felsic. Miller and Vervoort (1996) speculated that during this stage, mafic magmas became trapped in the lower crust by a feedback system of underplating and crustal anatexis. Mafic underplating caused partial melting of the lower crust, creating rheological and density barriers, which trapped more mafic magmas and created more anatexis and so on. Magnetic polarity switched to a normal field orientation during this stage.

The main magmatic stage (1102-1094 Ma) represents renewed surface volcanism in a time of normal magnetic polarity (Fig. 4C). Magmatism produced largely

uncontaminated, but compositionally diverse, magmas as lower crustal magma chambers were evacuated. Felsic magmatism was also prevalent indicating ongoing crustal melting. However, isotopic data indicate that the crustal source was likely more radiogenic and perhaps older (Archean) than felsic magmatism in the early and latent stages (Vervoort et al., 2007).

The late magmatic stage (1094-1086 Ma) produced continued rift-basin subsidence, but rapidly diminished volcanism was progressively replaced by the deposition of clastic sediments as the main rift fill (Fig. 4-D). Volcanism during this stage consisted of relatively primitive basalts with depleted mantle isotopic signatures and the local development of evolved composite volcanoes (Nicholson et al., 2007). Waning volcanism and the thermal collapse of the rift basin might indicate plate drift, moving the rift off of the plume heat source (Davis and Green, 1997).

In northeastern Minnesota, the overwhelming majority of MCR rocks are igneous intrusions and volcanics (Fig. 1). The only sedimentary rocks are thin units of sandstone at the base of the volcanic pile and as scattered interflow sediments. The overlying sediments of the Bayfield and Oronto groups are not exposed in northeastern Minnesota, but are inferred from seismic data to onlap the volcanics just offshore (Cannon et al., 1989). In the following section, the volcanic rocks and hypabyssal intrusions, which occur along the north shore and collectively form the hanging wall of the Duluth Complex, are described.

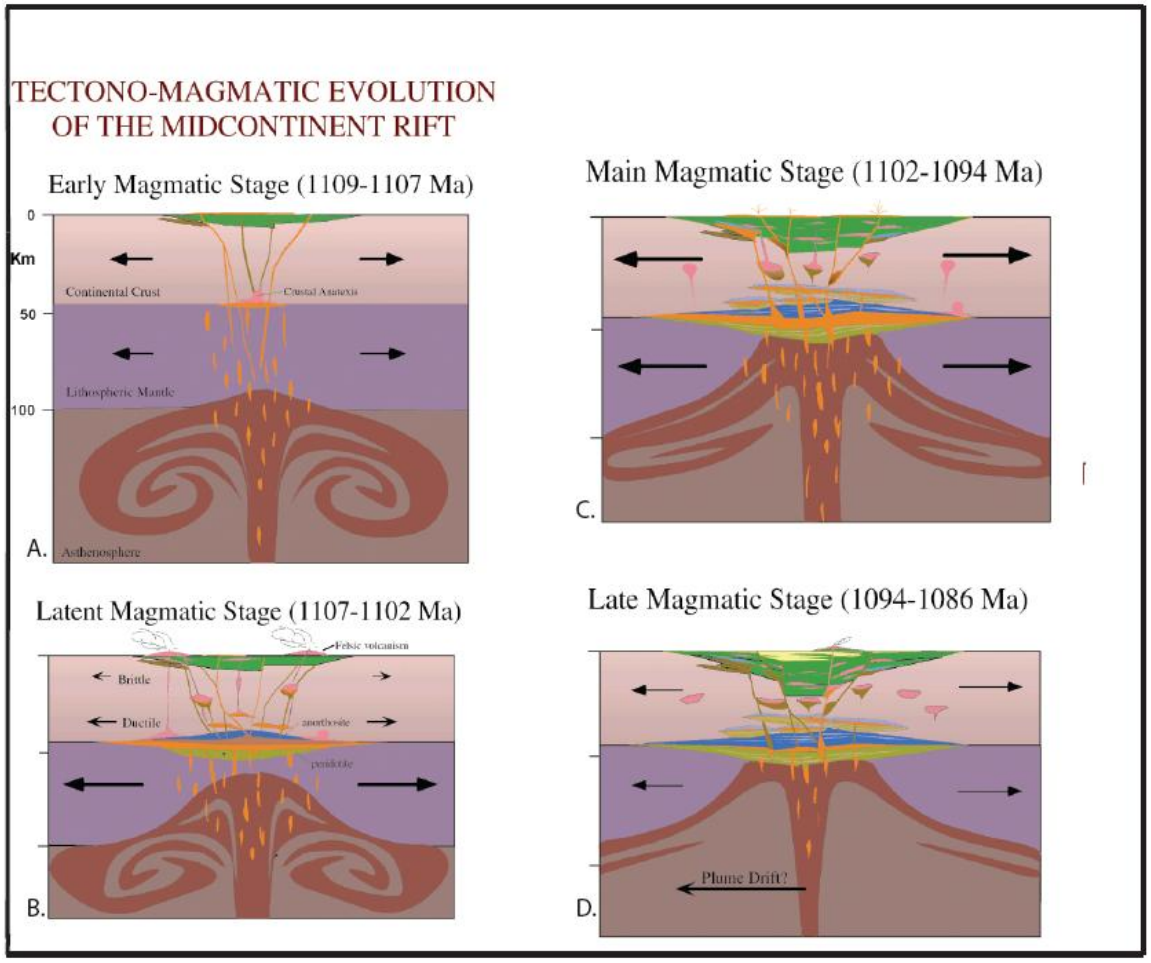


Figure 4: The four tectonomagmatic stages of Midcontinent rift evolution including: A. early magmatic stage, B. latent stage, C. main magmatic stage, and D. late magmatic stage (J. Miller, unpublished).

### 1.1.4 North Shore Volcanic Group, Beaver Bay Complex, and Related Intrusions

The North Shore Volcanic Group (NSVG) is exposed along a 150 km-long section of the north shore of Lake Superior from Duluth to Grand Portage (Green, 2002). Overall, the volcanic pile dips gently (10-20°) to the south and east with strike arcing from north-south near Duluth to east-west near Grand Portage. The stratigraphically highest flows in the volcanic package occur in the Tofte-Lutsen area. The stratigraphic column between Duluth and Tofte (southwest limb) measures 9.7 km thick, whereas the

northeast limb between Tofte and Grand Portage measures 6.2 km thick (Green, 1972). The lithostratigraphies of the two limbs are distinctly different and cannot be correlated (Fig. 5). One major difference is that felsic lavas comprise only 10% of the southwest limb, but up to 25% of the northeast limb.

A paleomagnetic reversal (R-N) has long been recognized in both limbs of the NSVG and has been used to correlate the NSVG with other volcanic packages exposed in the Lake Superior area (Fig. 3A, Fig. 5). High resolution U-Pb age dating over the past two decades has allowed for more precise correlation of volcanic and intrusive units within the MCR. As found elsewhere in the western Lake Superior region, lower magnetically-reversed lavas generally yield ages of 1109-1107 Ma, whereas normal polarity lavas fall between 1101-1096 Ma (Fig. 5). As mentioned above, the time gap between 1107-1102 Ma represents a period of extrusive inactivity, though felsic volcanism is evident in this time interval elsewhere.

Geochemically, the mafic to felsic lavas of the NSVG range from tholeiitic to mildly alkalic. The sequence is dominated by moderately evolved olivine tholeiitic basalt; however, compositions include primitive olivine tholeiite, transitional basalt, basaltic andesite, ferroandesite, icelandite, and rhyolite (Green, 2002).

The Beaver Bay Complex (BBC) is a group of hypabyssal intrusions occurring in the medial part of the NSVG and exposed along the central part of the north shore (Fig. 1). U-Pb ages of younger phases in the BBC indicate emplacement at around 1096 Ma, which is about 3 million years younger than the main phase of the Duluth Complex (Paces and Miller, 1993). Compositionally, BBC intrusions include a range of mafic,

intermediate, and felsic bodies (Miller and Chandler, 1997). Most intrusions occur as thin sheets and dikes, showing little evidence of internal differentiation with the exception of the Sonju Lake intrusion. Other intrusions similar to Beaver Bay Complex rocks occur in the far northeast and southwest reaches of the NSVG (Miller et al., 2002).

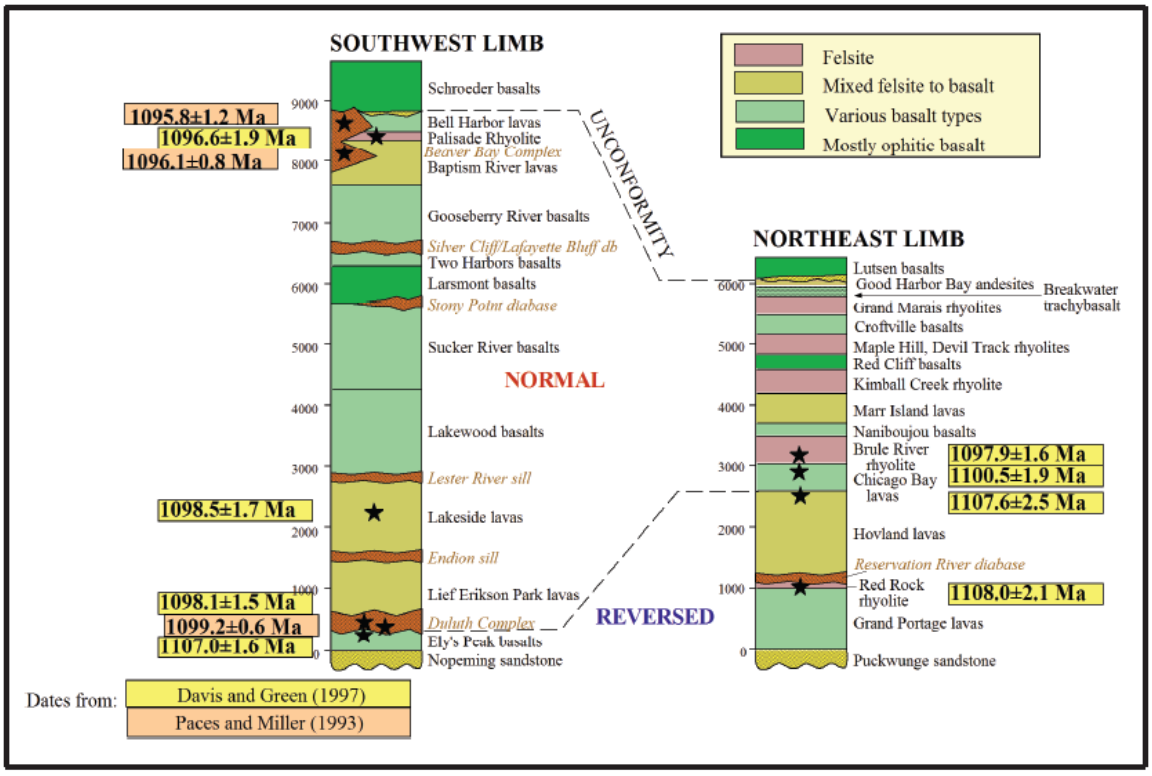


Figure 5: Lithostratigraphy of the southwest and northeast limbs of the North Shore Volcanic Group, modified from Green and Davis, 1997.

### 1.1.5 Duluth Complex

The multiple intrusions of the Duluth Complex occur within an arcing band from Duluth to near the Canadian border that is 270 km long and up to 40 km wide (Fig. 1). In terms of areal exposure, it is the second largest mafic intrusive complex on Earth after the Bushveld Complex of South Africa. The Duluth Complex is enclosed by a footwall of

Paleoproterozoic and Archean rocks, and a hanging wall of mixed volcanics and hypabyssal intrusions, as described above.

The Duluth Complex is typically subdivided into four intrusive series on the basis of dominant lithology, general age, and internal structure. In order of relative decreasing age, these series are the felsic, the early gabbro, the anorthositic, and the layered (Miller and Severson, 2002).

The felsic series consists of massive granophyric granite with lesser intermediate rocks emplaced during early stage magmatism along the eastern and central roof zone of the complex (Vervoort et al., 2007). Also emplaced during early stage magmatism, the early gabbro series consists of layered gabbroic cumulates located along the northeastern contact of the complex (Fig. 1). The anorthositic series is found throughout the complex as structurally complicated, plagioclase-rich, gabbroic cumulates emplaced during main stage magmatism. Also emplaced during main stage magmatism, the layered series consists of numerous stratiform troctolitic to ferrogabbroic cumulates residing at the base of the complex (Miller and Severson, 2002).

U-Pb dates from the felsic and early gabbroic series yield irresolvable emplacement ages of about 1108 Ma for the gabbroic rocks (Paces and Miller, 1993) and 1109-1106 Ma for granophyric rocks (Vervoort et al., 2007). The two series appear to be genetically unrelated as differentiation of the early gabbroic series intrusions would be volumetrically inadequate to produce the enormous volume of granophyre in the felsic series (Miller and Severson, 2002). Instead, the gradational contact relationships between the two series more likely indicates that the early gabbro series intruded beneath the felsic

series and caused it to partially melt and assimilate. Miller and Severson (2002) suggest that the felsic series may have acted as a density and rheologic barrier for the early gabbro series magmas. Isotopic data (Vervoort et al., 2007) suggest that the felsic series most likely originated from partial melting of Paleoproterozoic crust beneath the felsic rocks.

Both the anorthositic series and the layered series were produced in the main magmatic stage (1102-1094 Ma), however the layered series commonly contains abundant inclusions of anorthositic series rocks and layered series rock are often found as intrusions into anorthositic series rocks. Historically, this led most workers studying the Duluth Complex to interpret the anorthositic series as significantly older than the layered series (Miller and Severson, 2002). However, precise U-Pb dates obtained by Paces and Miller (1993) show the anorthositic series and layered series to be virtually identical in age at 1099 Ma. Miller and Severson (2002) provide two possible explanations linking the anorthositic and layered series. The first explanation calls for both series forming from the same batch of moderately plagioclase-enriched magma with intratelluric plagioclase crystals segregating to the roof zone by flotation, leaving the underlying evolved magma to crystallize from the floor up. The second explanation calls for both series tapping the same deep crustal source, initially rich in suspended plagioclase with the anorthositic series resulting from early extractions of crystal-rich magmas, and the layered series resulting from progressive depletion of these crystal-rich magmas.

Whereas the multiple emplacements of plagioclase-rich magma mushes that produced the structurally complex anorthositic series are very difficult to discriminate

into individual intrusions, the layered series can be subdivided into at least 11 discrete bodies (Fig. 1) that have relatively well defined margins and show varying degrees of internal differentiation (Miller and Ripley, 1996). The majority of the intrusions of the layered series form 3-4 kilometer thick, sheet-like bodies that typically dip gently to the east and southeast (i.e., toward the axis of the Midcontinent Rift). Exceptions include the funnel-shaped Bald Eagle intrusion, the plug-like Osier Lake intrusion, and the north-dipping Wilder Lake gabbro (Fig. 1). Layered series intrusions were largely emplaced between an anorthositic series hanging wall, and a pre-Keweenawan footwall of Paleoproterozoic sedimentary rocks or Archean granite-greenstone terrane rocks. However, many intrusions were emplaced higher in the volcanic pile and structurally above other layered series intrusions (e.g., Bald Eagle intrusion and Greenwood Lake intrusion). Miller et al. (2001) interpreted that successively higher intrusions were progressively younger, although age data are presently insufficient to bear this out.

All layered series intrusions display some degree of fractional crystallization-driven differentiation that is manifest as phase layering and cryptic mineral layering. However, individual intrusions display marked differences in the details of their igneous stratigraphy that can be variably attributable to recharge and eruption events, country rock assimilation, parental magma composition, and crystallization conditions (Miller and Ripley, 1996). The SKI is a poorly-differentiated mafic layered intrusion within the layered series that displays a limited range of differentiation.

# CHAPTER TWO: PREVIOUS STUDIES OF THE SOUTH KAWISHIWI INTRUSION

The discovery of Cu-Ni mineralization in the SKI in the 1950's spurred the Minnesota Geological Survey to begin quadrangle-scale mapping studies across the state in 1961. A stated goal of the MGS at this time was to produce bedrock maps for the entire state at a scale of 1:250,000, with more detailed mapping completed in areas needing critical evaluation of resource potential (Sims, 1965). One of the first areas to receive detailed mapping was the Gabbro Lake 15' Quadrangle, which includes much of the SKI. The results of this mapping (Green et al., 1966) effectively demonstrated that the SKI and the Bald Eagle intrusion were separate, composite, mafic layered bodies within the Duluth Complex, thus dispelling the long-held notion that the complex was a single lopolithic intrusion (Grout, 1918; Grout et al., 1959). This initial contribution to detailed mapping was followed by years of mapping in the Duluth Complex conducted largely by University of Minnesota graduate students that still persists today (Miller et al., 2002). This chapter will summarize: 1) the major bedrock mapping studies conducted in the SKI, 2) drill core logging activities that sought to determine the igneous stratigraphy of the SKI, 3) the history of mineral exploration of the SKI and the related Partridge River Intrusion, 4) petrologic and metallogenic studies that have attempted to interpret the magmatic history and metal sulfide mineralization of the SKI, and 5) the open vs. confined style mineralization model of Peterson (2001).

## 2.1 Geologic Bedrock Mapping

The first detailed bedrock mapping study of the South Kawishiwi intrusion was conducted by William Phinney in the mid-1960's and was published as MGS Miscellaneous Map M-2 (Green et al., 1966). Phinney recognized six map units within the SKI, four of which reside in the main body of the SKI. The two main units are a heterogeneous contact zone, which hosts most of the Cu-Ni sulfide mineralization, overlain by several varieties of augite troctolite with local anorthositic gabbro inclusions. The other two units reside in what has come to be known as the Nickel Lake macrodike, which is now proposed to be a feeder system to the SKI (Peterson et al., 2006), and will be described later in this section.

Following the mapping of Green et al. (1966), a number of reconnaissance-scale to detailed geologic mapping studies were conducted in the SKI (Phinney, 1967; Bonnichsen, 1970a-d; 1971; Morey and Cooper, 1977; Foose and Cooper, 1978), serving to subdivide the relatively well-exposed SKI into various troctolitic map units. Map units in all these studies were typically distinguished on the basis of augite mode and habit (ophitic to subophitic), and the occurrence of anorthositic rocks either as conformable layers within the troctolitic rocks or as inclusions. Most significant to this project, these studies also documented the extent of a heterogeneous, sulfide-bearing basal contact zone dominated by a complex mix of troctolitic, gabbroic, and noritic rocks variably enriched in Cu-Ni-Fe sulfide.

Figure 6 shows an integrated summary of the map units of the SKI defined by these early studies portrayed in MGS Miscellaneous Map M-119 (Miller et al., 2001).

Map M-119 was published to summarize the current regional picture of the Duluth Complex and related rocks. Accompanying this map, MGS Report of Investigation 58 (Miller et al., 2002) detailed the geology and mineral potential of the Duluth Complex and gave an extensive summary of mapping and exploration studies completed in the Duluth Complex up to 2001. M-119 and RI-58 provide a comprehensive, contemporary picture of the state of knowledge of the Duluth Complex.

Since publication of the M-119 compilation, NRRI/MAP-2002-01 (Peterson, 2002) depicts the basal contact of the SKI in three-dimensional shaded relief. NRRI/MAP-2002-02 (Peterson et al., 2002) and NRRI/MAP-2004-02 (Peterson et al., 2004) both show the bedrock geology of the SKI's basal contact zone west of the Birch lake area, and NRRI/MAP-2004-02 also includes additional field data and copper assay data.

In 2005, four maps were published by the MGS of the Babbitt 7.5' quadrangles from mapping largely conducted by Jim Miller (MGS) and Mark Severson (NRRI). These maps, (M-159, Severson and Miller, 2005; M-160, Miller, Severson, and Foose, 2005; M-161, Miller and Severson, 2005; M-162, Miller, 2005) which cover an area encompassing parts of the Partridge River intrusion, the southern South Kawishiwi intrusion, and the southwestern Bald Eagle intrusion, were intended to update the unpublished reconnaissance maps of Bonnichsen (1970a-d) and part of Foose and Cooper's (1978) map of the Harris Lake area.

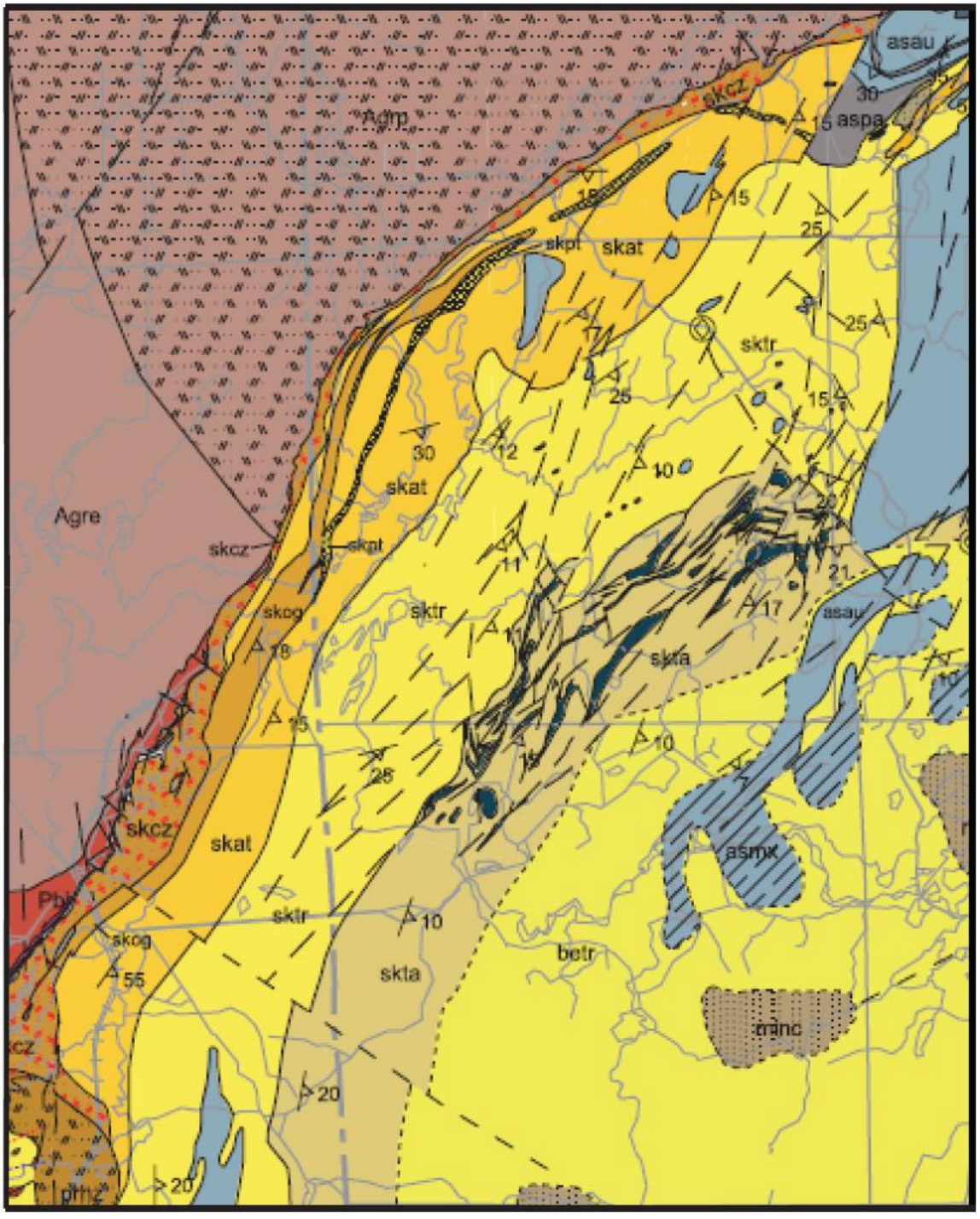


Figure 6: Excerpt from M-119 (Miller et al, 2001) containing the South Kawishiwi intrusion as of 2001; SKI unit include: skcz-sulfide-bearing contact zone, sktr-troctolite cumulates, skat-augite troctolite cumulates, skta- interlayered troctolitic and anorthositic rocks, skpt-poikilitic leucotroctolite cumulates, skgp-gabbroic pegmatite, skog-olivine oxide gabbro to augite troctolite cumulates.

The Babbitt NE quadrangle (M-160) is most pertinent to this study, in which, Miller, Severson, and Foose (2005) describe the SKI as composed of a heterogeneous, sulfide-bearing polylithic contact zone overlain by multiple, randomly alternating troctolitic, and augite troctolitic units. Although the SKI and PRI are not observed in outcrop contact, the authors note that drill cores logged by Severson and Hauck (1990) show the SKI to be in intrusive contact with the PRI in the southwest corner of the map. At the contact between the two intrusions, the trace of the SKI units bends sharply back to the east with at least one unit pinching out. The PRI is very heterogeneous at the contact, which Severson and Hauck (1990) interpreted as recrystallization and possibly partial melting resulting from intrusion of the SKI. The map shows the SKI to contain multiple anorthositic series inclusions largely confined to two troctolitic units (Mkl, Mku) and occurring mostly well above the sulfide-bearing contact zone. The map also shows the areal extent of three known SKI deposits including the Birch Lake deposit, the Dunka deposit, and the Serpentine deposit.

In 2006, Peterson digitized topographic contours and created a 5-meter spaced digital elevation model (DEM; NRRI/MAP-2006-01, Peterson, 2006), which greatly increased the detail (36x's) of standard U.S. Geological Survey DEM's, and was generated to be used as a base map for further mapping in the northern SKI area. In that same year, Peterson et al., (2006) produced a map of the Nickel Lake macrodike (NRRI/MAP-2006-02) to the northeast of the SKI. The map shows the northeast-trending macrodike is composed of a core of pegmatitic oxide gabbro mantled by heterogeneous troctolites with intermixed sulfide-bearing troctolites to the west and

layered troctolites and dunites to the east. The discovery of previously unreported Cu-Ni sulfide mineralization in the margins of the macrodike and its geometric relationship to the SKI led Peterson et al., (2006) to interpret the Nickel Lake macrodike as being a possible feeder system to the SKI.

One of the most recent mapping projects in the vicinity of the SKI was conducted in the Nickel Lake-Gabbro Lake area by several students participating in UMD's Precambrian field camp (Tharalson et al., 2007). Their mapping focused on the connection between the Nickel Lake macrodike and the Bald Eagle intrusion, previously mapped by Paul Weiblen (Weiblen, 1965; Green et al., 1966). This mapping confirms that the macrodike connects with the northern Bald Eagle intrusion, a connection that Green et al. (1966) described as "tenuous."

Recently, Peterson (2008) released a compilation of mapping in the northern South Kawishiwi intrusion (Fig. 7). The map shows the Nickel Lake macrodike geologically connected with the northern SKI. In the explanatory note for the map, Peterson (2008) interprets that the macrodike served as a major conduit to the SKI. This interpretation is a central tenet of Peterson's (2001) mineralization model and has important implications for the emplacement of SKI magmas and sulfide mineralization of the Nokomis deposit. The map also shows that the strike and dip of igneous foliation and layering in the northeastern part of the SKI defines a funnel-shaped or synformal body, in contrast to the previously held view that the SKI occurs as a sheet-like body that consistently dips to the southeast and projects beneath the Bald Eagle intrusion. However, additional mapping along the eastern margin of the SKI is needed to confirm

this. Peterson's ideas for the formation and mineralization of the South Kawishiwi intrusion and its connection to Nickel Lake macrodike will be elaborated on in the Petrologic and Metallogenic Studies section below.

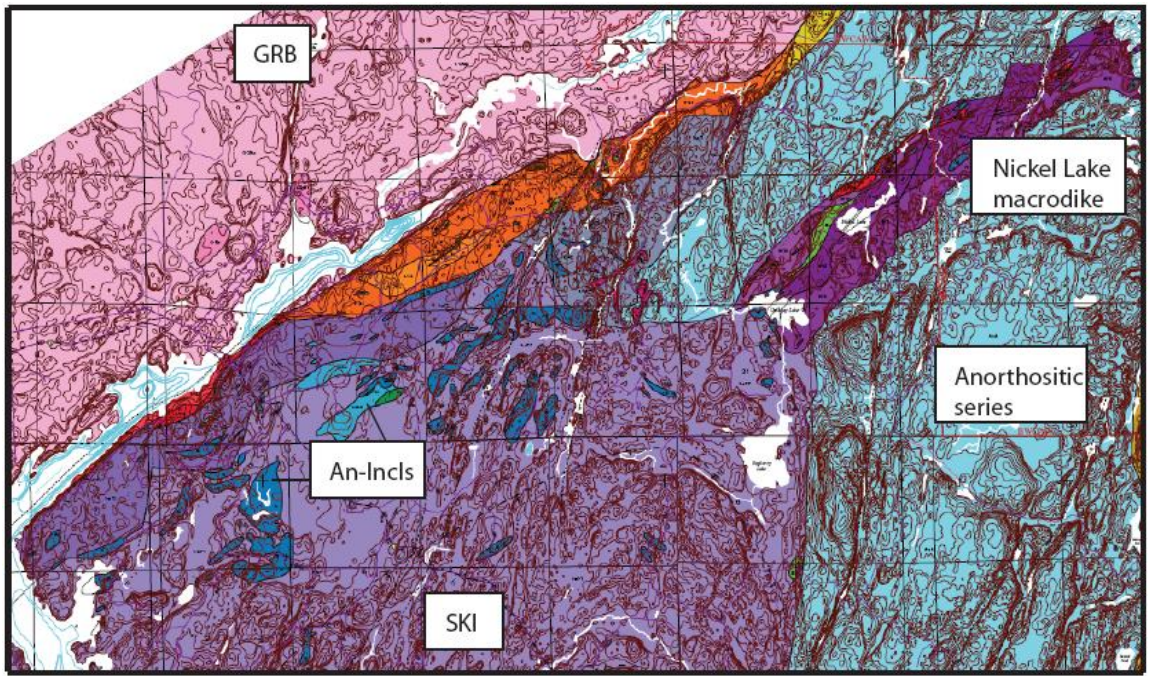


Figure 7: Excerpt from NRRI/MAP-2008-01, showing important features significant to this study, modified from Peterson, 2008.

## 2.2 Core Logging Studies

In addition to surface mapping, many studies beginning in the 1970's sought to define the igneous stratigraphy along the mineralized basal zone of the SKI by relogging the abundant exploratory drill cores that were turned over to the Minnesota Department of Natural Resources. Bonnichsen (1972) examined core from four drill holes in the Dunka Pit area and defined nine units: Giants Range batholith footwall rocks, inclusions of Biwabik iron formation, hornfels basalt, anorthositic rocks, and five SKI mafic units.

Bonnichsen's igneous units, which were largely based on pyroxene mode, habit, and composition, portray a very complex, bifurcating internal structure.

Foose (1984) subsequently defined six stratigraphic units along the basal zone of the SKI in nine drill cores located northeast of the Dunka Pit area over a six-mile strike length. He noted a "plagioclase-rich pegmatoidal layer" that consistently showed up immediately above the "sulfide-bearing basal zone" and later called the PEG unit by Severson (1994). Foose (1984) also reported an olivine-rich troctolite unit immediately above the pegmatoidal layer. His three units above this, from bottom to top, include: lower troctolite, troctolite with pegmatoidal layers, and troctolite with anorthositic layers.

The reports of Bonnichsen (1972) and Foose (1984) both highlighted the extreme heterogeneity found in the mineralized basal portion of the SKI. Although correlation between these two studies is difficult, independently they both show that the igneous stratigraphy of the lower SKI can be correlated in drill core and that the SKI is generally a stratigraphically cohesive intrusive body. These core logging studies, as well as the early mapping projects noted above, set the stage for more detailed and focused work to follow.

Severson (1994) conducted the most complete public core-logging report on the SKI to date. He divided the SKI into 17 stratiform igneous units (Fig. 8) through examination of drill core from 193 drill holes. At the time, this included every publicly archived drill core from the SKI in existence (Severson, 1994). Drill core for this study is housed at the Minnesota Department of Natural Resources (MDNR) core library in Hibbing.

The main characteristics of the igneous units defined by Severson (1994) are summarized in Figure 9. From bottom to top, the units are: BAN (bottom augite troctolite/norite), BH (basal heterogeneous), U3 (ultramafic three), PEG (Pegmatoidal unit of Foose, 1984), U2 (ultramafic two), U1 (ultramafic one), AT-T (anorthositic troctolite-troctolite), Main AGT (main augite troctolite), HP#1 (high picrite #one), HP#2 (high picrite #two), AT&T (anorthositic troctolite and troctolite), AT(T) (anorthositic troctolite (troctolite)), AN-G (anorthositic group), Upper GABBRO (upper gabbroic) , INCL (basalt inclusion), Upper PEG (upper pegmatoidal), and T-AGT (troctolite-augite troctolite). The uppermost units (AT-T, U2, U1, Main AGT, AT&T, AT(T)) include multiple homogeneous, sulfide-barren rock types consisting largely of anorthositic troctolite, augite troctolite, and troctolite. These units conformably overlie a sulfide-bearing basal contact zone composed of several units - BAN, BH, U3, and PEG. Several relatively narrow intervals of ultramafic rocks (dunite, melatroctolite, oxide melatroctolite) occur throughout the stratigraphy. In upper units, these ultramafic units are U2, U1, HP#1 and HP#2, while the sulfidic basal contact zone contains only the U3 unit. Severson (1994) recognized an enormous inclusion block of anorthositic series rocks capped by a thick zone of hornfels metabasalt in the Highway 1 area, which he termed the AN-G unit (Figs. 8 & 9). As explained below, this inclusion will come to play a major role in explaining the mineralization of the Nokomis deposit. Barren troctolitic units of the SKI surround and encase this package of anorthositic rocks with the sulfide-bearing basal contact zone present immediately beneath it.

Severson's (1994) report remains the most complete study to date covering the igneous stratigraphy of the entire SKI. It provides a robust template for additional investigations focused on specific areas of the SKI. The igneous stratigraphic unit terminology for the SKI developed by Severson has been accepted by many workers both in academia and industry, allowing for easy correlation between contemporary data sets, and large-scale characterizations of the SKI. One of the objectives of this study is to reevaluate Severson's general stratigraphy in the Nokomis deposit area to determine what modifications, if any, are required by new study of the area immediate to the Nokomis deposit. The part of Severson's (1994) igneous stratigraphy that applies to this study is highlighted in red on figure 8.

A principal conclusion of Severson's (1994) study was that the SKI formed by multiple injections into a sheet-like chamber and that each injection had limited and variable areal extent leading to a highly compartmentalized configuration of rock units. This is evident in Figure 8 and was reconfirmed by mapping in the Babbitt NE quadrangle (Miller, Severson, and Foose, 2005). Severson's interpretations on magmatic emplacement and mineralization will be summarized below in section 2.4. The following section describes Cu-Ni-PGE exploration by private companies in the SKI over the past 60 years.

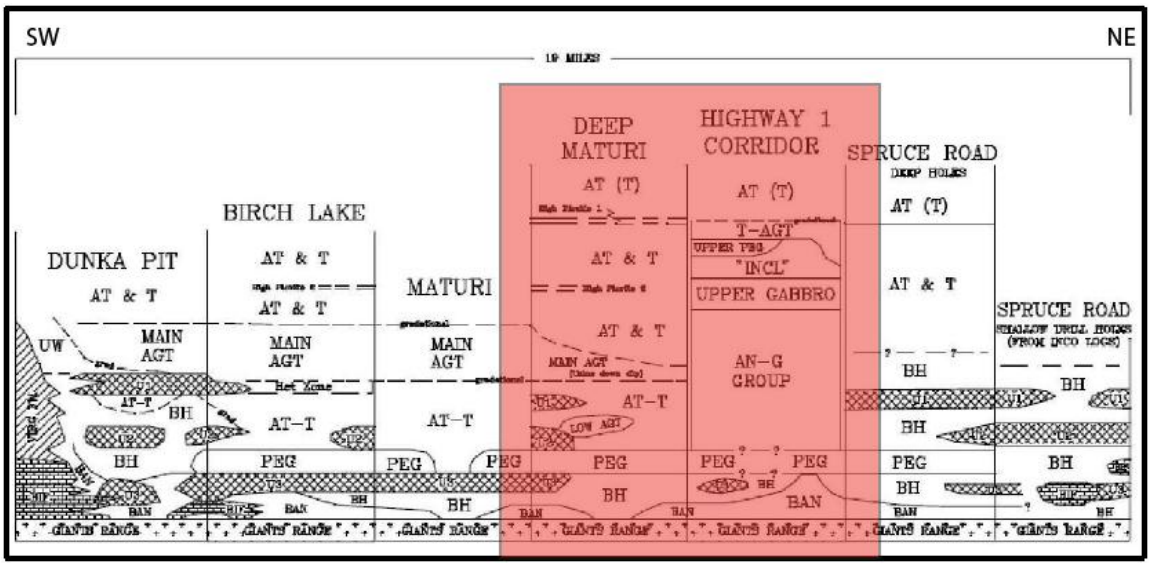


Figure 8: Stratigraphic section showing the 17 lithostratigraphic units of the South Kawishiwi intrusion as defined by Severson (1994), the area pertaining this study is highlighted in red, modified from Severson, 1994.

| UNIT | MAJOR ROCK TYPE | THICKNESS (ft) (range) | PLAG SYMP | ILM/MGT COMPOSITE | ILM/Ti-Cr COMPOSITE | MISCELLANEOUS |
|---|---|---|---|---|---|---|
| AT (T) | Anorth. Tract. | + 1,200 | ✓ | ✓ | | |
| AT & T | An. Tract & Tract. | (1,200–2,000) | ✓ | ✓ | | High Picrite #1 at top |
| UW | Sulf-barg Tract. | (100–900) wedge-like | ✓ | ✓ | | two ultramafic zones (UW1 & UW2) |
| MAIN AGT | Augite Troctolite | 900 (270–1,380) | ✓✓ | ✓ | | hybrid rocks common near base at Dunka Pit area |
| U1 | 55% ultramafics 45% troctolites | 110 (5–430) | Rare | Ilm dominant | ✓ | uppermost sulfide-bearing unit at Dunka Pit and Spruce Road |
| BH | Sulf-barg Heterog. Troctolite | (90–1,700) | Rare | Ilm dominant | | Highly variable thickness ! |
| AT-T | An. Tract to Tract. | 380 (70–1,200) | ✓ | ✓ | | locally sulfide-bearing at Dunka Pit area |
| U2 | 36% ultramafics 64% troctolites | 90 (5–425) | — | Ilm dominant | ✓ | sulfide-bearing at Dunka Pit and Spruce Road; mass ox in B1-68 |
| PEG | Tract with common pegmatitic zones | 95 (10–260) | ✓ | Ilm dominant | ✓ | locally sulfide-bearing |
| U3 | 33% ultramafics 67% troctolites | 100 (3–410) | Rare | ✓ Mgt is dominant in mass oxides | ✓ | PGE-bearing zones; massive oxide and BIF incl's common; green pleonaste common. |
| BAN | Augite Tract (top) Norite (bottom) | 125 (10–380) | Rare | Ilm dominant | | sulfide-bearing; contains most mass. sulf. occurrences; mass ox and BIF incl's at Dunka Pit |
| HIGHWAY 1 CORRIDOR | | | | | | |
| T-AGT | Tract & Aug. Tract. | (70–450) | | | | |
| UPPER PEG | Pegmatoidal Tract. | (77–139) | | | | |
| "INCL" | Granular "Ox Gab" | (300–540) | — | Mgt dominant | | sheet-like CC Inclusion (basalt?) |
| UPPER GABBRO | Gabbro | (20–855) | ✓ | ✓ | | |
| AN-G GROUP | 40–79% Anorthosite 13–24% Gabbro | 1,850 (1600–2,450) | Tr ✓ | Ilm dominant ✓ | | contains semi-mass graphite veins |

Figure 9: Summary table of the major attributes of Severson's (1994) lithostratigraphic units comprising the SKI.

## 2.3 Cu-Ni Sulfide Mineral Exploration of the SKI

Exploration of the SKI began in 1948 when Ely prospector F.S. Childers, exploring the basal contact in the South Kawishiwi River area, recognized sulfide gossan stains in weathered gabbro during excavation of Spruce Road. Childers and his partner, R.V. Whiteside, drilled a 188 foot bore hole in 1951 into what is now called the Maturi deposit (Miller, Severson, and Hauck, 2002). Since then, more than a dozen different exploration companies have drilled hundreds of bore holes into at least seven different Cu-Ni-PGE prospects in the SKI. From southwest to northeast, these include the Serpentine, Dunka Pit, Birch Lake, Maturi, Nokomis, South Filson Creek, and Spruce Road deposit areas (Fig. 10). Five of these prospects (South Filson Creek, Spruce Road, Maturi, Birch Lake, and Nokomis) are currently in different stages of development and can justifiably be termed "deposits."

Maturi, Nokomis, Birch Lake, Dunka Pit, Serpentine, and Spruce Road all display similar styles of basal contact mineralization. However, they differ in that Nokomis, Maturi, and Birch Lake typically show a confined-style of basal contact zone mineralization, whereas Spruce Road, Dunka Pit, and Serpentine display an open-style of basal contact zone mineralization, as defined by Peterson (2001). Confined-style vs. open-style mineralization will be discussed in detail in the next section. The South Filson Creek prospect displays a "cloud" type of mineralization, meaning that disseminated Cu-Ni sulfide is 300-500 meters above the basal contact (Kuhns et al., 1990).

Drilling of the Maturi deposit commenced in the early 1950's with an aggressive drilling program by International Nickel Company (INCO). INCO's drilling program

proceeded through the 1970's, identifying a 247 Mt deposit with average grades of 0.5% copper and 0.19% nickel (Miller, Severson, and Hauck, 2002). In the late 1960's and early 1970's exploration drilling by INCO, Duval Corporation, Hanna Mining, and Newmont Mining confirmed a down-dip continuation of Maturi to the east termed Maturi Extension. Drilling in the area halted in the mid-1970's due to environmental pressures and economic conditions. Processing of low-grade Duluth Complex Cu-Ni ores was also an issue at the time, but current advancements in hydro-metallurgical processing techniques has alleviated many environmental problems with processing sulfide ores. Because early exploration of Duluth Complex deposits was focused largely on Cu and Ni, most companies did not assay for PGE's. Not until the mid-'80's were significant concentrations of palladium, gold and platinum discovered in Duluth Complex ores during studies by the University of Minnesota (Sabelin and Iwasaki, 1985, 1986; Morton and Hauck, 1987).

In the late 1990's, following Peterson's (1996) report on Cu-Ni-PGE mineralization in the SKI, Wallbridge America, a Canadian junior company out of Sudbury, Ontario, picked-up a lease option on the Maturi Extension properties from American Copper Nickel Company, and began conducting preliminary assessments of the property. In late 2005, Duluth Metals Ltd. was formed as a spin-off from Wallbridge America to explore the Maturi Extension properties (in late 2006, Duluth Metals was incorporated as an American company). Seven initial holes were drilled in early 2006 that contained significant copper, nickel, and precious metals values. In the fall of 2006, an aggressive drilling program was initiated by Duluth Metals Corp to define a resource

for Maturi Extension. The results of this drilling program produced significant enough resource estimates by early 2008 that the company decided to rename the Maturi Extension prospect, the Nokomis deposit. Table 1 displays tonnage and grade estimates as of mid-2008 for five Cu-Ni-PGE deposit/prospect areas in the SKI where information is available.

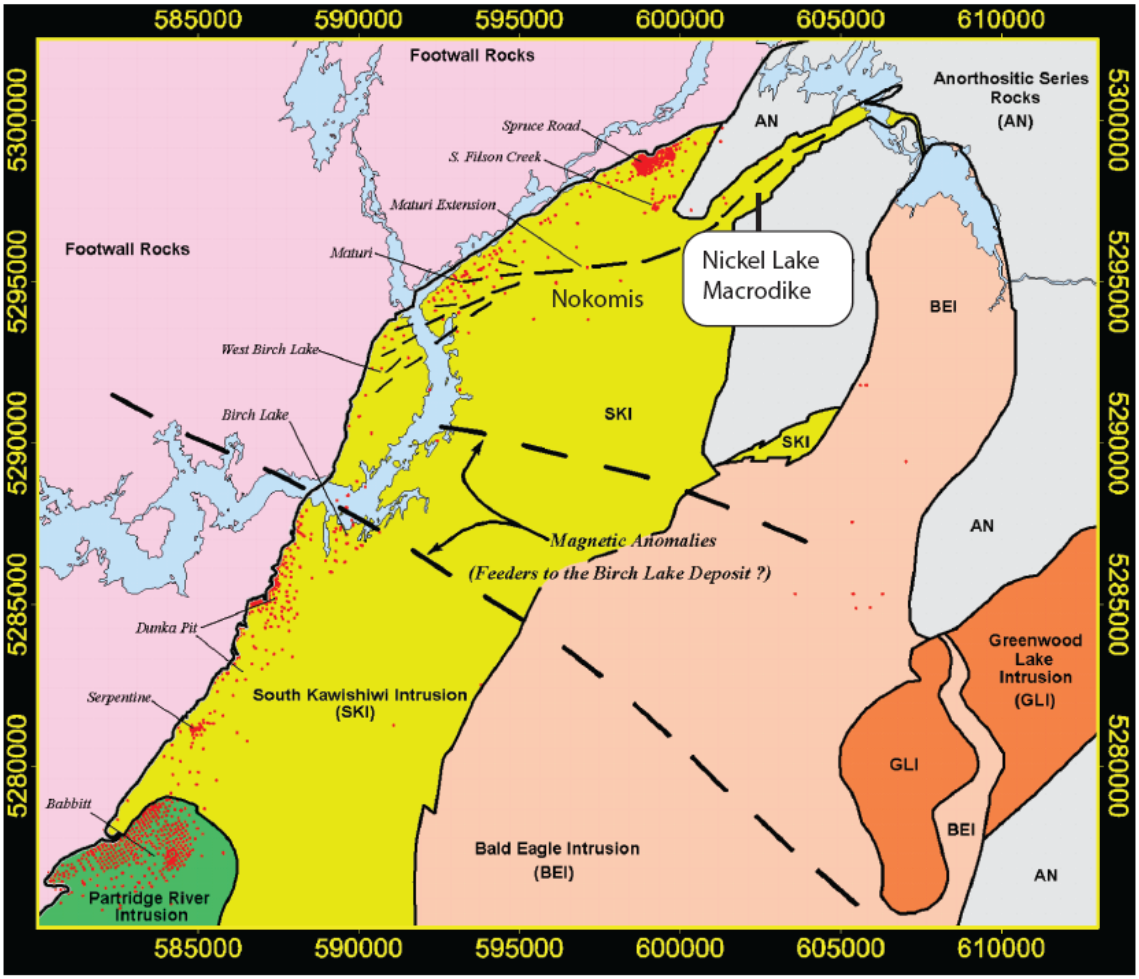


Figure 10: Cu-Ni-PGE deposits/prospects in the South Kawishiwi intrusion with accompanying table providing grade and tonnage information for selected deposits, red dots indicate drill hole density as of 2001, modified from Peterson, 2001.

Table 1: Metals grade and tonnage information for selected SKI deposits as available.

| DEPOSIT | Tonnage (million tonnes) | | Copper % | | Nickel % | | PGE's (g/t) | | Reference |
|---|---|---|---|---|---|---|---|---|---|
| | Inferred | Indicated | Inferred | Indicated | Inferred | Indicated | Inferred | Indicated | |
| Maturi | 83.1 | | 0.7 | | | | 0.43 | | Franconiaminerals.com (July 23, 2008) |
| Nokomis | 284 | 449 | 0.627 | 0.624 | 0.194 | 0.199 | 0.718 | 0.6 | Duluthmetals.com (July 23, 2008) |
| Birch Lake | 100.4 | | 0.59 | | 0.19 | | 1.19 | | Franconiaminerals.com (July 23, 2008) |
| Spruce Road | 28.4 | 376.7 | 0.23 | 0.39 | 0.109 | 0.14 | | | Franconiaminerals.com (July 23, 2008) |
| Serpentine | | >250 | | 0.41 | | 0.14 | | | Zanko et al., 1994 |

## 2.4 Petrologic and Metallogenic Studies

Many petrologic and metallogenic studies have focused on the magmatic and mineralization history of the SKI (and the PRI) and, in particular, on the heterogeneity of the basal contact zone and the Cu-Ni-PGE mineralization contained within. Ideas about the overall petrogenesis of the SKI range from *in situ* fractional crystallization of a closed system (Chalokwu and Grant, 1990) to an open system with an infinite number of magma recharge events similar to the formation of ocean crust gabbros (Sassani, 1992), and even suggestions that gabbroic and troctolitic rocks of the SKI and the PRI were in fact

completely different intrusions with interlayered contacts, producing the observed heterogeneity of the basal contact zone (Martineau, 1989). This section does not attempt to account for every petrologic and metallogenic study conducted in the SKI, but rather highlight conclusions pertinent to this study. Severson (1994) and Hauck et al. (1997) also provide thorough summaries. A brief discussion of the Partridge River intrusion is included, however, because of significant similarities in its petrology and sulfide mineralization to the SKI.

Accompanying the Gabbro Lake 15' quadrangle (Green et al., 1966), Phinney (1969) described "a northeast-trending dike between Omaday and Gabbro Lakes," that merges with the northeastern margin of the SKI and appears to link to the northern margin of the Bald Eagle intrusion (Fig. 10). Phinney (1969) was the first to interpret this dike as a feeder to the SKI. He cited modally layered troctolite to melatroctolite with elongated olivine grains and plagioclase laths oriented parallel with the dike walls, as well as numerous iron formation and anorthositic inclusions also aligned parallel with dike walls, as evidence that the dike was a feeder. Phinney (1969) also noted that at Gabbro Lake, the dike splits into several smaller, southeast-trending dikes cutting earlier anorthositic series rocks.

Phinney (1969) identified three main units within the main body of the SKI, which are also shown on the Gabbro Lake 15' quadrangle map (Green et al., 1966): a contact zone, augite troctolite, and poikilitic augite troctolite. He described the contact zone as a sulfide-bearing, inhomogeneous mixture of rock types and textures containing many fine-grained inclusions. Some inclusions are interpreted as representing autoliths

of a gabbroic chilled margin, while others were clearly Virginia Formation and anorthositic series. Phinney (1969) noted that the Cu-Ni sulfide mineralization consisted of mostly disseminated chalcopyrite, pyrrhotite, pentlandite and cubanite, and that sulfides were present with varying silicate assemblages and fine- to coarse-grained host rocks, typically forming interstitial to plagioclase and olivine. The upper troctolite units contain plagioclase and olivine as cumulus phases, and augite, magnetite, biotite, and hypersthene as interstial (post-cumulus) minerals. Petrographic observations and microprobe mineral analyses by Phinney (1969) show that olivine in the contact zone of the SKI was more iron-rich ($Fo_{50}$) than olivine in the upper units of the SKI ($Fo_{60}$). Plagioclase displayed normal zoning with a range of 5 to 10 percent anorthite content and commonly contained a schiller of ilmenite. Augite and iron oxides locally form subpoikilitic to poikilitic grains, and augite displays extensive exsolution lamellae of hypersthene with associated schiller of titaniferous magnetite and pseudobrookite.

Weiblen and Morey (1976, 1980) speculated that sulfide mineralization occurred early on in the formation of the SKI. From samples collected from INCO Test Pit Number 1 on Spruce Road, and from Bear Creek Mining Company drill hole B-1, they discriminated four distinct textures of sulfides intergrown with silicates: interstitial, included, intergrown, and fine-veinlet sulfides. They also noted that each textural type had a characteristic copper-nickel-iron sulfide mineralogy and modal abundance. They concluded that gravity settling of dense immiscible sulfide melt from the SKI mafic magma alone could not have produced the interstitial and disseminated nature of the ore zone. Instead, they argued that metamorphism of the country rocks produced a sulfur-

rich vapor phase which rose through the magma, scavenging metals that had already been concentrated in the magma. They called on pre-existing fault zones in the country rocks acting as channel ways for the sulfur-rich vapor, which also accounted for the textural and mineralogical assemblages they observed.

Sulfur isotope studies conducted in the related Partridge River intrusion (Ripley, 1981; Ripley and Al-Jassar, 1987; Andrews and Ripley, 1989; Ripley et al., 2007) documented highly variable values that are consistent with sulfur isotope values observed in Virginia Formation rocks. These studies concluded that sulfides in the PRI had a source of sulfur in different layers of Virginia Formation rocks with differing sulfur isotope values.

Foose and Weiblen (1986) followed up on Weiblen and Morey's (1976) earlier ideas about sulfide genesis, during a petrologic study of the upper sulfide-barren units of the SKI. Most interestingly, they uncovered two distinct whole rock nickel trends in different stratigraphic sections of the same drill hole. The first, in which nickel content decreases upward, is an expected trend resulting from normal fractional crystallization. However, the second trend shows nickel increasing up through the intrusion. Citing the complex, fault-bounded nature of Duluth Complex magma chambers, they suggested that magma in adjacent chambers fractionated to different degrees to explain this phenomenon. Continued rifting could cause mixing between chambers with variably fractionated magmas. This, coupled with a chamber undergoing periodic recharge of primitive magmas, could create the reversed nickel increase trend. Foose and Weiblen (1986) further concluded that sulfide genesis was caused by assimilating sulfur-rich

footwall rocks and xenoliths creating sulfur-rich vapors that moved through the magma when it was about 75% crystallized. They suggested that the heterogeneity of the sulfide-bearing contact zone reflected a dynamic magma chamber with abundant magma mixing, and continuous replenishment of fresh magma with entrained inclusions of Biwabik Iron Formation and Virginia formation. Addressing the abrupt contact between the sulfide-bearing rocks of the contact zone and the sulfide-barren rocks of the upper zones, they speculated that this implies a radical change in magmatic conditions from an early dynamic, restricted chamber switching to an open, quiescent period of emplacement.

Severson's (1994) extensive core-logging study of the SKI led him to conclude that it was a progressively-emplaced, multiply-intruded magmatic system. Based largely upon observations made from re-logging 193 drill cores, he described emplacement of the basal contact zone, *"as a series of repeated and rapid influxes of new magma into several restricted chambers that eventually coalesced with continued magmatic injection to produce the overall heterogeneous and compartmentalized nature of the lower SKTS,"* (p. 182, Severson, 1994). Severson (1994) stressed the discontinuous nature of many of the units, describing pinch-outs, drastic thickness variations, and changes of the stratigraphic positioning of units relative to other units. One of the more obvious examples of these changes is in the Dunka Pit area. Here, at the same stratigraphic level that the coarse, sulfide-barren, augite troctolites of the Main AGT unit occur over most of the SKI, the rock changes to heterogeneous, inclusion-rich, sulfidic troctolite containing several ultramafic intervals, a unit Severson calls the Updip Wedge (UW; Figs. 8 & 9). Severson (1994) suggested that the UW was an earlier unit cut-off by the later intruding

Main AGT. The upper sections of the SKI tell a much different story than the basal contact zone. Like Foose and Weiblen (1986), Severson (1994) interpreted a much calmer, quiescent emplacement of the upper units into an open system with very little interaction with surrounding country rocks and thus little sulfur contamination. He noted that homogeneous troctolitic units are periodically interrupted by thin melatroctolite units marked by sharp bases and more gradational upper contacts. He interpreted these ultramafic intervals as evidence of the progressive inflation of the chamber by sheet-like intrusions of slightly olivine over-saturated tholeiitic magmas.

During a mineralogical and oxygen isotope study of the SKI in the Spruce Road area, Lee and Ripley (1996) re-logged and sampled all or part of four drill holes from the area, developing a seven-unit stratigraphy. They concluded that magmatic genesis of the SKI included *in situ* equilibrium crystallization with residual liquid expulsion and subsequent magma recharge. Perhaps more importantly, their oxygen isotope work demonstrated that only their units I and II, located < 100 m from the footwall GRB contact displayed crustal contamination signatures.

Two other studies of the Partridge River intrusion have implications for SKI mineralization. Theriault et al. (1997) studied country rock assimilation and silicate magma/sulfide melt ratios (R-factor) in the Dunka Road deposit (now Polymet's NorthMet deposit) of the PRI. In this deposit, Animikie group sedimentary rocks form the footwall to the PRI. These sedimentary rocks are locally sulfide-rich and thus when present are presumed to have played a major role in the genesis of sulfide mineralization. They distinguished three main occurrences of disseminated sulfide mineralization: 1)

norite-hosted sulfides, 2) troctolite-hosted sulfides, and 3) PGE-rich sulfide horizons. The norite-hosted sulfides occur near the basal contact or are associated with country rock xenoliths. The PGE-rich sulfide horizons are usually found beneath ultramafic horizons, while the troctolite hosted sulfides comprise the bulk of the deposit. They concluded that two main parameters, degree of contamination of the magma from partially melted granites and sulfur-bearing hydrous fluids, and the R-factor, controlled the sulfide mineralization observed. They suggested that norite-hosted sulfides formed from high contamination and low R-factors, PGE-rich sulfides formed from uncontaminated magmas with high R-factors, and that troctolite hosted sulfides formed from low to moderately contaminated magmas with moderate R-factors.

In a recent study of the PRI, Ripley et al. (2007) focused on the heterogeneity of the basal contact zone. They concluded from isotopic and other geochemical evidence that high-Al olivine tholeiitic magmas produced both the gabbroic and troctolitic components of the basal contact zone. Furthermore, "*modification*" of these magmas occurred from fractional crystallization, country rock contamination, and *in situ* crystallization in a shallow environment. Most significantly, they stated that sulfur isotope values in leucotroctolitic rocks that overlie the basal contact zone are consistent with a mantle source, while sulfur isotopes in the basal contact zone indicate a crustal source, but that values are quite heterogeneous. They conclude that magmas "*at depth interacted with country rocks*" containing widely variable sulfur isotope values.

## 2.5 SKI Mineralization Model of Peterson (2001)

Following on his 1996 study of Cu-Ni grades in the SKI, Peterson (2001) recognized differing Cu-Ni-PGE grades associated with variations in the vertical thicknesses of disseminated sulfide-mineralized zones throughout the SKI. Peterson's (2001) mineralization model describes a physical system of magma flow in which low-grade (Cu, Ni, & PGE), vertically extensive (200-700 m) mineralization contrasts with high-grade, vertically restricted (<200 m) mineralization. The grades vary stratigraphically, but not particularly with lithology. Rather, sulfide-mineralized stratigraphic units simply vary in thickness and metal tenor (especially PGE). Peterson (2001) cited the grades and thicknesses shown in Figures 11 and 12 as examples of the two styles of mineralization, which he defined as follows:

**Open** - vertically extensive (> 200 m's) mineralization with low to high Cu-Ni grade and low Au+PGE grades (Examples: Serpentine, Dunka Pit, and Spruce Road; Figure 11). Cu-Ni grades typically increase towards the basal contact although the mineralized zones are typically erratic in their spatial extent and grade, and commonly interfinger in a random pattern with zones that are barren of sulfides. Restricted zones of massive sulfide occur locally at, and/or immediately below, the basal contact.

**Confined** - vertically restricted (< 200 m's) mineralization with moderate to high Cu-Ni grades and moderate to very high (locally) Au+PGE grades (Examples: Birch Lake, Maturi, Maturi Extension (Nokomis); Figure 11). Cu-Ni grades are typically the

highest near the top of the mineralized zone (units U3 and BH) and gradually decrease with depth toward the basal contact. Only limited areas of massive sulfide occur at and/or immediately below the basal contact. For example, the upper portion of the mineralized zone within the Maturi deposit consistently exhibits copper values in excess of 1.0% that decrease to ~0.25% at the basal contact (Fig. 11).

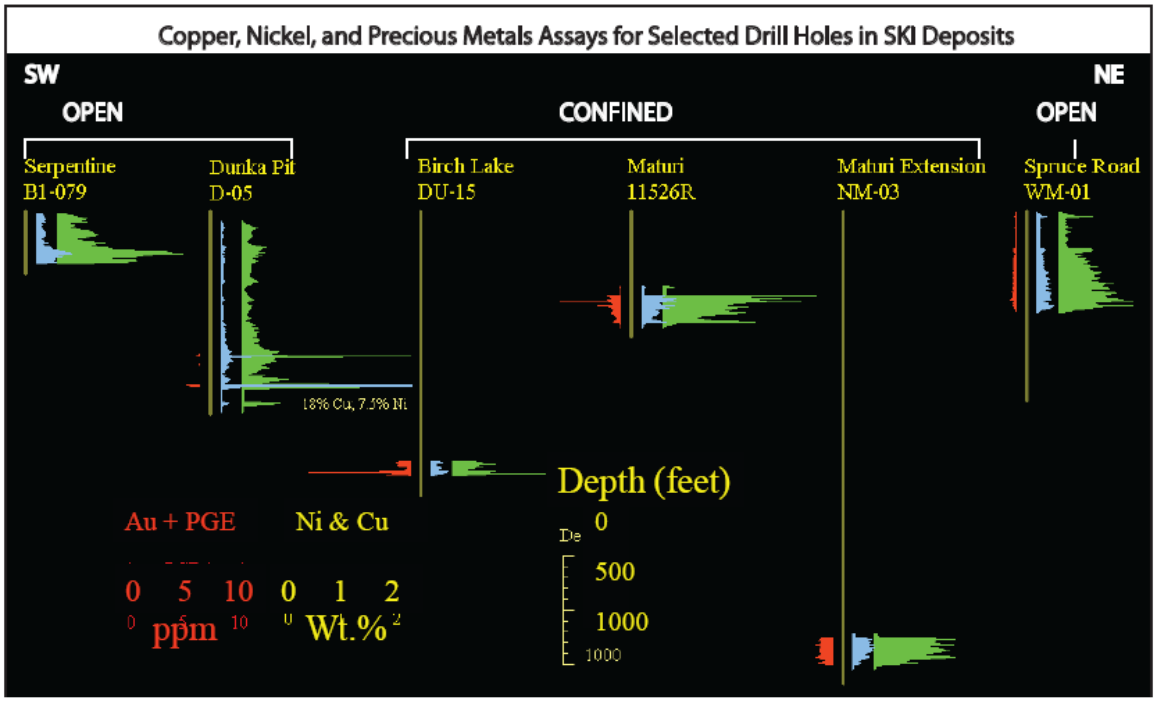


Figure 11: Specific drill holes from six different SKI deposits, showing drill depth versus thickness and grade of copper, nickel, and Au + PGE's. Drill holes are presented in rough geographic order from southwest to northeast. The two holes in the southwest and the hole to the northeast display open-style mineralization, while the remaining three holes represent confined-style mineralization, modified from Peterson, 2001.

Figure 13 shows the areas of the basal SKI where these two mineralization styles are inferred to occur according to Peterson (2001). Peterson (pers. comm. 2006) favored a model in which open-style deposits formed first followed by continued, subsequent magmatism creating the confined style deposits. However, the lack of obvious cross

cutting relationships does not preclude that the two mineralization styles formed contemporaneously whereby open-style deposits formed in thicker marginal parts of the magma sheet while confined mineralization formed in vertically restricted central parts of the chamber. In either situation, the hanging wall is thought to have been composed of anorthositic series rocks as will be discussed later.

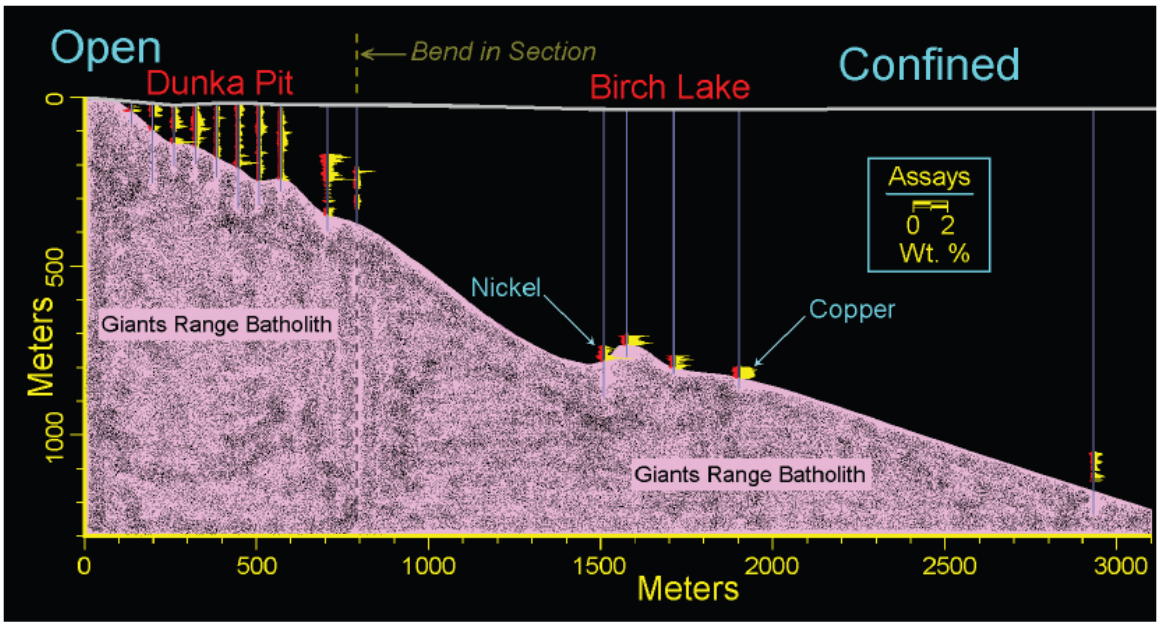


Figure 12: Section showing transition from confined-style mineralization of the Birch Lake deposit to the open-style mineralization of the Dunka Pit deposit, from Peterson, 2001.

The relationship between thickness and grade is further highlighted in Figure 14, which shows assay data compiled by Peterson (1996) from these six deposits plotted against distance from base. In these plots, Cu+Ni values in the confined deposits range to almost twice the concentration of average copper plus nickel grades in open style deposits. Plots of PGE+Au show even more enriched precious metals concentrations for confined style deposits than for open style deposits. Moreover, the more vertically restricted range of the confined style to within 100 m above the basal contact is also

evident in these plots. Peterson (2001) explained these two styles of mineralization as resulting from different flow regimes of sulfide-bearing, in-fluxing magma. He proposed a model whereby open-style mineralization resulted from low velocity, low-turbulence laminar flow into larger magma chambers whereas confined-style mineralization resulted from magma injections into confined areas resulting in constricted turbulent flow. The turbulent flow would promote high R-factors, which relates the volume of silicate magma that comes into contact with a volume of immiscible sulfide melt (Naldrett, 1999). A high R-factor means that a particular volume of immiscible sulfide melt came into contact with a very large volume of silicate magma thus allowing the sulfide melt to efficiently scavenge and concentrate metals from the silicate magma. A high R-factor would be expected to occur under conditions of confined, turbulent and prolonged flow in magma channels and conduits.

Peterson (2001) envisioned that early magma influxes into the SKI magma chamber emanated from the Nickel Lake macrodike and created an initial chamber by plying the anorthositic series off Giants Range granite footwall (Fig. 15). He suggested that this was first accomplished along a NW-SE trending transform fault to form open-style mineralization in a large static magma chamber in the Spruce Road area. Continued magmatic flow delaminated the anorthositic series further westward but the vertical separation of the anorthositic hanging wall was less. This resulted in confined style mineralization evident in the Nokomis, Maturi and Birch Lake deposit areas. Peterson (2001) postulated that constricted, turbulent magma flow beneath the anorthositic series cap resulted in high R-factors between the silicate magma and immiscible sulfide melt,

giving rise to increased Cu-Ni-PGE grades. Continued emplacement of unmineralized magmas continued to lift the anorthositic cap in most other areas of the SKI, but not in the Nokomis deposit area, where an anorthositic series pillar became isolated and engulfed by troctolitic cumulates of the upper SKI.

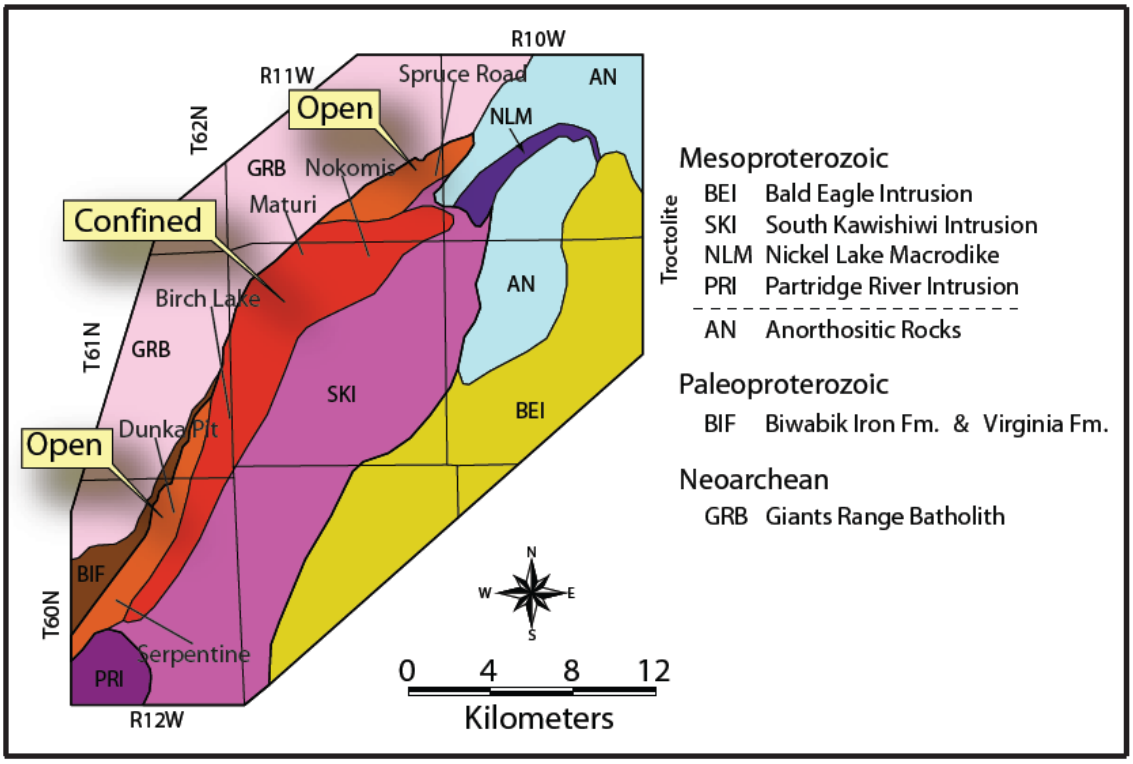


Figure 13: The six SKI deposit from figure 11 presented in map view categorized by mineralization style (confined in red; open in orange) including Serpentine and Dunka Pit (open-style) to the southwest, Birch Lake, Maturi, and Nokomis (Maturi Extension; confined-style) in the center, and Spruce Road (open-style) to the northeast, modified from Peterson, 2001.

Peterson's (2001) mineralization model was subsequently augmented by detailed mapping studies conducted in the northern SKI where it merges with the Nickel Lake macrodike (Peterson et al., 2006; Tharalson et al., 2007; Peterson, 2008). The Nickel Lake macrodike is composed of heterogeneous troctolite with intermittent sulfide-bearing troctolite to the west, and steeply layered troctolite and dunite to the east, sandwiching

coarse-grained to pegmatitic oxide gabbro (Fig. 16). Additionally, subvertical inclusions of hornfelsed basalt and Biwabik Iron Formation occur within the troctolite, along with many anorthositic series inclusions, especially in the area of Omaday Lake (Fig. 16). These observations of steeply inclined layering, foliation, and inclusion orientations led Peterson et al. (2006) to interpret that the Nickel Lake macrodike was a southwest trending near subvertical conduit that fed magma into the SKI. They further postulated that the macrodike is part of a larger magma feeder system that connects up with a larger conduit projecting beneath the Bald Eagle intrusion (BEI) (see Fig. 10). Detailed mapping by Tharalson et al. (2007) confirmed the original mapping by Green et al. (1966) that traced the Nickel Lake macrodike into the northwest margin of the BEI. The arcing of the macrodike was attributed by Peterson and Severson (2002) to deflection of the magma conduit where it encountered the extension of the Giants Range granite in the footwall to the north into a NE-SW trending rift parallel fault.

In a general statement on the relatively low grade of Duluth Complex Cu-Ni sulfide deposits compared to other magmatic sulfide deposits, Naldrett (1999) commented that *"No magma flow channels have been identified so far, and the lack of magma flow subsequent to the development of sulfide immiscibility is regarded as the reason why these deposits are not of economic grade."* However, Peterson's (2001, 2006) postulation of magma flow channels and conduits feeding out of the Nickel Lake macrodike and higher Cu-Ni-PGE grades observed "upstream" in the Nokomis deposit suggests that such flow channels exist and may be tied to high mineral grades. The

principal objective of this study, then, is to further test these ideas in the Nokomis deposit area.

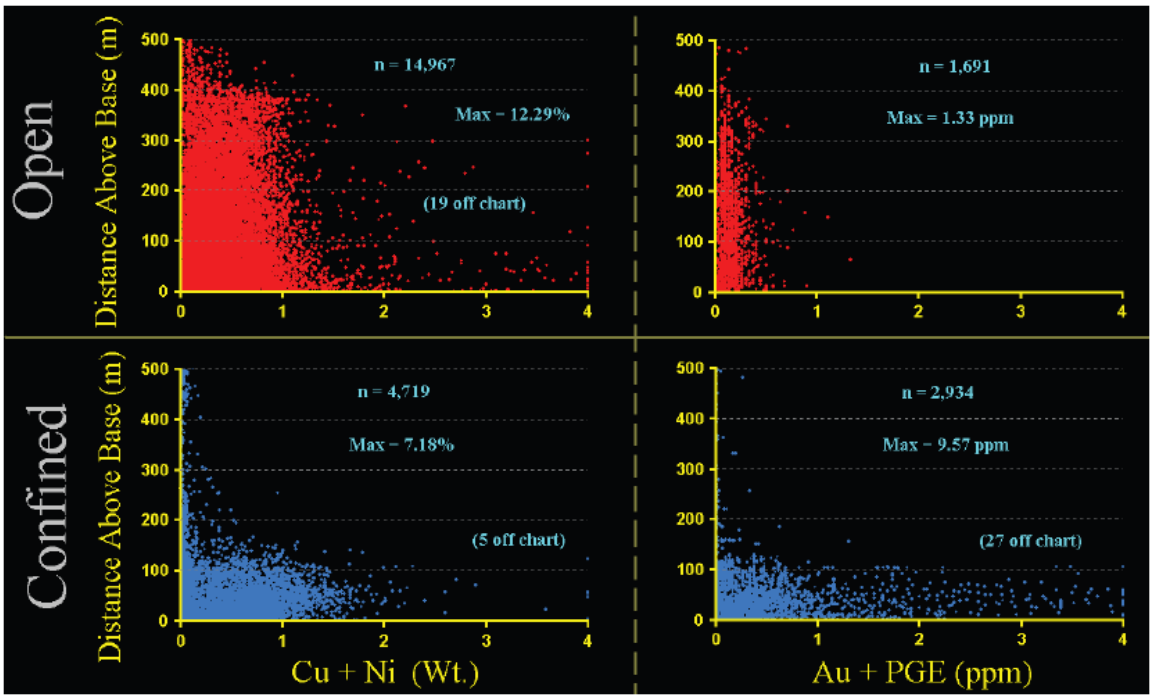


Figure 14: Plots of metal grades versus distance above base plots SKI deposits. Assay data for open style plots from Serpentine, Dunka Pit and Spruce Road deposits. Data for confined style plots from Dunka Road, Maturi, and Maturi Extension (Nokomis) compiled by Peterson (1996). Figure taken from Peterson, 2001.

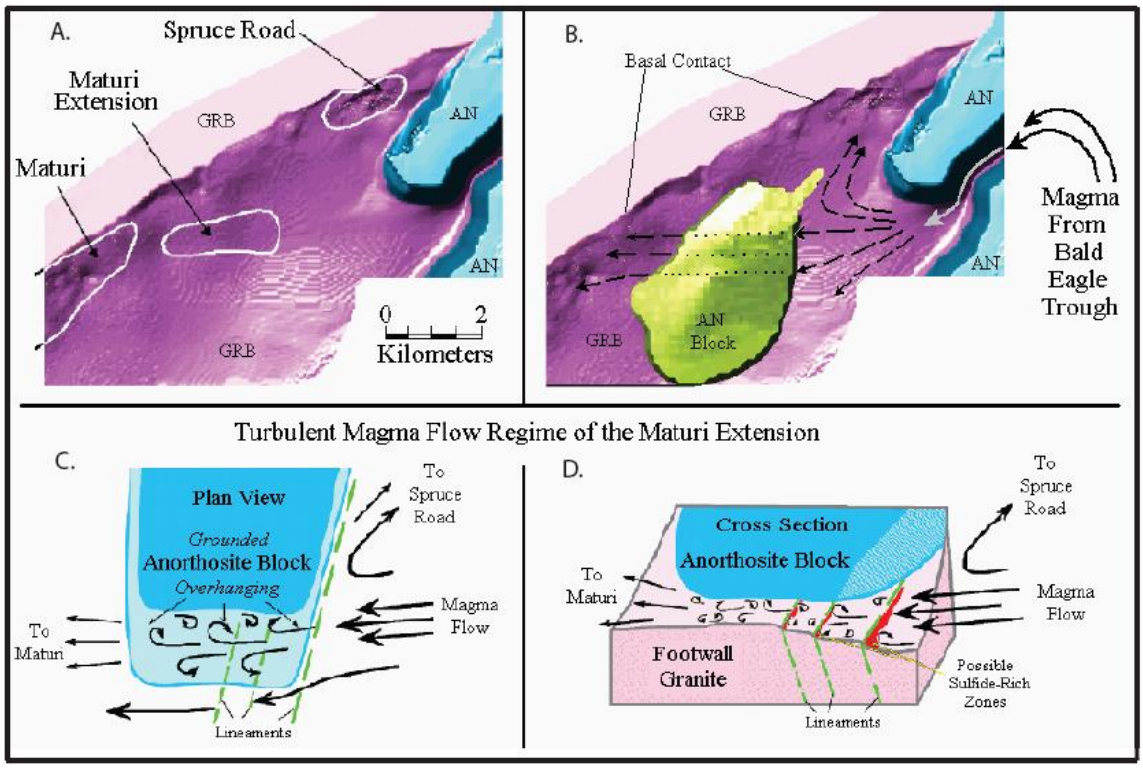


Figure 15: Peterson's open versus confined mineralization model for the South Kawishiwi intrusion: A. footwall contact in three dimensional relief, B. magma flow from Bald Eagle trough (now known as the Nickel Lake macrodike) flowing north to the open-style Spruce Road deposit, and west under the anorthosite block to the confined-style Nokomis deposit, C. plan view of confined-style mineralization flowing under the anorthosite block causing turbulent flow, D. cross-sectional view of confined-style mineralization under anorthosite block collecting sulfides along lineament traps, from Peterson, 2001.

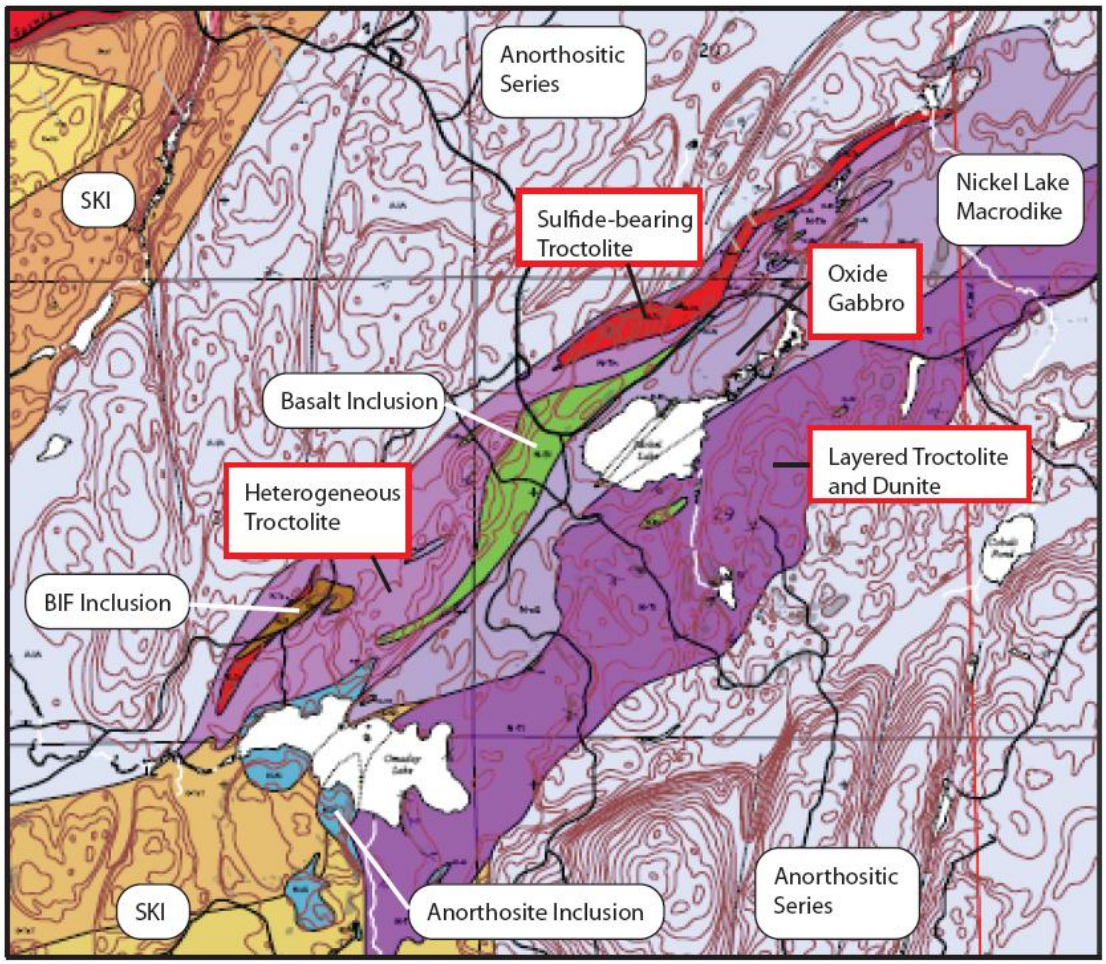


Figure 16: Excerpt from NRRI?MAP-2006-04 highlighting the major features of the Nickel Lake macrodike, modified from Peterson et al, 2006.

# CHAPTER THREE: GOALS AND OBJECTIVES

The variability in metal grade and ore concentration along the basal zones of the SKI is a well documented, but poorly understood characteristic of Duluth Complex mineralization. Some of this variability seems to be related to host rock type, as shown by Severson's (1994) detailed rendering of the lower igneous stratigraphy of the SKI. Peterson's (2001) model of an open vs. confined style of mineralization provides an intriguing explanation for the differing metal concentrations based on magma emplacement dynamics. However, the igneous stratigraphy of the mineralized lower SKI as laid out by Severson (1994) in the Nokomis deposit area (formerly the Maturi Extension, Fig. 8) was based on only a few drill holes (ten cores in the Nokomis deposit area; Fig 17). Similarly, Peterson's (2001) confined model of mineralization was based on assay data from a few cores. Since Severson's (1994) and Peterson's (2001) studies, Duluth Metals has drilled 154 more drill holes throughout the deposit as of the fall of 2008. This new drilling now allows for more detailed documentation of the igneous stratigraphy of this part of the SKI and for a more robust test of Peterson's mineralization model for the Nokomis deposit, which are the principal objectives of this study. Inherent to these prime objectives are the goals of better understanding the magmatic history of emplacement, and the petrogenesis and sulfide metallogenesis of this part of the SKI and other mineralized areas of the Duluth Complex.

This study sets out to accomplish these goals and objectives by documenting the vertical and lateral variation in modal rock type, textures, structures, mineral chemistry, sulfide concentration, and metal grade in a series of drill cores that profile an E-W section

of the Nokomis deposit area. This profile crosses the large anorthositic block that Peterson (2001) suggested was responsible for creating the confined-style of high-grade mineralization in the gabbroic and troctolitic rocks beneath it (Fig. 17).

Documenting the vertical and lateral changes in lithology and geochemistry in core that profile the Nokomis deposit will not only better establish the igneous stratigraphy of the deposit area, but will also serve to test whether these changes are consistent with the flow model of Peterson (2001). As described in the previous section, this model suggests that magmas and entrained sulfides flowed from east to west, emerging from the Nickel Lake macrodike feeder and developing as a confined, turbulent flow beneath the anorthositic block (Fig. 15). The metal tenor of the sulfides was presumably upgraded beneath the block by the turbulent flow leading to high R-factors for the entrained sulfides. This model predicts that a decrease in metal tenor might be expected "downstream" as metals are scavenged by "upstream" sulfides. This model also predicts that some lateral changes in silicate mineralogy (e.g., more olivine upstream and plagioclase downstream due to density differences) and composition (e.g., higher mg# upstream) may be expected. Documenting the vertical and lateral changes in rock type and mineralization in the Nokomis deposit area will not only help to better understand the petrogenesis of this deposit, but will also provide useful criteria for evaluating other enriched areas of the SKI and other mineralized intrusions of the Duluth Complex.

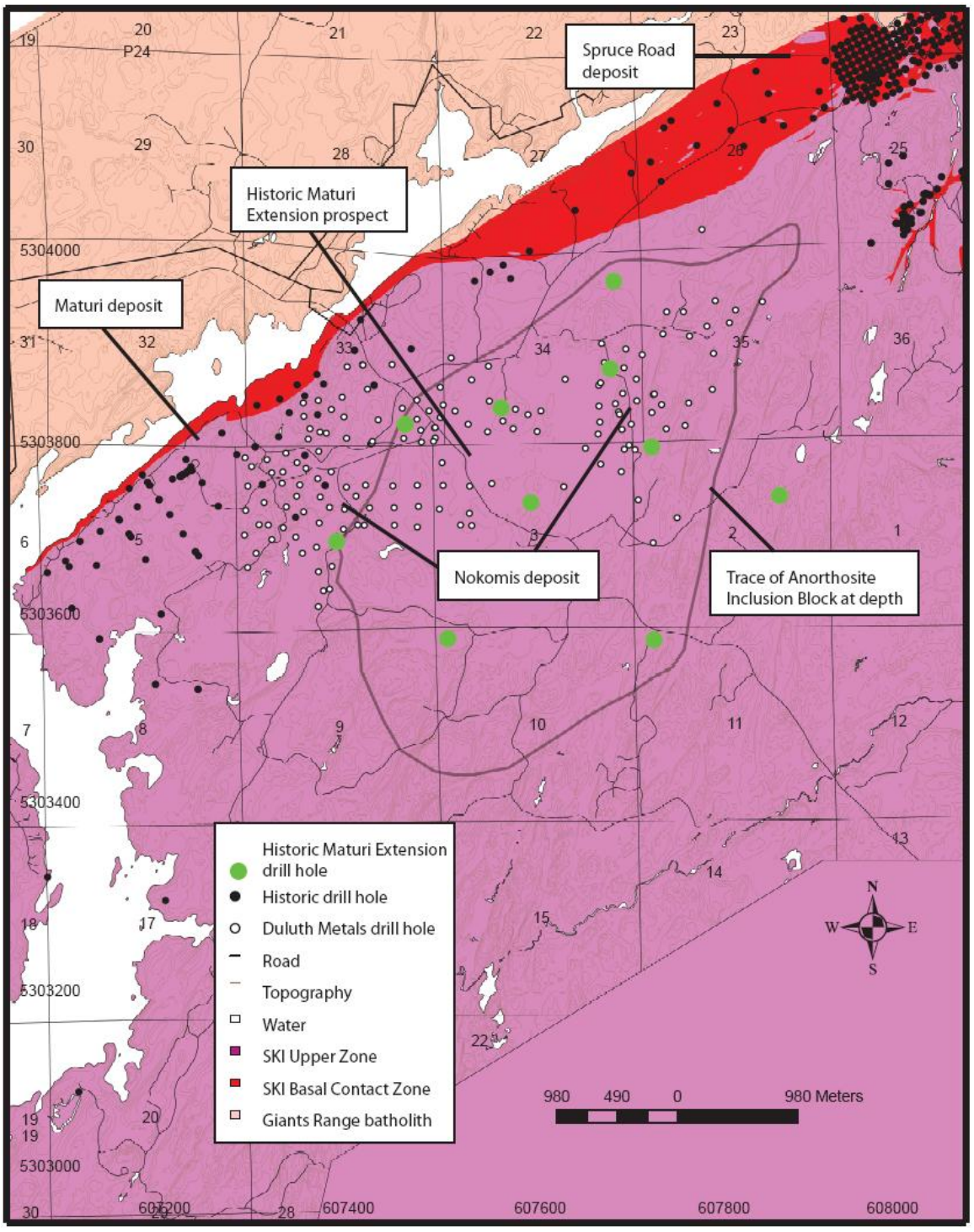


Figure 17: Locations of ten historic drill holes that initially defined the Maturi Extension prospect, which has come to be known as the Nokomis deposit from recent drilling completed by Duluth Metals. Locations of other historic drill holes in the area and Duluth Metals holes are shown for reference, geology modified from Peterson, 2008.

Some specific questions that this study will attempt to answer include:

- Is the SKI an open magmatic system as suggested by Severson (1994)?
- If so, how many magma pulses, and of what composition, were involved?
- Were successive magmas emplaced from bottom to top, or did later magmatic pulses intrude into earlier pulses?
- What role, if any, did differentiation play during crystallization during evolution of SKI magmas?
- How is the sulfide-bearing basal contact zone related to the largely sulfide-barren upper parts of the intrusion?
- What role did the previously emplaced anorthositic series magmas play in the development of the SKI magma chamber and in the concentration of high grade sulfide ore?
- Were magma flow dynamics a major factor in controlling the metal grade of sulfide ore as suggested by Peterson (2001)?

In addition to a study of drill core across the Nokomis deposit, I conducted detailed bedrock mapping of the Maturi deposit area. The Maturi is interpreted to be the updip surface expression of the Nokomis deposit (Severson, 1994). The goals of this field study are to 1) determine the extent to which the igneous stratigraphy established in drill core at depth can be recognized by surface mapping, 2) document sulfide-bearing outcrops of the Maturi deposit, and 3) improve the overall understanding of the field geology of the SKI beyond what was first documented by Green et al. (1966).

# CHAPTER FOUR: METHODS OF INVESTIGATION

## 4.1 Rock Classification Nomenclature and Textural Terminology

In order to integrate the results of this study with previous studies and ongoing mineral exploration activity by Duluth Metals, it is critical that a common nomenclature is established. Most geologists working in the SKI over the past 35 years have adopted a modal classification similar to that shown in Figure 18. This scheme, which was proposed by Severson and Hauck (1990), is based on modal percentages of plagioclase, olivine and pyroxene. It is modified from a 4-phase system (Ol-Pl-Cpx-Opx) originally proposed by Phinney (1972). Note that the Severson and Hauck (1990) scheme assumes most pyroxene is clinopyroxene (augite), which is the case for most Duluth Complex rocks. For orthopyroxene-rich rocks, Phinney's (1972) terminology is used. This classification scheme is readily adopted because it provides simple, common names to mafic rocks for use in mapping and logging drill core. Miller et al. (2002) criticized this scheme because it does not account for the natural "cotectic proportions of mineral phases expected to crystallize from basaltic magmas at low pressures", especially concerning plagioclase abundance. Miller et al. (2002) proposed a different modal classification scheme. However, because Severson and Hauck's (1990) modal classification scheme was used not only in Severson's (1994) extensive study of the SKI, but has also been adopted by Duluth Metals geologists, this study adopts it as well. This scheme does not consider the expected crystallization sequence that results from the olivine tholeiitic magmas that are assumed to have created most layered series intrusions,

accounting for the subtle variations in modal proportions of olivine and clinopyroxene in the troctolitic rocks common to layered series intrusions.

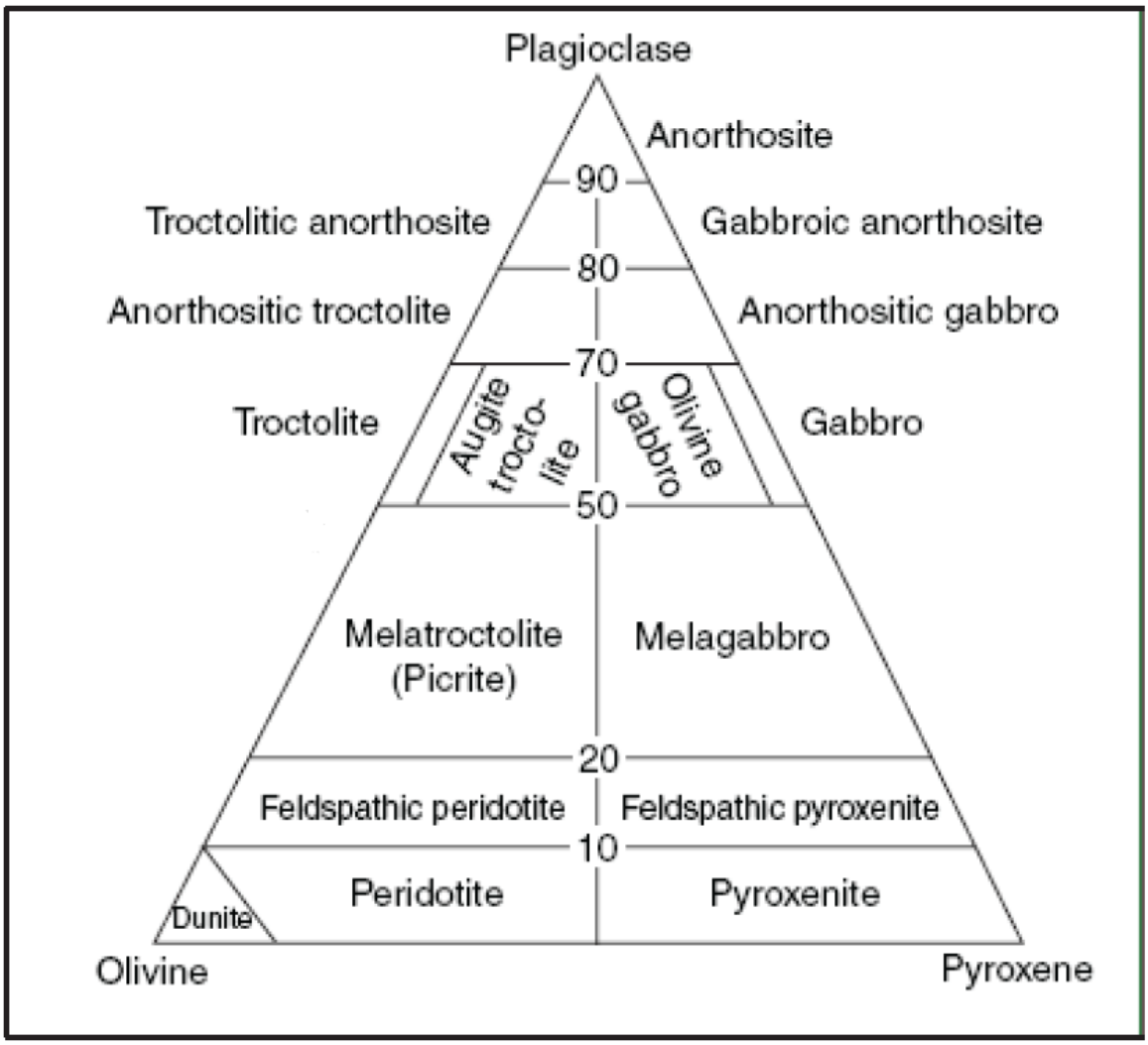


Figure. 18: Modal rock classification scheme for gabbroic rocks used in this study (from Severson and Hauck, 1990).

Textural terminology used in this study follows definitions given in Bates and Jackson (1987). Miller et al. (2002a) suggested that modal rock names be modified by terms that highlight the textural relationships between clinopyroxene and plagioclase (e.g., ophitic, subophitic, intergranular) because this relationship qualitatively reflects the degree of

differentiation of the olivine tholeiitic magmas thought to be parental to most layered series intrusions of the Duluth Complex. Where clinopyroxene is interstitial (ophitic to subophitic), it is interpreted to be intercumulus and thus not saturated in the parent magma (e.g. pt A, Figure 19). Where it occurs as anhedral granular crystals, it is interpreted to be saturated in the magma (e.g., pt. B, Figure 19). In most Duluth Complex Layered Series rocks, olivine is subhedral to anhedral granular in habit and thus is interpreted to be a cumulus/primocryst phase. The same is true of plagioclase, which typically occurs as a subhedral lath-shaped crystal. In rare cases, layered series rocks may contain subpoikilitic to poikilitic olivine and, less commonly, plagioclase.

Absolute grain sizes stated in this study are based on the primary phase of mineralogy with size ranges defined as: *fine-grained* (<1 mm), *medium-grained* (1-5 mm), *coarse-grained* (5-12 mm), and *pegmatitic* (>12 mm). Relative grain size descriptors include: *equigranular* (similar grain sizes for all primocryst phases), *seriate* (gradational range of grain sizes), and *porphyritic* (bimodal range in grain sizes for one or more primary phases).

This study uses the term *foliation* when describing a planar alignment of elongate or platy minerals, most commonly plagioclase. Modifiers follow the convention of Miller et al. (2002a): *non-foliated* (platy minerals show random alignment), *poorly foliated* (25-50% of crystals are aligned within 10° of a common plane), *moderate* (50-75% are coplanar), *well foliated* (75-90% are coplanar), and *very well foliated* (>90% are coplanar).

Additionally, several terms used to describe packages of rocks include: *homogeneous* (largely uniform in grain size, rock type, and texture), *vari-textured* (non-uniform in grain size and habit), and *taxitic* (non-uniform in modal mineralogy and texture, especially grain size).

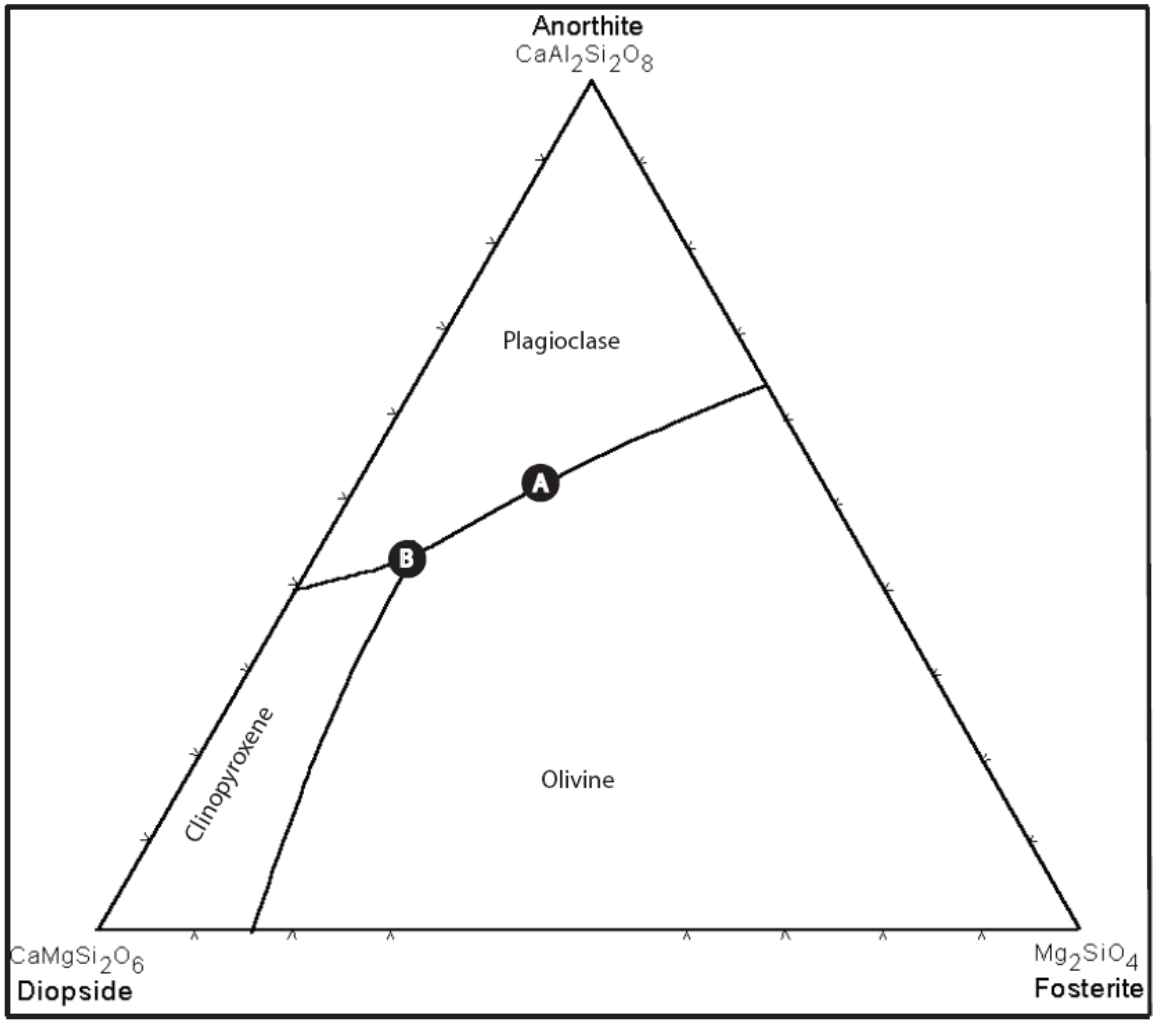


Figure 19: Phase diagram of the plagioclase, diopside, fosterite system. A magma crystallizing from point A will contain cumulus plagioclase and olivine, and if present intercumulus pyroxene. At point B all three phases will be cumulus.

**4.2 Bedrock Mapping**

Detailed bedrock mapping at a scale of 1:5,000 was conducted to document the igneous stratigraphy of the SKI in an area corresponding to surface projections of the Nokomis deposit and to provide more detail than shown on the 1:31,680 scale map of the Gabbro Lake 15' quadrangle (Green et al., 1966). Mapping focused in an area extending southwest of MN Highway 1 to Birch Lake, including parts of sections 4, 5, 6, 7, 8, 9, 32, and 33 in townships T61N, R12W, and T62N, R11W (Fig. 20). The base map for the geologic mapping was taken from Peterson (2006). This map area was selected because it includes the sulfide-bearing rocks of the Maturi prospect exposed along the eastern shoreline of the South Kawishiwi River, as well as the sulfide-barren rocks of the upper SKI. The Nokomis deposit is located down-dip and due east of the exposed basal contact zone. The map area partially includes both the Maturi prospect and the Nokomis deposit.

Bedrock mapping was conducted periodically through the summer and fall of 2007. Over 500 outcrops were documented, taking note of lithology, mineralogy, texture, grain size, foliation, homogeneity, outcrop appearance, and general field conditions. Generally outcrops were clean and fresh with a variety of flat-lying pavement surfaces, cliff faces, and whaleback morphologies. Many outcrops were covered with lichen and moss, however stripping of moss was typically easily done and resulted in the exposure of relatively clean, fresh surfaces beneath. The field area was easily accessible by truck along Kawishiwi River Road off of MN Hwy 1 with many new drill roads in place from recent and on-going exploratory drilling. The terrain was a mix of densely wooded areas, clear cuts, and swampy, boggy areas. Typically, multiple traverses were

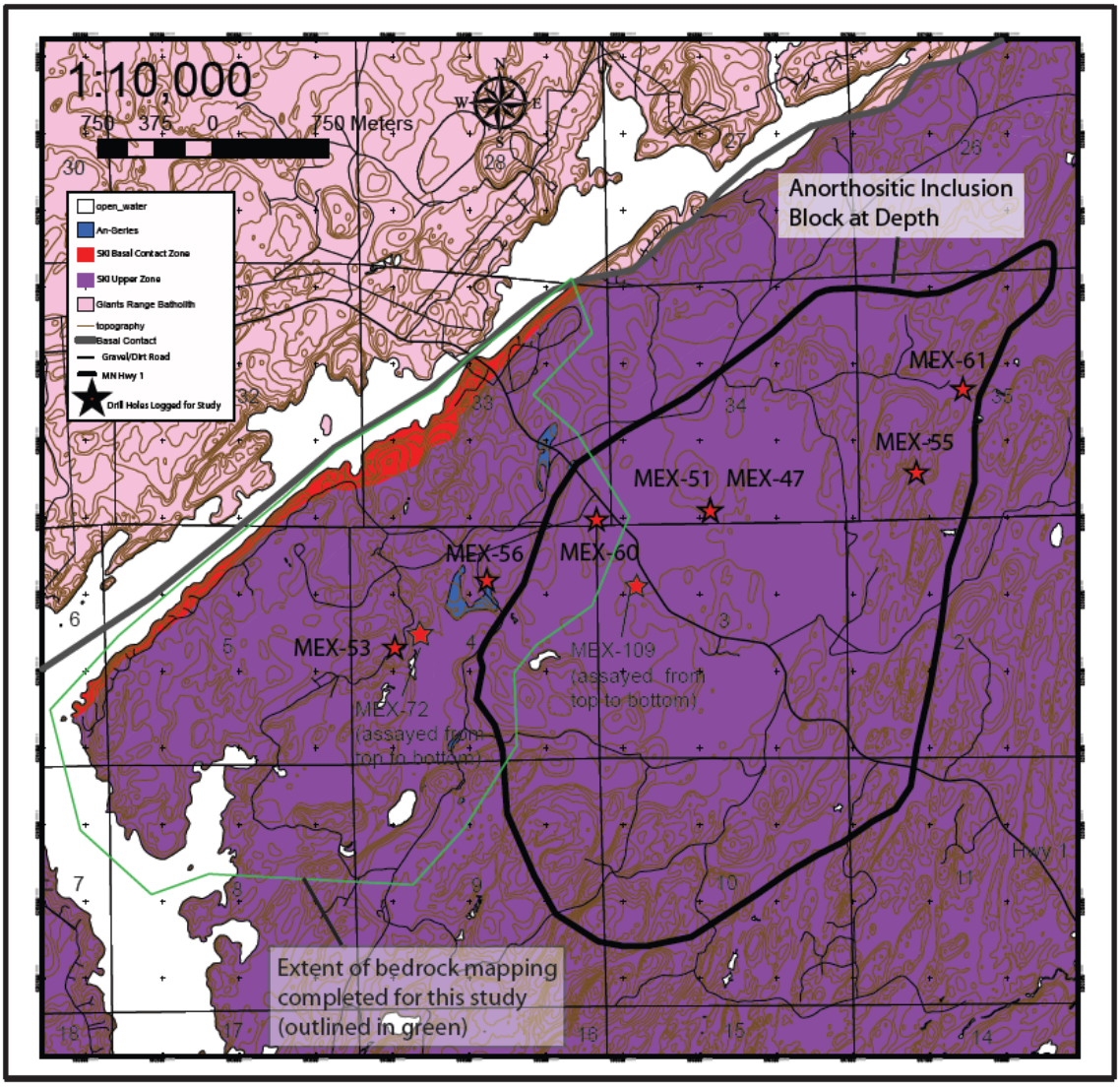


Figure 20: Generalized geologic map of the study area showing drill holes logged for this study (bold red stars), drill holes assayed from top to bottom (red stars), and areal extent of bedrock mapping conducted for this study (blue outline). The approximate outline of the anorthositic inclusion block at depth is outlined by a heavy black line.

conducted daily due to the network of roads in place. Traverses usually followed ridges or swamp boundaries where bedrock was likely to be exposed. Several days were devoted to mapping the shoreline of the South Kawishiwi River by canoe. This was especially useful in the southwestern portion of the map, where access by land was quite difficult. Field notes from bedrock mapping are located in Appendix I and the resultant

geologic map is presented as Plate I. The highlights and main conclusions from the mapping will be discussed in the next chapter.

### 4.3 Drill Core Logging and Sampling

Drill core for this study was selected in order to create a cross-section through the Nokomis deposit that traversed the anorthositic series inclusion block (Fig. 20) and roughly followed Peterson's (2001) east-west channelized flow patterns. Duluth Metals current in-fill and exploratory drilling program has resulted in an abundance of new drill holes scattered throughout the study area (Fig. 17). Seven holes totaling 24,115 feet and spread out over a profile length of roughly 3.5 kilometers were selected for detailed study (Fig. 20). From southwest to northeast, drill holes logged for this study include: MEX-53, MEX-56, MEX-60, MEX-47, MEX-51, MEX-55, and MEX-61. Logging was conducted at Duluth Metals facilities in Ely, Minnesota during the summer of 2007. Observations recorded in the logs included: silicate and sulfide mineralogy, modal mineral abundance, texture, grain size, alteration intensity and type, and internal structures (foliation and layering).

Detailed logging served to establish the lithostratigraphy through the study area, which could then be compared to Severson's, (1994) stratigraphy. Also, logging identified specific points of interest for sampling, which was conducted concurrently with logging. Samples were selected for the purpose of obtaining representative examples of the main rock types, textures, and primary mineralogy for each lithostratigraphic unit. Samples were also chosen at distinct unit contacts. In total, 256 samples were selected

from the seven drill cores. Results from core logging including complete drill core logs can be found in Appendix II. A fence diagram compiled from drill core logs can be found on Plate II. The unit lithostratigraphy interpreted from both drill core logging and follow-up petrography is discussed in the next chapter.

### 4.4 Petrography

All 256 samples collected from the seven drill cores and the 36 samples collected during field mapping had thin sections prepared for petrographic study. Of these, 190 samples were made into polished thin sections for later microprobe analysis. Thin sections were studied, described, and photographed to document features including primary and secondary mineralogy, modal mineral proportions, grain size, mineral habit, textural relationships, planar alignment, and alteration. Petrographic observations were very useful in verifying mineralogy, textures, and alteration assemblages not always obvious in hand sample. These observational data were also useful in documenting subtle differences in lithologic characteristics between samples. Reflected light petrography of oxide and sulfide phases was not conducted. Appendix III contains petrographic descriptions of all 292 thin sections presented in spreadsheet format. These petrographic data provide important information about the style and timing of crystallization and mineralization, as will be discussed in the next chapter.

## 4.5 Mineral Chemistry

Electron microprobe analyses using wavelength-dispersive spectrometry (WDS) were conducted at the Electron Microprobe Laboratory in the Department of Geology and Geophysics, University of Minnesota-Twin Cities on a JEOL 8900 Electron Probe Microanalyzer. All analyses used 10 second peak count times and 5 second background count times. Operating conditions included an accelerating voltage of 15 Kv, a beam current of 20 nA, and a beam diameter of approximately 5 microns. Over 4,000 separate analyses were acquired from 150 polished thin section samples. Microprobe point analyses focused on the major and minor element chemistries of the main solid solution silicate phases: olivine, pyroxene, and plagioclase. Typically, 10-15 analyses were obtained for each mineral phase in each sample. Three standardization tables were set up to analyze for olivine, pyroxene-hornblende-biotite, and plagioclase. Olive was analyzed for Mg, Ca, Al, Si, Ni, Fe, and Mn; pyroxene-hornblende-biotite was analyzed for Na, Ca, Al, Cr, Fe, Mg, K, Si, Ti, and Mn; plagioclase was analyzed for Na, Ca, Al, Fe, Mg, K, and Si.

Ample exploration assay data and whole-rock geochemical analyses from selected previous studies exist in this area of the SKI. However, datasets containing mineral chemistry are minimal to non-existent. Interpretations of magma composition and differentiation rely heavily on solid-solution mineral compositions. The new dataset supplies a comprehensive view of the silicate mineral chemostratigraphy across the Nokomis deposit area. These data will be used to profile lateral and vertical changes in mineral chemistries through the deposit area. Vertical profiles will be used to document

differences between units, while lateral profiles will document differences within units. Appendix IV contains the results of microprobe analyses.

**4.6 Geochemistry**

Duluth Metals provided access to a large volume of recently acquired assay data (over 15,000 analyses) from the Nokomis deposit for this study. In some cases, only data from the seven holes selected for this study have been used to evaluate geochemical variations along the main profile, while in other cases, the entire data set was used to give a deposit-wide view of its geochemical attributes. These data typically encompass only the mineralized portions of the SKI in the basal contact units with continuous sampling done every five feet. However, several drill holes (MEX-51, MEX-72, MEX-109, Fig. 20) were assayed from top to bottom with continuous sampling every 10 feet, except in the mineralized portions where sampling was every five feet. MEX-72 and MEX-109 were drilled and assayed after the core for this study was selected, but the geochemistry of these holes was incorporated into this study because they offer more complete chemical profiles through the intrusion. Logs for these add-on holes completed by Duluth Metals geologists are used in this study. Analyses contain most major elements (except Si) and trace metals and include: Ag, As, Au, Ba, Be, Bi, Ca, Cd, Co, Cr, Cu, Fe, Ga, K, La, Mg, Mn, Mo, Na, Ni, P, Pb, Pd, Pt, Rh, S, Sb, Sc, Sn, Sr, Te, Th, Ti, Tl, U, V, W, and Zn. However, many of these trace elements, including: As, Be, Bi, Cd, Ga, La, Mo, Sb, and W have concentrations generally too low for detection limits on these exploration grade geochemical assays.

Analyses of Duluth Metals core were conducted at ALS Chemex facilities in Thunderbay, Ontario, using sample codes PREP 31 (crushing), PGM ICP23 (Pt, Pd, and Au by fire assay and ICP-AES finish), and ME ICP61 (four acid leach with near total digestion). Although these are not complete whole rock analyses (e.g., Si was not analyzed), they are valuable to this study for several reasons: 1) they give continuous records of the lithogeochemical stratigraphy vertically through the deposit area, 2) the major element chemistries provided proxies for the continuous mineralogical variations across the deposit area, and 3) the whole rock data can be compared to microprobe mineral analyses (e.g., Ni in olivine/Ni in whole rock). The drill holes assayed from top to bottom (MEX-51, MEX-72, MEX-109) allow for an even more complete geochemical profile (e.g., Mg#) of the rock column at these locations. These holes are especially useful given their locations: MEX-51 profiles the northern part of the anorthosite block, MEX-72 profiles the troctolite section west of the anorthosite block, and MEX-109 penetrates the middle of the anorthosite block (Fig. 20). Data obtained from geochemical assays are confidential and can only be presented in graphical form.

# CHAPTER FIVE: DISCUSSION

In this chapter, I discuss and interpret the results of this study and their implications for petrogenesis and metallogenesis of the SKI in the Nokomis deposit area. The main points to be discussed and interpreted are: (1) the surface bedrock geology of the field study area; (2) the development of a workable lithostratigraphy for the Nokomis deposit area of the SKI implied by my mapping, core logging, and petrographic studies and Severson's (1994) previous work; (3) estimates of the parental magma composition(s) that produced the SKI based on mineral and whole-rock geochemical data; (4) the history of magmatic emplacement and crystallization of those magmas implied by stratigraphic and lateral variations in lithologic and geochemical attributes; and (5) evaluation of Peterson's (2001) lateral flow model of mineralization in light of lithologic and geochemical data. The discussion culminates with presentation of a proposed petrogenetic and metallogenic model for the South Kawishiwi Intrusion (Plate III).

Based on surface and subsurface geology, petrography, and whole-rock and mineral chemical data, the study area can be subdivided into three major zones: the basal contact zone, upper zone, and anorthositic inclusion block. Figure 21 shows the surface exposure of the basal contact and upper zones in the area mapped for this study (colored areas). It also shows the location of the inclusion block, based on drill cores logs and sparse outcrop. Line A-A' shows the surface trace of a cross section plane on to which most lithostratigraphic and chemostratigraphic data from the studied drill cores (red stars) will be projected.

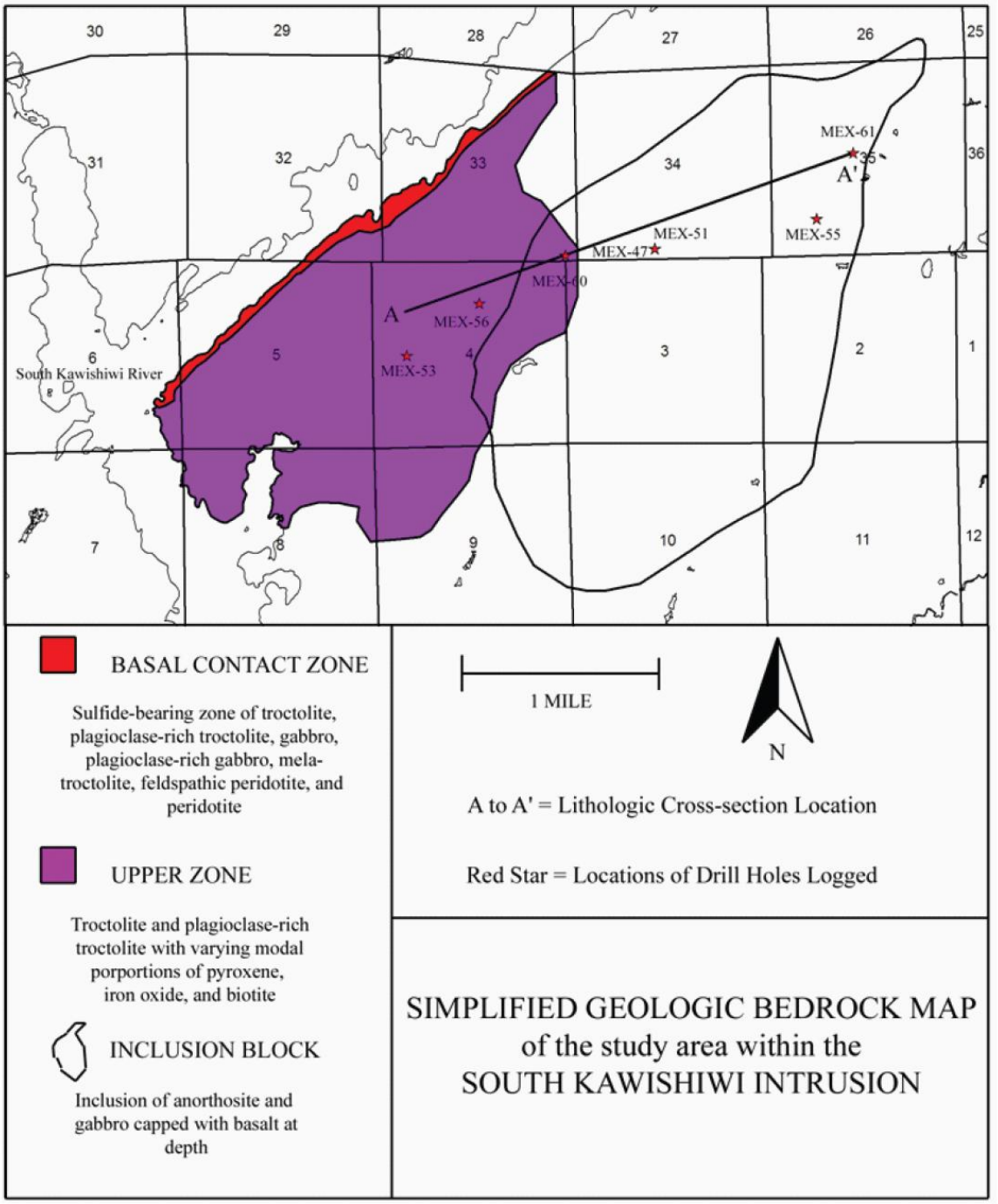


Figure 21: Simplified geologic bedrock map of the study area displaying the map area of the basal contact zone and upper zone, locations of drill holes logged for this study, and outline of the anorthosite inclusion block at depth.

## 5.1 Bedrock Geology of the South Kawishiwi Intrusion in the Maturi and Nokomis Deposit Areas

Previous bedrock mapping in the study area (Fig. 20) by Green et al. (1966) and Phinney (1967) generally subdivided the SKI into a lower thin, lithologically and texturally heterogeneous package of sulfide-bearing rocks overlain by a thick, homogeneous, sulfide-barren package of troctolitic rocks with scattered occurrences of anorthositic series inclusions and rare mafic hornfels. The upper troctolitic units consist mostly of troctolite to anorthositic troctolite with variable amounts of pyroxene, biotite, and iron oxide interstitial to olivine and plagioclase. New bedrock mapping for this study generally confirms this general dichotomy, but, at the larger (1:5,000) scale of mapping, I was able to subdivide these units further and correlate them with units identified by Severson (1994) in drill core. Moreover, the new mapping shows outcrop occurrences in detail, not depicted on earlier maps. The full results and interpretations from field mapping are presented in the geologic map on PLATE I. A summary of the geology is presented in Fig. 22 and discussed below.

### 5.1.1 Footwall Rocks

The Giants Range batholith forms the footwall everywhere in the field area, with the trace of the intrusive contact concealed beneath the South Kawishiwi River (Fig. 22). Better constraint of the position of this contact was attempted by thoroughly investigating both shorelines of the river, and by visiting islands in the river. However, it was found that the GRB comprises the entire western shoreline and all of the islands in the vicinity,

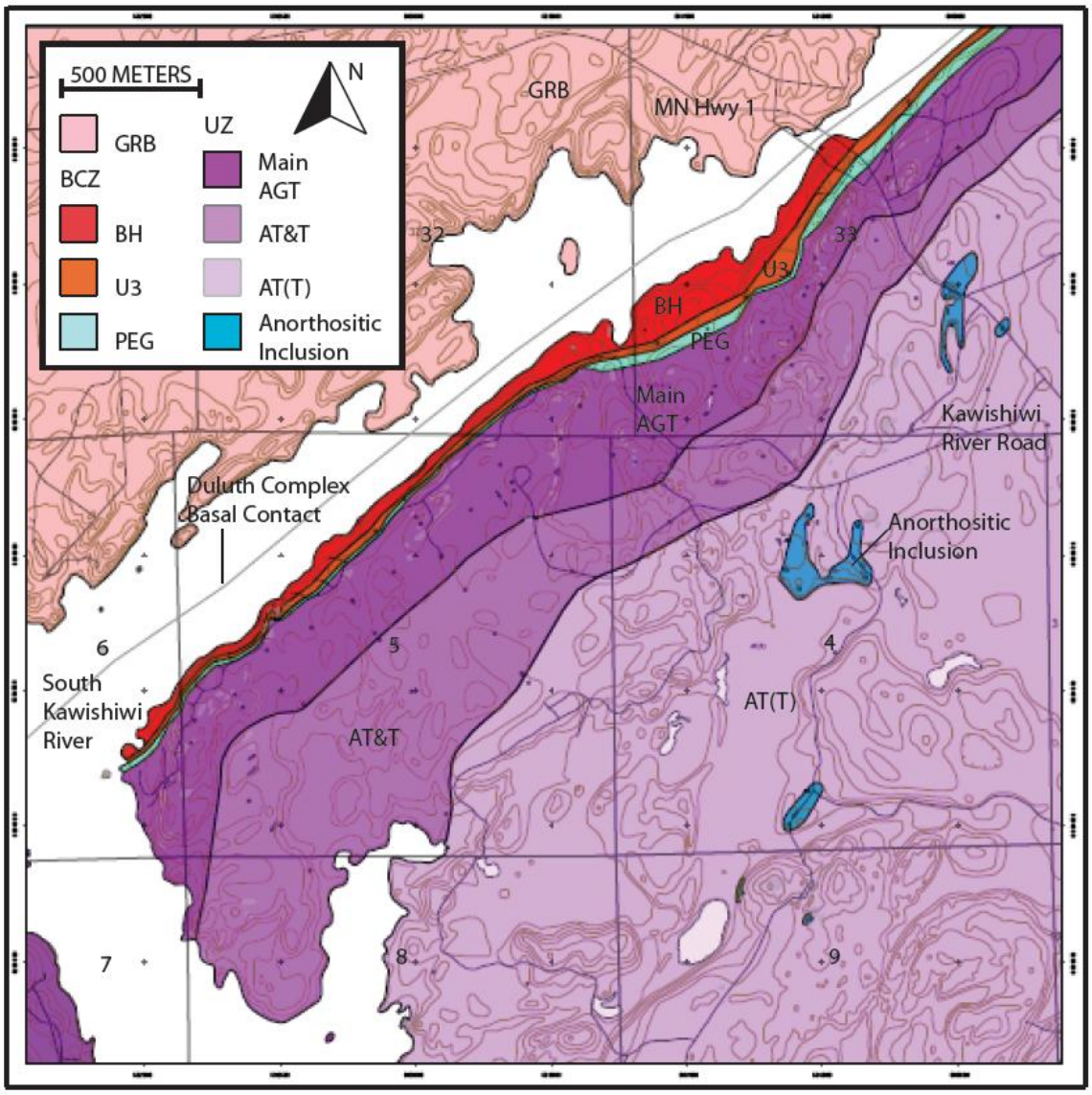


Figure 22: Geologic map of the field study area simplified from the 1:5,000 scale map presented in Plate I. Unit abbreviations defined in the text. Topographic base map from Peterson, 2006.

whereas rocks of the SKI compose the entire eastern shoreline. These observations confirm the conclusion of Green et al. (1966) that the basal contact resides beneath the river. Nearly the entire eastern river bank is composed of sulfide-bearing outcrops. For the most part these outcrops are barely exposed above the waterline and are quite

weathered and gossan-stained, making accurate lithologic descriptions difficult. Several samples were collected for petrographic study and are discussed with the lithostratigraphy in section 5.2.

### 5.1.2 Basal Contact Zone

Mapping for this study confirms that the SKI can generally be subdivided into a sulfide-bearing basal contact zone and a sulfide-barren upper zone (units skcz and skat/skt, respectively, of Green et al., 1966). Moreover, as identified by Green et al. (1966), the contact lies between individual outcrops of the sulfide-bearing basal zone and the sulfide-barren upper zone within a few meters of each other, although a directly observable contact was not found.

The mineralized basal contact zone can be subdivided into three mappable lithostratigraphic units that Severson (1994) identified in the subsurface (Fig. 22, Plate I):

1) BH (basal heterogeneous) unit - a lower interval of heterogeneous lithologies and textures,
2) U3 (ultramafic three) unit – a medial ultramafic interval of consistently medium- to fine-grained melatroctolitic to peridotitic rocks, and
3) PEG (pegmatite) unit - a coarse-grained package of augite troctolitic to olivine gabbroic rocks that commonly contain coarse-grained to pegmatitic pyroxene clots (high density, subophitic oikocrysts).

All but the PEG unit rocks are gossan-stained in outcrop. In fact, the PEG unit is notably unaltered when it is exposed.

The BH unit consists of a broad range of modal rock types dominated by troctolite, melatroctolite, augite troctolite, and anorthositic troctolite, with lesser amounts of gabbro, olivine gabbro, and anorthositic gabbro. Grain sizes range from fine-grained to pegmatitic, with olivine and plagioclase typically intergranular, and pyroxene commonly ophitic to subophitic. Contacts between differing lithologies, grain sizes, and textures are commonly sharp, but are also locally gradational on a variable scale of centimeters to meters. Conformable layering or foliation is not easily observed; however, chaotic or irregular foliation was locally observed and is interpreted as undulating flow foliation. The variable orientation of foliation, commonly on an outcrop scale, was noted but typically not measured. Gossan-staining from oxidation makes visual estimation of sulfide content difficult; however, breaking large sample blocks apart commonly reveals up to 3 modal percent sulfide with fine to coarse grain sizes and interstitial textures.

Severson (1994) found bifurcating lenses and stratiform intervals of olivine-rich rocks throughout the BH unit in drill core, but in the area of this study he distinguished the U3 unit as the highest interval that occurs among the heterogeneous rocks of the BH unit and beneath the consistently coarse-grained rocks he distinguished as the PEG unit. A significant thickness of melatroctolitic rocks interpreted to be the U3 was found in direct contact with the heterogeneous rocks in the field area. In the field, the U3 unit dominantly consists of fine- to medium-grained troctolite, melatroctolite, feldspathic peridotite, and peridotite. These rocks typically contain minor amounts of interstitial plagioclase and pyroxene. Outcrops are gossan-stained from strong oxidation of sulfides. This, coupled with fine grain sizes, gives the ultramafic rocks of the U3 unit a massive,

structureless appearance and makes accurate measurements of igneous foliation and layering difficult, and thus none were recorded. Sulfides in the U3 unit are fine-grained and disseminated. As in the BH unit, pervasive weathering makes modal estimations difficult, while the fine-grained nature of sulfides in the U3 makes identification difficult.

The PEG unit was rarely found in outcrop. It was identified based on comparisons to known PEG unit rocks found in drill core, and guided by surface projection from drill core. Rare field identification of this unit may be due to striking similarities to the Main AGT unit.

In the few outcrops where the PEG unit is exposed, it is dominantly composed of coarse-grained, subophitic augite troctolite. The augite in the rock commonly forms coarse to pegmatitic, anhedral to subophitic clots, which is the most distinctive field characteristic of the unit. The PEG is structurally massive and weather resistant. An absence of sulfide and gossan-staining makes the PEG unit easily distinguishable from coarser varieties of the BH unit. Although the contact between the PEG and U3 units was never directly observed, the close proximity of gossan-stained (U3 unit) and non-gossan-stained (PEG unit) outcrops makes it an easily inferred contact based on the absence of sulfides, and thus the absence of gossan-staining in the PEG unit.

### 5.1.3 Upper Zone

The field contact between the PEG unit and the base of the upper zone is mostly marked by a gradational change in texture and the disappearance of clotty augite. Overall, the upper zone rocks become medium-grained to locally coarse-grained and augite becomes ophitic containing oikocrysts up to 3 centimeters in diameter. In Severson's (1994) compilation of the SKI drill core, he identified three main units as comprising the upper zone in the Maturi deposit and Deep Maturi area: the Main AGT (main augite troctolite) unit, the AT&T (anorthositic troctolite & troctolite) unit, and the AT(T) (anorthositic troctolite (locally troctolite)) unit (Figs. 8 & 9). While the augite-rich and coarser Main AGT unit can be discriminated from the medium-grained anorthositic troctolites of the AT&T and AT(T) units in field exposures, the upper troctolitic units are indistinguishable in the field. The thin melatroctolitic units that are commonly observed in drill core to divide the upper anorthositic troctolite units have not been observed in outcrop. The contact between these AT&T and AT(T) units (Plate 1, Fig. 22) is inferred largely from drill hole projections.

In the field, the Main AGT unit is remarkable in its homogeneity. It consistently occurs as a medium-grained, subophitic to ophitic augite troctolite with 5-15% augite oikocrysts. It is massive and outcrops well. The Main AGT does contain local plagioclase-rich lens-like bodies, usually on a scale of meters with gradational contacts less than 10 centimeters wide, showing variability in plagioclase and olivine content. Modally, these bodies are usually anorthositic gabbro to gabbroic anorthosite, but it is not clear if these are anorthositic series inclusions. Anorthositic series inclusions elsewhere

in the upper zone typically display sharp contacts with the enclosing troctolitic rocks and commonly display internal plagioclase foliation. These lens-like bodies typically display neither sharp contacts nor internal plagioclase foliation. In the field, the contact between the Main AGT unit and the overlying troctolitic unit above is gradational. This contact was observed directly in at least one outcrop area where augite changed from ophitic to subophitic and decreased in mode from 5-10% to < 5% over a distance of several meters.

The anorthositic troctolite and troctolitic units of the upper zone are also distinctive in their textural and mineralogic homogeneity, but unlike the Main AGT unit, they are consistently low in augite and iron oxide abundance and tend to be coarser grained. Typically, the AT&T, and AT(T) units are modally dominated by medium- to coarse-grained olivine, and subhedral granular plagioclase and may contain up to 5% subophitic to ophitic oikocrysts of augite and up to 2% subpoikilitic iron-titanium oxide. Troctolitic rocks of the AT&T and AT(T) units can be poorly to moderately foliated, but rarely display modal layering. Minor fluctuations in modal mineralogy on a meter-scale create broadly diffuse layering between anorthositic troctolite and troctolitic rocks. The thin ultramafic horizons (HP#1 and HP#2) commonly found in drill core between the Main AGT, AT&T, and AT(T) units evidently are very poor outcrop formers as they were not found in the field.

### 5.1.4 Inclusions in the SKI

Although the above observations are in general agreement with previous mapping, this study documented a heretofore undescribed relationship with regard to the

abundance and type of inclusions of anorthositic series rocks and basaltic hornfels occurring in the upper zone units. While both inclusion types are found throughout the SKI, mafic hornfels inclusions predominate just above the basal contact zone in the Main AGT. They are usually rather large, encompassing tens of meters, and display relict pipe amygdules filled with iron-oxide-rich, medium-grained gabbroic material, and healed fractures filled with massive quartz.

Anorthositic series inclusions, which range in size from several meters to hundreds of meters and can be found throughout the map area, are particularly abundant in the AT(T) unit. Although small, isolated anorthositic series inclusions locally occur in and just above the basal contact zone, several large groups of inclusions occur in the AT(T) unit. One notable difference between the two upper zone troctolitic units (AT&T and AT(T)) is that the AT(T) unit commonly contains anorthositic series inclusions up to 300 meters long. The AT&T unit and the Main AGT unit also contain anorthositic series inclusions, but typically not to the extent seen in the AT(T) unit. Lithologies include anorthosite, troctolitic anorthosite, and gabbroic anorthosite that commonly display coarse-grained ophitic textures with well-developed plagioclase foliation and contains olivine that ranges in habit from poikilitic to granular.

More complete descriptions of inclusions within the SKI, as well as interpretations of their origin will be discussed in the following subsection (5.2).

## 5.2 Lithostratigraphy of the South Kawishiwi Intrusion in the Nokomis Deposit Area

The drill core logging and bedrock mapping conducted for this study provide an up-to-date, detailed igneous stratigraphy for the Nokomis deposit area of the SKI. Severson's (1994) igneous stratigraphy defined the entire intrusion, but only ten holes existed in the study area at that time (Fig. 17). With more than 150 holes drilled by Duluth Metals, a more complete picture of the intrusive stratigraphy can now be developed. Rather than develop the igneous stratigraphy of the SKI in the Nokomis area from scratch, this study adopts Severson's (1994) general unit nomenclature for the SKI (Figs. 8 & 9) for two reasons. First, observations from logging and field mapping indicate that Severson's (1994) basic classification scheme is a valid and useful stratigraphic subdivision of the SKI. Second, since Severson's (1994) seminal work, all published reports (e.g. Lee and Ripley, 1996; Hauck et al., 1997) and exploration work conducted by Duluth Metals have adopted Severson's (1994) unit nomenclature for the SKI (Figs. 8 & 9), allowing for correlation of the geology of the Nokomis deposit area with other parts of the SKI. In this section, I report the detailed lithologic characteristics and internal variations of these stratigraphic units in the Nokomis deposit area, describe the nature of the boundaries between the units, and point out where the unit stratigraphy is ambiguous or in need of revision.

Figure 23 is an idealized geologic cross section through the study area constructed from seven logged drill cores (Fig. 21) that shows the major zones and lithostratigraphic units of the Nokomis deposit area. This cross section subdivides the subsurface geology

into the three main zones noted previously: the anorthositic inclusion block, upper zone, and basal contact zone. These zones are further subdivided into the lithostratigraphic units noted by Severson (1994) and described below. The anorthositic inclusion block is largely subdivided into the Anorthositic-Group (AN-G) and the Upper GABBRO units, with a thin cap of mafic volcanic hornfels. The basal contact zone is subdivided from bottom to top into the Bottom Augite Troctolite/Norite (BAN), the Basal Heterogeneous (BH), the Ultramafic Three unit (U3), and the Pegmatitic unit (PEG). The upper zone dominantly consists of the Main Augite Troctolite unit (Main AGT), Anorthositic Troctolite and Troctolite unit (AT&T), and the Anorthositic Troctolite (locally Troctolite) unit (AT(T)). It also contains thin intervals of olivine-rich rocks consisting of the lower Ultramafic One unit (U1) and Ultramafic Two unit (U2) at the base of, or within the Main AGT unit, and thin horizons of olivine-rich rocks at the base of the AT&T and AT(T) units consisting of the High Picrite # Two (HP#2) and High Picrite # One (HP#1), respectively. Also shown in Figure 23 is an area of heterogeneous rocks situated above the anorthositic inclusion block and referred to as the Gabbro-in-Troctolite unit (G-in-T). A second possible inclusion block of anorthositic rocks, not previously recognized by Severson (1994), occurs just inside the limits of this cross section and is called the Poikilitic Anorthosite unit (PAN). PLATE II displays a more complete and detailed fence diagram created from the same drill hole data for the Nokomis deposit. A correlation diagram presented in Figure 24 portrays the temporal relationships interpreted for these units. The following sections provide detailed descriptions from field data, drill core logs, and petrography for the units shown in Figure 23.

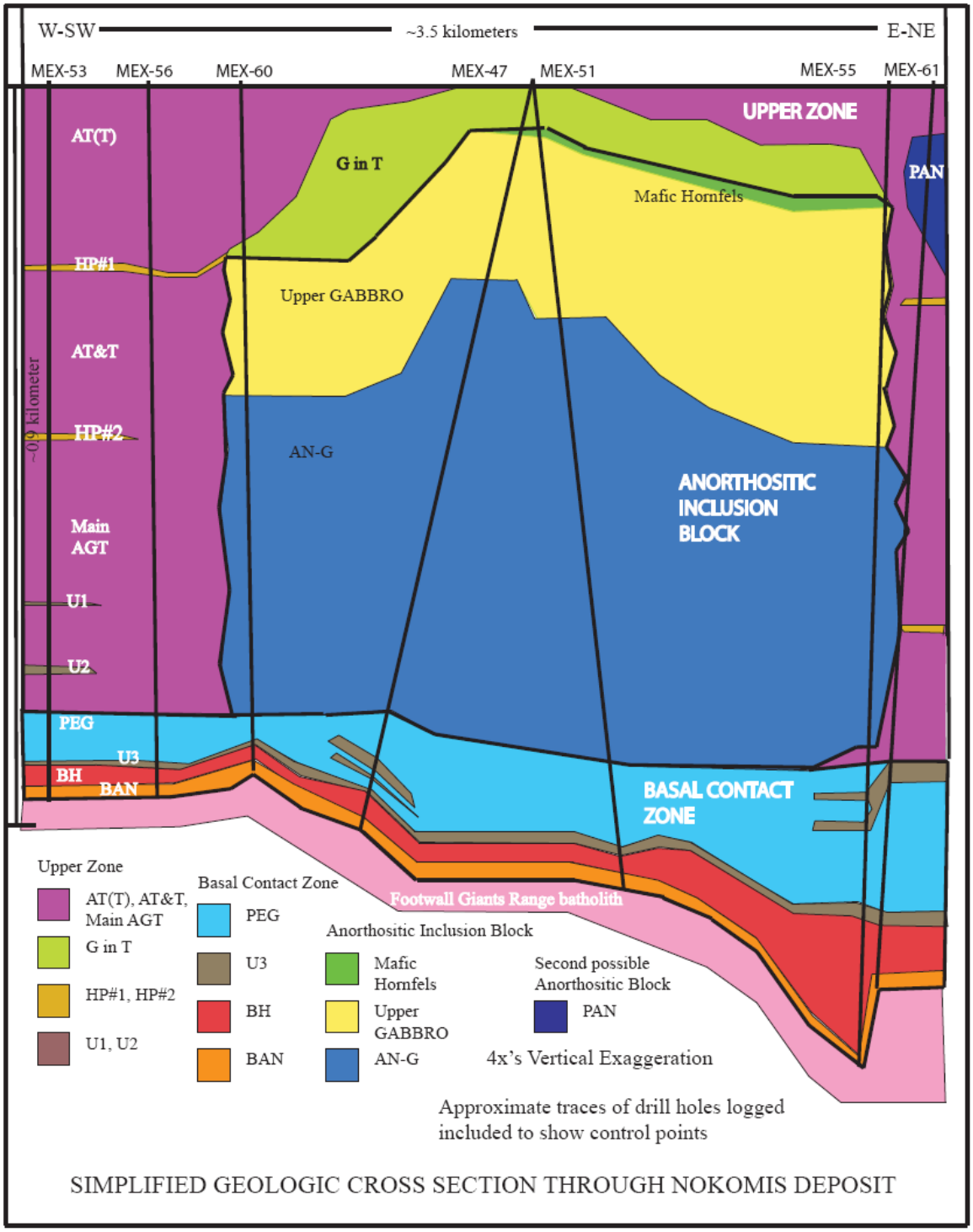


Figure 23: Geologic cross-section displaying the igneous stratigraphy of the study area. Drill hole locations and profile line shown in Figure 21. Vertical exaggeration equals 4X.

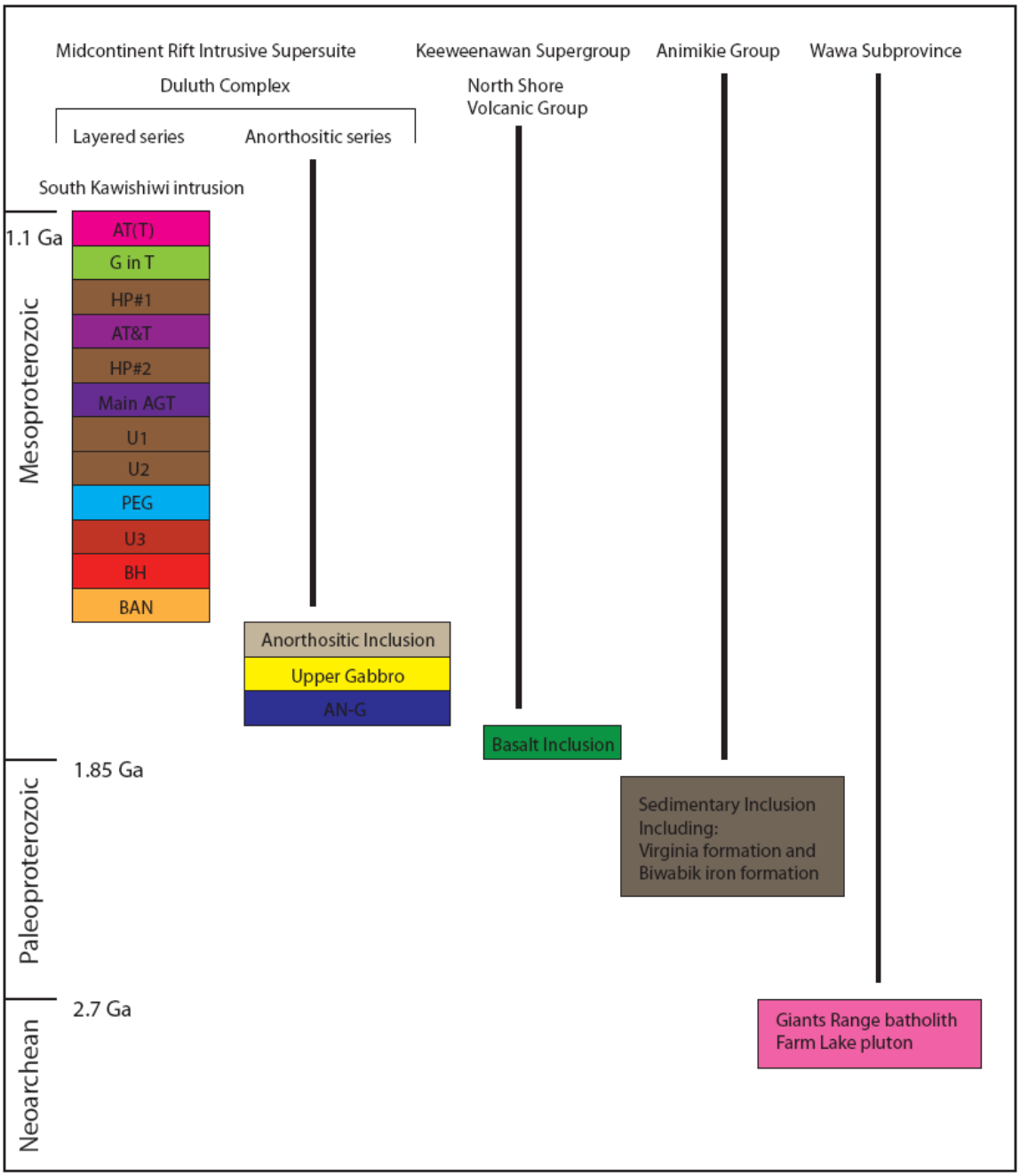


Figure 24: Correlation diagram summarizing the temporal relationships of the units interpreted from this study.

### 5.2.1 Footwall - Giants Range Batholith

Granitic rocks of the Giants Range batholith (GRB) exclusively form the footwall to the SKI in the Nokomis deposit area. Although the main rock type mapped in contact with the SKI in the Maturi area is a porphyritic, hornblende-rich quartz monzonite of the Farm Lake pluton (Boerboom and Zartman, 1993), lithologies directly at the GRB-SKI footwall contact in drill core are predominantly hornblende-biotite monzodiorite, with lesser diorite, quartz diorite, and quartz monzodiorite. The monzodiorite is typically coarse-grained with a well developed foliation and porphyritic texture defined by whitish alkali feldspar phenocrysts (<2 cm). The dioritic rocks are coarse-grained, intergranular, and absent of phenocrysts. Another minor lithology is fine- to coarse-grained hornblendite, which occurs as centimeter- to meter-scale irregular masses. Grading downward from the contact with the SKI, the quartz-poor and plagioclase-rich granitic rocks irregularly become enriched in quartz and alkali feldspar, with the latter becoming progressively pinkish in color. By 10-30 meters below the contact, monzonite and quartz monzonite predominate. These transitions in quartz concentration, plagioclase/alkali feldspar ratio and the bleaching of alkali feldspar in the contact zone are likely features related to thermal metamorphism of the granite by the SKI. Perhaps the local occurrence of fine-grained, massive syenitic veins (<1cm – 3m) can also be attributed to partial melting of the granite during emplacement of the Duluth Complex.

Another distinctive feature of the footwall granites that is likely related to the emplacement of the SKI is the occurrence of significant sulfide mineralization. Commonly, the upper 20-40 meters of the footwall contains 0.25-0.5% (locally up to

1.5%), fine- to medium-grained, disseminated sulfide composed of chalcopyrite >> pyrrhotite. In some drill core, sulfide mineralization has been noted up to 80 meters into the footwall. These occurrences of sulfide mineralization in the footwall are poorly understood and deserve further study.

### 5.2.2 Inclusions in the South Kawishiwi Intrusion

Igneous and metasedimentary rock inclusions are observed throughout the study area in outcrop and in drill core. The main inclusion types are metasedimentary hornfels, mafic hornfels, and anorthositic rocks. Most inclusions observed in outcrop range in size from 1 meter to 10's of meters, while anorthositic inclusions up to 300 meters in length have been noted and in many instances can be found in large groupings. In drill core, where only the minimum size of inclusions can be estimated, inclusions range from several centimeters to several meters across. The large inclusion block of anorthositic series and minor mafic volcanic hornfels (anorthositic inclusion block in Fig. 23) is discussed separately in the next section, but a possible second large inclusion block of anorthositic rocks called the PAN unit is discussed below.

*Metasedimentary Rock Inclusions*

Metasedimentary rock inclusions occur throughout the SKI in both outcrop and drill core. Both sharp, well-defined contacts, occasionally with a notable chilled margin, and irregular, gradational contacts have been observed. Some inclusions display relict bedding, while others are texturally massive. The mineralogy of metasedimentary inclusions is usually quite difficult to ascertain macroscopically as they are typically very

fine-grained. They are typically quartz rich and locally contain strongly magnetic iron-oxide-rich horizons or clots, massive cordierite, or massive and/or globular (<1 cm in diameter) graphite (Fig. 25). Locally, apophyses or dikes of, medium-grained gabbroic and troctolitic material, featuring plagioclase, olivine, clinopyroxene, and orthopyroxene penetrate, or intermix within, the matrix of metasedimentary inclusions, which indicates intrusion of mafic magmas into the inclusions. Generally, the metasedimentary rock inclusions are fine-grained and granoblastic. Metasedimentary inclusions commonly contain fine-grained, disseminated sulfide mineralization (pyrrhotite >> chalcopyrite) in minor concentrations (< 2%, but rare occurrences with up to 40% sulfide have been noted). Metasedimentary inclusions are found in the anorthositic inclusion block, and are rarely found in the upper zone of the SKI. The lower parts of the basal contact zone, though still rare, hosts the vast majority of metasedimentary inclusions. Animikie Group rocks of the Biwabik Iron and Virginia formations are likely to be the protoliths for most if not all of these inclusions.

Severson (1994) interpreted the quartzose sedimentary rock inclusions to have been derived from the Virginia Formation, and the iron-oxide-rich inclusions to be of Biwabik Iron Formation descent. Their presence in the basal contact zone suggests that the Virginia formation and presumably the underlying Biwabik Iron formation may have originally composed at least part of the footwall to the SKI in this area. The possibility that these inclusions were transported from the southwest, where the Virginia formation clearly forms the footwall (Fig. 1), would contradict the flow model that magmas filling the SKI chamber came from the northeast. Additionally, mapping in the Nickel Lake

Macrodike area (Peterson et al., 2006) documents Biwabik Iron Formation inclusions up to one kilometer long orientated sub-vertically with the long axis parallel to dike walls within the macrodike as if to have been carried through the macrodike. These sediments are rich in sulfur and are considered to have provided the sulfur source for sulfide mineralization in the Partridge River intrusion (Ripley, 1981; Ripley and Al-Jassar, 1989), though there have been no sulfur isotope studies done in the SKI to date.


Figure 25: Metasedimentary inclusion featuring globular graphite with a matrix of quartz; Drill core MEX-47 - depth 1809 feet.

*Mafic Hornfels Inclusions*

There are numerous mafic hornfels inclusions throughout the stratigraphy of the SKI, but most commonly they reside in the lower upper zone units (Main AGT and AT&T). The following characteristics were observed in both drill core and field studies, and in three samples collected from drill core for petrographic study (Appendix II). The mafic hornfels inclusions are typically tens of meters in dimension, but lengths spanning several hundred meters have been observed. Sharp contacts with the enclosing gabbroic and troctolitic rocks are common. Mafic hornfels inclusions display homogeneous,

equigranular, granoblastic textures, are consistently fine-grained, and have uniform (on a sample by sample basis) modal mineralogies with 40-50% granular plagioclase, 20-54% granular augite, 15-20% granular olivine, and 1-15% granular iron-oxide. The mafic hornfels inclusions are remarkably unaltered.

Most occurrences contain coarse gabbroic clots interpreted to represent metamorphosed amygdules based on their size and distribution (Severson, 1994; Miller and Severson, 2002; Patelke, 1996). Some elongated clots (Fig. 26) have distributions resembling relic, metamorphosed pipe amygdules. Many mafic inclusions are strongly magnetic. They commonly display healed voids and fractures (Fig. 26), which are filled with medium-grained gabbroic, troctolitic, and anorthositic material mantled by thin rims (<3 mm thick) of iron-oxide.

Based on relic textures and mafic mineralogy, mafic hornfels inclusions are considered to be of volcanic origin, representing thermally metamorphosed blocks derived from the basal section of the North Shore Volcanic Group. The well-developed granoblastic textures provide evidence of re-crystallization due to thermal metamorphism. Miller and Severson (2002) suggested that the strongly magnetic inclusions may indicate that the protolith was an evolved Fe-rich (or transitional) basalt.

*Anorthositic Inclusions*

Anorthositic inclusions of various sizes and lithologies occur throughout the stratigraphy of the SKI, though they are most prevalent and densely concentrated in the uppermost units. The rock types range in texture from medium- to coarse-grained,


Figure 26: Mafic hornfels inclusion in outcrop. A. close-up of an elongate area of coarse gabbro interpreted to be a metamorphosed pipe amygdule; B. network of mineralized joints common to mafic hornfels inclusions; Both photographs from outcrop station 62107-06 (Appendix I).

Figure 27: Meter-sized inclusion of medium-grained, troctolitic anorthosite with poikilitic olivine enclosed by augite troctolite containing coarse to pegmatitic clots of augite typical of the Main AGT unit. Photos from outcrop station 80607-03 (Appendix I).

intergranular to ophitic, weakly to strongly foliated, and with olivine ranging from anhedral granular to poikilitic (1 to >10 cm oikocrysts; e.g., Fig. 27). Modal rock types include troctolitic anorthosite, gabbroic anorthosite, and anorthosite. Contacts between the anorthositic inclusions and the host troctolite can be sharp (e.g., Fig. 27) to gradational, though usually less than one meter thick. When contacts are sharp, olivine in the troctolite is commonly concentrated around the anorthositic inclusions creating a rim (< 5 cm thick) of medium-grained olivine.

The lithologic, textural and structural characteristics of these inclusions are consistent with these masses being derived from the anorthositic series of the Duluth

Complex. As noted in the regional geology section, anorthositic series rocks have similar U-Pb ages (~1099 Ma) as the troctolitic rocks of the layered series, but consistently occur as solid inclusions within layered series intrusions such as the SKI (Miller and Severson, 2002).

*PAN (Poikilitic Anorthosite) Unit*

The PAN unit (poikilitic anorthosite) was discovered from drilling conducted in the fall of 2007 in the far northeastern part of the study area (east of Spruce Road and north of Hwy 1; Fig. 23). Numerous (~15) holes drilled in the area encountered a distinctive poikilitic troctolitic anorthosite and establish its size to be at least hundreds of meters wide and several hundred meters thick. It occurs just east of the anorthositic inclusion block first defined by Severson (1994), which he termed the Hwy 1 corridor anorthosite, and it (the PAN) appears to be a second separate large inclusion block of anorthositic series rocks with troctolitic rocks of the SKI between the two blocks.

The extent of this second large inclusion block of anorthositic series rocks is defined not only by drill core, but also by numerous outcrops of poikilitic anorthosite that have been noted east of Spruce Road, north of the field area for this study. These outcrops display a medium- to coarse-grained poikilitic troctolitic anorthosite with olivine oikocrysts up to seven centimeters in diameter (Fig. 28). These outcrops have been correlated to similar rocks found in drill core, which consist of randomly alternating medium- to coarse-grained, poikilitic troctolitic anorthosite and anorthositic troctolite,


Figure 28: The PAN (Poikilitic anorthosite) unit in outcrop featuring olivine oikocrysts up to seven centimeters in diameter, outcrop located east of Spruce Road in section 35 of NRRI-MAP-2008-01 (not in field area of this study).

with troctolitic anorthosite dominating the unit. Olivine oikocrysts average about three centimeters in diameter. This rock type has been found in many holes drilled in the farthest eastern exploration areas of the current Nokomis deposit, although it is only present in one drill core (MEX-61) logged for this study. Its actual dimensions to the east, northeast, and southeast are unknown due to insufficient data.

Though locally present in SKI rocks, poikilitic troctolitic anorthosite is not a dominant rock type of the SKI, especially not to the extent seen in the PAN unit. However, poikilitic troctolitic anorthosite is a common lithology of the anorthositic series

(Miller and Weiblen, 1990). Based on this association, this unit has been tentatively identified as a large inclusion block, or possibly a cluster of inclusions of anorthositic series rocks. Continued exploration and petrologic studies are needed to define the extent of this unit and determine its influence on sulfide mineralization in the SKI.

### 5.2.3 Anorthositic Inclusion Block

The mapping of Phinney (included in Green et al., 1966) documented many anorthositic outcrops within the SKI in an area that is now recognized as being underlain by a large anorthositic inclusion block. Not having the drill core information now available and showing the subsurface extent of anorthositic rocks, Green et al. (1966) reasonably interpreted these outcrops as individual anorthositic inclusions. Severson (1994) concluded from outcrops and early drilling of six holes that these exposures represent a single large block, calling the entire anorthositic mass the Highway 1 corridor. Severson (1994) stated that the uppermost and lowermost portions of these drill holes contain rocks with SKI affinity that reasonably correlate with nearby SKI unit lithostratigraphy.

Severson (1994) estimated that the block is approximately 2.4 kilometers wide by 4 kilometers long and up to 1 kilometer thick. Drilling by Duluth Metals subsequent to Severson's study has allowed better constraints on the dimensions of the anorthositic inclusion block. These new drilling data indicate that the inclusion is approximately three kilometers wide from east to west, with a maximum thickness of about 1 kilometer. The block's north-south length is still in question as drilling has not yet defined its

southern extent, but a minimum length of 4 kilometers is possible. The three-dimensional shape of the block is also coming into focus from continued Duluth Metals drilling. Its western and northwestern borders are near-vertical, while its eastern and northeastern borders dip steeply to the west and southwest, respectively. Severson (1994) defined three major units within the block, which he termed INCL (Inclined Inclusion of Basalt), Upper Gabbro, and AN-G (Anorthosite-Gabbro Group). This study found Severson's (1994) units to properly describe the rocks present in the anorthositic inclusion block, though the INCL unit is here renamed the Mafic Hornfels unit.

*Mafic Hornfels*

The Mafic Hornfels unit was found in three drill cores logged for this study: MEX-47, MEX-51, and MEX-55 (Fig. 21). It thickens to the east and northeast from 13 meters to 24 meters thick, and dips slightly to the east (Fig. 23). The upper and lower contacts of the Mafic Hornfels unit are always sharp, but the upper contact is locally irregular with SKI apophyses inter-fingering into the unit, creating sharp centimeter- to meter-scale layering in core between fine-grained hornfels and medium- to coarse-grained troctolitic to gabbroic SKI magmas.

The Mafic Hornfels unit typically consists of very fine- to fine-grained, strongly magnetic, equigranular, granoblastic mafic hornfels. Thin section inspection of five samples from the unit indicates that the mineralogy and texture of the unit is slightly different compared to other mafic hornfels inclusions in the SKI in that the Mafic Hornfels unit contains significant orthopyroxene. The mineralogy consists of 40-60% plagioclase, 10-35% augite, 0-30% olivine, 0-11% orthopyroxene, and 9-20% iron-oxide.

A strongly granoblastic equigranular texture predominates as is typical of other mafic hornfels.

The Mafic Hornfels unit is interpreted as a remnant of iron-rich basalts of North Shore Volcanic Group that originally formed the hanging wall to the early intruding anorthositic series. Multiple emplacements of SKI magmas likely caused the combined anorthositic series and included basalt to become separated from the main anorthositic series mass as the SKI magma chamber developed.

*Upper Gabbro*

The Upper Gabbro unit occurs in four drill holes logged for this study: MEX-60, MEX-47, MEX-51, and MEX-55 (Figs. 21 & 23). A maximum thickness of 295 meters was found in MEX-47 in the center of the block, and a minimum thickness of 180 meters was found in MEX-60 to the west, with MEX-55 in the east showing a thickness of 273 meters. The Upper Gabbro unit was found in every drill core that pierced the anorthositic inclusion block, being situated atop the thick sequence of AN-G anorthositic rocks. The upper contact of the Upper Gabbro unit is usually sharp and marked by a relatively thick, laterally extensive mafic hornfels inclusion (Mafic Hornfels unit), while the lower contact is gradational as gabbroic lithologies become randomly mixed and inter-layered with anorthositic rocks. This lower contact usually displays gradational contacts between gabbroic and anorthositic rock types highlighted by variability in clinopyroxene and iron-oxide mode over several meters.

Based on petrographic inspection of 22 samples, the Upper Gabbro unit dominantly consists of coarse-grained, intergranular, iron-oxide-rich (≤10%) olivine

gabbro to locally augite troctolite (Fig. 29). Intermixed anorthosite, gabbroic anorthosite, and anorthositic gabbro lithologies, especially near the lower contact, are common. The

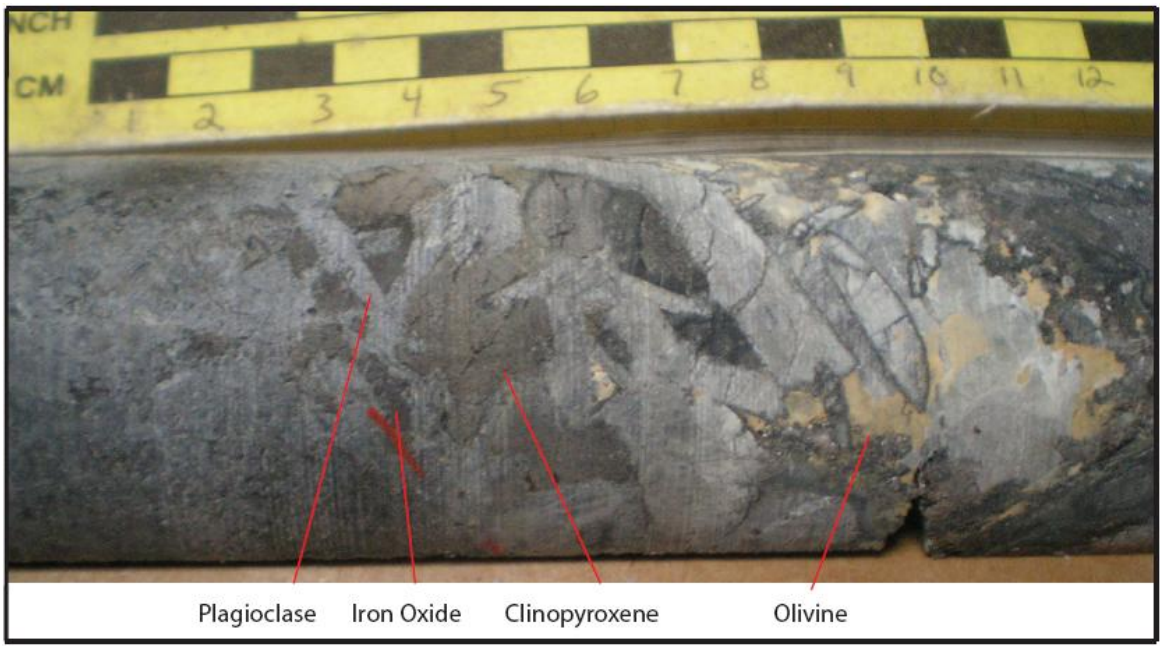


Figure 29: The Upper GABBRO unit in drill core; Drill hole MEX-51 - depth 2450 feet.

Upper Gabbro unit is typically composed of 55-70% anhedral to subhedral granular plagioclase, 2-15% poikilitic to subhedral granular olivine, dominantly subhedral granular clinopyroxene (10-30%) and orthopyroxene (0-10%), and 5-10% subhedral granular iron-titanium oxide with variable magnetic strength. Biotite (usually <1%) commonly rims oxide, and locally rims clinopyroxene. Sulfides are typically present in rare to minor amounts (<0.5%) and are predominantly fine- to medium-grained disseminated chalcopyrite > pyrrhotite. Locally, the rock typically shows moderate to strong uralite alteration (after pyroxene), serpentine alteration (after olivine), kelyphitic rims (after olivine), and sericite (after plagioclase).

*AN-G (Anorthosite-Gabbro Group)*

The extensive AN-G unit was found in four drill holes logged for this study: MEX-60, MEX-47, MEX-51, and MEX-55 (Fig. 21 and 23). A maximum thickness of 586 meters was found in the central area in MEX-51, a minimum thickness of 184 meters was found on the eastern edge in MEX-55, and MEX-60 at the western border showed a thickness of 393 meters (Fig. 23). The upper contact is gradational with the Upper Gabbro unit as described above, while the lower contact is typically sharp with the PEG unit or locally the U2 unit.

The AN-G typically consists of coarse-grained to pegmatitic, intergranular to ophitic, poikilitic (olivine) anorthosite, troctolitic anorthosite, and gabbroic anorthosite with local gabbro, anorthositic gabbro, olivine gabbro, and anorthositic troctolite lithologies. Plagioclase commonly displays moderate to well-developed foliation (figure 30) with variable orientations. Petrographic study of 22 sections reveals that the AN-G is composed of 75-96% anhedral to subhedral granular plagioclase, 1-18% anhedral granular to poikilitic olivine with oikocrysts up to several centimeters across, 1-22% ophitic to subophitic clinopyroxene as low-density ophites (1-2 cm diameter), 1-10% largely subophitic to anhedral granular orthopyroxene, and typically less than 1% interstitial biotite and iron oxide, respectively. Pervasive needle-like iron oxide and small sheafs of biotite occur in plagioclase, clinopyroxene, and orthopyroxene as exsolution schiller that parallels cleavage planes (Fig. 31). This phenomenon implies that these


Figure 30: Well foliated anorthosite of the AN-G unit; Drill hole MEX-51 – depth 2401 feet.

rocks experienced very slow cooling or reheating and provides supportive evidence that SKI magmas intruded into the anorthositic series country rock shortly after the anorthositic series itself was emplaced. Typically, the AN-G is sulfide-barren with local rare to trace, fine- to medium-grained, disseminated pyrrhotite, in much greater abundance than chalcopyrite. When present, sulfide is usually associated with sedimentary hornfels inclusions. This spatial relationship supports the generally held conclusion that these rock types, which presumably represent inclusions of Virginia Formation, provided the dominant sulfur source for mineralization (Ripley et al., 2007). Common alteration includes: moderate to strong localized uralite and serpentine, weak sericitization, moderate to strong, localized sausseritization, and local kelyphitic rims on olivine.

The mineralogic, textural and structural characteristics of the AN-G unit share many similarities to anorthositic series rocks described by Miller and Weiblen (1990), and are thus thought to be a remnant of the anorthositic series country rock intruded by the SKI. The pervasive shiller of iron-oxide and biotite present in plagioclase,

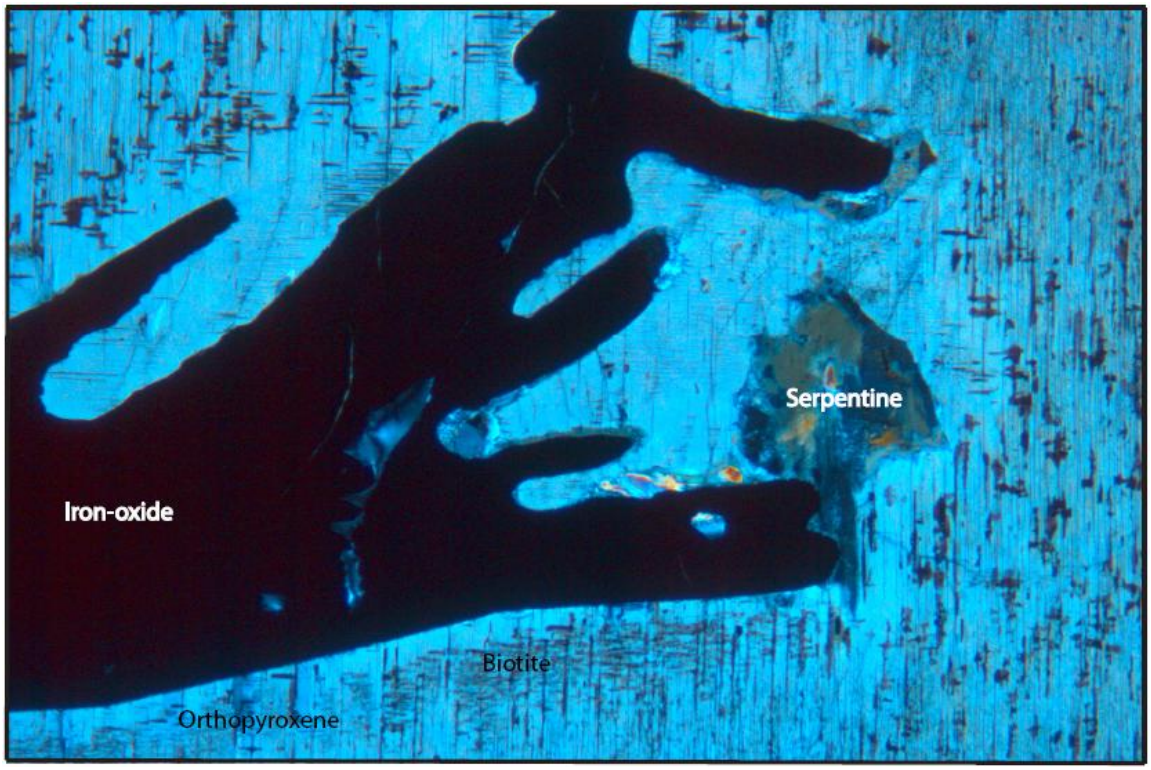


Figure 31: Amoeboidal iron-oxide embaying into orthopyroxene with biotite and oxide exsolution schiller in clinopyroxene (field of view = 2.5 mm wide; Sample ID – 51-1868).

orthopyroxene, and clinopyroxene is consistent with reheating of these anorthositic rocks by the SKI magmas.

The stratigraphic position of the Upper Gabbro unit between the Mafic Hornfels unit and the AN-G, and the gradational lower contact of the Upper Gabbro unit with the AN-G, may imply a genetic association between the Upper Gabbro and the AN-G such that the Upper Gabbro is an upper differentiate of the AN-G. However, without

geochemical data, this is largely speculation. Moreover, the Mafic Hornfels unit is likely a remnant of the hanging wall North Shore Volcanic Group basalts intruded by anorthositic series magma. Miller and Severson (2005) describe a similar gabbroic lithology occurring in the anorthositic series rocks in the Babbitt SW quadrangle. They note that this unit was termed the Powerline gabbro unit G1 of Bonnichsen (1970, 1974), and the PLG unit of Severson and Hauck (1990). Green and Miller (2008) describe a similar series of rocks associated with the Layered Series at Duluth, in which they postulate that the upper gabbroic rocks are a flow differentiate of the anorthositic rocks below.

### 5.2.4 Basal Contact Zone of the SKI

The basal contact zone of the SKI consists, from bottom to top, of the Bottom Augite Troctolite/ Norite (BAN) unit, the Basal Heterogeneous (BH) unit, the Ultramafic Three (U3) unit, and the PEG (Pegmatoidal Unit of Foose, 1984) unit. All four of these units were found in every drill hole logged for this study. Descriptions of these units are presented below, including comparisons to Severson's (1994) characterizations.

*BAN (Bottom Augite Troctolite/Norite) unit*

The BAN unit as described by Severson (1994) consists of a dominantly medium-grained mixture of norite, gabbronorite, and olivine gabbronorite with local augite troctolite. Thickness of the unit is variable from several centimeters to ten's of meters, though a thickness of several meters is most common. The lower contact is commonly sharp and irregular with granitic rocks of the footwall GRB. The upper contact with the

overlying BH unit is typically gradational and marked by a rapid decrease in orthopyroxene.

Logging and petrographic study of the BAN unit show it to typically consist of fine-grained, ophitic gabbro, and gabbronorite (Fig. 32), with local olivine gabbronorite

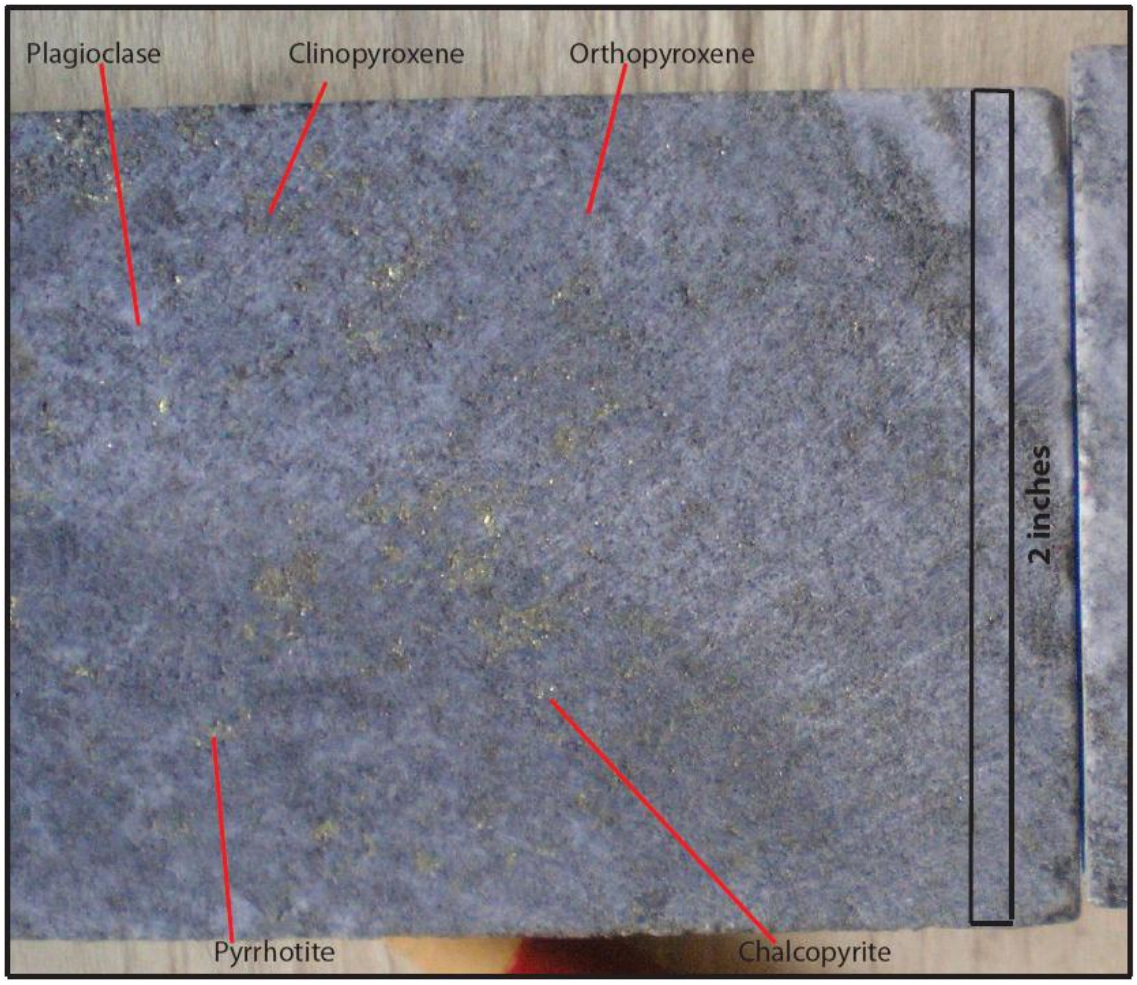


Figure 32: The BAN unit in drill core, featuring fine-grained norite to gabbro norite with disseminated pyrrhotite and chalcopyrite; Drill hole MEX-51 – depth 3449.5 feet.

and augite troctolite. Plagioclase (50-65%) is anhedral to subhedral granular. Olivine (0-19%) is anhedral granular to poikilitic, while (8-25%) orthopyroxene and (8-18%) clinopyroxene are commonly ophitic with orthopyroxene generally more abundant

toward the bottom. Biotite (<1%) and iron oxide (<5%) commonly occur interstitially. Locally, the groundmass consists of alkali feldspar and quartz with common micrographic textures and fine-grained, euhedral apatite needles. Alteration in the BAN unit is patchy and usually consists of weak to strong serpentinization of olivine, weak to strong uralitization of pyroxene, and moderate to strong sericitization of plagioclase.

The BAN unit typically contains prominent fine-grained, disseminated chalcopyrite and pyrrhotite. Locally, within 10 centimeters of the footwall contact, it contains massive sulfide marked by pyrrhotite in much greater abundance than chalcopyrite. Sulfide minerals locally display graphic intergrowth textures with orthopyroxene (Fig. 33) and fine disseminations in plagioclase (Fig. 34), but more commonly, they display an interstitial relationship with the primary silicate and oxide minerals.

The BAN unit is interpreted as a contaminated zone of the BH unit. Common micrographic alkali feldspar and quartz suggest intermingling of GRB felsic melts with the SKI mafic magma. The observed increase in orthopyroxene in the BAN is also consistent with silica contamination of mafic magmas by partial melts from the granitic footwall rocks. As described above (5.2.1), this implied enrichment in silica and alkalies is matched by a significant depletion of quartz and alkali feldspar in the footwall immediate to the basal contact of the SKI.

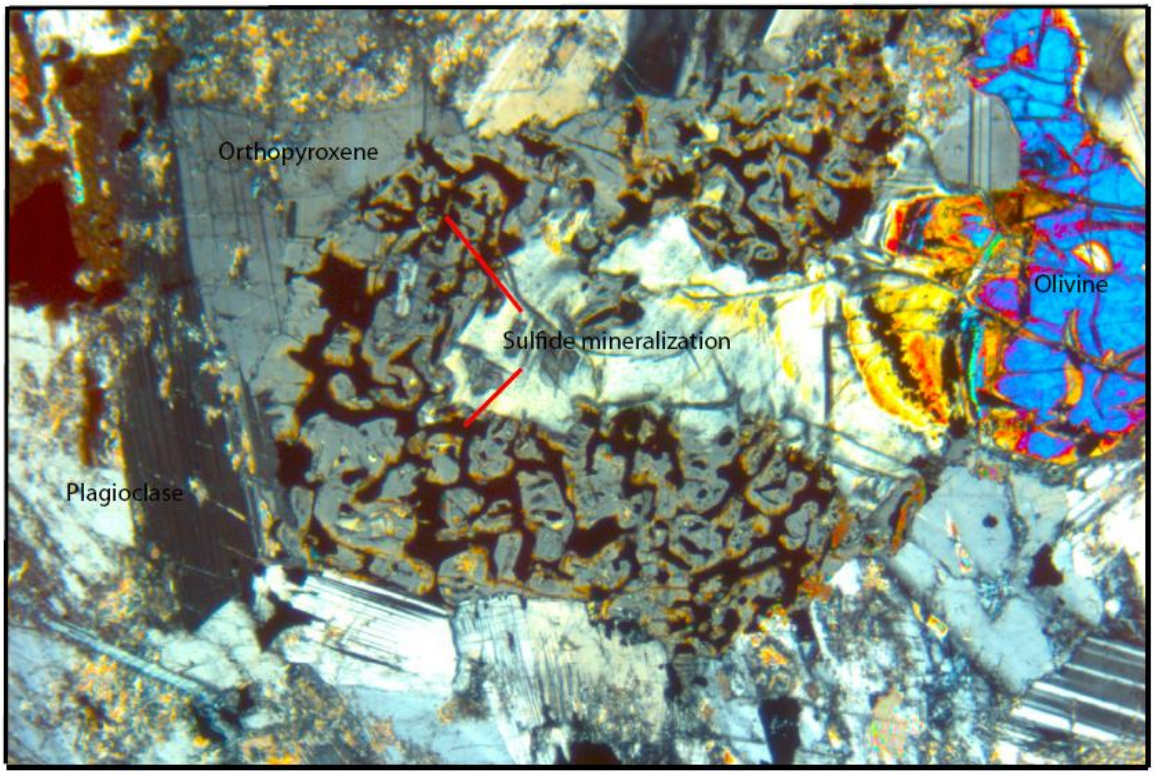


Figure 33: Graphic intergrowths of sulfide and orthopyroxene from the BH unit (Field of view = 2.5 millimeters wide; Sample ID - 8033).

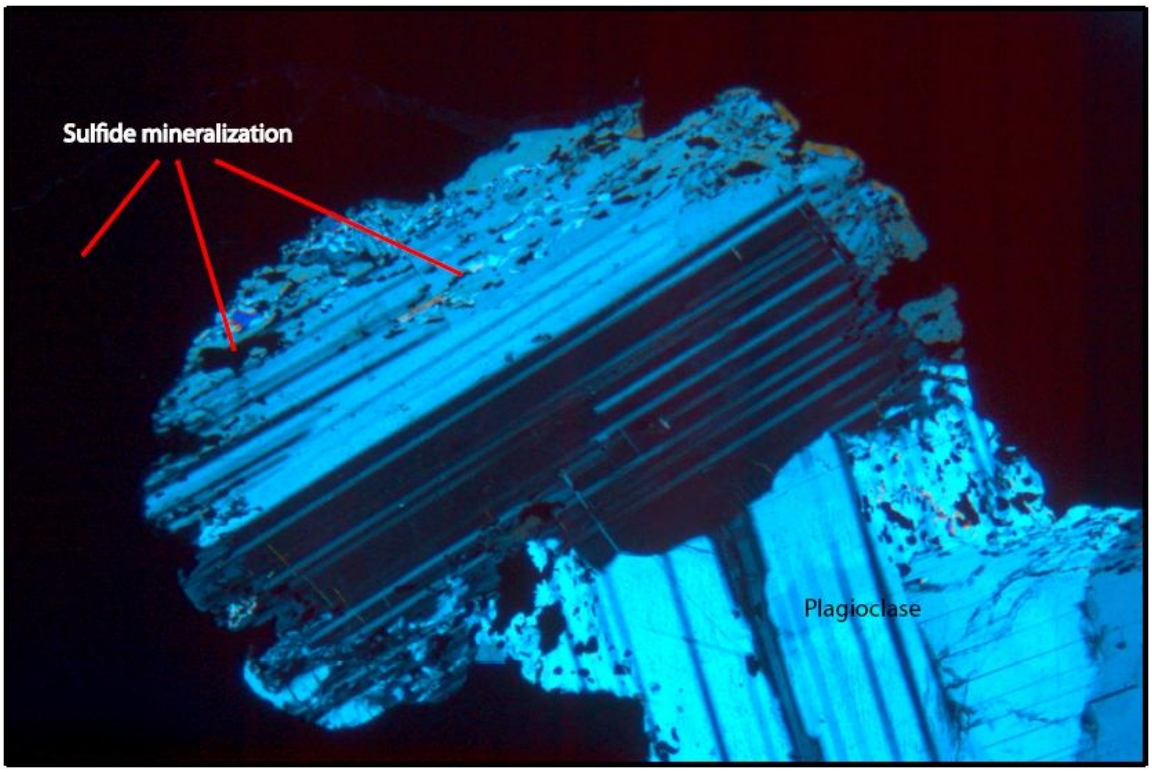


Figure 34: Disseminations of sulfide mineralization within plagioclase in the BAN unit (Field of view is 2.5 mm wide; Sample ID – 51-3396).

*BH (Basal Heterogeneous) unit*

Severson (1994) characterized the basal heterogeneous (BH) unit as the main sulfide-bearing zone of the SKI that is lithologically composed of a mixture of troctolite, anorthositic troctolite, and augite troctolite with grain sizes ranging from fine- to coarse-grained (and locally pegmatitic) on a meter scale. A maximum thickness of greater than 100 meters in the eastern region of the study area (MEX-55) thins to the west to as little as 15 meters (MEX-53). Contacts are typically mineralogically and texturally gradational with respect to both the U3 unit above and the BAN unit below. In outcrop the BH unit is typically gossan-stained, strongly oxidized, and weathered to grus (Fig. 35A).

In this study, the BH unit was found to consist of a vari-textured troctolite, augite troctolite, and anorthositic troctolite with local gabbro and anorthositic gabbro intervals (Fig. 35B). Texturally, it varies from fine-grained to pegmatitic and intergranular to ophitic. In places, it contains lenses and stratiform intervals of olivine-rich troctolite, melatroctolite, feldspathic peridotite, and peridotite very similar to the rocks of the U3 unit. Locally, these ultramafic layers show bifurcations and pinch-outs suggesting that many of the ultramafic intervals may be interconnected on a large scale.

In most BH unit samples, plagioclase (50-88%) is anhedral to subhedral granular (i.e., lathy to tabular) but locally may be poikilitic containing chadacrysts of opaques and olivine. Olivine (15-40%) ranges from subhedral granular to poikilitic and is locally mantled by kelyphitic rims that commonly include orthopyroxene, hornblende, biotite, and plagioclase - orthopyroxene symplectite.. Clinopyroxene (<1-15%) is usually ophitic with local iron oxide/biotite schiller in the cleavage. Orthopyroxene (<1-8%) is subophitic to ophitic, and locally interstitial, and commonly forms peritectic rims around olivine. Subhedral to anhedral granular iron-titanium oxides (<5%) commonly occur interstitial to silicates. Biotite (<1-3%) occurs interstitial to other phases and as rims on sulfides and iron oxides. Interstitial alkali feldspar and euhedral apatite locally occur in trace amounts. Alteration is typically weak to moderate, but locally strong, typically consisting of serpentine (after olivine), uralite (after pyroxene) and sericite (after plagioclase).

The BH unit typically displays fine- to coarse-grained disseminated, sulfide throughout. Sulfide minerals include chalcopyrite, cubanite, talnakhite, pentlandite, and


Figure 35: A. the BH unit in outcrop with a weathered, gossan-stained, grussy appearance, (Outcrop station 60407-01; Appendix I); and B. the BH unit in drill core displaying heterogeneity in lithology and grain size with sharp internal contacts; red dashed lines outline lithologies; Drill hole MEX-61 – depth 3384 feet.

pyrrhotite occurring typically as disseminated to semi-massive aggregate grains interstitial to silicates and oxide phases. Sulfides locally form embayments and fine disseminations in plagioclase and biotite. Cubanite and talnakhite typically occur as exsolution lamellae within chalcopyrite, and pentlandite lamellae can occur in pyrrhotite. Ratios of Cu sulfides and Fe sulfides vary throughout the unit, but talnakhite, cubanite, and chalcopyrite are generally more abundant than pyrrhotite near the top of the unit. Pentlandite occurs throughout the unit and tends to be more abundant in the pyrrhotite-dominant lower section of the unit.

*U3 (Ultramafic Three) unit*

Severson (1994) described the Ultramafic Three (U3) unit as consisting of up to 20 ultramafic horizons composed of peridotite, melatroctolite, oxide melatroctolite, and olivine-rich troctolite alternating with horizons of troctolite. In the study area, the U3 unit averages 5.5 meters thick, but increases to 24 meters under the eastern margin of the anorthositic inclusion block (MEX-55; Fig. 23). The upper contact with the PEG unit is sharp, while the lower contact with the BH is usually gradational and consists of multiple, thin (centimeter-scale) olivine-rich horizons bifurcating through the BH. In outcrop, the U3 is typically massive and colored dark brown from sulfide gossan-staining, oxidation, and strong weathering (Fig. 36).

The U3 unit is predominantly composed of homogeneous, fine- to medium-grained troctolite, melatroctolite, feldspathic peridotite, and peridotite with local anorthositic troctolite, but it can also be locally coarse-grained. Plagioclase (10-60%) is typically either subhedral granular (lath-shaped; Fig. 37) with poor to moderate foliation,

or poikilitic enclosing granular olivine (Fig. 38). Olivine (25-85%) is predominantly anhedral granular but locally displays poikilitic and subpoikilitic textures (Fig. 37). Minor interstitial clinopyroxene (up to ~6%) is typically subophitic with moderate

Figure 36: The U3 unit in outcrop showing a massive structureless morphology and brownish, oxidized weathering surface (Outcrop station 60807-05; Appendix I).

density ophites, usually less than 1 cm in diameter. Orthopyroxene is rare (usually <1%) and typically occurs as peritectic rims around olivine. Anhedral granular iron oxide (<5%) and interstitial biotite (<1%) are also present. The U3 unit is consistently sulfidic,

usually containing up to 3% (ave. 1-2%) disseminated, fine- to medium-grained, Cu-rich sulfide (chalcopyrite, talnakhite, cubanite, and minor pyrrhotite; Fig.39). Alteration of the U3 unit is typically patchy and is dominated by both serpentinization of olivine and kelyphitic assemblages at contacts between olivine and plagioclase (Fig. 40).

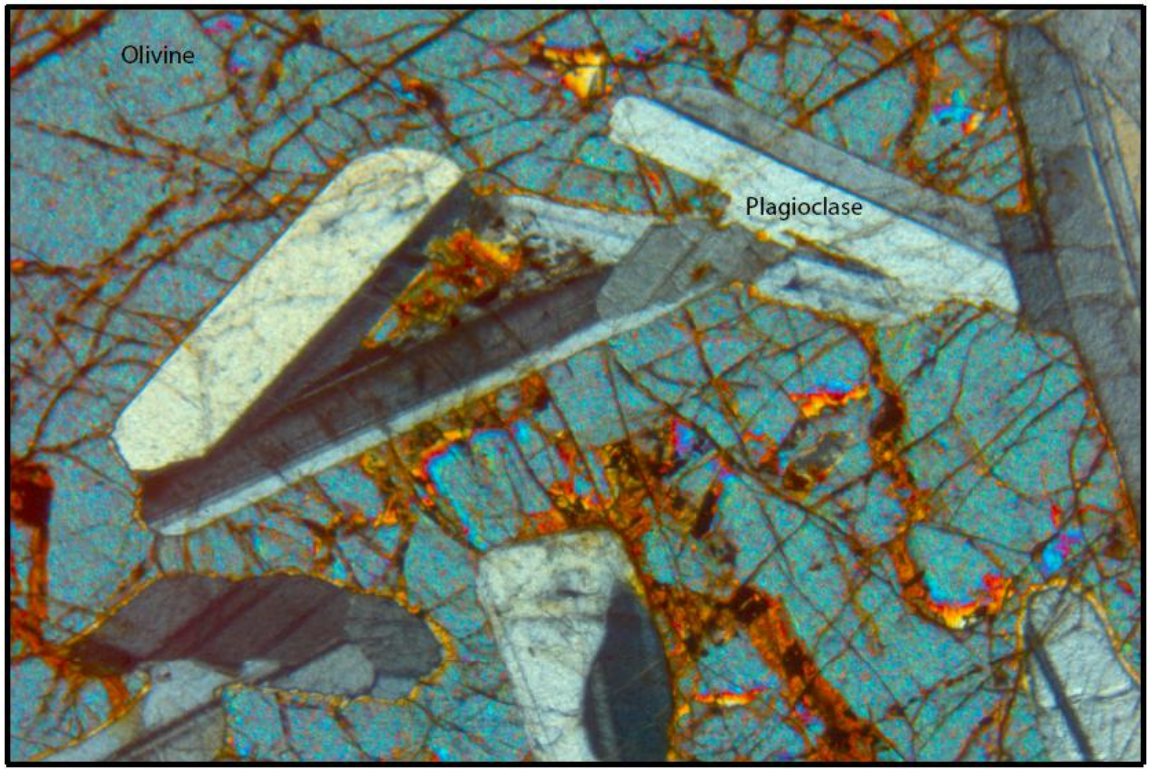


Figure 37: Poikilitic olivine with lath-shaped plagioclase displaying weak to moderate planar alignment in the U3 unit (field of view = 2.5 mm wide; Sample ID - 7112).

Severson (1994) encountered much thicker zones of the U3 unit than were found in this area of the intrusion; however, this discrepancy might be due to differences in how the U3 unit is defined. Severson (1994) described the U3 as thick sequences of alternating troctolites and ultramafic rocks. In this study, the U3 unit is limited to intervals dominated by olivine-rich troctolites to ultramafic rocks. In several instances, olivine-rich troctolites and ultramafic rocks persist downward as thin layers, but troctolite

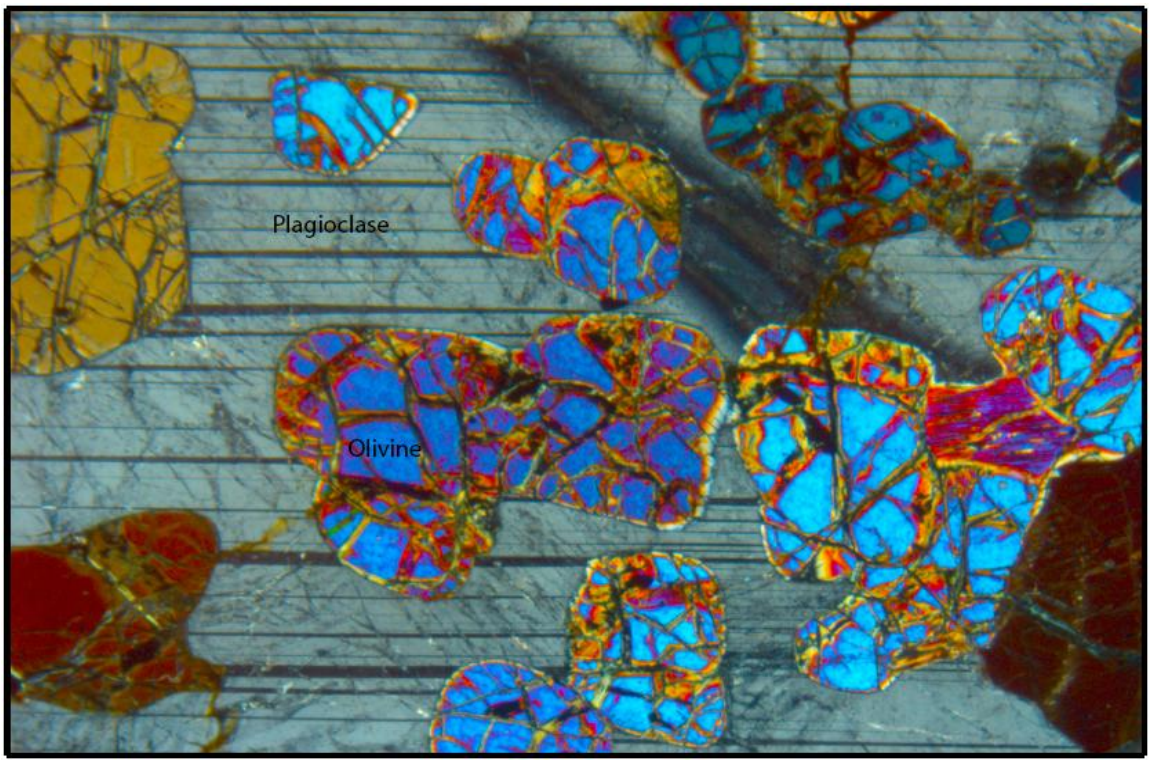


Figure 38: Poikilitic plagioclase in the U3 unit (field of view = 2.5 mm wide; Sample ID - 7312).

is dominant. In these instances, the contact between the U3 unit and the BH unit is placed where the dominant lithologies change, instead of down to the last occurrence of olivine-rich troctolite or ultramafic rocks. This study interprets these outlying, or more appropriately underlying, olivine-rich layers as bifurcations of the U3 unit down into the BH unit.

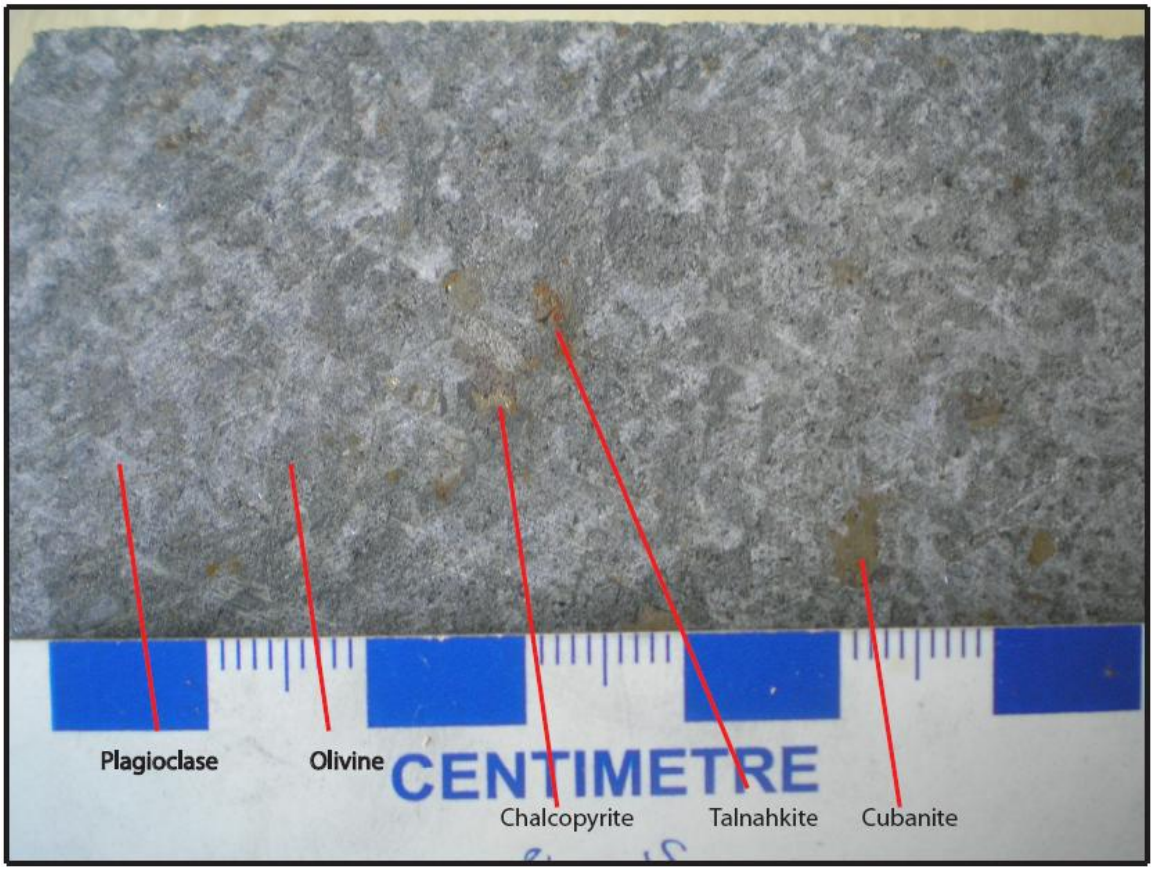


Figure 39: Medium-grained sulfidic melatroctolite in drill core, typical of the U3 unit; Drill hole MEX-56, depth 2677 feet.

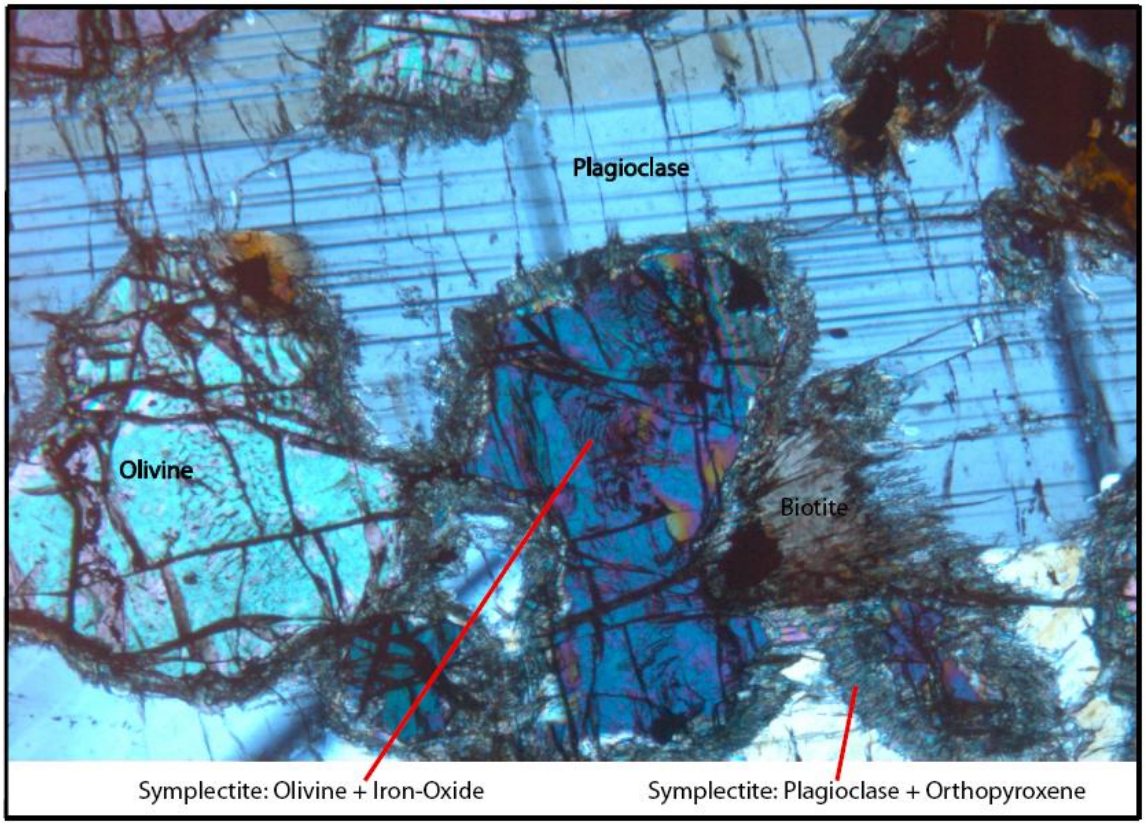


Figure 40: Kelyphitic rims around olivine composed of thin orthopyroxene, biotite, Fe oxide, and fine symplectitic intergrowths of orthopyroxene in Ca-plagioclase. Locally, olivine internally contains symplectic intergrowths of iron oxide (field of view = 2.5 mm wide; Sample ID – 60-2682).

*PEG (Pegmatoidal) unit*

Severson (1994) described the PEG unit as consisting dominantly of texturally heterogeneous troctolite to anorthositic troctolite with homogeneous zones that grade into pegmatoidal and pegmatitic zones composed of anorthositic troctolite, troctolitic anorthosite, anorthositic gabbro, and gabbroic anorthosite. Severson (1994) noted that the PEG unit can be very difficult to identify in drill core without first identifying the U3 unit. Once the U3 unit is identified, the presence of the PEG unit above it becomes clear. While the lower contact is always sharp with the U3 unit, the upper contact of the PEG unit can be gradational with the Main AGT unit (or with the AN-G in the vicinity of the anorthositic inclusion block), or sharp if the U2 unit is present. The average thickness of

the PEG unit is 25 meters. Like the U3 unit below, a maximum thickness in the PEG unit was recorded beneath the eastern margin of the anorthositic inclusion block (40 meters, MEX-55; Fig. 23).

This study found the PEG unit to usually occur as homogeneous to locally heterogeneous, coarse-grained to pegmatitic, subophitic anorthositic troctolite, troctolite, and augite troctolite. Petrographic observations reveal that, the PEG unit contains (60-90%) subhedral to anhedral granular, lath-shaped plagioclase that show no preferred orientation. Olivine (5-30%) is typically poikilitic to subhedral granular and is locally rimmed by orthopyroxene or by kelyphitic assemblages. Clinopyroxene (<1-27%) is typically subophitic to anhedral granular, commonly displaying pegmatitic, subophitic clots (Fig. 41 [drill core]; Fig. 42 [outcrop]). When not rimming olivine, orthopyroxene is typically ophitic with modal amounts of less than 5%. Interstitial biotite (<1%) is often associated with interstitial iron-oxide (<7%) and rare sulfides. Additionally, interstitial alkali feldspar, quartz, and primary hornblende are common accessory minerals with rare euhedral apatite also present. Rare to trace amounts (<0.5%) of interstitial chalcopyrite and pyrrhotite also occur. Alteration is typically weak to moderate and patchy in distribution consisting of serpentine, sericite, and uralite.

A common aspect of the basal contact zone units is that they are dominated by sulfide-bearing rocks. However, the PEG unit is an exception to this in that it contains only trace amounts of sulfide. However, the PEG unit's inclusion in the basal contact zone is based on its presence beneath the anorthositic inclusion block. Whether it is more

appropriate to put the PEG unit in the basal contact zone or the upper zone will be discussed in detail in the remaining sections.


Figure 41: The PEG unit in drill core composed of coarse-grained augite troctolite with pegmatitic, subophitic oikocrysts of augite; Drill core MEX-133M – depth 789 feet.


Figure 42: The PEG unit in outcrop with the same lithology and texture as that seen in figure 40, (Outcrop station 80607-02, Appendix I).

### 5.2.5 Upper Zone of the SKI

The upper zone of the SKI was subdivided by Severson (1994) into three major troctolitic units and a series of relatively thin olivine-rich, ultramafic units. From bottom to top, the troctolitic units consist of the Main Augite Troctolite (Main AGT) unit, the Anorthositic Troctolite and Troctolite (AT&T) unit, and the Anorthositic Troctolite (locally troctolite) (AT(T)) unit (Fig. 23). Olivine-rich, ultramafic units consist of the Ultramafic Two (U2) unit, the Ultramafic One (U1) unit, the High Picrite # 2 (HP#2) unit, and the High Picrite # 1 (HP#1) unit. Both the U2 and U1 units are associated with the Main AGT unit with the U2 at the base of the Main AGT, and the U1 within the Main

AGT typically toward the top. The HP#2 unit occurs at the base of the AT&T unit, and the HP#1 unit occurs at the base of the AT(T) unit.

The boundary between the upper zone and the basal contact zone is placed between the PEG unit and the Main AGT unit in this study. Although the PEG unit is typically barren of sulfide, which is characteristic of the upper zone, the unit is always present beneath the anorthositic inclusion block and therefore is included in the basal contact zone.

*Main Augite Troctolite (Main AGT) unit*

Severson (1994) describes the Main AGT unit as a zone where the dominant rock type is medium-grained, ophitic augite troctolite. He notes that the Main AGT unit is present nearly everywhere in the SKI, but consistently thins from west to east and loses its identity northeast of the anorthositic inclusion block. In this study, the Main AGT unit was found in most drill cores logged (MEX-53, MEX-56, MEX-55, and MEX-61; Fig. 23), but is absent beneath the anorthositic inclusion block except at the east and northeast margins of the block.

The Main AGT-PEG contact is sometimes marked by the occurrence of a melatroctolite layer, termed the U2 unit by Severson (1994), which has a sharp lower contact. When the U2 unit is absent, the Main AGT is in gradational contact with the PEG unit that is marked by a shift from dominantly medium- to coarse-grained rocks with an ophitic texture to dominantly coarse-grained to pegmatitic rocks with subophitic clots of clinopyroxene of the PEG unit. The upper contact of the Main AGT unit is commonly defined by the occurrence of a melatroctolitic unit which Severson (1994)

calls the HP#2, and is usually gradational, but observable. When the HP#2 is absent, the upper contact is gradational with the AT&T unit marked by a shift from dominantly augite troctolite to dominantly augite-poor anorthositic troctolite.


Figure 43: The Main AGT unit in outcrop featuring the characteristic medium- to coarse-grained augite troctolite, (Outcrop station 73107-01; Appendix I).

The Main AGT unit typically consists of massive homogeneous, medium- to coarse-grained, ophitic to locally subophitic and intergranular augite troctolite (Fig. 43). Locally, the modal rock type may include olivine gabbro, troctolite, and anorthositic troctolite, the latter containing poikilitic olivine. Petrographic study of 16 samples shows the unit to be composed of 65-68% subhedral granular plagioclase and 17-25% poikilitic to anhedral granular olivine with minor peritectic rims of orthopyroxene. Biotite and iron

oxide typically occur interstitially in modal amounts of less than 1%, but locally up to 3-5% iron oxide is present. Its most diagnostic feature is the occurrence of 5-15% augite forming ophitic to subophitic oikocrysts of moderate to high density (Fig. 43). In some sections, euhedral apatite crystals (<1%) have been observed. Locally, the unit contains thin layers of melatroctolite, inclusions of basalt and anorthosite, and small irregular areas of pegmatitic iron-oxide-rich gabbro, olivine gabbro, and anorthositic gabbro. Sulfide is rare (<0.5%) and, when present, is predominantly chalcopyrite. Alteration of primary phases is moderate to weak.

*Ultramafic Two (U2) and Ultramafic One (U1) units*

Severson (1994) defines the U1 unit as the top ultramafic unit when three ultramafic units are present within the Main AGT and PEG units. In this case, the U2 unit is considered the middle ultramafic unit and the U3 unit is the stratigraphic lowest of the three. When only one ultramafic unit is present above the U3 unit within the PEG and Main AGT units, Severson (1994) considered it to be the U2 unit. The U2 and U1 units are described together here because in the study area they are lithologically identical and both reside within (U1) or at the base (U2) of the Main AGT unit (Fig. 23). Severson (1994) describes both the U2 and the U1 units as being lithologically and structurally similar to the U3 unit (see section 5.2.5) in that they consist of intermittent to rhythmic layering of troctolite, melatroctolite, feldspathic peridotite, peridotite, and feldspathic dunite. The only lithologic difference between the U2 and U1 units and the U3 unit in the study area is that significant concentrations of sulfides occur only in the U3 unit.

Contacts between the U1 and U2 units and enclosing rocks are almost always sharp at the top, and gradational (cm-m) to sharp at the bottom. Neither unit was found in outcrop.

Petrographic study of six samples shows the U2 and U1 units as consisting of thin (meter-scale) packages of homogeneous, fine- to medium-grained, moderately to well-foliated, intermittently layered troctolite, melatroctolite, feldspathic peridotite, and peridotite with minor intervals of anorthositic troctolite (Fig. 44). The units are generally

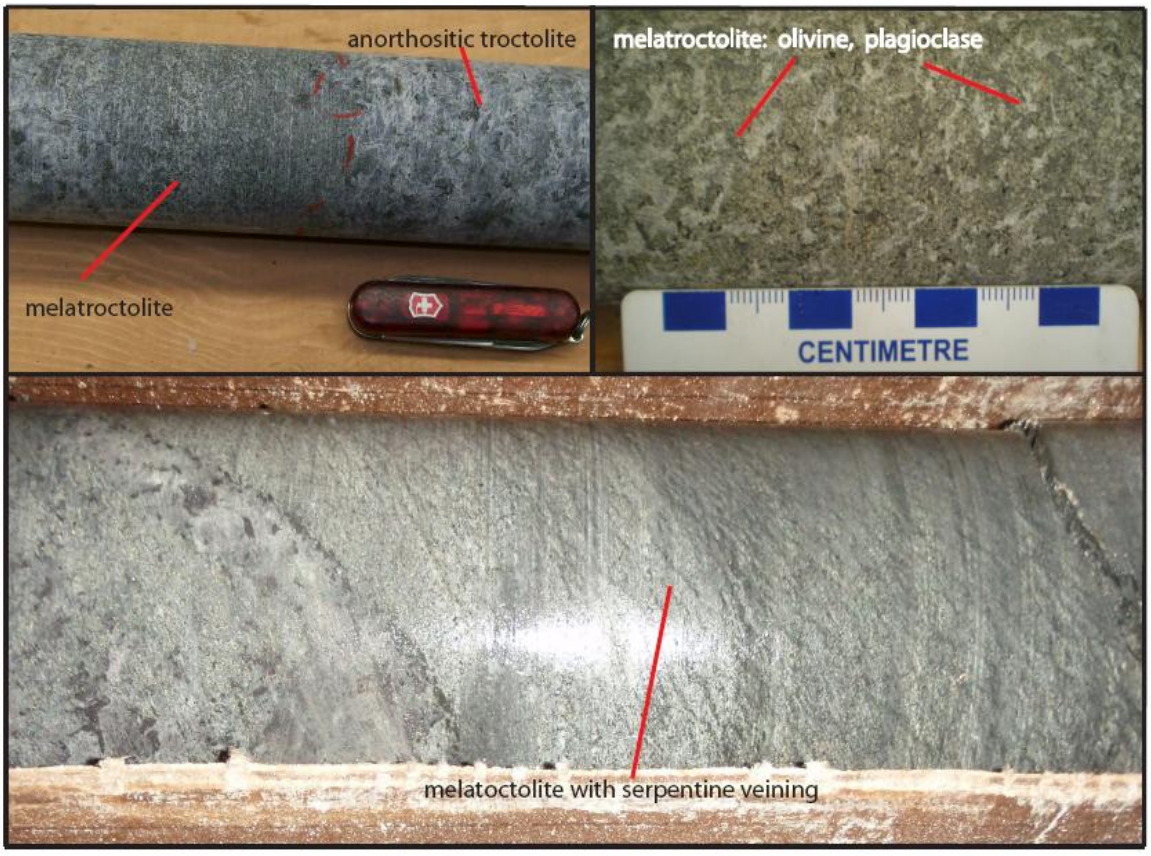


Figure 44: The U2 unit in drill core; top left (Drill core MEX-128M – depth 3030 feet) melatroctolite with sharp upper contact and gradational lower contact; top right (Drill core MEX-55 – depth 2947 feet) showing unaltered melatroctolite; and bottom (Drill core MEX-128M – depth 3058.5 feet) melatroctolite with moderate serpentine veining.

composed of 50-82% subhedral granular olivine, 1-15% ophitic to subophitic clinopyroxene, and 25-50% subhedral granular and locally subpoikilitic to poikilitic

plagioclase. Orthopyroxene, biotite and iron-oxide are rare (<1%). As noted above, sulfide is rare (< 0.5%) and is predominantly chalcopyrite and pyrrhotite. Both ultramafic units display moderate to strong serpentine alteration of olivine and serpentine veining. The serpentine veins form a subhorizontal network of subparallel veins that crosscut multiple grains of olivine and adjacent minerals.

*Anorthositic Troctolite and Troctolite (AT&T) unit*

Severson (1994) describes the AT&T unit as a monotonous mix of anorthositic troctolite and troctolite with narrowly gradational (cm-scale) internal contacts between plagioclase-rich and relatively plagioclase-poor lithologies. The AT&T unit is present in every drill core logged for this study that flanks the anorthositic inclusion block (MEX-53, MEX-56, MEX-61; Fig. 23), and numerous outcrops were recorded during field mapping. The upper and lower contacts vary from sharp to gradational depending on whether melatroctolitic to dunitic units are present. Severson (1994) named the ultramafic units bounding the AT&T unit the upper HP#1 and the lower HP#2. When the HP#2 is not present, the lower contact with the Main AGT unit is gradational (on a scale of meters) and defined by a decrease in pyroxene mode and an increase in plagioclase mode. When the HP#1 unit is not present, the upper contact with the AT(T) is similarly difficult to identify, being defined by a subtle increase in plagioclase mode.

Lithologically, the AT&T unit consists of randomly alternating sequences of medium- to coarse-grained, ophitic troctolite, ophitic and/or poikilitic anorthositic troctolite, and subophitic to ophitic augite troctolite. Local lenses (<1 m) of intergranular to subophitic pegmatitic anorthositic gabbro and anorthositic troctolite are also present as

are anorthositic inclusions (usually >1 to 10's of m thick). Anorthositic lenses differ from anorthositic inclusions in that anorthositic lenses are typically not foliated, and that they display an abrupt large differential in grain size from the enclosing rocks. Petrographic study of 20 sections shows the unit to contain 60-75% subhedral to anhedral granular plagioclase, 12-40% granular, subpoikilitic, and poikilitic olivine with kelyphitic rims commonly developed on oikocrysts, 0-10% subophitic to ophitic clinopyroxene. Subophitic orthopyroxene is common with modes typically less than 1%, but in rare cases up 12% has been observed. Minor (<1%) interstitial biotite, apatite, and iron oxide commonly occur, but up to 5% poikilitic iron oxide has been locally observed. The AT&T unit is generally sulfide barren, but where present, chalcopyrite is greater than pyrrhotite. Alteration consists largely of locally strong uralitization of pyroxene and serpentinization of olivine (Fig. 45).

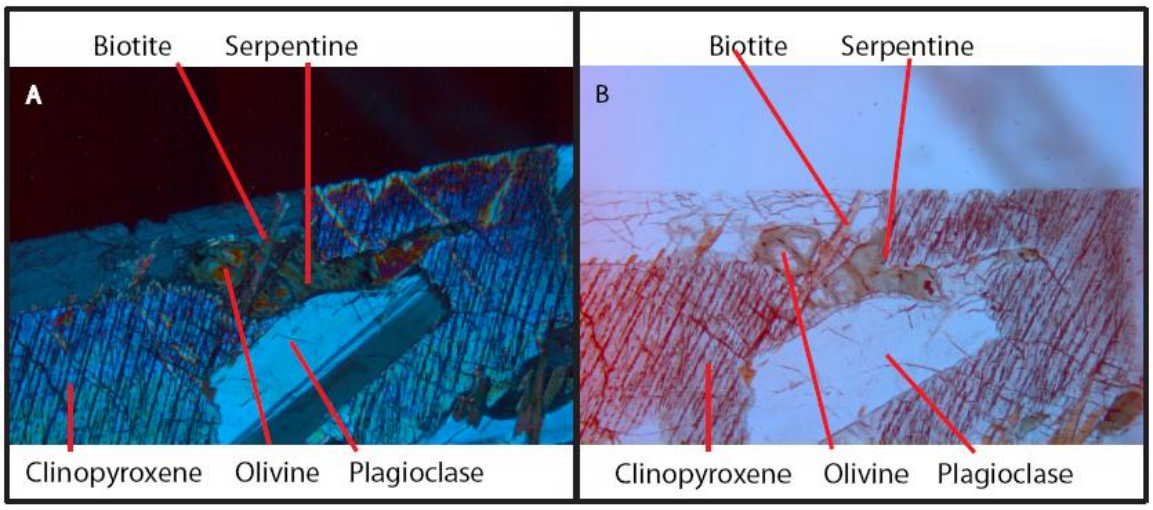


Figure 45: Serpentine alteration of olivine in the AT&T unit A. cross polarized light, B. plane polarized light, (field of view = 2.5 mm wide in each photomicrograph; Sample ID – 53-732).

*High Picrite Two (HP#2) unit, and High Picrite One (HP#1) unit*

Severson (1994) does not provide detailed descriptions of the HP#2 and HP#1. They are described here because when visibly present, they are obvious marker horizons that define the AT&T unit in an otherwise monotonous expanse of troctolitic rocks. The HP#2 unit was found only in the farthest west (MEX-53) and the farthest east (MEX-61) drill cores logged for this study and was not found in outcrop, while the HP#1 was found in drill holes MEX-53, MEX-56, MEX-60, and MEX-61 (Fig. 23). Typically, the upper contacts of both the HP#2 and HP#1 are sharp and the lower contacts are gradational on a centimeter to meter scale.

In drill core, the HP#2 and HP#1 units typically consist of a thin interval (several meters) of medium-grained, sulfide-barren troctolite inter-layered with ultramafic rocks including melatroctolite, feldspathic peridotite, peridotite, and feldspathic dunite. Petrographic study of five sections shows the dominant mineralogy to consist of 60-87% subhedral granular olivine, 0-10% subophitic to interstitial clinopyroxene, and 1-35% anhedral granular to poikilitic plagioclase. Subophitic to ophitic orthopyroxene, and interstitial biotite, and iron oxide are minor, however, up to 10% iron oxide has been noted. Sulfides have not been found in these units. Common alteration includes moderate to strong serpentine veining cross-cutting olivine grains (Fig. 46) as in the U2 and U1 units.

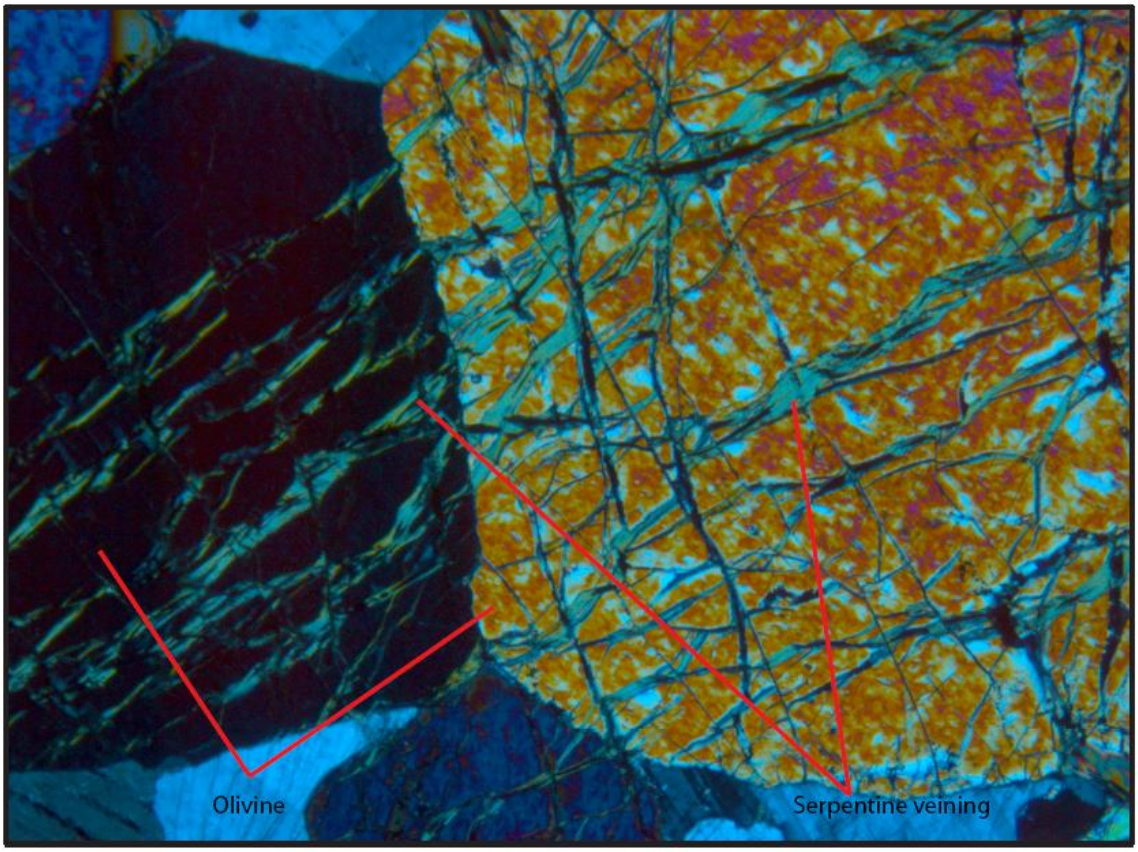


Figure 46: Serpentine veining cross-cutting olivine grains in the HP#1 unit, (field of view = 2.5 mm wide; Sample ID – 56-739).

*Anorthositic Troctolite (locally troctolite) (AT(T)) unit*

Severson (1994) describes the AT(T) unit as a monotonous zone of medium- to coarse-grained anorthositic troctolite and troctolitic anorthosite with local troctolite and rare augite troctolite. The AT(T) unit is present in nearly every drill hole logged for the study (MEX-53, MEX-56, MEX-60, MEX-55, MEX-61; Fig. 23), and abundant outcrops were observed and documented. The AT(T) unit is very similar to the AT&T unit, but constitutes a separate unit for several reasons. First, the AT(T) unit shows a subtle overall increase in plagioclase mode (~5%) from the AT&T unit. This general increase

in plagioclase is manifest by much less troctolite, and augite troctolite, more anorthositic troctolite, and by the common occurrence of troctolitic anorthosite (Pl>80%) in the AT(T) unit. The AT(T) unit is open-ended at the top with the present erosional surface. When the lower contact is marked by the HP#1, the contact is usually sharp, but when the HP#1 unit is absent, the lower contact is effectively indiscernible.

Lithologically, the AT(T) unit consists of a thick sequence of randomly alternating intervals of medium- to coarse-grained, ophitic anorthositic troctolite and troctolitic anorthosite with lesser troctolite and augite troctolite. It also contains local anorthosite inclusions and heterogeneous zones of pegmatitic anorthositic gabbro and anorthositic troctolite. Petrographic study of 13 sections showed the AT(T) unit to contain 60-87% subhedral to euhedral lath-shaped granular plagioclase, 6-26% granular to subpoikilitic to poikilitic olivine with kelyphitic rims common on poikilitic olivine, and typically 0-5% ophitic augite. Subpoikilitic and poikilitic olivine are more common in anorthositic troctolite and troctolitic anorthosite. Orthopyroxene commonly occurs as peritectic rims around olivine (Fig. 47) and locally as subophitic grains (<7%). Biotite and iron-oxide (<1% respectively) both display poikilitic and interstitial textures. The AT(T) unit is typically sulfide barren with local rare chalcopyrite greater than pyrrhotite (<0.5%).

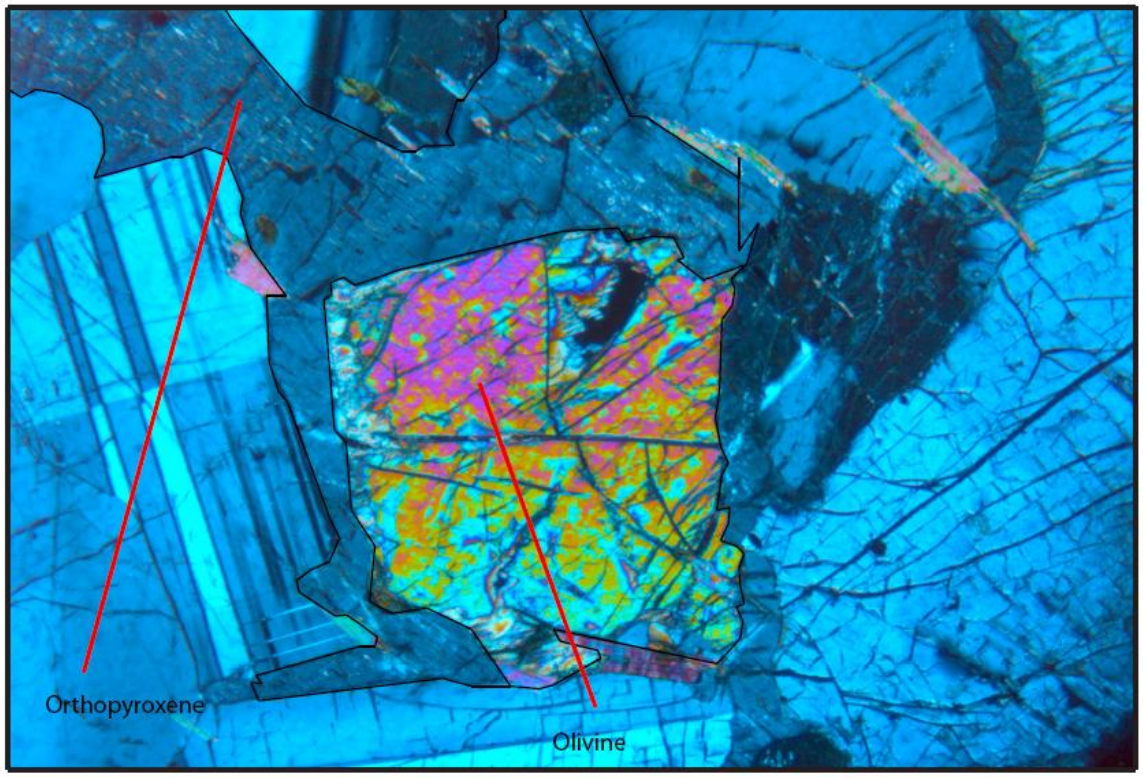


Figure 47: Orthopyroxene as a peritectic rim and subophitic overgrowth on olivine in the AT(T) unit, cross polarized light, (field of view = 2.5 mm wide; Sample ID – 53-506).

*Gabbro in Troctolite (G-in-T) unit*

The G-in-T unit is a new unit recognized in the upper zone which occurs above and adjacent to the anorthositic inclusion block. The G-in-T unit replaces Severson's (1994) Upper Peg and T-AGT units. In this study, the G-in-T unit was found in all drill cores overlying the anorthositic inclusion block (Fig. 23). It was discovered and named from outcrops found in the Spruce Road area displaying medium-grained, intergranular, olivine-rich troctolite intermixed with pegmatitic, intergranular gabbro (Fig. 48).

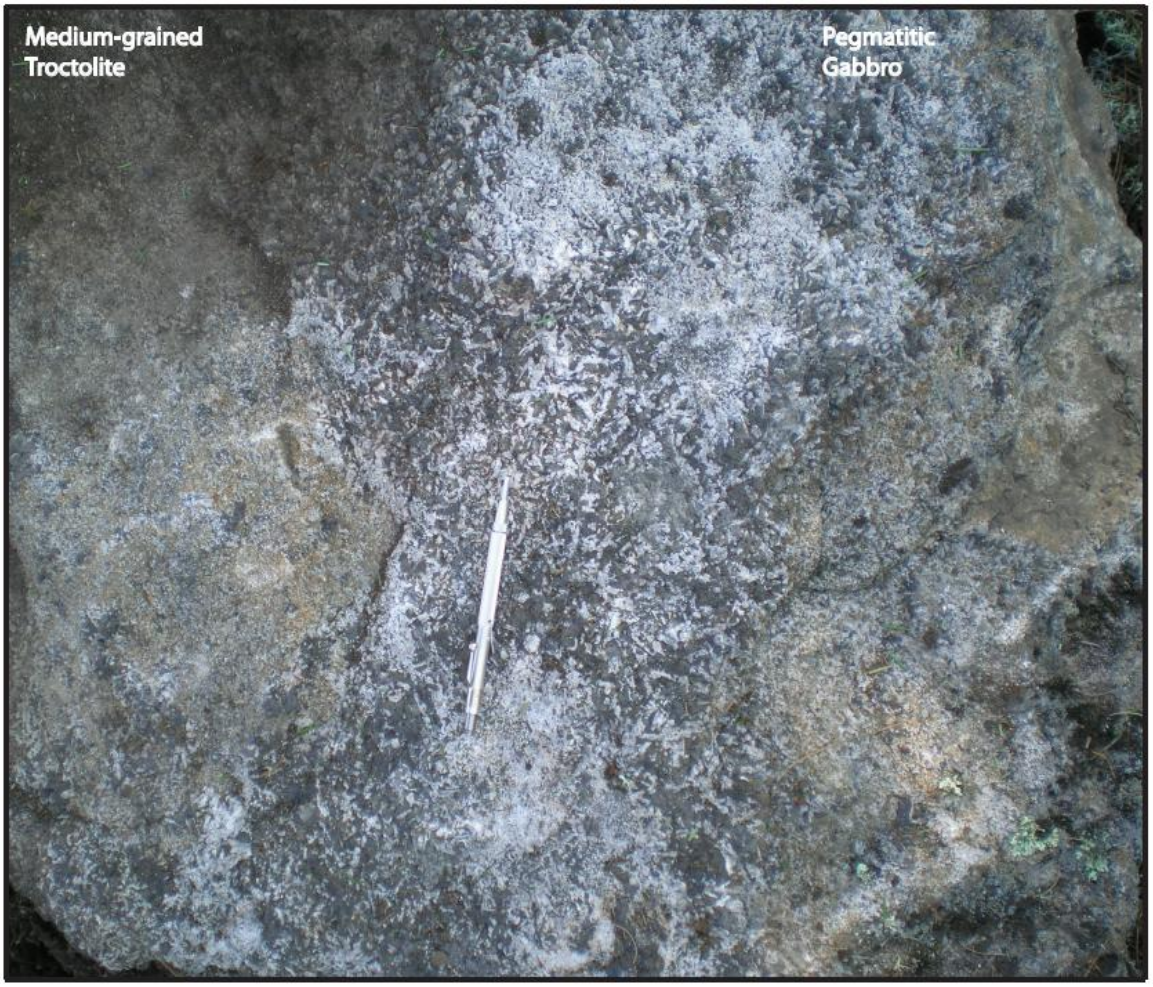


Figure 48: The G-in-T unit in outcrop featuring coarse-grained to pegmatitic gabbro intermixed with medium- to fine-grained troctolite; located in section 34 of NRRI-MAP-2008-01 (not in field area of this study).

In some drill holes (e.g., MEX-60), the G-in-T unit is overlain by the AT(T) unit across a gradational contact over several- to ten's of meters. The lower contact is sharp with the Mafic Hornfels unit. In drill core, the G-in-T unit displays a heterogeneous mix of medium-to-coarse-grained troctolite with local ophitic augite troctolite and coarse-grained to pegmatitic oxide gabbro. Petrographic study of 14 sections showed the troctolite of the G-in-T unit to be very similar to the AT(T) unit with 60-65%

equigranular plagioclase, and 25-40% granular to locally subpoikilitic olivine commonly displaying peritectic rims of orthopyroxene and locally a kelyphitic assemblage. Biotite and iron oxide occur interstitially in amounts less than 1%. Local occurrences of augite troctolite contain less than 7% granular to subophitic augite. The coarse grain size and mineralogic heterogeneity of the gabbro in the G-in-T unit makes accurate modal mineralogy estimates difficult. However, drill core and outcrops show the gabbro to contain approximately 55-70% granular plagioclase, 25-40% granular to subophitic augite, and 5-10% granular iron-oxide. Locally, granular olivine is present in amounts generally less than 5%, and rarely up to 7%. Moderate to strong uralitization and actinolite plus chlorite alteration (Fig. 49) of pyroxene and serpentinization of olivine are common.

The G-in-T unit is noted in core when heterogeneous packages of rocks occur above and adjacent to the anorthositic inclusion block, and it is found consistently above and to the northeast of the anorthositic inclusion block. The G-in-T unit is considered here to be a component of the magmatism that created the AT(T) and AT&T units. Several ideas concerning the formation of the G-in-T unit include: 1) intruding magmas ripping apart, transporting, and partially assimilating chunks of the anorthositic inclusion block creating a heterogeneous halo around the block, and 2) late stage hydrous gabbroic melts being driven off the semi-molten anorthositic inclusion block promoting the formation of the pegmatitic gabbro within the medium-grained troctolite.

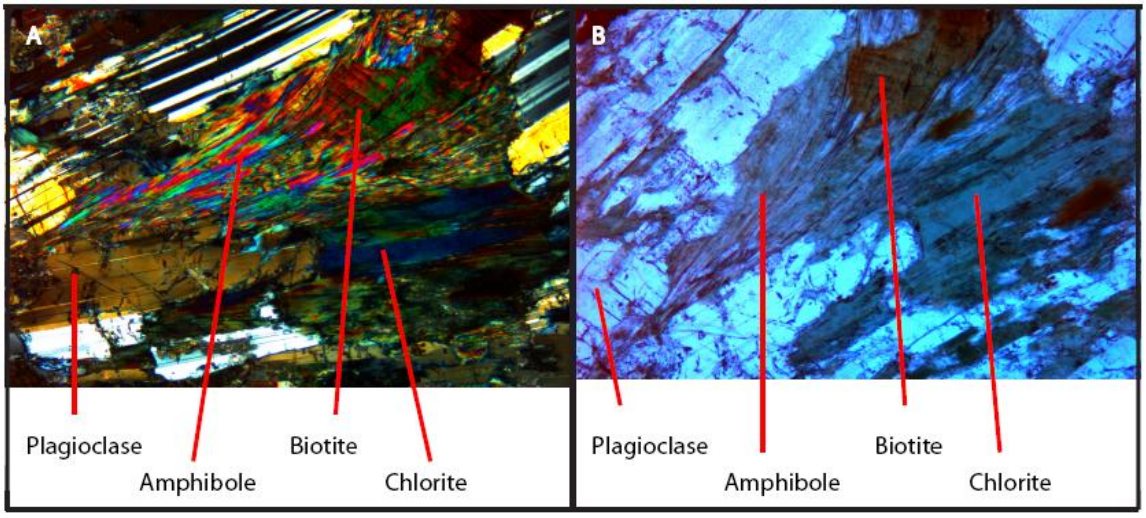


Figure 49: Actinolite and chlorite alteration in the G-in-T unit, A. cross polarized light, B. plane polarized light (field of view = 2.5 mm wide in each photomicrograph; Sample ID – 60-126).

### 5.2.6 Summary and Comparison to Severson's Lithostratigraphy

One of the main changes from Severson's (1994) lithostratigraphy for the SKI adopted in this report is the distinction of the basal contact zone and the upper zone. Severson's (1994) report hinted at distinguishing a sulfide-bearing basal contact zone from a sulfide-barren upper zone, but did not formally identify them as distinct zones. The motivation for distinguishing these zones for this study comes not only from the fact that the lower zone units are generally well mineralized, whereas the upper zone is barren of sulfide, but also that the lower contact zone occurs throughout the SKI, whereas the upper zone units do not occur beneath the anorthositic inclusion block. The observations suggest that the two zones represent very distinct episodes of magmatism. This summary section highlights other observations and interpretations made in this study that differ from, or add to Severson's (1994) igneous lithostratigraphy of the SKI.

In Severson's (1994) Hwy 1 Corridor area, which corresponds to the region overlying the anorthositic inclusion block in this study, he distinguished the Upper Peg and T-AGT units. In this study, these two units have been lumped together and renamed the G-in-T unit. This designation is based on the occurrence of an extremely heterogeneous package of rocks above and adjacent to (northeast, east) the anorthositic inclusion block. This package of rocks was found not only in drill core, but also in outcrop in the Spruce Road area. The G-in-T unit is interpreted to be associated with the AT(T) and AT&T units and likely owes its formation to assimilation and mixing with basalts, gabbros, and anorthosites of the anorthositic inclusion block.

A newly discovered unit east of the anorthositic inclusion block is the PAN unit. At the time of Severson's study there were no drill cores in this area of the SKI. This unit is interpreted as a possible second large anorthositic series inclusion to the immediate east-northeast of the anorthositic inclusion block. This finding could have important implications in Peterson's (2001) open vs. confined model of sulfide genesis since the anorthositic inclusion block is called upon to produce confined magmatic flow and concentrate metals in Peterson's model. A second large block may have also generated confining magmatic flow to concentrate metals in this area as well.

Another departure from Severson (1994) unit descriptions concerns the upper ultramafics (HP#1, HP#2), which Severson describes as thick (meters to 10's of meters) packages with multiple ultramafic horizons. This study found these units to be composed of much thinner zones (cm to meters) with very few ultramafic horizons. These much thinner, restricted and commonly absent upper ultramafics have been interpreted to

indicate major influxes of magma (Severson and Hauck, 1990; Severson, 1994; Miller and Severson, 2002) and are used to distinguish the major units of the upper zone (Main AGT, AT&T, AT(T)). The absence of these upper ultramafics in outcrop compelled Peterson (2008) to lump the AT&T and AT(T) units together as one in his map of the northern SKI.

Severson (1994) described the U3 unit as being composed of a thick (10's of meters) package of troctolitic rocks with multiple ultramafic horizons. In the study area, fewer ultramafic horizons were observed. Therefore, the U3 unit is defined here as a much more vertically restricted (5-24 m thick) unit with local layers of ultramafic rocks within the upper BH unit that may be thin bifurcations of the U3 unit.

Given these minor revisions, Severson's (1994) lithostratigraphy is remarkably valid in the study area. Table 1 presents a summary of the major characteristics of the unit lithostratigraphy identified and defined in the Nokomis deposit area. The following section presents mineral chemistry and geochemical assay data for the study area.

Table 2: Summary of the major characteristics of the lithostratigraphic units of the SKI in the Nokomis deposit area.

| **Unit** | **Dominant Modal Rock Types** | **Secondary Modal Rock Types** | **#Grain Size/ Foliation** | ***Bulk Rock Textures** | ****Alteration** | **Other Distinguishing Characteristics** |
|---|---|---|---|---|---|---|
| UPPER ZONE | | | | | | |
| **AT(T)** | Anorthositic troctolite, Troctolitic anorthosite | Troctolite, Augite troctolite | M-C/P-M | IG-Oph; locally w/ Poik Ol | Local Md KA | Abundant anorthosite inclusions, Opx rimming Ol, rare Ap |
| **G in T** | Troctolite, Oxide gabbro, Olivine oxide | n/a | T: M-C/N-P<br>G: C-P/N | T: Oph-IG<br>G: IG-SO | Md to St; Url, Act + Chl, Srp, KA | Inhomogeneous, Opx rimming Ol |

| | | | | | | |
|---|---|---|---|---|---|---|
| | gabbro | | | | | |
| **HP#1** | Troctolite, Melatroctolite, Peridotite, Feldspathic peridotite, Feldspathic dunite | Anorthositic troctolite | M/N-P-M | SO | Md to St SV | Multiple Ol-rich horizons, Separates AT(T) from AT&T |
| **AT&T** | Anorthositic troctolite, Troctolite | Augite troctolite | M-C/N | IG-Oph; locally w/Poik Ol | Local Md KA; local, St Url and Srp | Local Ap |
| **HP#2** | Troctolite, Melatroctolite, Peridotite, Feldspathic peridotite, Feldspathic dunite | Anorthositic troctolite | M-C/N-P-M | IG | Md to St SV | Multiple Ol-rich horizons, Separates AT&T from Main AGT |
| **Main AGT** | Augite troctolite | Olivine gabbro, Anorthositic troctolite, Troctolite | M-C/N | IG-Oph | Local KA, Md to Wk Url, Srp, and Ser | Local high-density SO Cpx |
| **U1** | Troctolite, Melatroctolite, Peridotite, Feldspathic peridotite, Feldspathic dunite | Anorthositic troctolite | F-M/N-P-M | IG | Md to St SV | Multiple Ol-rich layers, Within Main AGT |
| **U2** | Troctolite, Melatroctolite, Peridotite, Feldspathic peridotite, Feldspathic dunite | Anorthositic troctolite | F-M/N-P-M | IG | Md to St SV | Multiple Ol-rich layers, At base of Main AGT |
| BASAL CONTACT ZONE | | | | | | |
| **PEG** | Anorthositic troctolite, troctolite, augite troctolite | n/a | C-PEG/N | IG | Wk to Md and patchy Ser, Url, Chl, Local KA | Common high density SO Cpx Common minor Ksp, Qtz, Hb, Ap; Poorly mineralized |
| **U3** | Troctolite, Melatroctolite | Anorthositic troctolite | F-M-C/N-P- | IG | Md to St pervasive SV, | Layered; Abundant Cp, |

| | | | | | | |
|---|---|---|---|---|---|---|
| | , Peridotite, Feldspathic peridotite, Feldspathic dunite | | M-W | | local Md Url, Md Srp, and Local KA | Po, Cb, and Tal; Ol-rich horizon always at top of BH but also bifurcates down into the BH |
| **BH** | Troctolite, Anorthositic troctolite, Augite troctolite | Anorthositic gabbro, gabbro | F-M-C-PEG/N | IG-Oph | Wk to Md, locally St Srp, Ser, and Local KA | Strongly mineralized with Cp, Po, Cb, and Tal, Very heterogeneous in texture, lithology, and grain-size |
| **BAN** | Norite, Gabbro norite, Olivine gabbro | Augite troctolite | F-M-C/N | IG | Wk to St Srp, and Md to St Ser | Opx-rich with increasing mode down section, Commonly <10 cm of massive Po >>Cp at footwall contact, Locally abundant Ksp and Qtz |
| ANORTHOSITIC INCLUSION BLOCK | | | | | | |
| **Mafic Hornfels** | Mafic volcanic hornfels | n/a | F/N | Grano-blastic | n/a | Significant (<11%) Opx |
| **Upper Gabbro** | Olivine gabbro | Augite troctolite | C/N | IG | Local Md to St Url, Srp, Ser, Local KA | Commonly iron-oxide rich |
| **AN-G** | Anorthosite, Troctolitic anorthosite, Gabbroic anorthosite | Gabbro, Anorthositic gabbro, Olivine gabbro, | C-PEG/P-M-W | IG-Ol-Poik-Oph | Md to St Url, Srp, Ser, and Sausserite | Common Pl foliation |
| INCLUSIONS | | | | | | |
| **Basalt Inclusion** | Mafic volcanic hornfels | n/a | F/N | Grano-blastic | n/a | Metamorphosed pipe amygdules |
| **Anorthosite Inclusion** | Anorthosite, Troctolitic anorthosite, Gabbroic anorthosite | n/a | M-C/P-M-W | IG-Ol-Poik-Oph | Md Ser, Srp, Url | Common Pl foliation |
| **Sedimentary** | Hornfels sedimentary | n/a | F-M-C/N-P- | Grano-blastic | n/a | Commonly graphitic, |

| | | | | | | |
|---|---|---|---|---|---|---|
| **Inclusion** | rocks | | M-W | | | commonly contains massive iron-oxide |
| **PAN** | Troctolitic anorthosite | Anorthositic troctolite | M-C/N-P-M | Ol-Poik | n/a | Ol-oikocrysts <7 cm |
| FOOTWALL | | | | | | |
| **GRB** | Monzonite, Quartz monzonite, Diorite, Quartz diorite, Monzodiorite, Quartz monzodiorite | Hornblendite, Granite | M-C/N-P-M-C | Porphyritic, IG | Md Chl | Local Cp usually <1% |

*Abbreviations used in Table:*

Minerals: Ol-olivine, Pl-plagioclase, Cpx-clinopyroxene, Opx-orthopyroxene, Ox-Fe-Ti oxide, Bio-biotite, Ap-apatite, Ksp-alkali feldspar, Gp-granophyre (Ksp+Qtz), Qtz-quartz, Hb-hornblende, Cp-chalcopyrite, Po-pyrrhotite, Cb-cubanite, Tal-talnakhite

# Grain Size: F-fine, M-medium, C-coarse, P-pegmatitic
Foliation: N-nonfoliated, P-poorly foliated, M-moderately foliated, W-well foliated

* Textures: (based on Cpx habit)
IG-intergranular; SO-subophtic; Oph-ophitic
Poik-poikilitic

** Alteration: (in order of prominence)
Intensity Wk-weak; Md-moderate; St-strong
Type: Srp-serpentine after olivine, Url-uralite after pyroxene, Ser-sericite after plagioclase, Act-actinolite, Chl-chlorite, KA-kelyphitic assemblage, SV-serpentine veining

## 5.3 Whole Rock and Mineral Chemostratigraphy of the South Kawishiwi Intrusion in the Nokomis Deposit Area

This section discusses and interprets both whole-rock geochemical data obtained from Duluth Metals assay analyses and the results of mineral chemistry data from microprobe analyses within the framework of the unit lithostratigraphy described above. As discussed in previous sections, the lithostratigraphy of the SKI in the Nokomis deposit area can be subdivided into three major zones: the basal contact zone, the upper zone, and the anorthositic inclusion block (Fig. 23). Specifically, this section will present the major element lithochemical and mineral chemical attributes observed between and stratigraphically through these major zones. The stratigraphic variations in base and precious metal concentrations in the basal contact zone will also be evaluated.

### 5.3.1 Major Element Whole Rock Chemostratigraphy of the South Kawishiwi Intrusion in the Nokomis Deposit Area

As explained in the methods and results section (4.6), Duluth Metals has assayed several drill holes at roughly two-meter intervals from top to bottom (MEX-51, MEX-72; Fig. 20). MEX-51 penetrates the anorthositic inclusion block, while MEX-72 shows a complete section through the SKI to the west of the anorthositic inclusion block (Fig. 20). MEX-51 was logged for this study, but MEX-72 was not, however it was drilled roughly 200 meters northeast of MEX-53 (Fig. 20), which was logged for this study. Given the close geographic proximity of these two drill holes, the unit lithostratigraphy of MEX-53 will be used to approximate the unit lithostratigraphy of MEX-72.

The major element geochemical profiles through MEX-51 and MEX-72 provide strikingly complete record of the chemostratigraphy of the SKI and clues to the magmatic and mineralization relationships between and within the upper zone, basal contact zone, and anorthositic inclusion block. The following discussion focuses on concentrations of the major elements Mg and Ca. These two elements are chosen because they are abundantly present, and variations in their abundance have implications for changes in the modal mineralogy within the SKI and consequently its emplacement and crystallization history. In particular, Mg is a useful proxy for the variation in mafic mineral abundance (olivine and pyroxene) and Ca is a general proxy of plagioclase plus augite abundance. Figure 50 shows the stratigraphic variations in weight percent Mg and Ca in drill core MEX 51, which penetrates the anorthositic inclusion block, the basal contact zone, and the footwall. Figure 51 shows variations in Mg and Ca abundance through MEX-72, which cuts the upper zone, the basal contact zone, and the footwall.

*Footwall Contact and Basal Contact Zone*

One of the most surprising results of the major element data is that despite the sharp change in mineralogy and texture at the contact between the footwall GRB and SKI rocks (described in section 5.2.1 and 5.2.4), Mg and Ca abundances show gradational changes across the contact. Across the basal contact at a depth of about 3640 feet in MEX-51, both Mg and Ca show general trends of upward increasing concentrations (Fig. 50). Similar trends in Mg and Ca are evident across the basal contact in MEX-72 (Fig. 51). Greater than 50 meters below the basal contact, the concentration of Mg in the footwall granite is generally less than 2 %, but in the vicinity of the basal contact, the

concentration locally spikes to over 8% (MEX-51; Fig. 50). Above the contact, Mg increases steadily from about 3.5% in the BAN unit to greater than 8% in the U3 unit in MEX-51. However, in MEX-72, Mg concentration irregularly increases to a maximum of 5%.

Calcium shows an even smoother transition across the basal contact in MEX-51 (Fig. 50). Starting with concentrations of 2% to 3% in the lowest granites, Ca steadily increases starting at a depth of about 3550 feet (~30 m below the contact) to maximum concentrations of 6.5% at roughly 3350 feet deep in the upper BH unit (~30 m above the contact). The concentrations of Ca in the upper BH and U3 units become much more variable, likely reflecting the modal variability of plagioclase. In MEX-72 (Fig. 51) Ca shows a similar trend, in minimum and maximum values, but deviates from the trend below (~2900 ft) the contact and actually increases from 1% to 3%.

The gradual upward increasing trend in Mg and Ca through the sulfidic BAN, BH, and U3 units abruptly changes to a more constant compositional range in the overlying PEG unit within the two drill cores. In MEX-51 (Fig. 50), Mg shows a range of values between about 3% and 5%, with an abrupt drop at the PEG - AN-G contact. Magnesium in MEX-72 (Fig. 51) shows a similar range (3-5 %), but the upper contact with the U2 unit is less clear. Like Mg, calcium in MEX-51 shows limited variability, with values from 6-7% and a sharp break at the upper contact. Calcium in MEX-72 for the PEG unit largely remains between 5-7%, however it drops to as low as 3.5% towards the top of the unit.

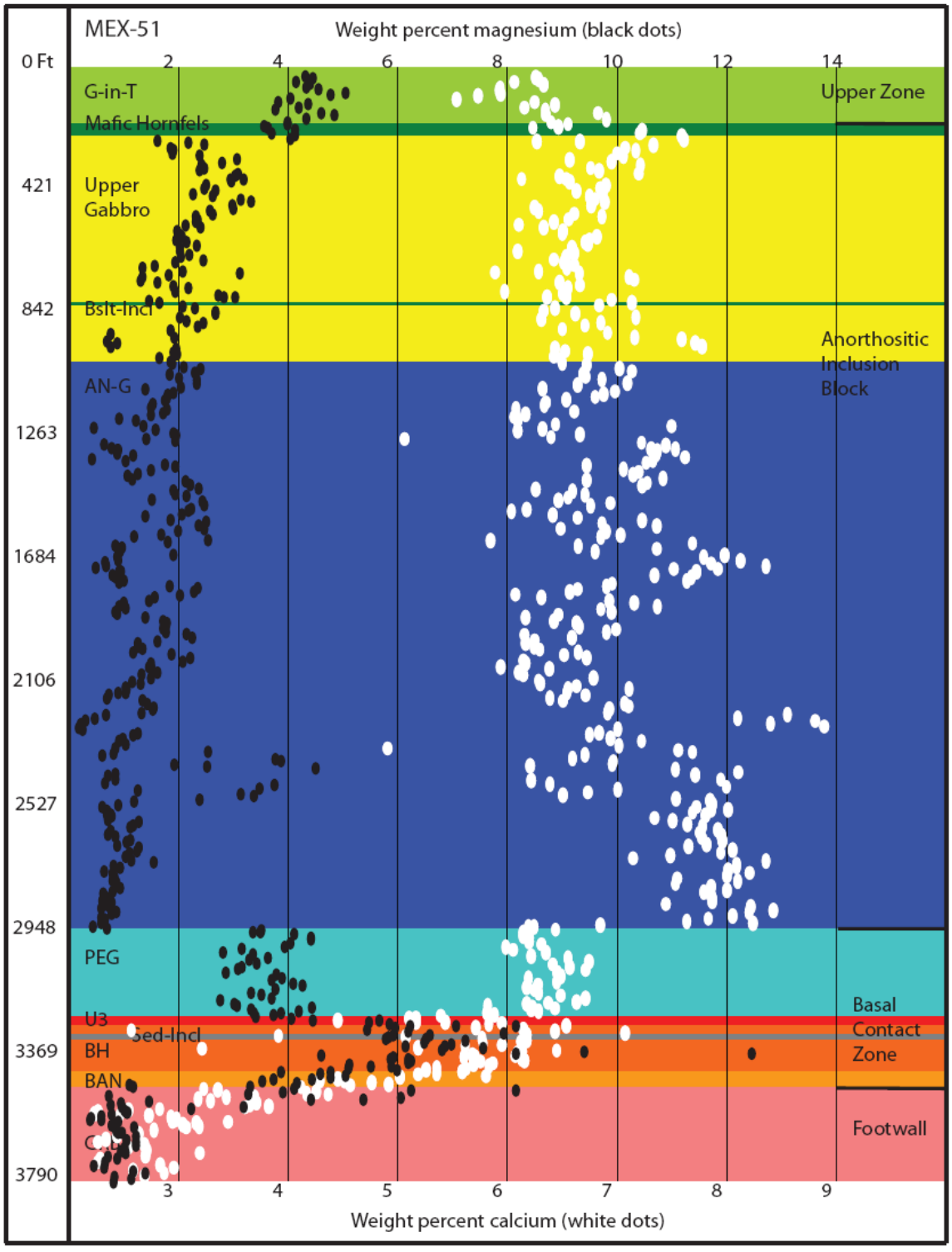


Figure 50: Whole rock concentrations (wt. %) of magnesium (black dots), and calcium (white dots) from Duluth Metals assay data for drill hole MEX-51 plotted versus depth and set against unit lithostratigraphy.

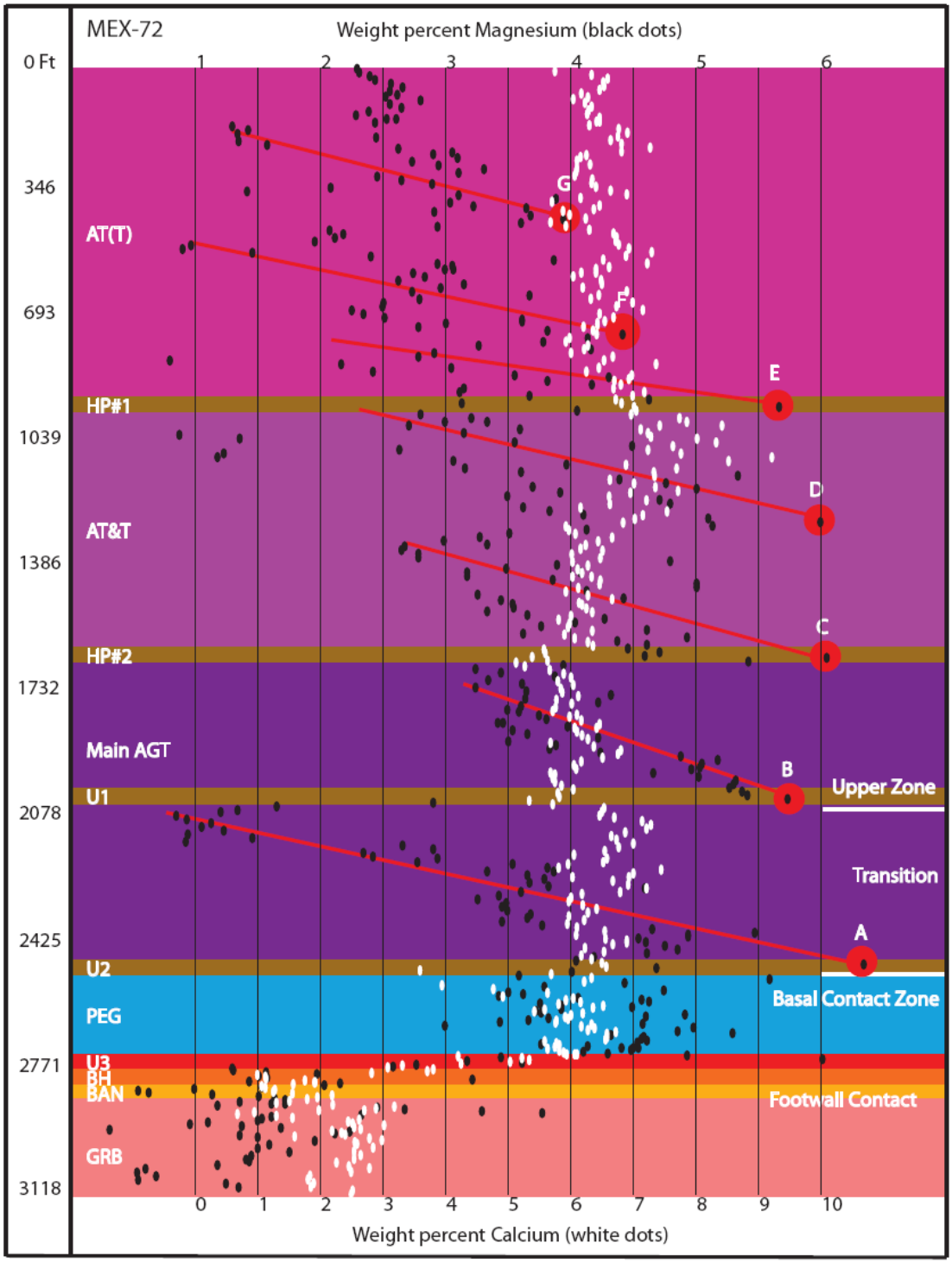


Figure 51: Whole rock concentrations (wt. %) of magnesium and calcium from Duluth Metals assay geochemistry data for drill hole MEX-72 plotted against depth. Large red dots mark magnesium maximums and red lines projecting from red dots show upward decreasing magnesium trends. Unit lithostratigraphy is approximated from MEX-53 as explained in the text.

*Anorthositic Inclusion Block*

Variations in Mg and Ca concentrations through the remainder of MEX-51 portray significant differences between the basal contact zone of the SKI and the anorthositic inclusion block (Fig. 50). The base of the anorthositic inclusion block (@~2950 ft) is chemically defined by a sharp increase in Ca and decrease in Mg. These changes obviously reflect the abrupt mineralogic changes at the PEG - AN-G contact, in particular, the increased abundance of plagioclase in the anorthositic gabbro and a complimentary decrease in mafic mineral abundance.

The upper contact between the anorthositic inclusion block and the upper zone of the SKI (@~200 ft) displays a similar, but reversed break. Here, the Upper Gabbro and Mafic Hornfels units of the anorthositic inclusion block are overlain by the heterogeneous G-in-T unit of the SKI. A sharp (~3%) change in Mg concentration occurs between the Upper Gabbro and Mafic Hornfels units. This is followed by a gradual increase through the contact (between the Mafic Hornfels and G-in-T units), which continues upward through the G-in-T unit to the top of the hole. The Ca profile (Fig. 50) displays comparatively similar, but as would be expected, reversed trends with increased Ca in the plagioclase-rich anorthositic inclusion block both above and below the anorthositic inclusion block.

*Upper Zone*

Magnesium concentrations in drill hole MEX-72 display an interesting series of cyclical trends in the upper zone when plotted versus depth (Fig. 51). At least seven cycles of upwardly decreasing Mg concentrations (Fig. 50, red lines) emanating from

maximum Mg values of ~4-6% (Fig. 51, red dots) can be discerned beginning at the base of the upper zone (~2050 ft). The trends generally begin in accordance with an ultramafic horizon (U2, U1, HP#2, HP#1; Fig. 51 trend lines A, B, C, E).

*Interpretations of Whole Rock Chemostratigraphy*

The ~60-meter-thick, chemically gradational (Mg and Ca profiles) interval that straddles the lithologically sharp basal contact is actually consistent with changes in lithologies present on either side of the contact. The granitic footwall develops intermediate compositions (quartz monzodiorite) in the immediate footwall and the basal contact zone rocks become dominated by biotitic norite (see Section 5.2). These chemical and lithologic changes across the contact also bracket a zone of fairly consistent Cu-Ni sulfide mineralization (~0.3%). Collectively, these chemical and lithologic attributes seem best explained as having resulted from partial melting of the GRB by the SKI magmas. Upward infiltration of siliceous and volatile-rich anatectic melts from the granite would result in the stabilization of orthopyroxene and biotite in the basal SKI and would leave behind a more intermediate residual composition in the GRB contact zone. The influx of silica into the already sulfide-saturated mafic magma would further lower its sulfide carrying capacity and thus promote further liquation of sulfide from the magma. Some of this dense sulfide liquid evidently infiltrated downward into the granite, perhaps by a *lit par lit* replacement process contemporaneous with upward infiltration of anatectic melts.

The abrupt change in smooth compositional trends evident in the footwall and lower basal contact zone at the U3 - PEG contact is more difficult to explain. Perhaps,

rising fluids or siliceous melts emanating from both the footwall and SKI magmas below became trapped in the PEG unit by the overlying anorthositic series beneath which the basal contact zone was emplaced. For this explanation to be plausible the same signature should be observed for the basal contact zone in the Mg profile for MEX-51 (Fig. 50), and for MEX-72 (Fig. 51). The two basal contact profiles bear striking resemblance (Fig. 50, MEX-51; Fig. 51, MEX-72), showing significant breaks in compositional trends at the U3 - PEG contact. Basal contact zone Mg concentrations are quite similar beneath both the anorthositic inclusion block and beneath the upper zone{MEX-51 (3-5%), MEX-72 (2-5%)}, while Ca concentrations dip to ~4% in MEX-72 (beneath the upper zone) with a slightly upward decreasing trend, and remain fairly static (6-7%) in MEX-51 (beneath the anorthositic inclusion block). These similar whole-rock geochemical trends in the basal contact zone in two very different environments seem to support that initially the anorthositic series capped the entire basal contact zone, and that the SKI was emplaced at the boundary between the granitic GRB footwall and the anorthositic series hanging wall. Sharp jumps in (~3%) Mg and (~ 1-2%) Ca corresponding to the upper and lower lithologic contacts between the SKI and the anorthositic inclusion block unquestionably confirm the presence of a large exotic mass residing within the SKI stratigraphy, which was likely derived from the anorthositic series of the Duluth Complex. These chemical and lithologic data strongly support suggestions (Severson, 1994; Peterson, 2001, Miller and Severson, 2002) that SKI magmas intruded beneath and lifted a large block of anorthositic series rocks up delaminating them from the GRB rocks below.

As already discussed in Section 5.2.5, the lithologic attributes of the heterogeneous G-in-T unit situated above the anorthositic inclusion block is thought to have formed by either (1) intruding upper zone magmas which detached, transported, and partially assimilated parts of the anorthositic inclusion block, (2) evolved magmas from the partially molten anorthositic inclusion block which rose up into and mixed with the overlying SKI magmas, or (3) that some combination of both processes may have produced the heterogeneous halo observed around the perimeter of the anorthositic inclusion block. The Mg and Ca abundances in the G-in-T unit show a distinct break from those abundances in the anorthositic inclusion block and the variability in abundances are not as great as the heterogeneity of the unit might predict. Nevertheless, there is a gradational change up through the G-in-T that is consistent with mixing between an anorthositic component and a more mafic component similar to the upper zone chemistry/mineralogy, with the mafic component becoming more prevalent up-section.

Upward decreasing Mg trends in MEX-72 (Fig. 51) may indicate that the upper zone of the SKI was formed by episodic emplacement of mafic magmas that were given time to cool and fractionate prior to subsequent magma recharge. The generally homogeneous mineralogic and textural character of the Upper Zone rocks, save for the thin ultramafic intervals, and their lack of significant sulfide mineralization suggest that such repeated inputs of upper zone magmas did not create physically turbulent and chemically chaotic conditions within the resident magma chamber, unlike recharge events which likely created the heterogeneous, sulfide-bearing basal contact zone. The

reason for this difference in emplacement dynamics probably relates in part to the thermal maturity of the SKI intrusive environment due to pre-heating by the basal contact zone and to the "drying out" and isolation of potential wall rock contaminants by previous intrusions through the SKI feeder conduits.

The interpretation that the cyclical variations in Mg concentration in the upper zone (Fig. 51) reflect the progressive differentiation of successive inputs of magma is by no means definitive. Indeed, the cyclical increases in Mg may instead, or additionally, indicate cyclical variations in the modal ratios of plagioclase to olivine in the troctolitic rocks. These modal variations could be created by periodic convective overturn of the magma chamber such that higher density olivine settles to the floor of the chamber faster than lower density plagioclase. If this were the case, however, one would expect to see a complimentary increase in Ca concentration as Mg decreases, which is not obvious in figure 51. Unfortunately, the effect of clinopyroxene concentration in the rocks also affects the whole rock MgO and CaO concentrations. Determining the process that best accounts for the cyclical variation in Mg concentration may be better tested by evaluating the cryptic variation in the magnesium number (Mg/(Mg+Fe), mole %) of mafic minerals, particularly olivine. Magmatic differentiation and recharge should leave a clear signature in the cryptic variation of mafic minerals, whereas compositional variations due to convective overturn should be minimal. This will be evaluated in the next section.

### 5.3.2 Cryptic Variations in Olivine, Pyroxene, and Plagioclase Compositions

Unlike whole rock concentrations of Mg and Ca from assay geochemistry, mineral chemistry data of forsterite, enstatite, and anorthite content are independent of any modal mineral proportions. Instead, these mineral compositions represent a better proxy for the degree of magma differentiation, because they inherently relate to the chemistry of the magma at the time of crystallization, assuming equilibrium conditions. It is important, though, to bear in mind that the SKI is largely composed of cumulate rocks, and thus all chemical variations are subject to the combined effects of cumulus and post-cumulus processes. This section discusses the chemical compositions of olivine, pyroxene, and plagioclase, how these mineral chemistries compare to the whole rock data discussed in the previous section (5.3.1), and what this data implies as to possible processes of magmatic emplacement, differentiation, convective overturn, and other phenomenon. Because the focus of this study is on the sulfide-bearing basal contact zone, only a cursory evaluation was made of cryptic variations through the upper zone in one drill core (MEX-53, Figs. 52 & 53). Mineral chemical data from six drill cores profiling the basal contact zone (Figs. 54 and 55) are used to evaluate not only stratigraphic variations in this zone, but also lateral changes across the Nokomis deposit area.

The average compositions of olivine, clinopyroxene, and plagioclase were calculated from 10 to 15 analysis points on each thin section sample. Olivine and pyroxene compositions are reported respectively by their Fo and En' contents (= Mg/(Mg+Fe)*100, cation%). Plagioclase is reported in terms of its An content

(=Ca/(Ca+Na+K)*100, cation%). In the plots below, olivine and clinopyroxene data are plotted by their average and standard deviation. In contrast, all plagioclase analyses are plotted. This is done because plagioclase is typically significantly zoned. A line is drawn connecting the most calcic compositions because these generally correspond to the core composition of the zoned plagioclase, and thus should be most representative of variations in the parent magma composition. A rare exception occurs when a group of analyses includes a lone analysis of significantly higher An content. These anomalous compositions may correspond to xenocrystic plagioclase or to some recrystallized portion of plagioclase (e.g., An content commonly increases due to plagioclase symplectite formation), and are not included in the profile.

*Cryptic Layering in the Upper Zone*

Sample spacing in the upper zone was sparse and predominantly focused on the contacts between units with subtle in-fill sampling conducted within major units to provide control points. Sampling was conducted largely at unit contacts in order to better evaluate whether these contacts represent major magma recharge events as concluded by Severson (1994). In drill hole MEX-53 (Fig. 52), these contacts are well defined by the presence of the ultramafic units (U2, U1, HP#2, HP#1), with all four ultramafic units both found in drill core, and sampled for mineral chemical analysis. The U2 and U1 units, located at the base of, and within the Main AGT unit, respectively are rather non-descript chemically, not differing much if at all from analyses in the basal contact zone below (Fig. 52), or from the hosting Main AGT unit. However, the HP#2 and HP#1 units, which represent the bases of the AT&T and AT(T) units, respectively, are

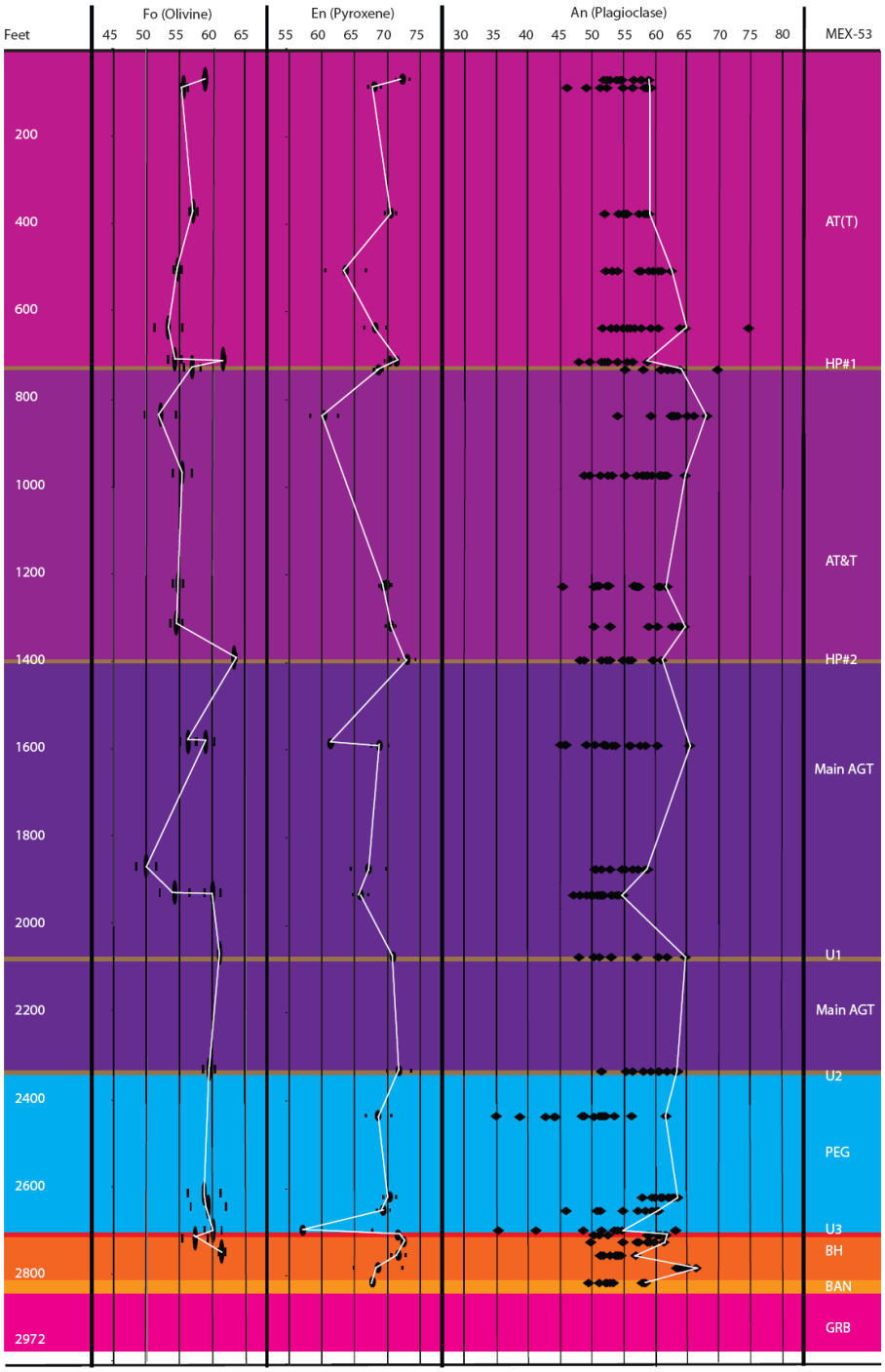


Figure 52: Forsterite (Fo) content in olivine, enstatite (En') content in pyroxene, and anorthite (An) content in plagioclase from microprobe data obtained from drill core MEX-53. Large black ovals show average Fo and En' contents; smaller ovals show one standard deviation of variation among multiple analyses; white line connects average compositions. All individual analyses of An content are shown for the plagioclase data with the white line connecting to most An-rich compositions (see text for discussion).

distinctive in their increased mg# contents of olivine and clinopyroxene, and their decreased An contents of plagioclase. Olivine composition increases 7-8% in Fo from the troctolite below upward into the ultramafic units, while clinopyroxene composition increases about 5% in En content. Conversely, plagioclase composition decreases at these horizons by about 5% An. Cryptic variations in mineral chemistry within the major upper zone units (Main AGT, AT&T, AT(T)) are best evaluated in concert with the whole rock Mg data (Fig. 53).

The whole rock Mg profile from drill hole MEX-72 is scaled to a best fit with the cryptic variation in Fo content measured from olivine in MEX-53 in Figure 53. Upward from the U1 unit in the middle of the Main AGT unit (Fig. 53, point A), a smooth decrease in Mg whole rock concentration is generally matched by a decrease in Fo content from 61% to 51% defined by 3 samples. An analysis of Fo in the upper Main AGT unit falls in line with another trend of decreasing Mg emanating from point B in Figure 53. This second Main AGT trend is truncated by the HP#2 unit with a third (Fig. 53, point C) upward decreasing trend in Mg through the lower AT&T unit that also has decreasing Fo contents (~1400 ft). Olivine compositions in higher parts of the upper zone generally fall in line with the Mg whole rock data but the sample spacing is insufficient to show progressive trends. In the AT(T) unit, Fo contents of olivine remain similar to those found in the AT&T and Main AGT unit below, but whole rock Mg abundance, while still cyclic in nature, shows overall lower values. This decrease in the whole rock Mg abundance of the AT(T) unit may reflect the fact that the AT(T) unit

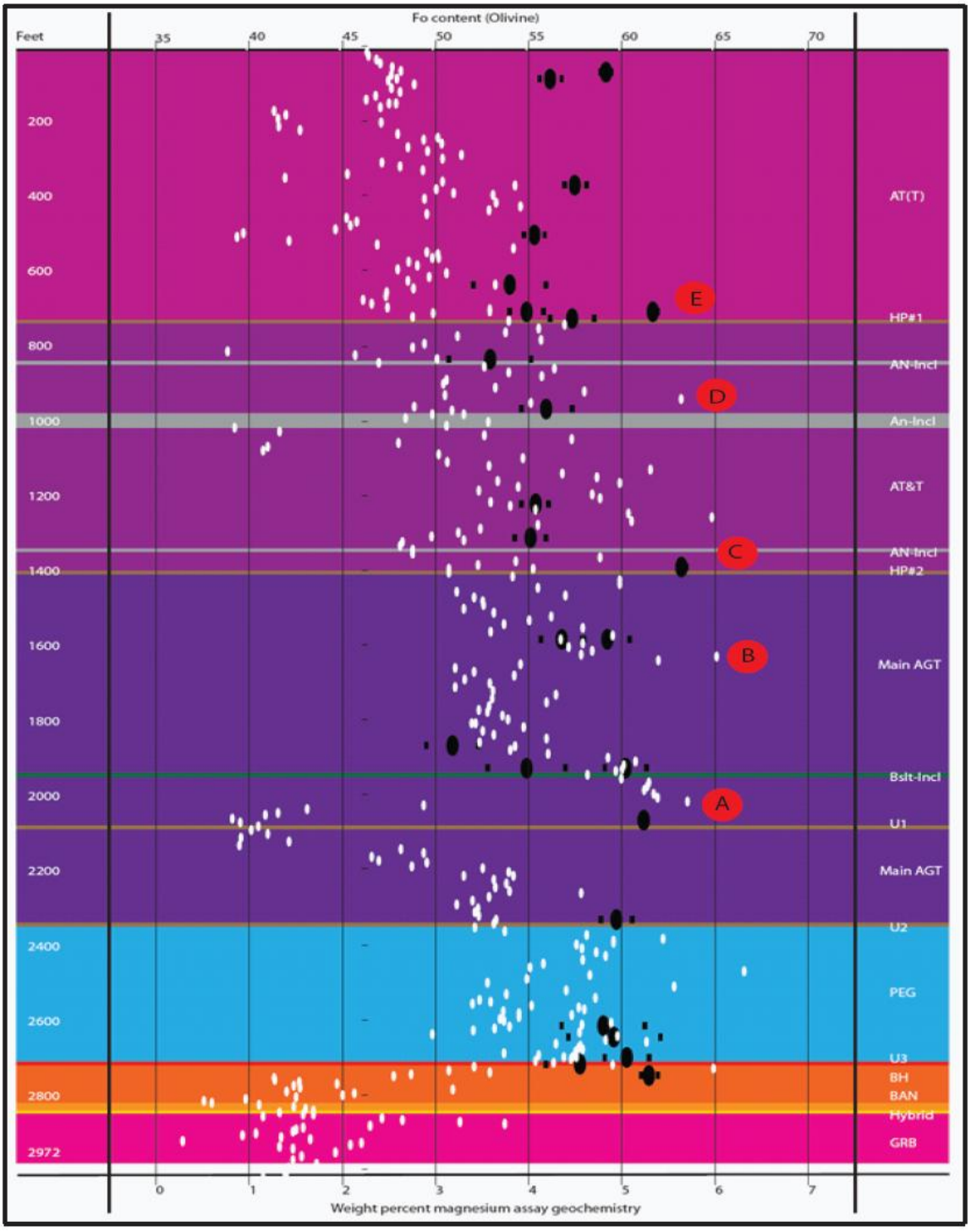


Figure 53: Fo content of olivine (black ovals) from MEX-53 and magnesium whole rock abundance (white dots) from MEX-72 plotted against the unit stratigraphy for MEX-53.

contains less modal augite and olivine and greater plagioclase abundance than the AT&T unit. It should also be kept in mind that the mineral chemical data and the whole rock data are from different, albeit proximal, core. Samples collected from the upper ultramafic horizons, HP#1 (53-713.5; Appendix II) and HP#2 (53-1395; Appendix II) show these units to have increased forsterite and enstatite compositions (Fig. 52) in comparison to adjacent troctolite in the units that they constrain (AT(T) and AT&T). The olivine-rich lithologies of these units (5.2.4), the apparent fractionation trends displayed by whole rock Mg abundances (Figs. 51 & 53), and the mineral chemistry data (Figs. 52 & 53) are all consistent with the interpretation put forth by Severson (1994) that these horizons more likely represent magmatic recharge events, than the products of convective overturn and graded accumulation of olivine. The absence of olivine-rich horizons corresponding to several peaks in Mg (e.g., Points B & D Fig. 53) may indicate that magma recharge did not always involve an overproduction of olivine crystallization or the input of phenocrystic olivine.

Interestingly, anorthite contents in plagioclase for these ultramafic horizons decrease (Fig. 52). Given the poikilitic texture of plagioclase in the melatroctolitic intervals, a possible explanation for their lower An content is that they crystallized as intercumulus minerals from evolved magmas trapped in the olivine-rich cumulus framework. A second possibility could be that the magmas forming the HP#1 unit (and the AT(T) unit) intruded just below the top crystallization front of the AT&T unit, causing the residual melt of the HP#1 unit (and the AT(T) unit) to mix with the evolved

melt of the AT&T unit below, lowering the anorthite content of intercumulus plagioclase slightly.

Both of the above ideas assume constant modal amounts of pyroxene. If pyroxene were to increase above average modal percentages in these samples, the decrease in anorthite content could be attributed to contemporaneous crystallization of pyroxene and plagioclase with pyroxene then accounting for some of the Ca that should be in the plagioclase. However, the modal percentage of pyroxene does not increase above average pyroxene modes of the intrusion for these samples (Appendix II; 53-713.5; 53-1395), therefore the decrease in anorthite content (Ca) in plagioclase is likely not attributable to an increase in pyroxene mode. This idea is only relevant in the microenvironment of trapped liquid, where intercumulus clinopyroxene and plagioclase would both compete for the Ca present, whereas in a crystallizing body of magma there would be ample Ca for both minerals crystallize.

*Cryptic Layering in the Basal Contact Zone*

Although a greater density of samples were analyzed for their mineral chemistry in the basal contact zone, the stratigraphic cryptic variations indicated are less systematic and thus more difficult to interpret than their upper zone counterparts. The stratigraphic variations in Fo content of olivine and the An content of plagioclase are plotted along with whole rock compositions of Mg and Ca into two figures here. Figure 54 shows data from core that profiles the basal contact zone where it is overlain by the upper zone. Figure 55 shows core data that profiles the basal contact zone where it is capped by the anorthositic inclusion block. When comparing these plots it is evident that these two sets

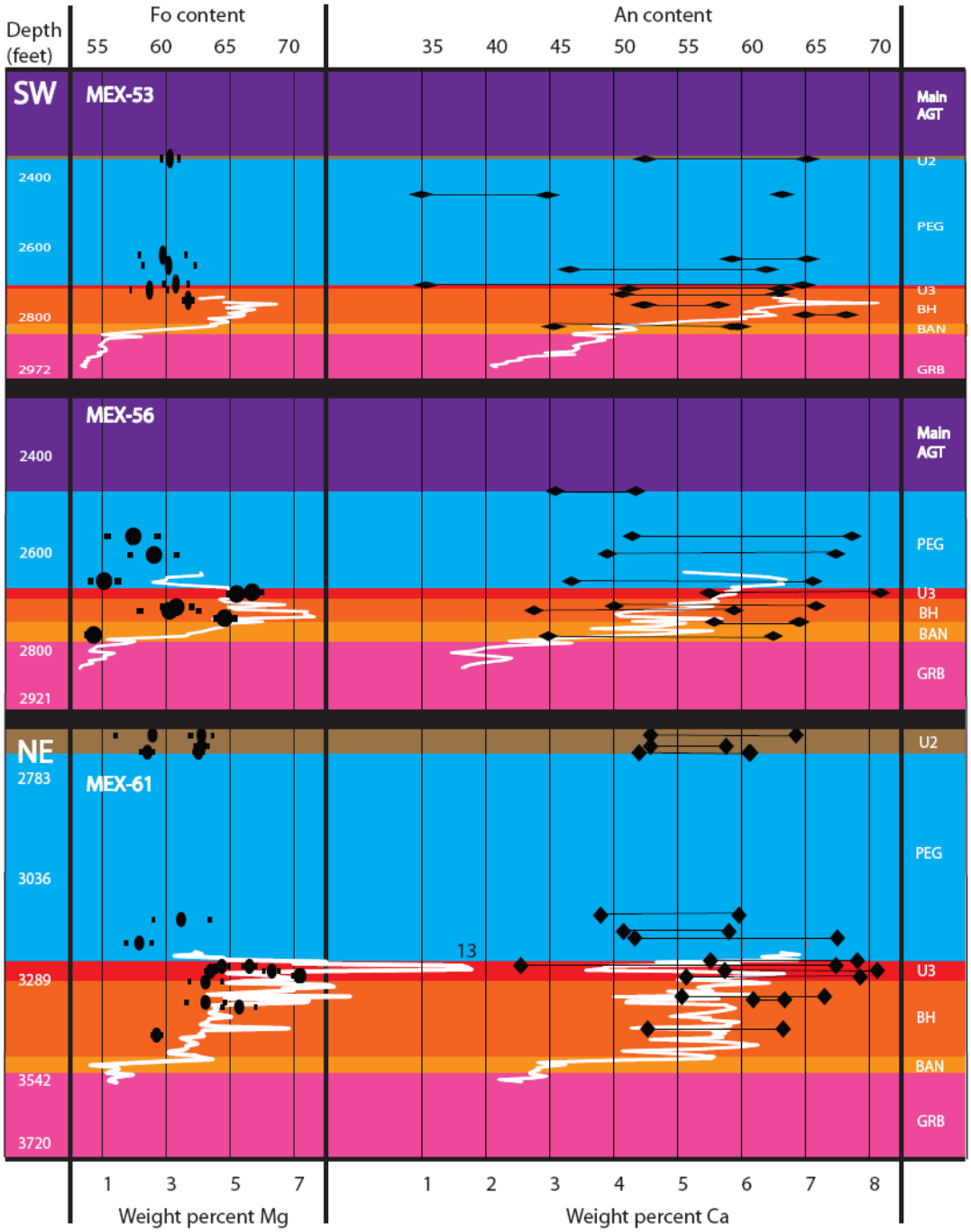


Figure 54: Stratigraphic variation in Fo contents of olivine, An contents of plagioclase and whole rock Mg and Ca abundance, through drill cores MEX-53, MEX-56, and MEX-61, which profile the basal contact zone where it is overlain by the upper zone. Fo and An data shown by black symbols; Mg and Ca abundances indicated by white curves. Olivine data shows average (large oval) and standard deviation (small ovals) of multiple (10-15) microprobe analyses per sample. Two black diamonds connected by a line indicates the range of An content measured from each specific sample. Vertical scales for all three core profiles are approximately equal.

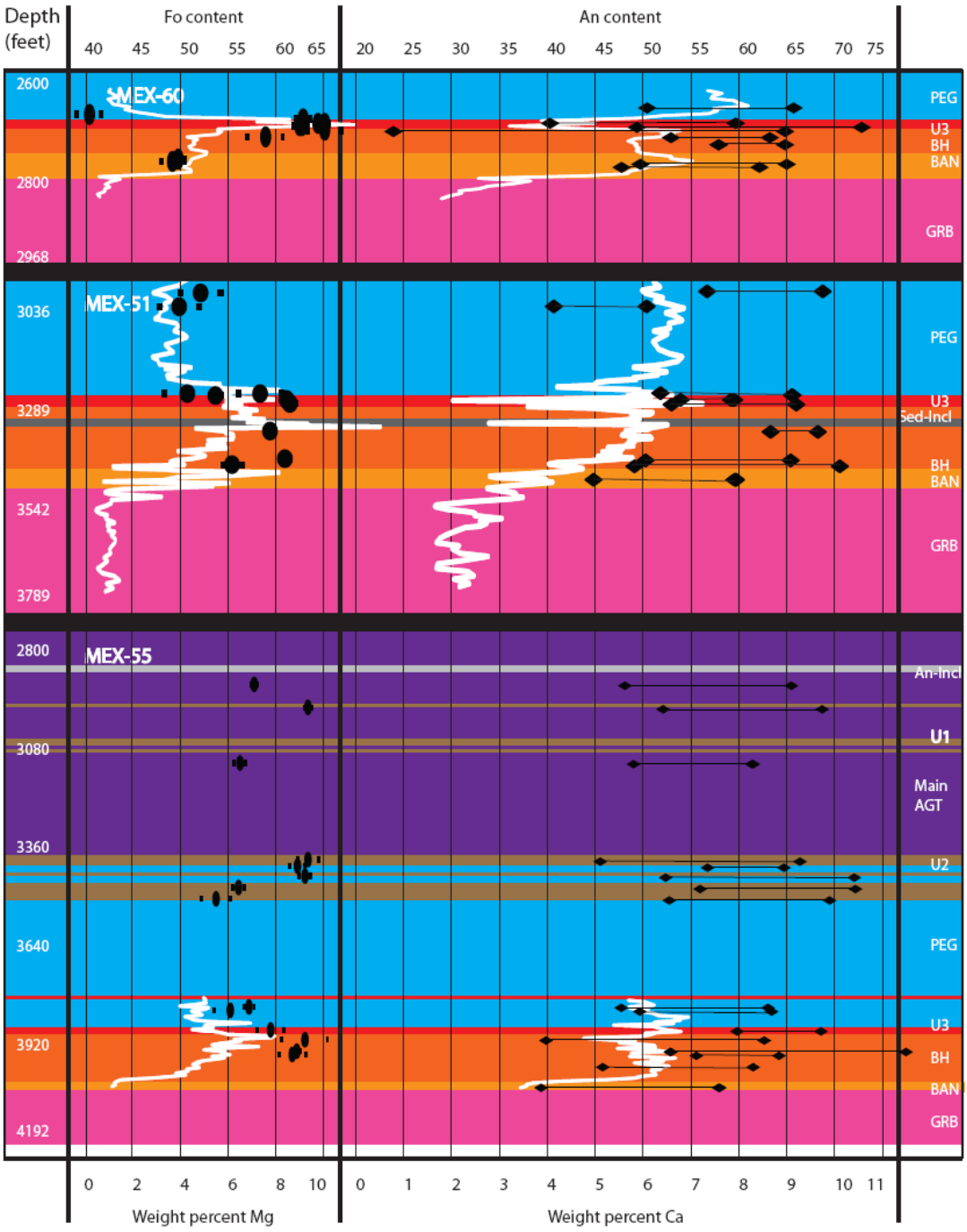


Figure 55: Stratigraphic variation in Fo contents of olivine, An contents of plagioclase and whole rock Mg and Ca abundance, through drill cores MEX-60, MEX-51, and MEX-55, which profile the basal contact zone where it is overlain by the anorthositic inclusion block. Fo and An data shown by black symbols; Mg and Ca abundances indicated by white curves. Olivine data shows average (large oval) and standard deviation (small ovals) of multiple (10-15) microprobe analyses per sample. Two black diamonds connected by a line indicates the range of An content measured from each specific sample. Vertical scales for all three core profiles are approximately equal.

of geochemical profiles do not show any obvious difference in geochemical trends from one setting to the other with regard for the basal contact zone.

Although not obvious at first glance, the geochemical profiles of Fo content and whole rock Mg abundance through the basal contact zone show several consistent trends (Figs. 54 and 55). First, the PEG unit typically contains some of the lowest Fo contents (40-60%) in the BCZ. Second, there is typically a peak in both Fo content of olivine (60-72%) and whole rock Mg in, or just below, the U3 unit. Third, both Fo content of olivine (48-61%) and whole rock Mg are highly variable in the BH unit until both sharply decrease downward into the BAN.

Anorthite content of plagioclase and whole rock Ca concentrations show no obvious systematic variability in profile compared to Fo and Mg data. Shown in Figures 54 and 55 are the maximum and minimum values of An content in plagioclase determined by multiple (10-15) microprobe analyses per sample. The spread of values for all samples (up to 40% An) highlights the well zoned nature of plagioclase in all units. Assuming that the most An-rich compositions generally represent the cumulus cores of the plagioclase, the maximum An data do not show any obvious trends through the basal contact zone units. Nor do the An data show obvious correlation with the whole rock Ca data. This is perhaps not surprising since Ca whole rock abundances are affected by augite mode, which is significant and variable in basal contact zone rocks. Although there is less petrologic information that can be gleaned from the plagioclase data compared to the olivine data, it is generally true that plagioclase in the U3 unit tends to have high maximum An (65-73%) which correlates with relatively high Fo contents of

olivine. Also, the variability of Fo in the BH unit is matched by the An data. One significant difference is that the maximum An content in the PEG unit does not decrease as much as the Fo content of olivine.

While some of the highest Fo contents are found in the U3 unit (Figs. 54 and 55), the highest concentrations of Mg do not always correspond to the highest Fo values. Instead, the highest Mg concentrations are sometimes found just below the U3 unit. These peak Mg concentrations could indicate an increase in clinopyroxene at these horizons, however if that were the case we would expect to see a complimentary increase in Ca at these horizons. Instead, there is generally a decrease in Ca accompanying the maximum Mg concentrations. Regardless, it is reasonable to conclude that the high Fo olivine comprising the U3 unit (up to $Fo_{71}$) likely represents the most primitive magmas associated with the SKI.

The high variability observed in all facets of the geochemical data from the BH unit match the physical heterogeneities described in the textures, grain-sizes, and rock types of this unit, its abundance of xenoliths, and obvious evidence for footwall contamination (sulfide, hydrous mineral phases, and orthopyroxene). This heterogeneity is consistent with the generally held idea that the BH formed from multiply emplaced, variably contaminated magmas and crystal-laden mush, which incorporated abundant country rock and autolithic inclusions as it passed into the SKI magma chamber (Severson, 1994; Miller and Severson, 2002; Peterson, 2006).

### 5.3.3 Chemostratigraphy of Copper, Nickel, and Platinum Group Elements in the Basal Contact Zone

This section discusses the stratigraphic variations in copper (Cu), nickel (Ni), and platinum group element (PGE = platinum, palladium, and gold) abundances and their relationships to major element geochemistry and the lithostratigraphy of the basal contact zone. Cu-Ni-PGE sulfide mineralization occurs in all basal contact zone units except the PEG unit (and the rare exception of the U3 unit in drill hole MEX-53), where sulfide is typically rare (<1%) to absent (Figs. 56 & 57). Significant sulfide mineralization may also occur in the immediate granitic footwall. A general clue into the chemostratigraphic variance of metals concentrations in the basal contact zone and footwall come from the stratigraphic distribution of sulfide minerals observed during core logging. The sulfide mineralogy consists dominantly of copper-rich minerals (chalcopyrite, cubanite, talnakhite) toward the top of the mineralized zone, with a decrease of these minerals and an increase in iron- and nickel-rich sulfides (pyrrhotite, pentlandite) towards the base of the mineralized zone. Chemostratigraphic profiles of copper and nickel concentrations (Figs. 56 & 57) agree with this observed stratigraphic variation in sulfide mineralogy.

In general, concentrations of Cu, Ni and total PGE's through the basal contact zone units tend to vary congruently. In detail, however, there are some distinct trends and variations to the peak concentrations. In sections overlain by the upper zone, Cu typically spikes near the top of the mineralized section, whereas Ni peaks toward the bottom (Fig. 56). In contrast, Cu and Ni concentrations vary similarly in basal contact zone sections overlain by the anorthositic inclusion block (Fig. 57). Here, both metals

show peak concentrations at both the top and bottom of the mineralized section. Total PGE concentrations in both settings seem to more closely follow Cu trends (Figs. 56 & 57).

A rather enigmatic feature of the chalcophile element chemostratigraphy is that peak concentrations in Cu, Ni, and PGE do not seem to be closely associated with any specific lithostratigraphic unit. In some cases (e.g. MEX-55, 60, & 61) the peak Cu and Ni occurs in the vicinity of the U3-BH contact. In other cores (e.g., MEX-51, 53, & 56), the highest grades occur in the BH unit. Curiously, Cu and Ni grades in the granite footwall range from negligible to significant, with the best mineralization seeming to occur when the peak mineralization in the basal contact zone occurs in the BH unit (e.g, MEX-51, 53, & 56), rather than the U3 unit. Additionally, the highest Cu and Ni grades appear to generally correspond to intervals enriched in olivine with high Fo contents (correlating to elevated Mg concentrations in Figs. 56 & 57).

These trends indicate a complicated history of Cu-Ni-PGE sulfide mineralization that may have involved sulfide fractionation, R-factor upgrading by resurgent magma pulses, and secondary remobilization by hydrothermal fluids. It is clear that all magma that created the basal contact zone, save probably the PEG unit, were sulfide oversaturated upon emplacement into the SKI chamber. The subtle zonation of predominantly Ni- and Fe-rich sulfides in the lower part of the basal contact zone and Cu-sulfides and PGE minerals in the upper part of the BH and into the U3 unit (Figs. 56 ad 57) suggests that fractionation of sulfide melt may have been involved. Nickel is

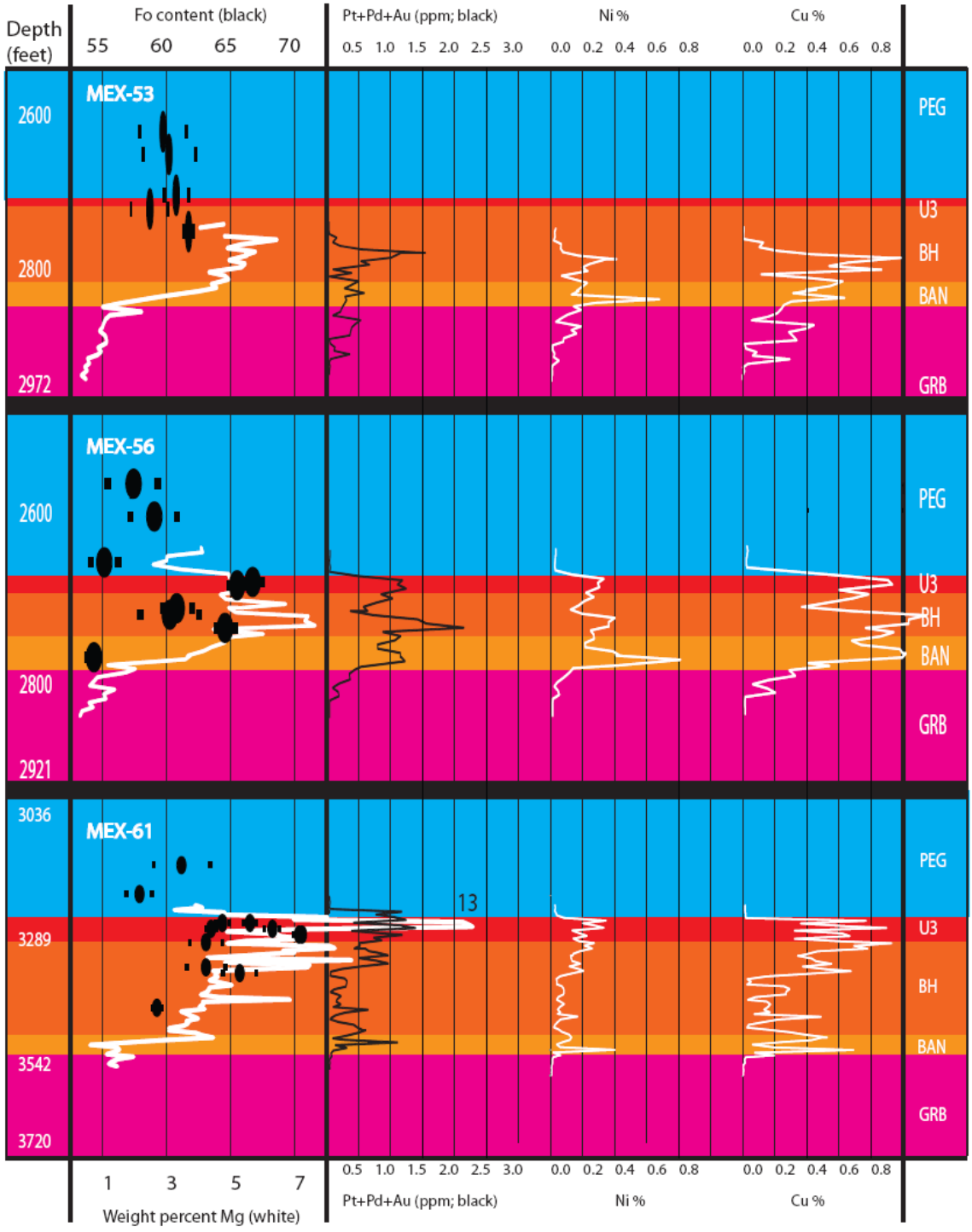


Figure 56: Stratigraphic variation in copper, nickel, and total PGEs concentrations in the basal contact zone where overlain by the upper zone and profiled in drill holes MEX-53, MEX-56, and MEX-61; Whole rock concentrations of Mg and forsterite content of olivine are shown for comparison.

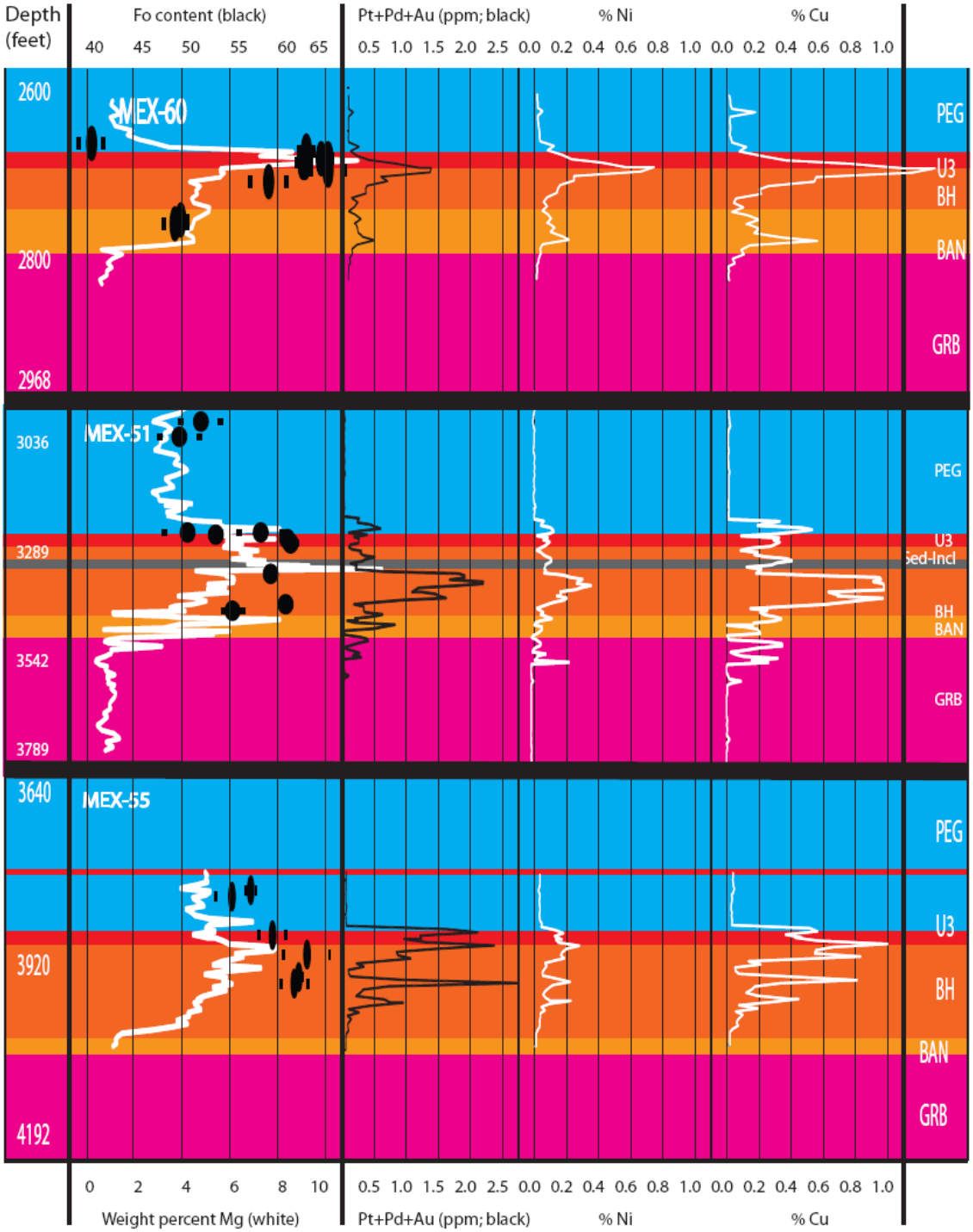


Figure 57: Stratigraphic variation in copper, nickel, and total PGEs concentrations in the basal contact zone where overlain by the anorthositic inclusion block and profiled in drill holes MEX-60, MEX-51, and MEX-55; Whole rock concentrations of Mg and forsterite content of olivine are shown for comparison.

preferentially taken up by early crystallizing MSS (later unmixing to form pyrrhotite and pentlandite), which results in enrichment of residual sulfide liquid in Cu and PGE (Naldrett, 2004). Sulfide fractionation is evident in the deposit at least on a localized scale as several instances of apparent Fe-Ni-Cu fractionation have been observed (Fig. 58). In some areas at the base of the deposit, several centimeters to several meters of massive to semi-massive sulfide occur which are characterized by pyrrhotite and pentlandite surrounding an inner core of chalcopyrite (Fig. 59).

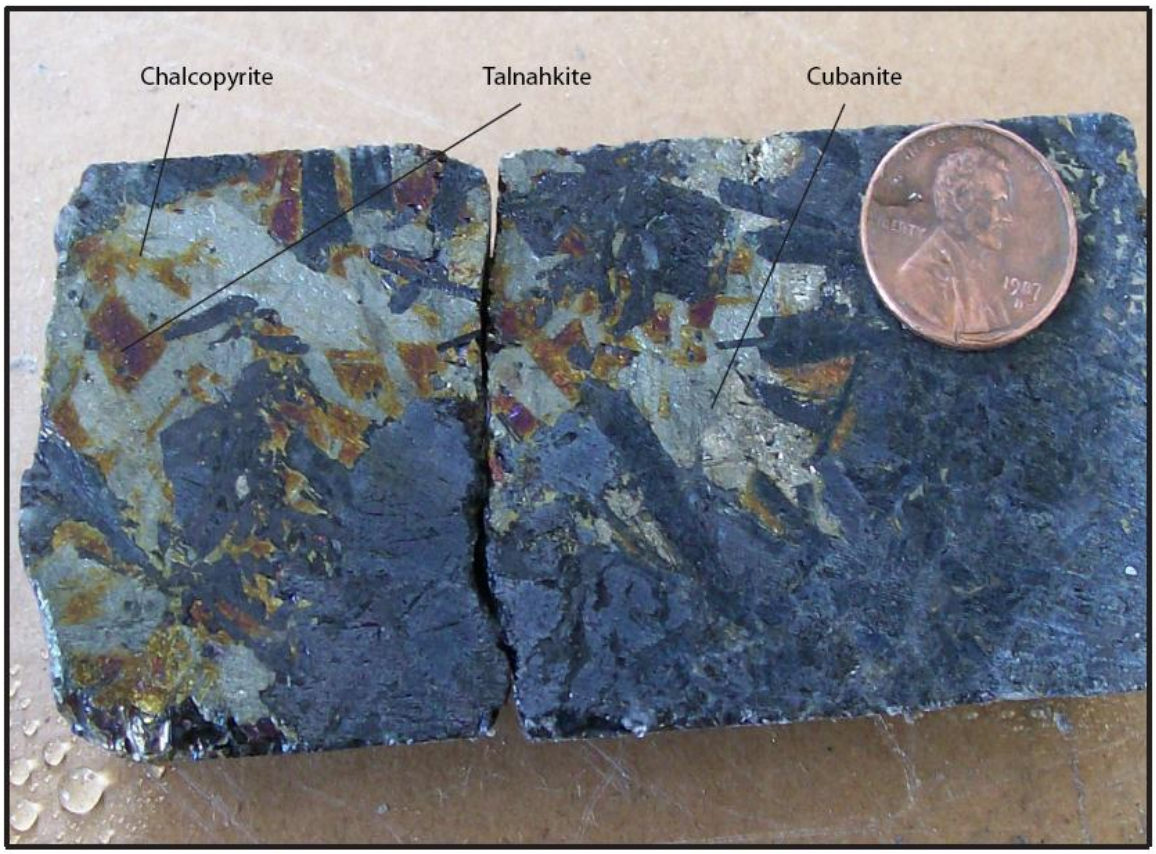


Figure 58: Pegmatitic clumping of chalcopyrite, cubanite, and talnahkite, displaying Cu-Ni-Fe sulfide fractionation in the upper part of the basal contact zone, photograph from Duluth Metals drill core MEX-51 at 3357 feet.

The upward increase in Cu+PGE/ Ni and of the overall metal grade suggests that sulfide fractionation alone was not at play. Rather, the general increase in grade up from the basal contact suggests that the metal tenor of the sulfide was repeatedly upgraded by turbulent mixing with new pulses of undepleted silicate melts. Such repeated inputs of magma are consistent with the lithologically and structurally heterogeneous character of the BH unit and with the correlation of higher grades with olivine-rich portions of the basal contact zone. The latter are thought to mark new inputs into the SKI chamber. If fractionation of sulfide liquid was occurring within the basal contact zone, the resident

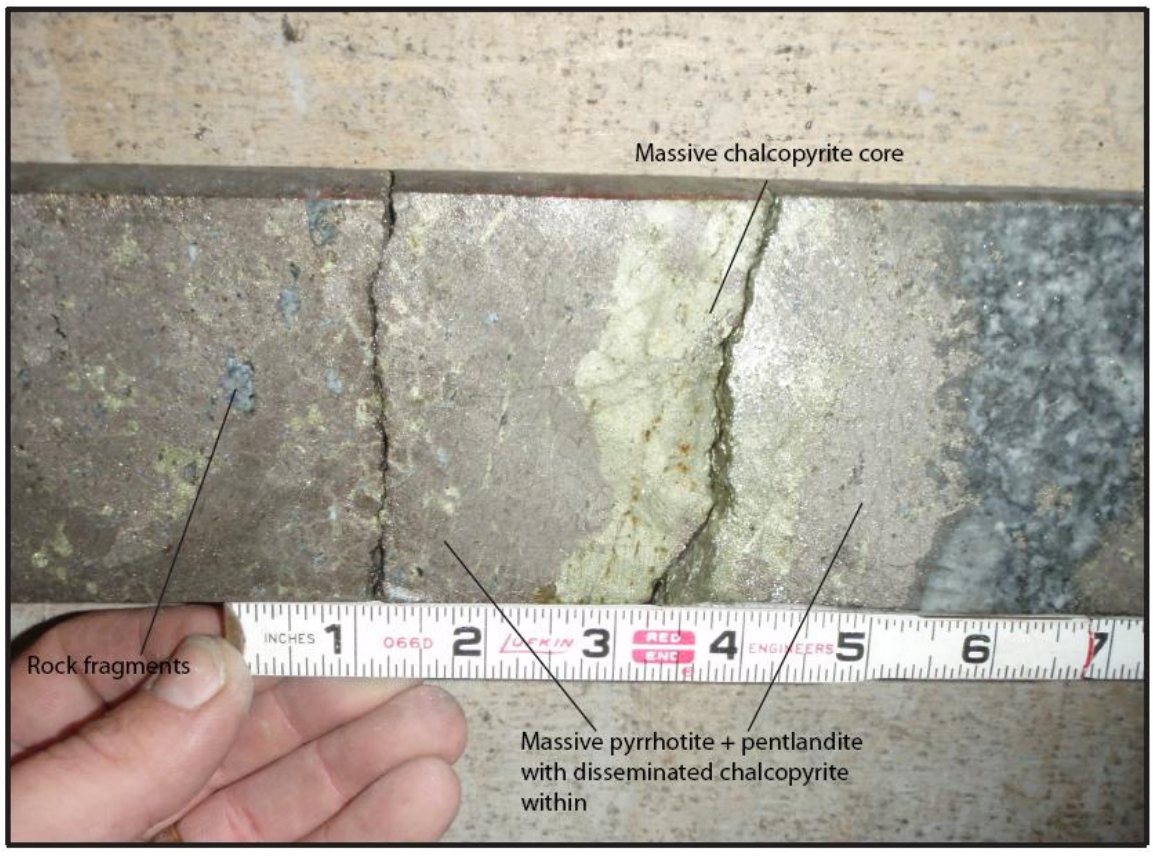


Figure 59: Massive sulfide at the base of the Nokomis deposit, displaying a chalcopyrite core surrounded by pyrrhotite and pentlandite, photograph from Duluth Metals drill core MEX-133M at 1350 feet.

sulfide liquid encountered, disturbed, and upgraded by each new pulse of magma would be progressively more Cu-PGE rich. This upgrading of fractionating sulfide may have also (or instead) occurred within the conduit feeding the magma chamber. As interpreted for Voisey's Bay (Naldrett, 1997), each pulse of magma through the vertical feeder churned up and upgraded the sulfide liquid that, because of density, had drained back down into the conduit. While some of this roiled up sulfide would again pool back into the feeder, a significant amount would be transported with the new magma pulse into the sheet-like magma chamber.

Finally, given the evident abundance of volatiles associated with the basal contact zone, it is also likely that secondary redistribution of sulfide occurred by dissolution and reprecipitation from hydrothermal fluids. Evidence for elevated volatiles includes the common occurrences of biotite, pegmatitic textures, and locally extensive alteration of primary minerals. Stable oxygen isotope data (Lee and Ripley, 1996) indicate that these volatiles were derived by dehydration of the granites and metasediments in the footwall. The degree to which secondary remobilization of sulfide is responsible for the complex mineralization patterns observed (Figs. 56 & 57) is difficult to access. However, given the generally consistent patterns of upward enrichment in grade and Cu+PGE/Ni, it seems likely that this process was minor or at least occurred on a local scale.

## 5.4 Estimation of the South Kawishiwi Intrusion Parent Magma Composition

Determining the parental magma compositions of mafic layered intrusions is difficult because of the nature of the cumulate rocks that compose them. Cumulates are considered to be mixtures of primocyrsts (cumulus minerals) and a magma component with the additional complication that the primocrysts are typically solid solution minerals (Wager et al., 1960; Wager and Brown, 1967; Irvine, 1982). Although chill margins or satellite dike might provide direct representative samples of possible parental compositions (e.g., Thy et al., 2006), such features are not associated with the SKI. Another method of estimating the parental magma composition is to subtract the compositional component of the cumulus minerals from the whole rock composition whereby the residual composition may be interpreted to approximate the parental liquid (e.g., Miller and Weiblen, 1990). However, it is difficult to accurately determine the proportions and primary compositions of cumulus minerals, especially for mafic phases like olivine that do not retain zoning which helps distinguish cumulus cores from postcumulus overgrowths. Moreover, it is not clear that intercumulus magma becomes completely "trapped" in cumulus rocks (e.g., Meuer & Meuer, 2006). A third inverse method is to calculate the composition of magma that is in equilibrium with a particular primocryst mineral composition. Bedard (1994) developed a method for calculating the trace element compositions of a magma in equilibrium with primocrysts based on mineral-liquid partition coefficients and mass balance. This technique requires high precision trace element data, which this study did not obtain. Another variant of this inverse method is to calculate the mg# (MgO/(MgO+FeO), mol%) of the liquid from its

olivine composition using the experimental data of Roeder and Emslie (1970). Because mg# is a good qualifier of the degree of differentiation in mafic rocks, this value can be used to limit the possible magma compositions that may be represented in comagmatic volcanics. In the case of the SKI, such comagmatic magmas likely exist in the normal polarity mafic lavas of the North Shore Volcanic Group (Green, 1972; BVSP, 1981),

An inverse and analogue method will be used here to estimate plausible parent magma compositions for the basal contact zone of the SKI. Olivine compositional data collected during this study is used here to estimate the most primitive mg# for the parent magma to the SKI. This compositional parameter will then be used to sort through NSVG compositions in order to find possible parent magma candidates. The plausibility of these volcanic compositions being SKI parent magma analogues will then be evaluated with the MELTS algorithm (Ghiorso and Sack, 1995) to determine whether olivine and plagioclase are early liquidus phases from such magma compositions.

Roeder and Emslie (1970) determined experimentally that the partitioning of Mg and Fe between mafic magma and olivine is constant and independent of temperature. Therefore, knowing the composition of olivine, one can calculate the composition of the liquid in equilibrium with that olivine. Applying this simple calculation to cumulate rocks presents complications, however, because of the well-documented phenomenon termed the “trapped liquid shift” (Barnes, 1986; Chalokwu and Grant, 1987), whereby cumulus olivine readily equilibrates with postcumulus, Fe-enriched overgrowths during slow subsolidus cooling.

Figure 60 helps to illustrate the trapped liquid shift phenomenon. A parental liquid with a composition of L ($Fo_{46}$) at its liquidus temperature will generate cumulus olivine of composition C ($Fo_{77}$). Let us assume that the parental liquid becomes trapped in the intercumulus pore space in an amount whereby its olivine component corresponds to one-third of the equivalent amount of cumulus olivine – this would correspond to a mesocumulate (Wadsworth et al., 1960; Irvine, 1982). As this trapped parent liquid crystallizes, it will crystallize an overgrowth rim on the cumulus olivine whose bulk composition will eventually correspond to the composition of the trapped parent liquid (Fo 46). During subsolidus equilibration, the originally zoned olivine composed of a 75% cumulus core of $Fo_{77}$ and a 25% postcumulus rim that averages $Fo_{46}$ (C+P) will homogenize to a uniform composition of $Fo_{68}$ (CP).

The above example is an ideal case since, as pointed out above, it is unlikely that complete trapping of the intercumulus liquid occurs (Meuer & Meuer, 2006). Compaction of the cumulate pile and increased buoyancy of the fractionating intercumulus magma can lead to its being expelled during postcumulus crystallization. Moreover, given the ease with which Fe and Mg diffuse in olivine at high temperatures, it is probable that re-equilibration between the postcumulus rim and the cumulus core begins during postcumulus crystallization. Regardless of the ideality of the trapped liquid shift, the phenomenon has been shown to have a significant effect in lowering the Fo content of olivine from its cumulus composition (Barnes, 1986; Chalokwu and Grant, 1987).

To minimize the effects of the trapped liquid, I sought out cumulates that show evidence for the lowest proportions of trapped liquid component. For the plagioclase-olivine cumulates of the SKI, these would be rocks with very low modes of interstitial pyroxene, Fe-Ti oxide and other postcumulus phases (biotite, amphibole, apatite, etc…). Also, plagioclase crystals should have minimal thicknesses of Na-enriched overgrowth rims. Another characteristic that would promote a minimal amount of trapped liquid is the strong development of foliation, which would minimize the porosity of the cumulate.

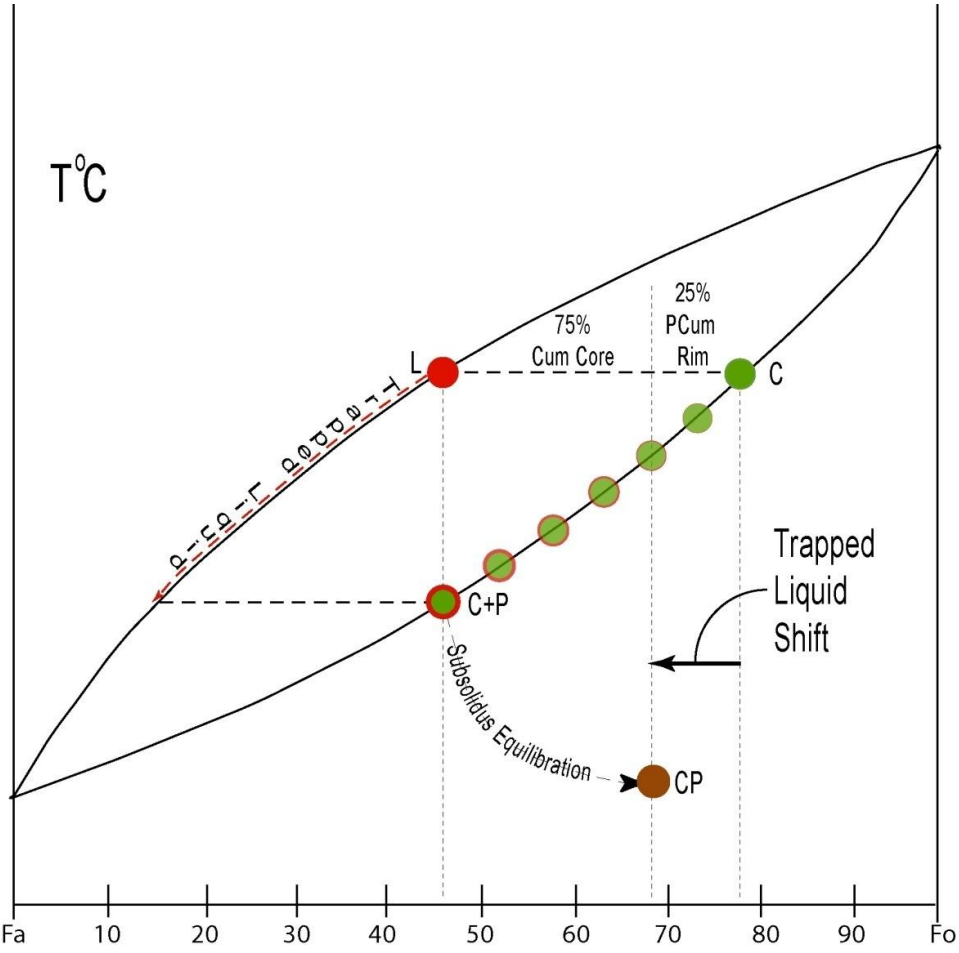


Figure 60: Idealized T-X phase diagram for olivine showing the trapped liquid shift in olivine composition due to cumulus and postcumulus crystallization and subsequent subsolidus equilibration.

In reviewing the petrographic attributes of samples from the basal contact zone, it was determined that melatroctolitic rocks from the U3 unit and ultramafic intervals in the BH unit best satisfy these criteria. As would be expected, these rock types also have olivine with high Fo contents. The maximum Fo content in olivine (71.7) was found in sample 61-3259 from the U3 unit (Fig. 55; Appendix III).

Using the equilibrium equation for iron and magnesium partitioning between basaltic liquid and olivine (Eq. 1), experimentally determined by Roeder and Emslie (1970), the FeO/MgO ratio and mg# of the parental liquid can be calculated for any olivine composition.

$$K_D = (X_{FeO}^{ol}/X_{FeO}^{liq})(X_{MgO}^{liq/}X_{MgO}^{ol}) = 0.3 \qquad \text{(Eq. 1)}$$

Reorganizing this equation to solve for the FeO/MgO ratio of the liquid, the equation becomes:

$$(X_{FeO}^{liq}/ X_{MgO}^{liq}) = ( X_{FeO}^{ol}/ X_{MgO}^{ol})(1/ K_D) = ( X_{Fe}^{ol}/ X_{Mg}^{ol})*3.03$$

The FeO and MgO concentrations measured by microprobe analysis from sample 61-3259 (Appendix III) are:

$$X_{FeO}^{ol} = 0.574, \text{ and } X_{MgO}^{ol} = 1.45$$

Applying these values to Equation 1, we get:

$$(X_{FeO}^{liq}/ X_{MgO}^{liq}) = (0.574/1.45)*3.03$$

$$(X_{FeO}^{liq}/ X_{MgO}^{liq}) = 1.2$$

To determine the mg# of the liquid, the mg# equation:

$$\text{mg\#} = MgO/(FeO+MgO)*100,$$

can be rearranged to equate mg# to the FeO/MgO ratio, which yields:

$$1 + (FeO/MgO) = 1/mg\#$$

Applying the FeO/MgO ratio determined above, yields an mg# of :

$$mg\# = (1/2.2)*100 = \mathbf{\underline{45.5}}$$

Assuming that the normal polarity basalts of the North Shore Volcanic Group, which have similar ages to the 1099-1098 Ma age of the SKI (Hoaglund et al., 2010), are generally comagmatic with the magmas that produced the subvolcanic intrusions of the Duluth Complex (Green, 1972), it seems reasonable to evaluate the NSVG compositions with mg#'s around 45.5 to determine whether they make plausible analogues for the parent magmas to the basal contact zone of the SKI. As part of the Basaltic Volcanism Study Project (1981), John Green compiled a reference suite of 20 mafic volcanic compositions from the North Shore Volcanic Group. Of the 20 mafic compositions, five samples have Mg#'s between 44.5 and 46.5 (these values are calculated assuming that FeO is 90% of the total Fe of the samples, with $Fe_2O_3$ comprising the remainder). The major element chemistries of these five volcanic compositions are listed in Table 3.

To evaluate which of the five compositions might be possible analogues to SKI parent magmas, the major element data were applied to the MELTS algorithm (Ghiorso and Sack, 1995) to determine the equilibrium mineral phases at or near their liquidus temperatures. These results are listed in the lower three rows of Table 3 and show that Kew-2, Kew-9, and Kew-12 are possible candidates because they are saturated in olivine and plagioclase near the liquidus temperature of the magma compositions. Note that the volcanic compositions are in equilibrium with olivine compositions between $Fo_{71}$ and $Fo_{73}$, thus providing an independent check on the mg# calculations based on $Fo_{71.5}$

olivine. Kew-11 is not an appropriate composition because its liquidus phase is only plagioclase over a 50° span of temperature and then becomes saturated in clinopyroxene. Kew-12 is also not appropriate since it has orthopyroxene as its sole liquidus phase followed by plagioclase after a 55° drop in temperature. Of the three compositions saturated in both olivine and plagioclase near their magma liquidus temperatures, none has an ideal composition as an SKI parent. Kew-2 and Kew-12 both have plagioclase as the first liquidus phase, although over an admittedly small temperature range (7-19°C) before olivine joins in. Still, this is inconsistent with the observation that melatroctolites tend to occur at the base of individual cooling units of magma, thus implying that olivine was the first liquidus phase. Although Kew-9 would seem to better fit this observation, since olivine is the initial liquidus phase and is saturated over an 8°C temperature range before plagioclase joins in, the composition of the plagioclase is significantly more sodic ($An_{60}$) compared to the observed range of most calcic plagioclase cores in the basal contact zone ($An_{65-73}$; Figs. 54 & 55). In contrast, the equilibrium An contents of plagioclase in Kew-2 ($An_{73}$) and Kew-12 ($An_{68}$) fall within this observed range. In conclusion, some hybrid combination of Kew-2, Kew-9, and Kew-12 would seem to be the most appropriate analogue for the parent magma to the basal contact zone of the SKI.

Table 3: Whole rock major element compositions of five volcanic samples from the *Keweenawan reference suite of the North Shore Volcanic Group* (BVSP, 1981) which have similar Mg#'s to that determined as the best estimate for an SKI parent magma. Lower three rows show the liquidus temperatures, the liquidus phase, and the temperature and stable phases at the point of two-phase saturation for the five NSVG samples as determined by MELTS (Ghiorso and Sack, 1995). Unshaded columns indicate compositions that are interpreted to be possible analogues for an SKI parent magma. See text for further discussion.

| Wt.% | KEW-2 | KEW-9 | KEW-11 | KEW-12 | KEW-20 |
|---|---|---|---|---|---|
| $SiO_2$ | 46.64 | 50.49 | 50.54 | 49.54 | 55.20 |
| $TiO_2$ | 2.33 | 2.05 | 1.49 | 2.14 | 1.61 |
| $Al_2O_3$ | 15.21 | 16.24 | 16.59 | 15.05 | 13.51 |
| FeOt | 13.40 | 11.13 | 10.55 | 12.27 | 10.17 |
| MnO | 0.14 | 0.17 | 0.16 | 0.17 | 0.16 |
| MgO | 5.68 | 4.52 | 4.51 | 5.05 | 4.39 |
| CaO | 9.21 | 6.75 | 10.06 | 8.38 | 5.53 |
| $Na_2O$ | 2.56 | 3.98 | 3.23 | 2.67 | 3.74 |
| $K_2O$ | 0.54 | 1.93 | 0.76 | 1.29 | 1.90 |
| $P_2O_5$ | 0.25 | 0.24 | 0.23 | 0.29 | 0.22 |
| $H_2O+$ | 3.05 | 2.04 | 1.38 | 2.53 | 2.75 |
| Total | 99.99 | 100.22 | 100.83 | 100.43 | 99.67 |
| Mg# (FeO=0.9*FeOt) | 45.6 | 44.6 | 45.9 | 44.8 | 46.2 |
| Magma Type | Olivine tholeiite | Transitional, weakly alkaline | Transitional, weakly alkaline | Transitional, weakly alkaline | Basaltic andesite |
| MELTS Liquidus | 1192° | 1166° | 1215° | 1169° | 1191° |
| Liquidus Phase | Pl (An73) | Ol (Fo73) | Pl(An74) | Pl (An67) | Opx |
| Multiply Saturated | 1173° Pl+Ol(Fo71) | 1158° Ol+Pl(An60) | 1166° Pl+Cpx | 1162° Pl+Ol(Fo72) | 1136° Opx+Pl |

## 5.5 Emplacement of the South Kawishiwi Intrusion in the Nokomis Deposit Area

Like kindred intrusions of the Duluth Complex, the magmas that created the South Kawishiwi intrusion were largely emplaced into the base of the comagmatic volcanic rocks that comprise the North Shore Volcanic Group (Miller and Severson, 2002). Prior to emplacement of the SKI and the earlier anorthositic series magmas, the volcanic edifice that accumulated unconformably atop the erosional surface of Archean to Paleoproterozoic basement rocks was between three and five kilometers thick based on geobarometric estimates of 1.2 kb pressure attending the thermal metamorphism of the Biwabik Iron-formation by the Duluth Complex (Laskowski, 1986). Because the shallow southeasterly dip of internal structure of the SKI and related intrusions is similar to the regional dip of volcanic rocks of the NSVG, it is generally assumed that the SKI was emplaced as a sill or sheet-like body that delaminated the basal basalt flows.

Emplacement of the SKI was evidently preceded by the formation of structurally complex masses of plagioclase-rich gabbroic rocks of the anorthositic series (Miller and Weiblen, 1990). Although high precision age dates (Paces and Miller, 1993; Hoagland et al., 2010) indicate that the formation of the anorthositic series and layered series intrusions such as the SKI are effectively contemporaneous, being emplaced between 1099 and 1098 Ma, field relations consistently show anorthositic series rocks as inclusions in layered series intrusions (Miller and Severson, 2002). Therefore, it is clear that anorthositic series rocks, which are thought to have formed from multiple injections of plagioclase crystal mush (Miller and Weiblen, 1990), where emplaced and largely crystallized before the SKI and other layered series intrusions were formed. The

occurrence of mafic hornfels and anorthositic series inclusions within the basal contact zone of the SKI, especially to the west and south of the Nokomis deposit area (Severson, 1994), indicate that anorthositic magma/mushes did not intrude only along the unconformity, but also somewhat higher into the lower section of the volcanic pile.

In the Nokomis area and to the north, however, it seems likely that prior to emplacement of SKI magmas, anorthositic series rocks were largely in direct contact with the pre-Keweenawan basement, having intruded along the basalt-basement unconformity. Evidence of this is given by geologic mapping in the Gabbro Lake 15' quadrangle, where Green et al. (1966) show anorthositic series rocks in direct contact with the Archean Giants Range batholith. Also, at least one hole drilled by Duluth Metals (MEX-89) shows anorthositic series rocks in direct contact with granitic rocks of the footwall. MEX-89 was drilled through the anorthositic inclusion block (5.2.3) and never encountered a clearly definable SKI basal contact zone between the anorthositic inclusion block and the footwall GRB. A lack of chilled margins around anorthositic inclusions, regardless of size, and the common occurrence of plagioclase xenocrysts in troctolitic rocks indicate that the anorthositic series was still very warm, if not semi-molten, when the SKI magmas were emplaced.

The lithologic, textural, structural and mineralization characteristics of the SKI in the Nokomis deposit area can be best explained as forming by two major emplacement events within which multiple recharge episodes took place. The two major emplacement events correspond to the two major zones defined in the SKI – the basal contact zone and the upper zone. The first event, which created the basal contact zone, occurred by

delamination of the anorthositic series from the Archean granite footwall by multiple complex injections of sulfide-bearing, inclusion-rich magmas. The least contaminated of these magmas were moderately evolved (mg# ~46), tholeiitic magmas as discussed in the previous section. The second event, which created the upper zone, occurred by overplating the basal contact zone and uplifting the anorthositic series cap, except in the area of the anorthositic inclusion block. These olivine tholeiitic mafic magmas were sulfide-undersaturated and some were possibly olivine (and plagioclase) porphyritic. Upper zone magmas were forced around instead of under the large pillar of anorthositic rocks in the Nokomis deposit area. The gradational contacts between the PEG and Main AGT units that mark the zone contact further imply some hybridization of upper zone magmas with the semi-molten magmas of the uppermost basal contact zone. Within each emplacement event, multiple magma recharge episodes gave rise to the various stratiform units that comprise each zone as will be discussed in greater detail below.

### 5.5.1 Emplacement of the Basal Contact Zone

The four main units of the basal contact zone are distinct in ways that might lead to the conclusion that each was emplaced as its own intrusive episode. It is also the case, however, that these units share a number of common features, which might imply that some or all units are linked to a single emplacement episode and the difference between them are the result of *in situ* processes within the SKI magma chamber (e.g., crystal fractionation, flow differentiation, interstitial melt migration, fluid fluxing, etc…). If the units were emplaced in more than one episode, the question arises as to the sequence of

intrusion. Rather than discuss the possible comagmatic and sequencing relationships between the units in stratigraphic order, these relationships will be discussed in the order of BH to BAN, BH to PEG, and U3 to PEG and BH. As will become clear, the U3 unit is discussed last because its relationship to all other units in the basal contact zone is the least understood and perhaps the most unique.

Before discussing the genetic relationships of the BH unit to other basal contact zone units, it is necessary to consider the origin of its extreme internal heterogeneity. The Cu-Ni sulfide-mineralized BH unit features a taxitic package of troctolites, gabbros, and olivine-rich rocks with fine-grained to pegmatitic grain-sizes, and granular to ophitic textures, in direct, sharp contact with each other on a centimeter scale. The seemingly random variations in silicate and sulfide mineral assemblages and textures of rocks comprising the BH create a consistently heterogeneous unit that, when considered at the intrusion scale, could be considered homogeneous in its heterogeneity. The heterogeneity of the BH unit would seem to imply extreme thermal and chemical chaos attending the initial inputs of magma along the anorthositic series-granite contact. The number of individual magma pulses that formed this unit is unknowable, but it is clear that it itself was not emplaced in a single event.

*BAN-BH Units*

The BH unit shows a gradational contact relationship with the underlying noritic and finer-grained BAN unit. The smooth variations in lithology and chemistry from the granitic footwall, through the BAN, and into the lower BH unit (Figs. 54 & 55) suggest that the BAN unit most likely represents a somewhat chilled contamination zone of the

earliest magmas into the SKI that also formed the BH unit. This contamination was presumably the result of incorporated siliceous partial melts from the GRB footwall. Whether this zone formed just prior to the BH or contemporaneous with the BH is difficult to discern.

*BH-PEG Units*

The PEG unit is distinctive from the BH in that it is made of more intermediate lithologies and mineral compositions, is generally not sulfidic, more consistently displays coarse textures, tends to contain more late-stage magmatic phases (amphibole, biotite, apatite, alkali feldspar and quartz), and is more hydrothermally altered. All these characteristics suggest that the PEG unit generally formed from a more evolved, volatile-rich magma compared to other basal contact zone units. Given these distinct attributes, it seems possible that the PEG formed from an intrusive pulse unrelated to the BH (or the U3; see below). Its largely unmineralized character and high stratigraphic position would seem to imply that it is younger than the other basal contact zone units.

Given its somewhat heterogeneous character, plagioclase-rich mode, and geochemical attributes, it is also possible that the PEG unit represents a comagmatic upper differentiate of the BH unit. Although the whole rock abundances of Ca and Mg between the PEG and BH units are clearly distinct (Figs. 50 & 51), it was argued in the previous section that these differences dominantly reflect a greater modal abundance of plagioclase in the PEG unit. Mineral compositions of the solid solution phases between the two units generally show similar to more evolved compositions in the PEG unit (Figs. 52, 53, 54, & 55). Interestingly, plagioclase compositions show similar maximum An

contents, but the PEG unit tends to have stronger zoning to more albitic compositions (Figs. 52, 53, 54 & 55). This is noteworthy since plagioclase retains its primocrystic compositions and does not experience trapped liquid shift equilibration like olivine and pyroxene.

Collectively, these attributes of the BH and PEG are consistent with both units being related to a common magma sheet that evolved *in situ* after being emplaced in multiple, semi-continuous dynamic injections of sulfidic, crystal-laden, inclusion-rich magma. The plagioclase-rich mode of the PEG unit may be related to moderate flotation of cumulus plagioclase due to its low density. The more evolved nature of the PEG unit, as well as its higher concentration of hydrous minerals and granophyre and its more intense alteration, may be related to upward infiltration of fluid-rich evolved melts derived from fractionation of the BH and volatile-rich partial melts of the GRB footwall. These evolved liquids evidently became trapped in the upper part of the magma sheet by the overlying anorthositic series roof zone. That the PEG unit retains its coarse, evolved, and hydrothermally altered nature along its entire extent, even where overlain by the upper zone, affirms the interpretation that the anorthositic series rocks initially formed the hanging wall above the entire basal contact zone.

The general lack of sulfide in the PEG, compared to its ubiquitous occurrence in the BH unit, would seem to argue against the two units being comagmatic. However, the PEG is locally mineralized in its lower parts (Fig. 57). Perhaps the infiltration of fluid-rich evolved magma into the upper part of the magma sheet kept the unit well above

solidus conditions, such that the dense sulfide liquid had ample opportunity to drain downward into the lower magma sheet that became the BH.

*U3 and other Basal Contact Zone Units*

Although the BAN, BH, and PEG units seem to be best explained as forming from multiple semi-continuous bursts of sulfidic, crystal-laden, inclusion-rich magma emplaced along the granite-anorthositic series contact that subsequently experienced upward infiltration of volatile-rich evolved liquids and downward draining of sulfide, the genesis of the U3 unit within this petrogenetic model is more enigmatic. The sulfidic and melatroctolitic U3 unit is distinct from other basal contact zone units by having an olivine- and oxide-rich mode, medium- to fine-grained texture, well foliated and locally layered internal structure, and more forsteritic olivine composition. Interestingly, the U3 is typically in sharp contact with the PEG unit above it and in gradational contact with the BH unit below. Thinner melatroctolite intervals within the BH unit may be magmatically related to the U3 unit, though there is no direct evidence that these thin intervals are physically connected to the U3 unit. Overall, the U3 unit and the possibly related melatroctolite intervals in the BH unit display the most primitive olivine compositions ($Fo_{65-72}$) of the entire SKI stratigraphy. The inverse method of estimating possible parent magmas from these olivine compositions described in the previous section indicates an evolved tholeiitic composition. Because of the potential for strong trapped liquid shifts and variable assimilation of country rock, it is difficult to determine whether this was the

primary magma to all basal contact zone (and upper zone) rocks (Table 3) or if it was unique to the U3 unit.

Two possibilities for the petrogenesis of the U3 unit are considered. One possibility envisions a single phase system whereby the U3 formed *in situ* along with the other units during and after the bulk of the basal contact zone was emplaced. An alternative possibility considers that the U3 unit and related melatroctolite intervals intruded in a discrete second episode of emplacement shortly after the BAN, BH, and PEG were emplaced and had differentiated into their dominant lithologies.

In a single-phase emplacement model for the basal contact zone (Fig. 61), the U3 unit may have formed as the result of magmatic flow and density differentiation in the basal contact zone, which allowed dense, smaller olivine crystals to segregate from less-dense, larger plagioclase crystals. This considerable contrast in density between these two primary mineral phases could cause buoyant plagioclase to rise as dense olivine sinks, creating a segregation of the two minerals. This single-phase model envisions that this modal segregation initiates at the interface between the lower, crystal mush flow (BH unit), and the upper, evolved, volatile-rich liquid (PEG unit). The bifurcations, or "lenses" of olivine-rich rocks within the BH unit would be produced by drag or shear forces caused by differential flow stresses due to viscosity contrasts between the crystal mush and the liquid above it. These drag or shear forces could potentially drag portions of the crystal-mush from below over the progressively forming U3 unit to produce "lenses" of olivine-rich rocks within the upper parts of the BH unit. The contact between the U3 and overlying PEG unit may be sharpened by upward migration of intercumulus

melts out of the dense olivine-oxide rich mineral assemblage and into the overlying PEG unit. In contrast, the contact between the U3 and underlying BH unit may have become more diffuse by the upward migration of melt, from the BH unit and downward migration of olivine.

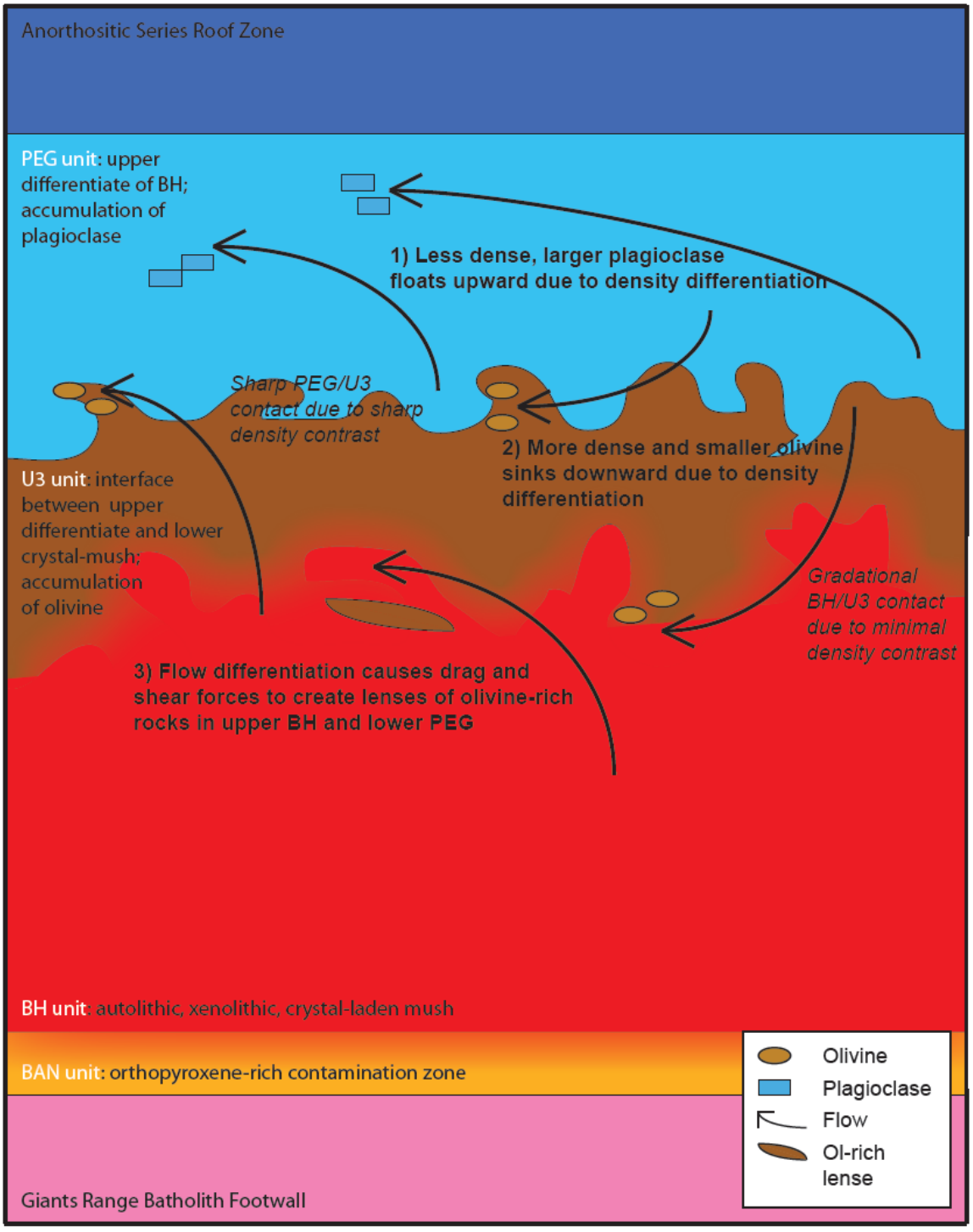


Figure 61: Single phase emplacement of all four basal contact zone units (BAN, BH, U3, PEG), featuring density segregation of (1) less dense but larger plagioclase (2) and more dense but smaller olivine at interface between upper differentiated liquid (PEG) and lower crystal mush (BH), and (3) drag or shear of free-moving crystals and less dense/less viscous liquid (not to scale).

A second explanation involves a two-phase emplacement model for the basal contact zone (Fig. 62) in which, the BAN, BH, and PEG units are generated in a similar fashion as in the single-phase model with the PEG unit differentiating from the BH unit (Fig. 62 A). The U3 unit, however, is generated by a second emplacement event occurring shortly after the formation of the BAN, BH, and PEG units (Fig. 62 B), but while these units are still in a molten, or semi-molten state. In this scenario, the U3 magmas, which were possibly slurries, laden with olivine and lesser plagioclase phenocrysts, are thought to have intruded roughly at the mushy-molten interface between the BH and PEG units. The sharp upper U3 contact with the PEG unit probably reflects the original intrusive contact between the intruding slurry and the semi-molten PEG unit. The contact would have initially been sharp since a more dense olivine slurry was intruding beneath the low density volatile-rich, feldspathic semi-crystalline PEG unit. This sharp contact would retain its sharpness after emplacement since the relatively more primitive interstial liquids in the olivine-plagioclase cumulates of the U3 unit were also more dense than volatile-rich evolved interstitial liquids in the overlying PEG unit, thus restricting migration of melt across the contact. In contrast, the lower U3 contact between the semi-molten BH unit would have developed a more diffuse boundary upon emplacement due to a density inversion. This density imbalance may have also promoted tongues of olivine-rich (plagioclase-poor) slurries penetrating into the low density mushes of the upper BH unit to generate the melatroctolitic intervals observed there.

In both of the above models the PEG unit is related to the BH unit as an upper differentiate, which poses a unique problem in that the PEG unit is rarely mineralized (as

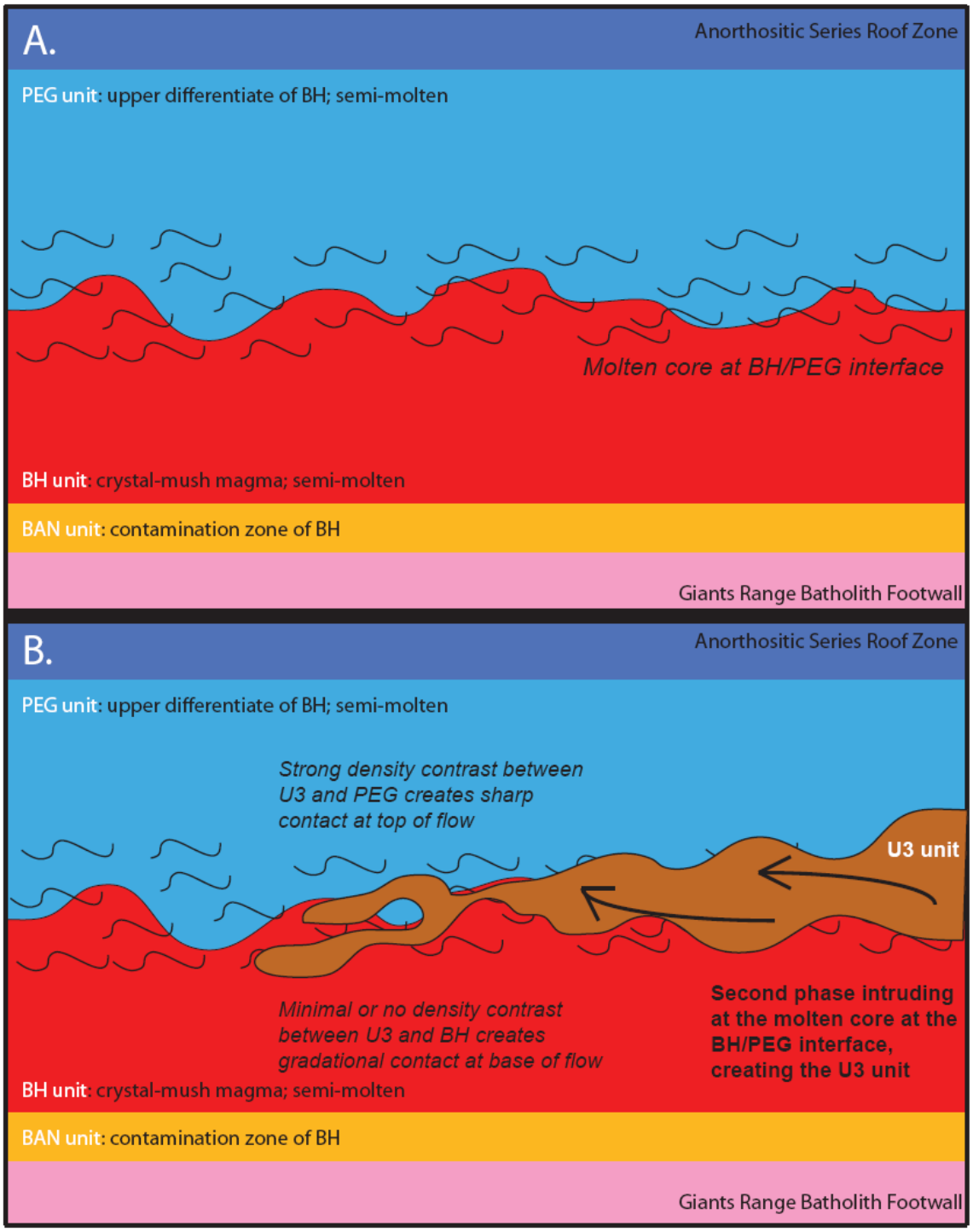


Figure 62: Two phase emplacement of the basal contact zone; A. (time one) the PEG unit differentiates from the crystal mush BH unit below as volatile-rich fluids and gasses rise upward along with siliceous partial melts from the GRB footwall; B. (time two) The U3 unit intrudes at the molten interface between the semi-molten BH and PEG units.

stated above), while the BH unit is always mineralized. It is possible that any sulfide contained within the PEG unit was able to drain downward and accumulate in the BH unit prior to the formation of the U3 unit. If the U3 unit was in place before or concurrently with the PEG unit it likely would have acted as a barrier to the downward migration of sulfide. This prompts the viewpoint of both of the above models, which envision the U3 unit as a late feature, forming after the generation of sulfide mineralization in the BH unit. The U3 unit itself displays significant sulfide mineralization, which in compliance with both of the above models would have to be inherent to the magmas that generated the U3 unit. These models will be further evaluated in the final section (5.7) of this chapter, taking better account of magma flow, and sulfide genesis.

### 5.5.2 Emplacement of the Upper Zone

The base of the upper zone is easy to identify when it is locally marked by a melatroctolite interval (U2), though in the Nokomis deposit area, this subunit is not always present. In this case, the contact between the PEG unit and the Main AGT unit of the upper zone is gradational and difficult to definitively identify. Although both units are typically augite troctolitic in mode, the transition from the PEG into the overlying Main AGT unit is best differentiated by a gradual decrease in grain size, a change from pegmatitic, high density clots of subophitic augite in the PEG to coarse-grained, moderate density, large (>5 cm) oikocrysts of ophitic augite in the Main AGT, and a reduction in the abundance of late magmatic phases and in the degree of alteration.

Very commonly another thin ultramafic interval (U1) will occur within the homogeneous mass of subophitic augite troctolite. This 1-5 meter thick interval typically has a sharp top and gradational to sharp base and seems to represent a new recharge event into the upper zone of magma similar to that which formed the lower part of the Main AGT unit.

The augite troctolite of the Main AGT unit distinctly contrasts with the troctolite and anorthositic troctolite of the overlying AT&T unit and is commonly marked by the occurrence of another thin melatroctolite subunit (HP#2). Above the AT&T unit, the AT(T) unit is differentiated by subtle differences in plagioclase mode with dominant lithologies consisting of anorthositic troctolite and troctolitic anorthosite. A second stratigraphically restricted marker horizon (HP#1) occasionally defines this contact. The melatroctolitic subunits (HP#2 & HP#1) typically have sharp upper contacts and gradational lower contacts, which is contrary to the expected sharp lower and gradational upper contacts that should form from an accumulating pile of crystals.

The contact between the Main AGT and the PEG units is so gradational that were the U2 unit not locally present and the PEG unit not the uppermost unit beneath the anorthositic inclusion block, it would be difficult to define a major unit contact let alone a major zone boundary at this contact. Still, on a macro-scale, this admittedly very gradational contact marks a fundamental change in the variability of the lithologies comprising the SKI, from the mineralogic, textural, and geochemical chaos of the basal contact zone to a homogeneous “sea of troctolite” in the upper zone with its systematic changes in modal mineralogy and cryptic layering. That the contact is gradational at a

minimum implies that the magmas forming the PEG and the Main AGT were similarly evolved olivine tholeiites and that some hybridization between the two units likely occurred before each became completely solidified. Despite the gradational nature of the PEG-Main AGT contact, the most important implication of this boundary in terms of the emplacement history of the SKI is that 1) the Main AGT and higher troctolitic units are absent beneath the anorthositic inclusion block, and 2) that pegmatitic-textured, subophitic, un-mineralized augite troctolite persists between the U3 and Main AGT units well away from the anorthositic inclusion block.

These two aspects of the PEG-Main AGT imply that the anorthositic series formed the hanging wall to the entire basal contact zone during its complex emplacement. The emplacement of the upper zone then was accommodated by the uplift of most of the anorthositic series hanging wall (or down-drop of the basal contact zone footwall), save the area now preserved as the anorthositic inclusion block.

The upper zone displays an entirely different chemical profile than that seen in the basal contact zone as presented in section 5.3 above. Lithologic and textural data occur in seemingly random sequences of troctolite, anorthositic troctolite, augite troctolite, and troctolitic anorthosite with a mix of intergranular, ophitic, and poikilitic bulk textures through the upper zone (Fig. 63). However, as discussed above (5.3.1) the chemostratigraphy of major element concentrations, specifically magnesium, displays a striking cyclical profile, which seems to indicate episodic magmatic emplacement with *in-situ* fractional crystallization between magmatic episodes (Fig. 64). Smaller magmatic events seem to only be recorded in the geochemical profile (Fig. 51; Sec. 5.3.1), while

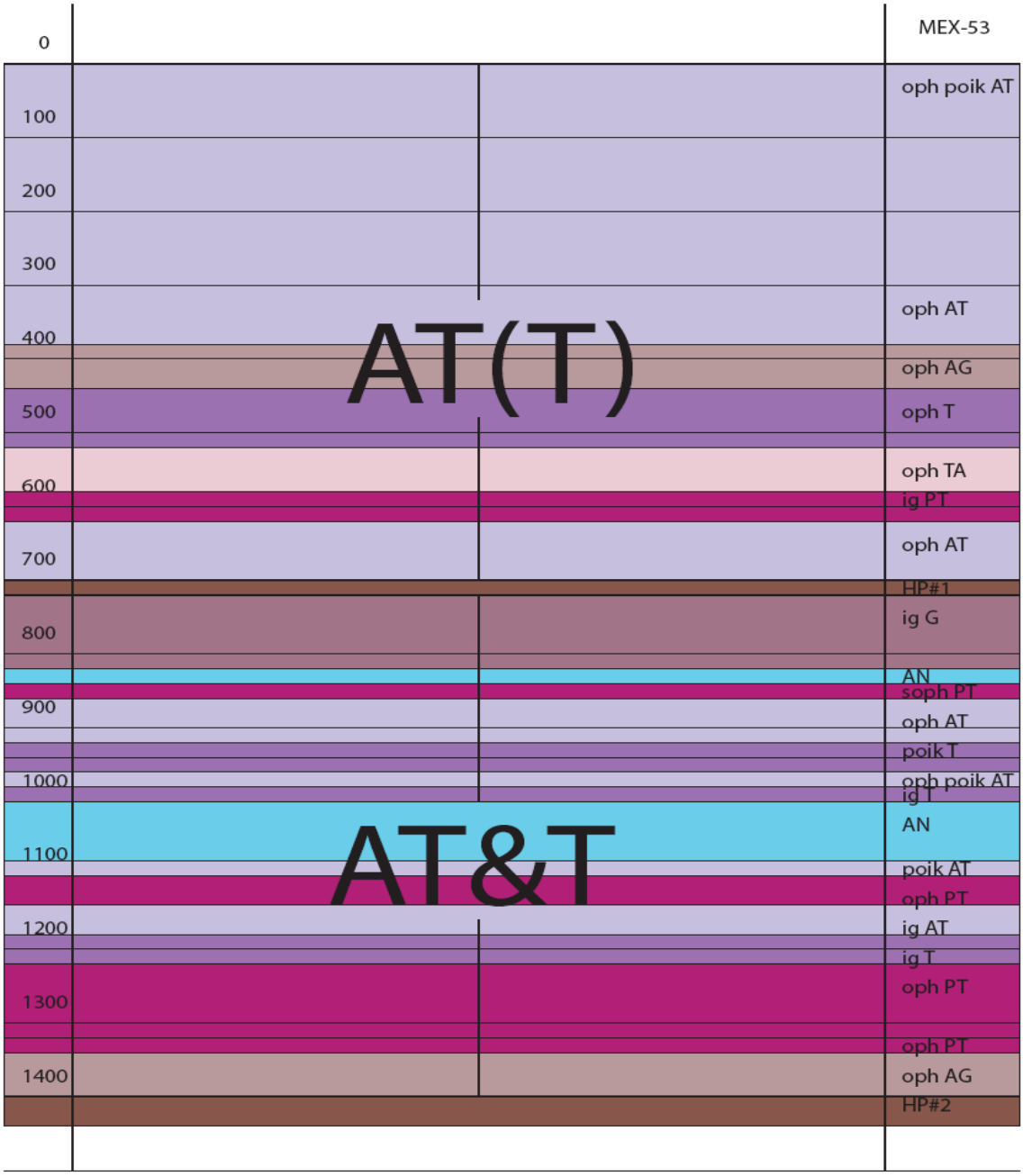


Figure 63: Profile through the AT&T and AT(T) units taken from drill hole MEX-53, illustrating randomly alternating lithologies and textures (T – troctolite, AT – anorthositic troctolite, PT – augite troctolite, TA- troctolitic anorthosite, G – gabbro, AG – anorthositic gabbro, AN – anorthosite, ig – intergranular, oph – ophitic, poik – poikilitic olivine).

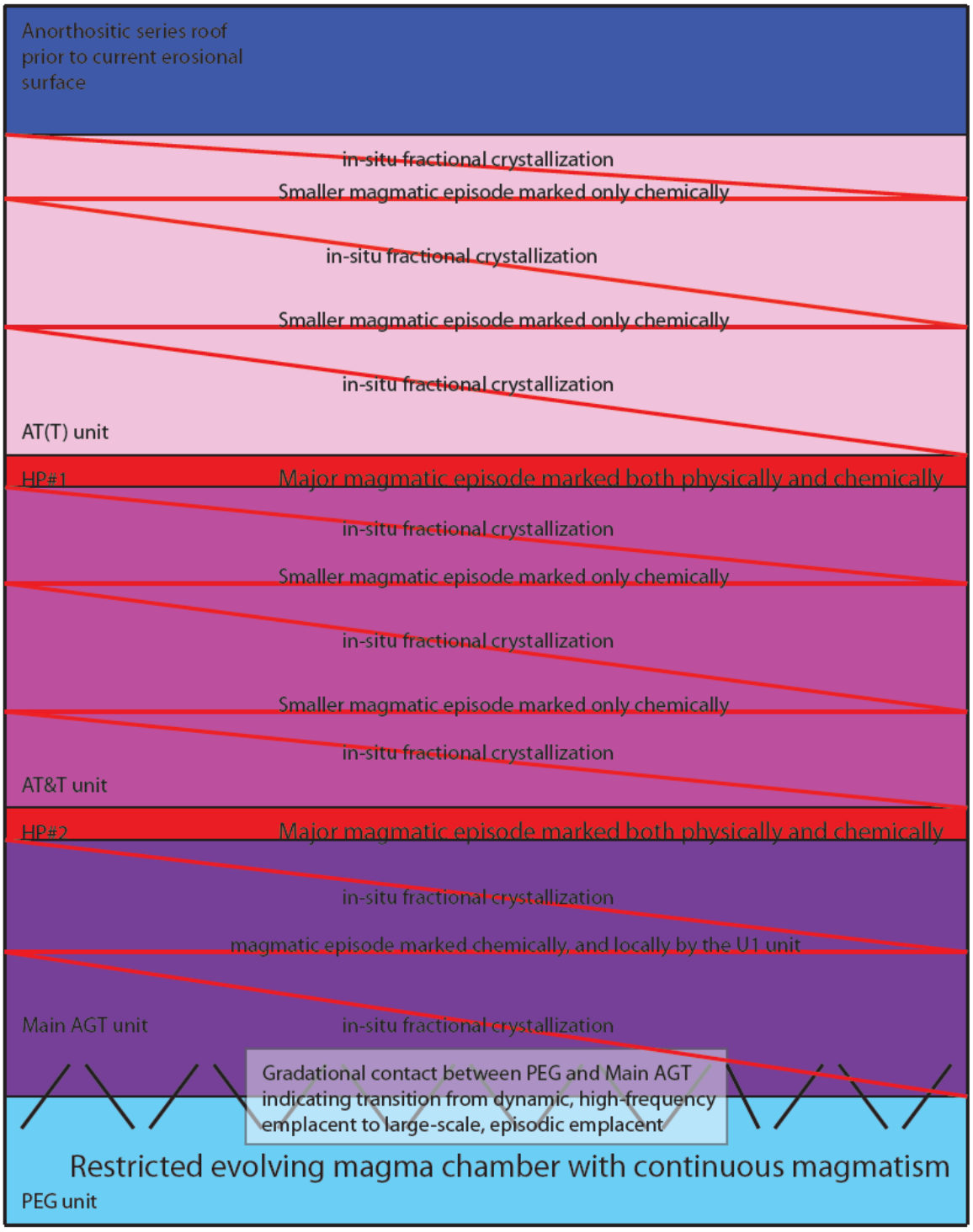


Figure 64: Model for emplacement of the upper zone, featuring *in situ* fractional crystallization with episodic magma recharge.

large-scale magmatic events are evidenced by both olivine-enriched horizons (HP#1 and HP#2) and spikes in magnesium concentration. The sharp upper contact of these units could be attributable to post emplacement migration of interstitial melt.

The relationship of the PEG unit, and the Main AGT unit implies that the two units may be genetically related, which also implies that the Main AGT unit may be somewhat of an evolved upper differentiate of the basal contact zone. The notable absence of clinopyroxene in the AT&T, and AT(T) units above the Main AGT unit seem to imply that these units are less evolved than the Main AGT, which indicates that they could have slightly different parent magmas, or that the parent magma for the AT&T, and AT(T) units may have been sourced from a different area of the same feeder magma chamber.

## 5.6 Evidence for Lateral Flow of Magmas Creating the South Kawishiwi Intrusion in the Nokomis Deposit Area

The ultimate purpose of this study is to test Peterson's (2001) open vs. confined style mineralization model and the idea that sulfide-bearing troctolitic magmas were emplaced into the Nokomis deposit area from the east via the Nickel Lake macrodike. To do this, petrographic, mineral chemical, and whole-rock/assay geochemical data are evaluated from the seven drill holes chosen for detailed study that form a cross-section through the Nokomis deposit (Fig.23; Sec. 5.2). This profile was set up to parallel Peterson's (2001) suggestion of lateral flow from the east to the west beneath the anorthositic inclusion block. In addition, whole-rock/assay geochemical acquired by

Duluth Metals from drill core throughout the Nokomis deposit area are evaluated for patterns and trends that might indicate lateral flow and progressive crystallization from east to west. Only data from the basal contact zone are evaluated, as it is the dominant host for the Nokomis deposit. The databases evaluated include modal mineralogy estimated from the petrographic study, incompatible element concentrations from whole-rock geochemistry, mineral chemistry of olivine, major element whole-rock geochemistry, and base and precious metal ratios.

Many physical and chemical variables could complicate the patterns that this data might show from a lateral flow perspective including the channelization of flow, and multiple emplacement episodes of variable magma compositions. Local variations due to channelization could be particularly problematic for the cross sectional profile. To overcome some of these possible complications, whole rock and assay data from drill core covering a broad area (~2.5 sq. miles) will be evaluated. Also, the possible effects of multiple emplacement episodes should be minimized by focusing some of the data evaluation on the U3 unit, which, as discussed above, may be the result of dynamic magma flow, or may have been emplaced in a single, late recharge event

### 5.6.1 Modal Evidence

Almost all SKI units contain cumulus olivine and plagioclase, which if occurring in experimentally determined cotectic proportions (McCallum et al., 1980), should have an Ol:Pl proportion of approximately 0.4. The lack of cotectic proportions may indicate that plagioclase and olivine were segregated by their density in a flowing crystal mush

sheet. In this case, lower density plagioclase might be expected to travel farther downstream, or in this instance to the west. To evaluate whether this type of flow segregation may have occurred in any of the basal contact zone units, the modal Ol/Pl ratios for core samples from the PEG, U3, and BH units are plotted relative to distance in Figure 65. The average Ol/Pl ratio does not change much across the Nokomis deposit

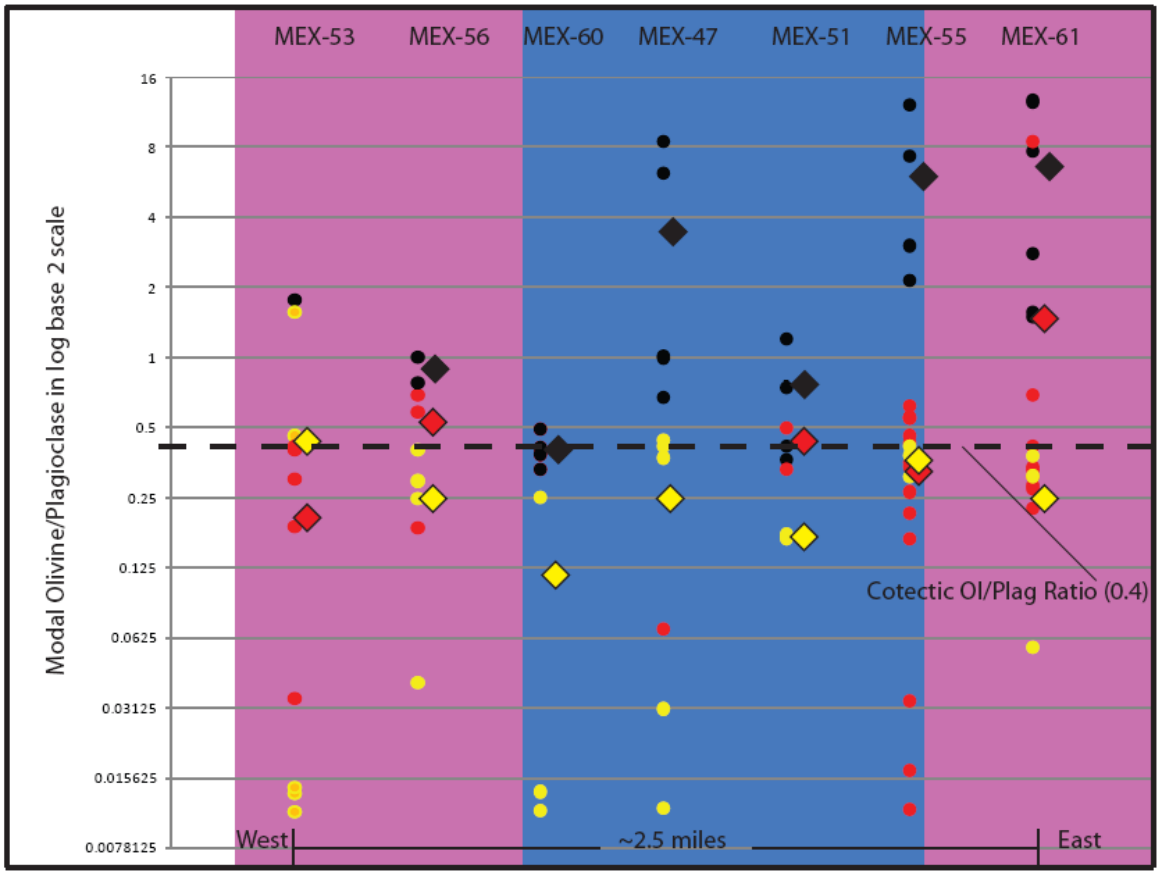


Figure 65: Modal mineralogy versus distance (olivine/plagioclase), yellow dots = PEG unit, black dots = U3 unit, red dots = BH unit, purple fields = holes drilled entirely through SKI, blue field = holes drilled through anorthositic inclusion block. Dashed line indicates the cotectic Ol/Pl ratio ~0.4. Diamonds indicated the approximate average Ol/Plag ratios.

area for the BH and PEG units. Both units have average Ol/Pl ratios that are typically less than the 0.4 cotectic ratio. In contrast, the Ol/Pl ratio in the U3 unit has average

compositions greater than the cotectic ratio, and shows a somewhat systematic decrease in that ratio from west to east. This trend of a gradual enrichment in plagioclase relative to olivine is consistent with density segregation by east to west flow of the U3 magma.

### 5.6.2 Incompatible Element Evidence

As a mafic magma crystallizes cumulus plagioclase and olivine, incompatible minor elements such as phosphorus, titanium, and potassium will become progressively enriched in the magma, while compatible trace elements such as nickel and chromium will be depleted. Compatible major elements such as calcium and magnesium would also become depleted in the magma as solid solution minerals (i.e. plagioclase, olivine) crystallize. Theoretically, a laterally flowing and fractionally crystallizing body of magma might show incompatible element enrichment and compatible element depletion in the magma as it moves downstream farther from the magmatic source. The whole rock concentration of the compatible elements would depend, however, on the proportions and compositions of cumulus phases and intercumulus liquid components, which vary independently of each other and are difficult to accurately determine. However, if we assume that all incompatible elements reside in the intercumulus liquid component and we compare only similar types of lithologies that have approximately similar proportions of cumulus and postcumulus minerals, then we can assume that any variation in incompatible element concentration will reflect changes in the (fractionated) composition of the intercumulus liquid. It is assumed here that at a large scale, the basic lithologies

comprising the BH and U3 units are internally similar and therefore compositional changes within each unit approximate changes in the intercumulus (parent) liquid.

This analysis is somewhat hindered by both limited types of incompatible elements that were analyzed by Duluth Metals and by the low precision detection limits for incompatible elements. Incompatible minor and trace elements that are available from the Duluth Metals analyses include phosphorous, titanium, potassium, and sodium. Concentrations of these elements in the BH and U3 units are plotted in figure 66 by drill hole, placed in geographic order (insufficient data were acquired from the unmineralized PEG unit). At first glance, there appears to be no systematic pattern. When comparing the incompatible element concentrations at the farthest west (MEX-53) and east (MEX-61) extremes, however, there is a general increase to the west, especially in the U3 unit. In between these two drill holes, however, the data becomes somewhat variable and inconsistent with a wide range of values. Most of these holes were drilled through or at the perimeter of the anorthositic inclusion block (MEX-60, MEX-47, MEX-51, MEX-55), with MEX-60 and MEX-55 on the edges of the block. This could indicate not only that magma flowed laterally from the east to the west (MEX-61 to MEX-53) in the intrusion, but also that flow-induced fractionation was hindered around the area of the anorthositic inclusion block. Perhaps flow channels may have been an early prominent feature of magma chamber dynamics, and that as the upper zone magma chamber opened up, the anorthositic inclusion block was left behind, acting as a trap for magmatic fluids emanating from magmas trapped under the block, which caused the elevations and inconsistencies in the incompatible element data below (Fig. 66).

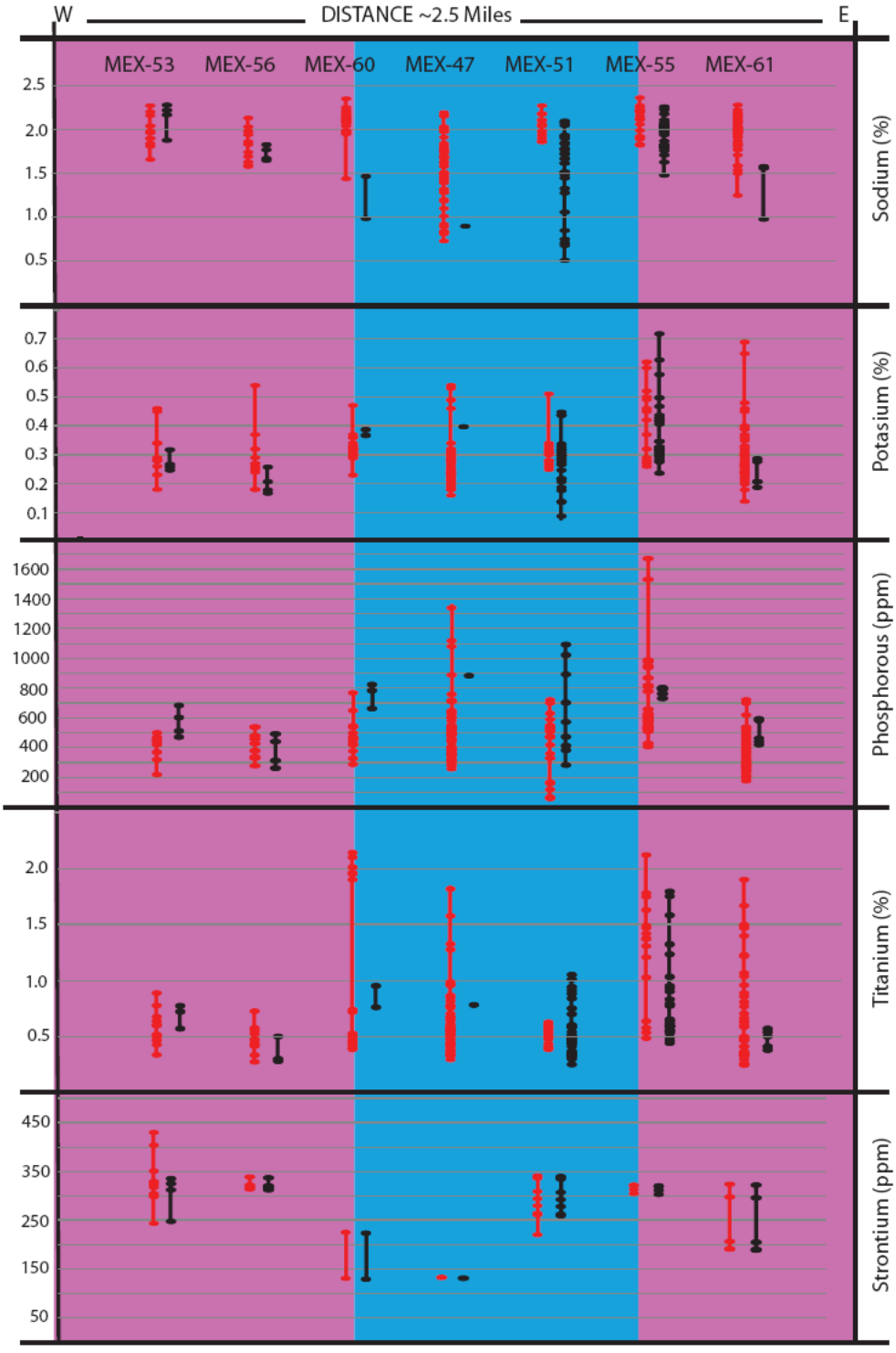


Figure 66: Selected incompatible element concentrations versus distance in the BH unit (red) and U3 (black) units from assay geochemistry; purple fields = holes drilled entirely through SKI, blue field = holes drilled through anorthositic inclusion block.

### 5.6.3 Mineral Chemistry of Olivine

It is well established that fractional crystallization of olivine produces progressively more fayalitic composition. Although the final olivine composition will depend on the degree of trapped liquid shift (Fig. 60), this effect can be minimized if similar cumulate rock types are considered. Another consequence of olivine fractionation is that it results in the progressive depletion of nickel in the magma. Nickel is compatible in olivine ($K_D \sim 5$); however, in the presence of an immiscible sulfide liquid, nickel will be strongly partitioned out of silicate magma and into sulfide liquid ($K_D = 100$, Rollinson, 1993). Assuming that sulfide saturation occurred shortly after or just prior to emplacement of SKI magmas forming the basal contact zone, nickel should become depleted from the magma downstream (west), and hence concentrations of nickel in olivine should be less downstream as well. Considering both olivine compositional factors described above, if magma flowed from the east to the west in the basal contact zone of the SKI, then olivine compositions should be more forsteritic with higher nickel concentrations in the east than in the west.

The U3 unit contains consistently adcumulate rock types which will promote a common, low degree of trapped liquid shift. This, as well as its relatively restricted stratigraphy, makes it the ideal focal point for this analysis. Forsterite and nickel contents are plotted in figure 67, according to drill hole in geographic order. Data from the easternmost core (MEX-61) shows the highest forsterite contents and is among the highest in nickel concentration, while the westernmost core (MEX-53) is at the low end of forsterite content and nickel concentration (Fig. 67). Data for MEX-56 generally falls

between these two holes (MEX-61, MEX-53), excluding a single outlying nickel concentration of just greater than 0.011 mole percent. These three holes (MEX-61, MEX-56, MEX-53) seem to demonstrate a downstream fractionating magma, becoming progressively depleted in nickel. However, the three holes that pierce the anorthositic inclusion block (MEX-55, MEX-51, MEX-60) display a completely opposite trend. That the data for the U3 unit beneath the anorthositic inclusion block does not follow suit with the data flanking the block shouldn't be surprising, considering the incompatible element data displayed in figure 66 above. This could again be a display of trapped liquids

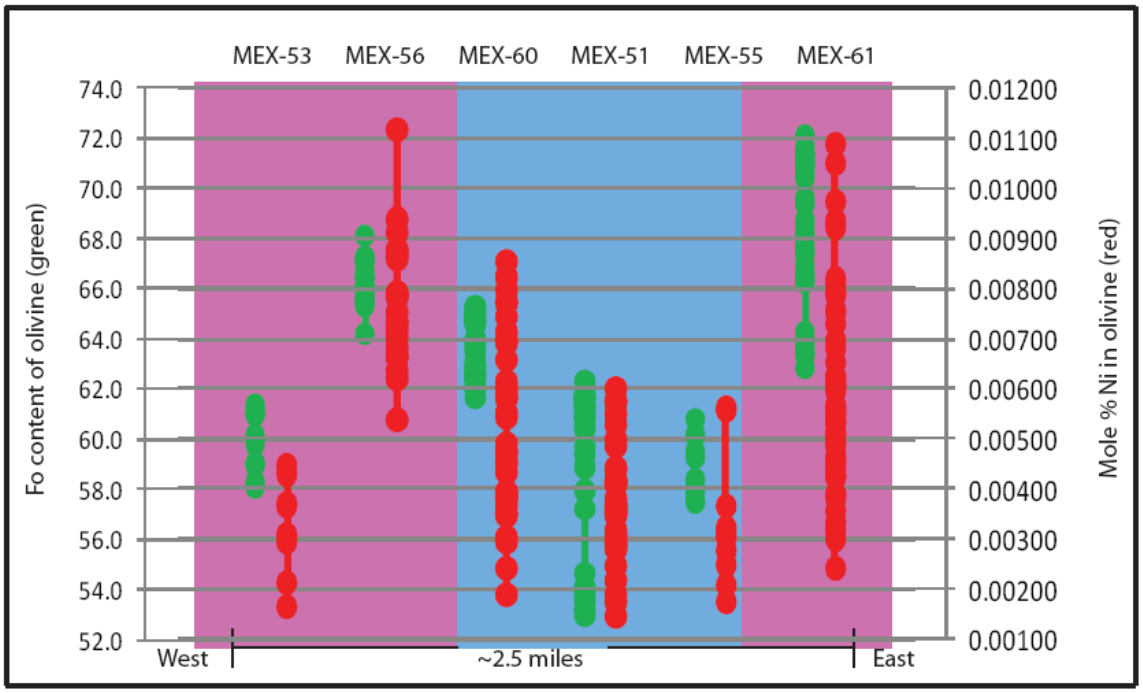


Figure 67: Fo content (green) and nickel concentration (red) in olivine from the U3 unit plotted by drill hole, purple fields = holes drilled entirely through the SKI, blue field = holes drilled the anorthositic inclusion block.

beneath the block not being given an opportunity to escape upon uplift and removal of the anorthositic series roof where the upper zone now exists. Lower Fo contents can be explained by this trapping and subsequent dilution of the magma, however nickel

concentrations should not be affected by this process. Perhaps the area beneath the block was more vertically restricted than other parts of the intrusion when the basal contact zone was emplaced, which caused constriction of magma flow beneath the block, resulting in higher R-factors between the silicate magma and sulfide melt. This process would cause more nickel to be taken up by the sulfide, leaving less nickel in the magma to crystallize with olivine. While the olivine compositional data are not conclusive by themselves, they are generally consistent with fractional crystallization accompanying E-W lateral flow, especially for the holes flanking the anorthositic inclusion block.

### 5.6.4 Major Element Whole-Rock Geochemistry

Given the physical and chemical variables that could affect the mineralogic and geochemical attributes along the two-dimensional profile defined by the seven drill cores previously described, perhaps a more regional view of geochemical trends can reveal patterns that can better test the E-W flow model. The mg# (MgO/(FeO+MgO), mol%) calculated from whole-rock geochemistry on a deposit-wide scale might provide insight into the presence or absence of channelized and/or general east-west magma flow in the basal contact zone. This parameter is generally a good measure of the fractionated character of ferromagnesian minerals in similar types of adcumulates. As such, the U3 unit is again the focus of this analysis because it is dominated by cumulus olivine. The regional variation of mg# (Fig. 68) does not show decreasing magnesium numbers from west to east as might be expected. Instead the data show mg depletion beneath the

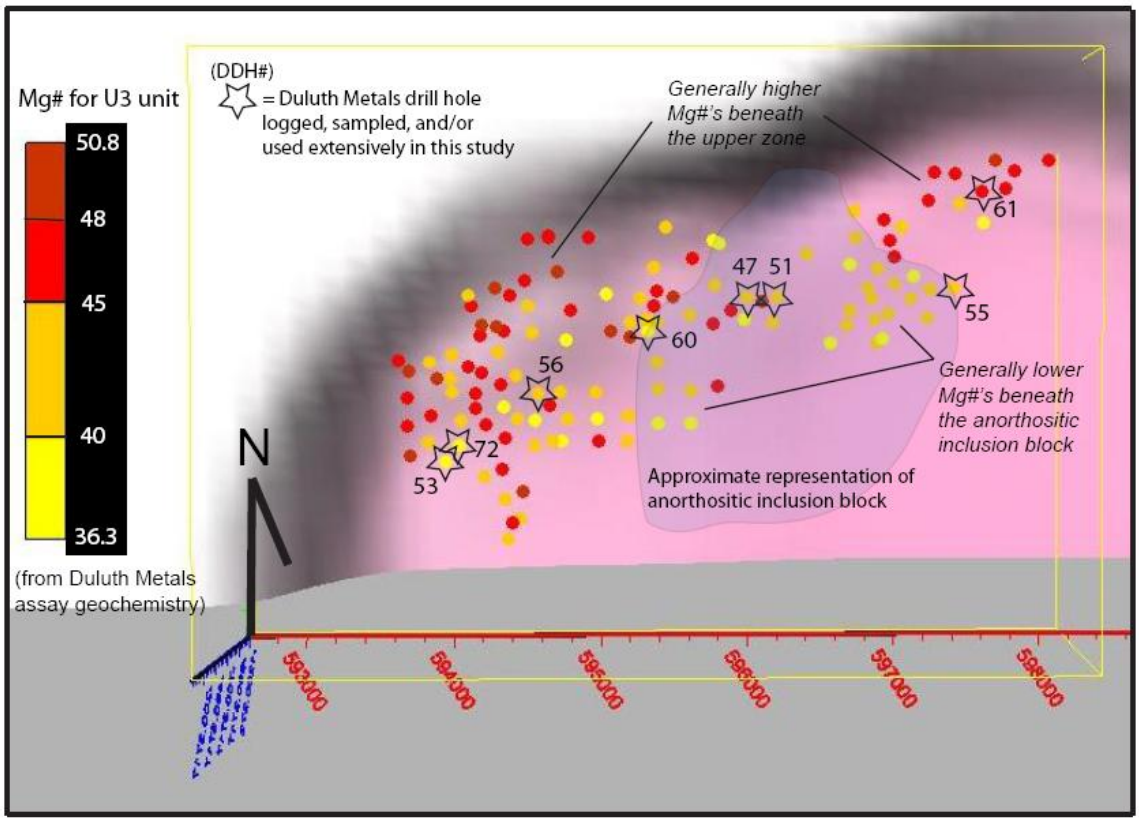


Figure 68: Plan view of whole rock mg# (Mg/(Mg+Fe)) in the U3 unit from drill hole assay geochemistry; shaded gray to pink area shows approximate footwall contact for reference.

anorthositic inclusion block and magnesium enrichment around the block (Fig. 68). This pattern is similar to that found with the profile in Fo and Ni content in Figure 67, which again may reflect a trapped liquid shift effect caused by evolved liquids being trapped and forced to equilibrate with cumulates beneath the anorthositic inclusion block. After the emplacement of the upper zone troctolites, the basal contact zone magmas could become "liberated" and infiltrate upward into the upper zone cumulates. The mg# data also seems to track magma flow channels developing from east to west, as magma first flows north of the block and then turns south as it encounters a steeply dipping GRB

footwall to the west. It could be that flow channels are actually marked by higher magnesium numbers with lower magnesium numbers flanking the channels.

### 5.6.5 Metals Ratios

Ratios of selected chalcophile metals can also indicate magmatic flow with relation to progressive sulfide exsolution from silicate melt. If magma flowed from east to west and sulfide liquation occurred throughout the flow, then copper over palladium ratio should strongly increase to the west, because palladium is preferably partitioned into sulfide liquid from silicate melt by several orders of magnitude greater than copper (Naldrett, 2004). Average copper/palladium ratios for the U3 unit from assay geochemical data in three dimensional plan view do increase from east to west (Fig. 69). This analysis is quite demonstrative, especially relative to the incompatible element analysis above (Fig. 66; Sec. 5.6.2). This analysis largely tests for progressive sulfide fractionation demonstrated through lateral flow in the basal contact zone, and displays a much more obvious signal because the depletion of strongly compatible elements is much more sensitive than the enrichment of incompatible elements (Rollinson, 1993) due to fractional crystallization. Notice that low Cu/Pd ratios ranging from 5663-15,000 are displayed throughout the map area, but are strongly concentrated in the northeast (Fig. 69). More compelling is the distribution of values ranging from 30,000-50,000, and 50,000-104,667. There are none of these data points located in the northeast, indicating that palladium concentrations are higher in the east than in the west. This analysis not only implies sulfide fractionation in the Nokomis deposit, but also displays a compelling

and straightforward demonstration of lateral flow from east to west in the SKI's basal contact zone.

While some of the data presented in this section is somewhat inconclusive, they certainly do not dismiss lateral flow as an element of genesis in the study area. In fact several areas of analysis (plan view whole-rock Mg#'s, plan view Cu/Pd ratios) strongly implicate lateral flow involved in both petro- and metallogenesis, and support Peterson's (2001, 2008) lateral flow model for the northern SKI. In the next section (5.7) I implement lateral flow into the emplacement models introduced in section 5.5 to present an interpretive petro- and metallogenesis model for the Nokomis deposit area.

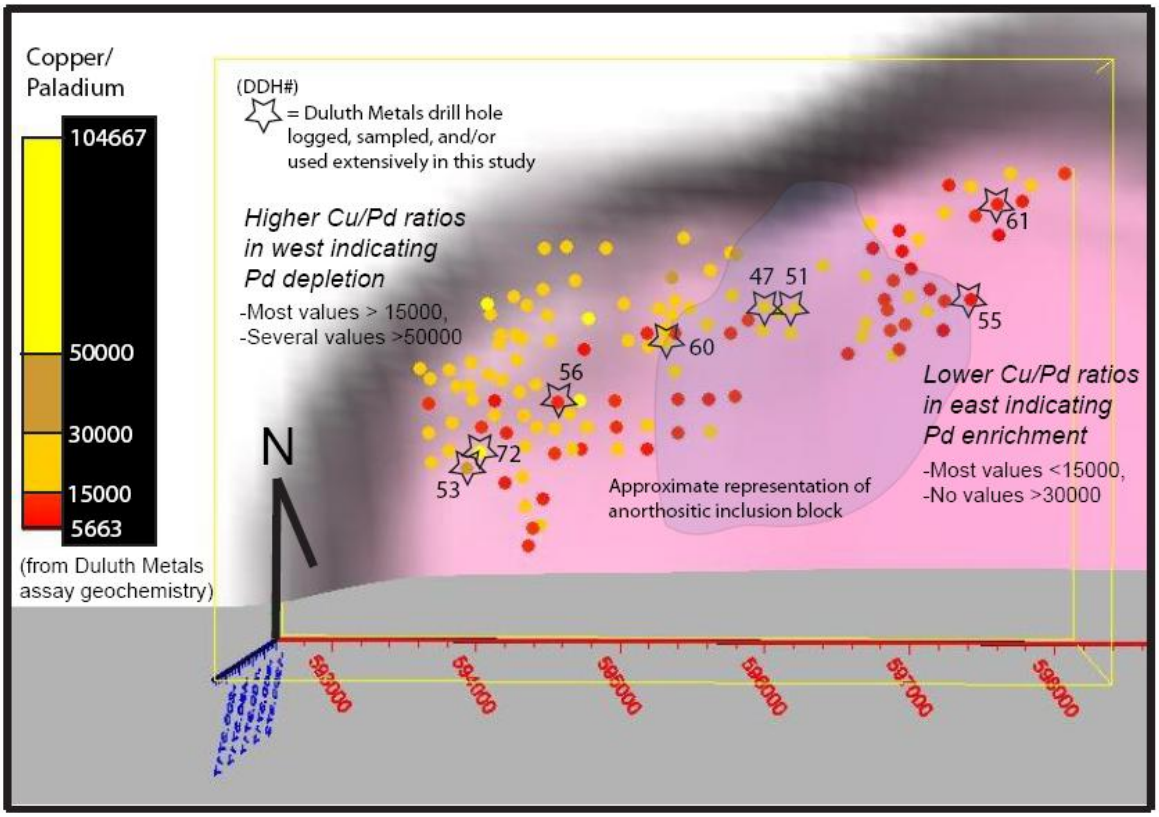


Figure 69: Plan view with approximate footwall contact for reference of Cu/Pd ratios in the U3 unit from drill hole assay geochemistry.

## 5.7 Petrogenesis and Metallogenesis of the SKI in the Nokomis Deposit Area

The analytic elements of this study (detailed bedrock mapping and core-logging, petrographic observations, mineral chemical analysis, and whole-rock geochemical/assay data (from Duluth Metals)) were conducted in order to develop a lithologic, mineralogic, and geochemical framework from which to evaluate the emplacement, crystallization and mineralization history of the SKI in the Nokomis deposit area. Through assembly of this framework, two lithologically and geochemically distinct zones of SKI rocks were identified (the basal contact zone and the upper zone) as well as a third, exotic package of rocks (anorthositic inclusion block) that had a significant influence on the petrogenesis and metallogenesis of the Nokomis deposit area. In the previous section (5.6), basal contact zone data were evaluated to determine whether they offered supporting evidence to Peterson's (2001) lateral flow model. It was found that, while complicated by the anorthositic inclusion block, evidence of east to west flow is supported by modal mineralogy and Cu/Pd ratio data, and to a lesser degree by incompatible element concentrations, olivine compositions, and whole rock mg# data. In section 5.5, single-phase and two-phase emplacement models for the basal contact zone were proposed and an *in situ* fractional crystallization model with periodic magma recharge in the upper zone was described. In this section, these emplacement models for the Nokomis deposit area are further embellished by incorporating processes of lateral flow and sulfide mineralization. Before presenting and discussing these models, it is necessary to discuss more recent developments made on the open versus confined model for mineralization in the SKI (Peterson, 2009, 2008, 2001).

### 5.7.1 Crystal slurry/channelized flow model for the basal contact zone of Peterson (2009)

Peterson (2001) defined two types of Cu-Ni-PGE sulfide mineralization in the SKI (open vs. confined) as described in section 2.5, and suggested that east-west lateral flow was a crucial component in the genesis of both types of mineralization. Recently, Peterson (2009, 2008) has expanded the open versus confined model by developing a crystal-slurry/channelized flow model for the genesis of the basal contact zone and the Nokomis deposit. Peterson's (2009; Fig. 70) crystal slurry model for the basal contact

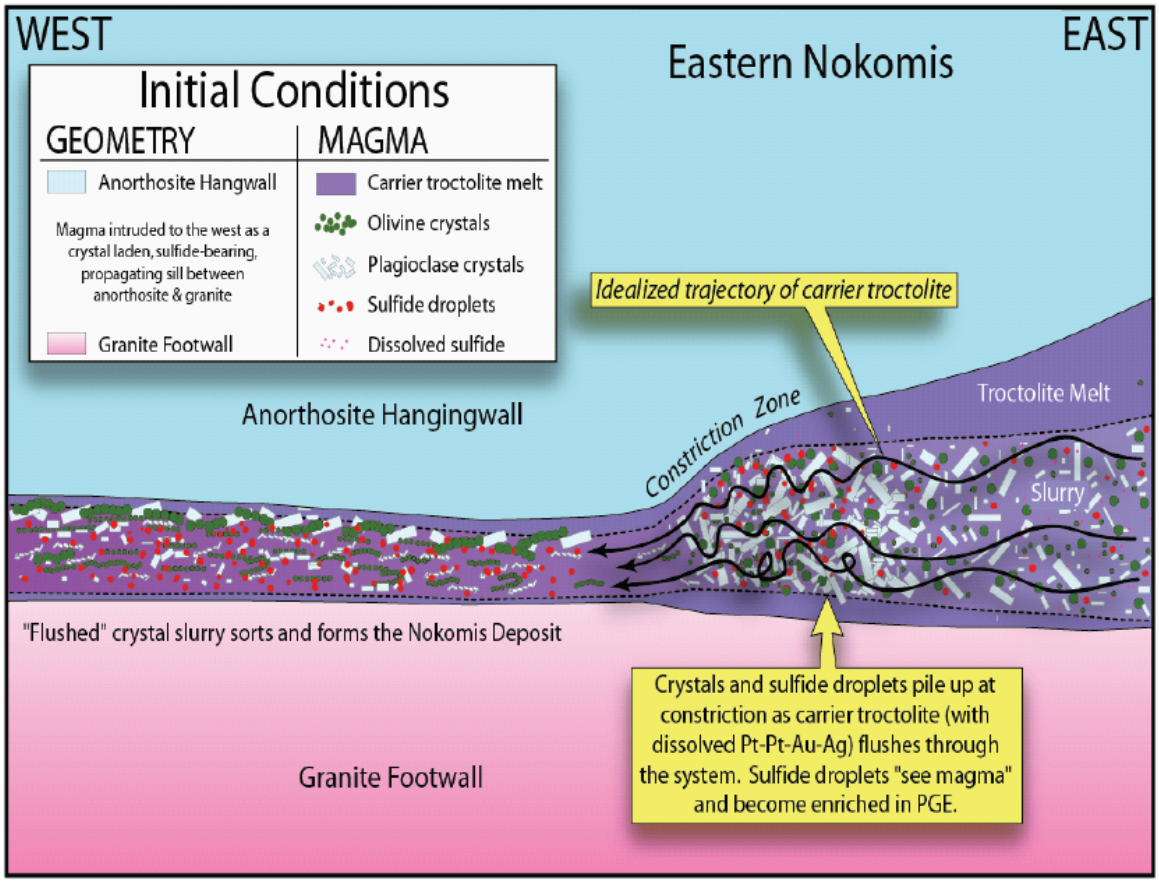


Figure 70: Peterson's crystal slurry model for the genesis of the basal contact zone (2009).

zone proposes that flow-induced crystal sorting created the stratigraphy (BH-U3-PEG) observed in the basal contact zone. In this model, the basal contact zone is emplaced as a sill, while lobes propagate laterally and vertically though a series of interfingering injections (Fig. 71; Pollard et al, 1975). Constriction at the forefront of lobes caused by the over-riding anorthositic series hanging wall causes both high R-factors and crystal sorting as magma and crystals are flushed downstream through the zone of constriction (Fig. 70). In this process, larger plagioclase crystals are forced upward as smaller olivine crystals flow downward, similar to the way in which turbidity flows are inversely graded as larger particles and fragments are pushed upward while smaller particles and fragments gravitate downward. Sulfide droplets also pile up at the point of constriction, causing the sulfide to encounter large volumes of magma and become enriched in PGE's.

Peterson (2009) identified physical depressions or scours in the GRB footwall of the Nokomis deposit by rotating cross-sections developed from Duluth Metals drill hole logs back to normal at the time of emplacement. He interprets these scours as flow channels (Fig. 72), noting differing metal profiles between 1) the channel edge, and 2) the channel center, as well as, 3) an anomalous increase in footwall mineralization below the channel center. These metal profiles include: 1) Cu-Ni-PGE disseminated sulfides, 2) Ni-Co enriched semi-massive sulfides, and 3) Cu-PGE enriched fractionated sulfides in the footwall. Peterson interprets these three confined-mineralization-style profiles to have been generated from 1) buoyant magmatic fluids carrying Cu-PGE metals up and out of the solidifying crystal-mush below, 2) Siliceous partial melts emanating from the granitic footwall within the channel, mixing with the sulfide-bearing troctolitic slurry triggering

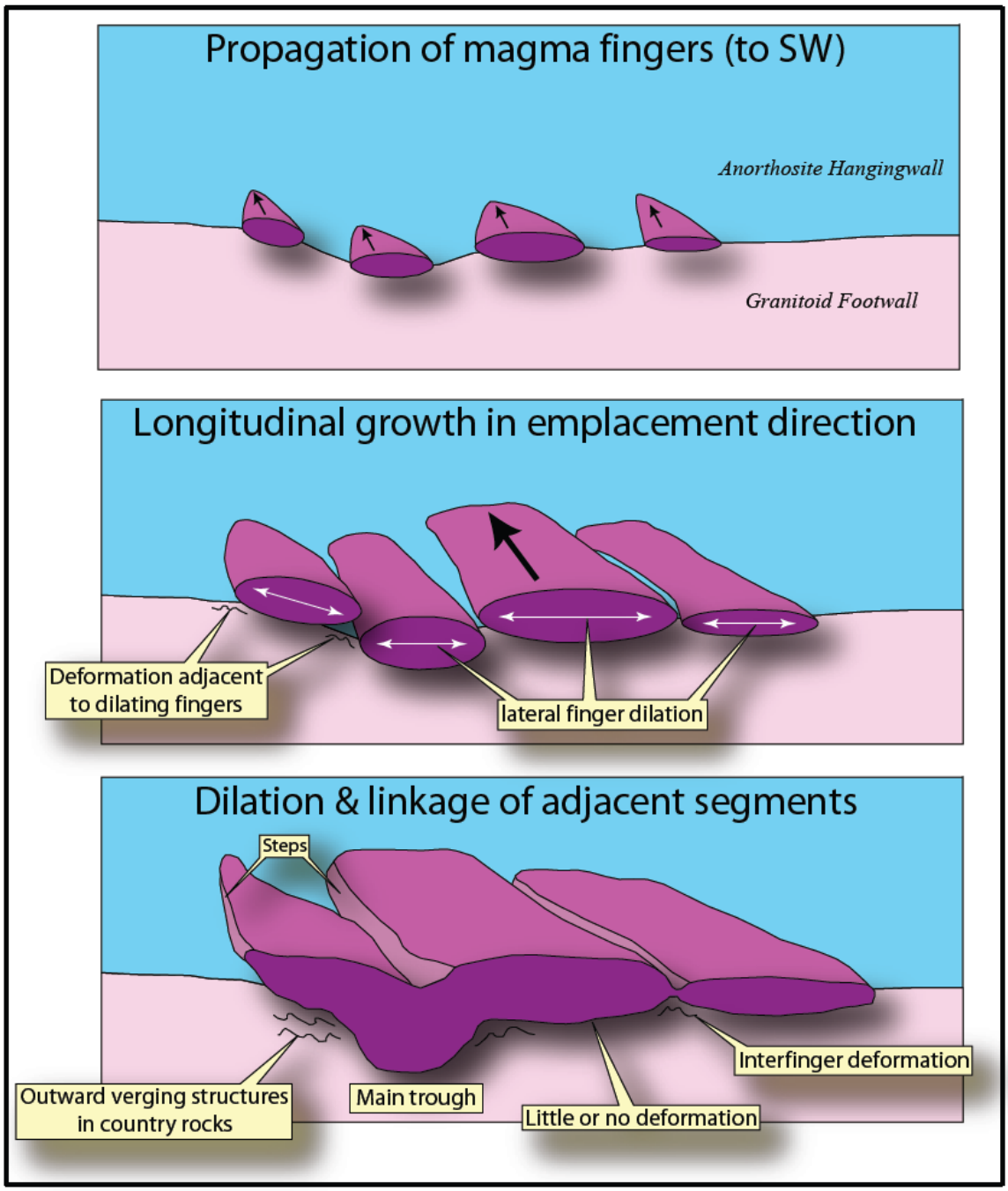


Figure 71: Propagation of a sill through advancement of fingers both laterally and vertically, modified from Pollard et al, 1975.

sulfide immiscibility which immediately scavenges and deposits Ni and Co from the magma, and 3) downward convecting hydrothermal fluids which carry and precipitate Cu and PGE's away from the thermal anomaly caused by channelized magma flow. With this model, Peterson (2009) was able to estimate dimensions on the channel width (300-500 m), and height (25-100 m), which is on scale with identified zones of Ni-Co enrichment in the Nokomis deposit. These zones of Ni-Co enrichment appear to track the main magmatic channel pathways through the Nokomis deposit (Fig. 73; Peterson, 2009).

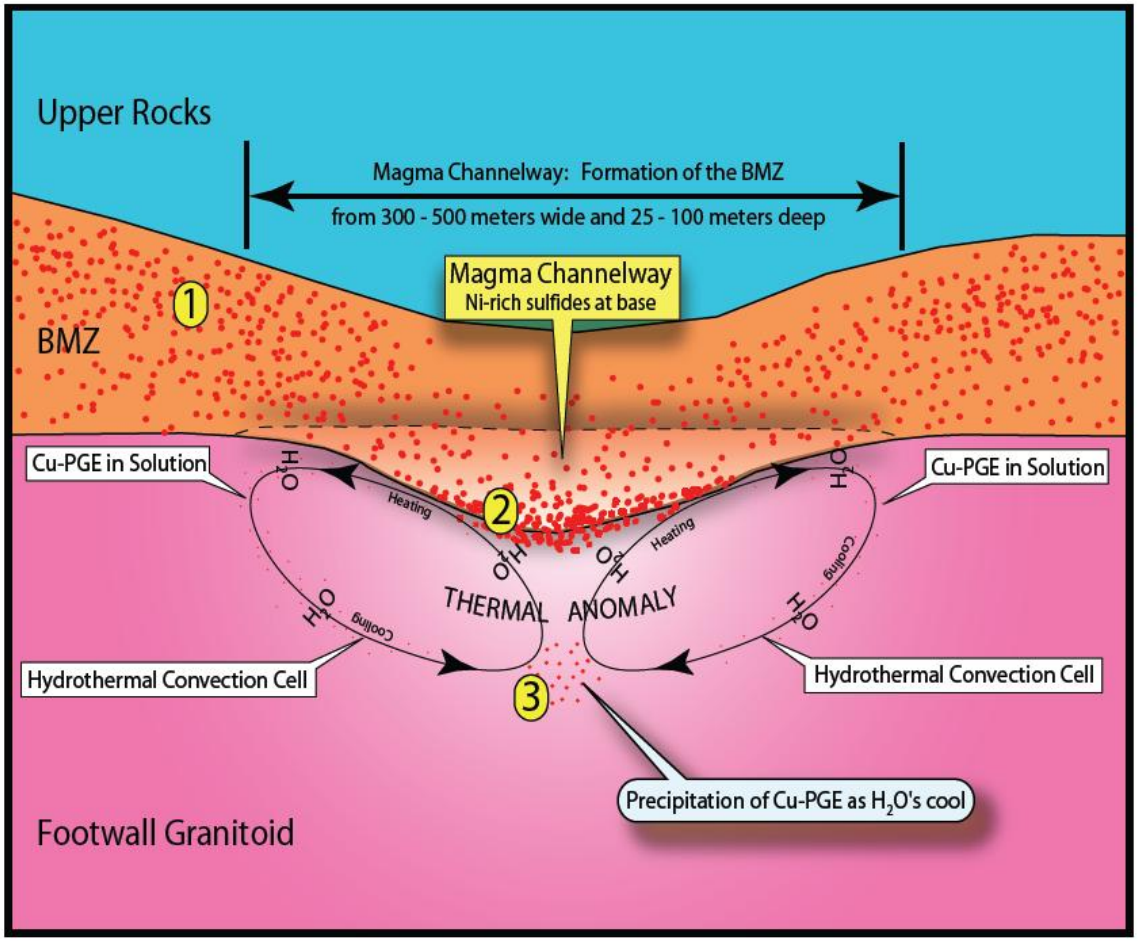


Figure 72: Peterson's channelized flow model of confined-style sulfide genesis, 1) Cu-Ni-PGE disseminated sulfides, 2) Ni-Co enriched semi-massive sulfides, 3) Cu-PGE enriched fractionated sulfides (2009).

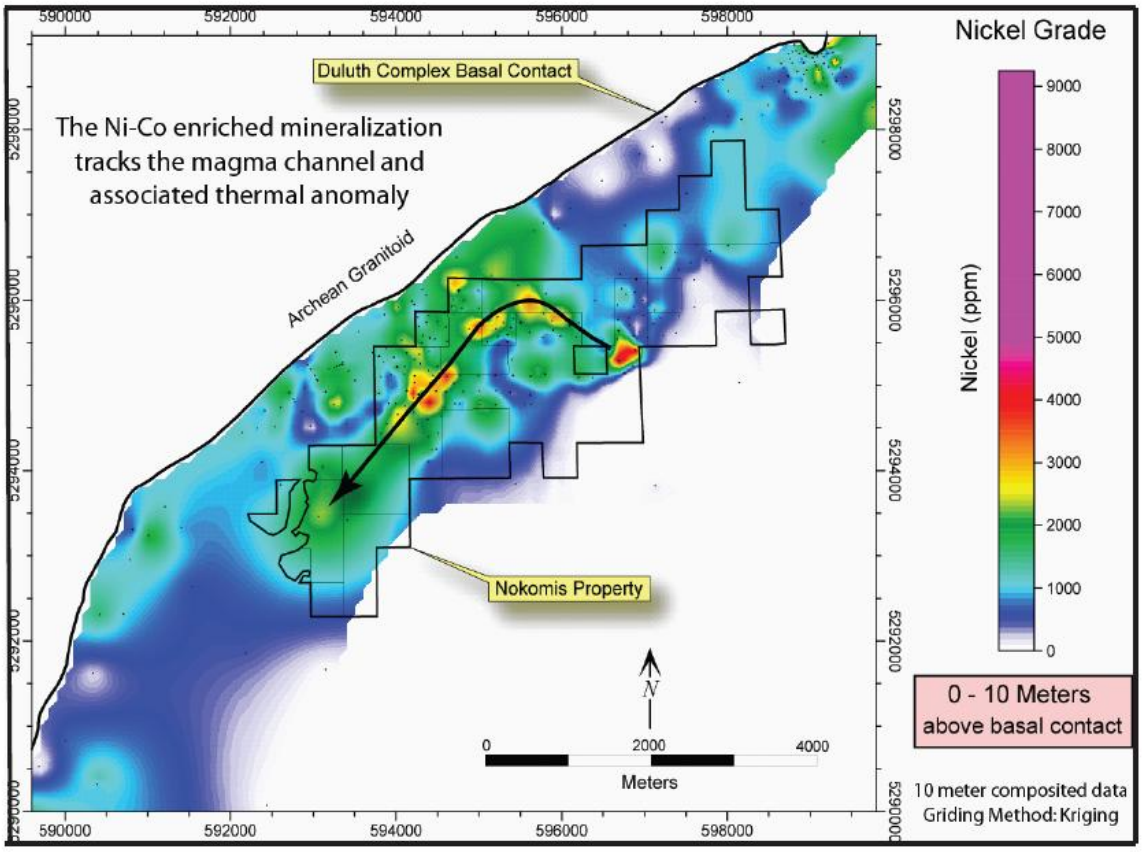


Figure 73: Magma channel tracked through the Nokomis deposit by zones of Ni-Co enrichment, Peterson, 2009.

### 5.7.2 Petrogenesis and metallogenesis of the basal contact zone in the Nokomis deposit area

As discussed in section 5.5, two general models for the genesis of the basal contact zone are envisioned - a single phase model and a two phase model. The models are similar to each other, while differences largely involve the formation of the U3 unit. In these models, the SKI magmas are assumed to have been sourced from the Nickel Lake macrodike (Fig. 74-1), and spread out as a sheet-like intrusion. The sheet was emplaced largely along the contact between a hanging wall of newly formed (and

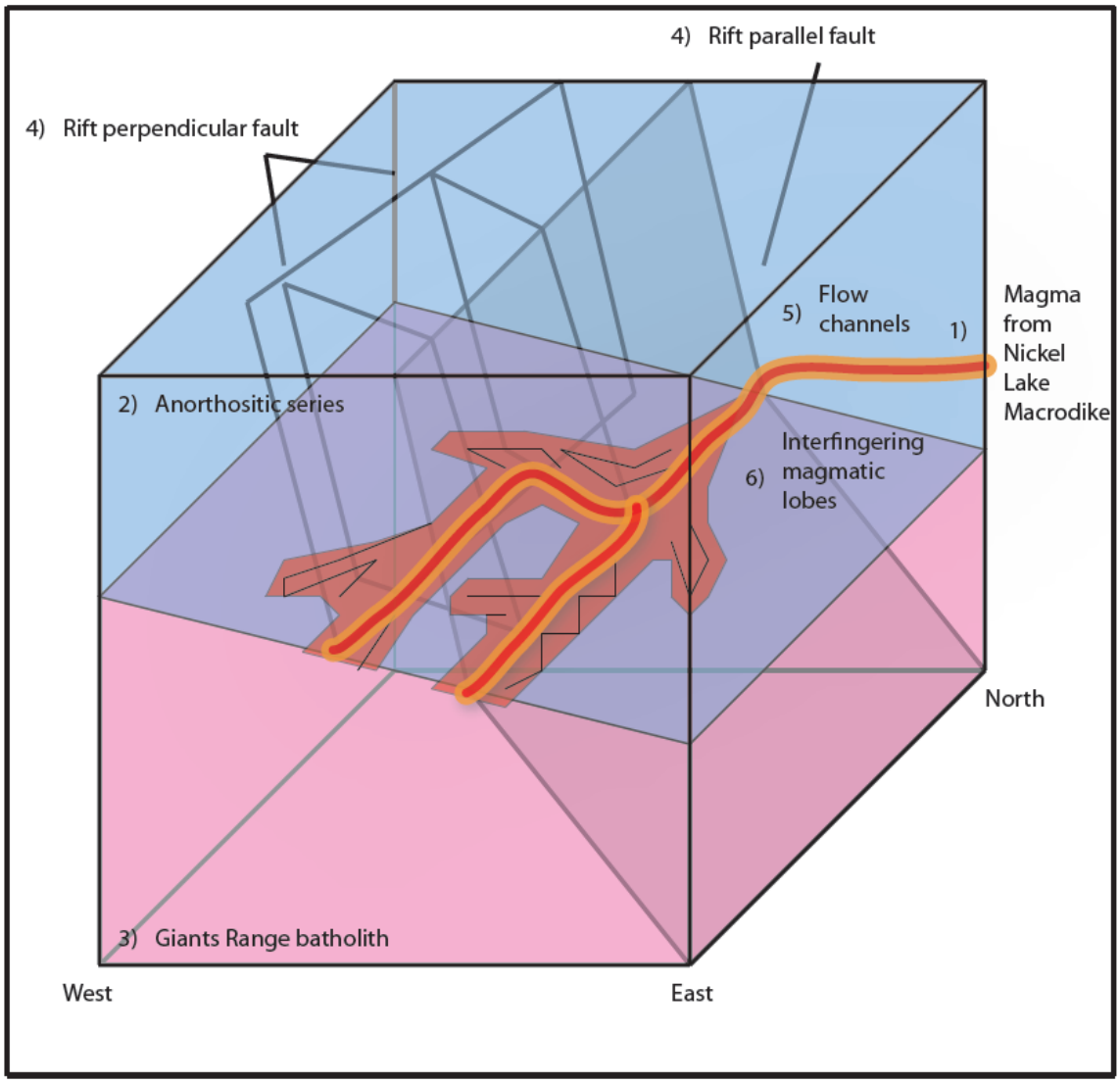


Figure 74: Initial conditions for emplacement intrusive flow channels to form the basal contact zone, see text for explanation.

therefore warm and possibly semi-molten) anorthositic series (Fig. 74-2) and footwall granitoids of the Giants Range Batholith (GRB; Fig. 74-3). Perhaps a network of rift parallel and perpendicular (transform) faults related to the Midcontinent Rift (Fig. 74-4) produced weaknesses in the anorthositic series and possibly in the GRB footwall for early SKI magmas to exploit and develop a network of flow channels mainly along the rift

parallel faults (Fig. 74-5). Continuous magmatic flooding propagated the development of numerous interfingering lobes with varying degrees of channel development (Fig. 74-6) that resulted in a coalescence of these lobes to form a continuous sheet-like, sulfide-bearing basal contact zone.

Single and two phase emplacement of the basal contact zone have the same initial conditions (Fig. 75-A), and were initially injected as interfingering lobes (Fig. 75-B) prior to coalescence into a single sheet-like sill. Early in the development of the basal contact zone, rift-related faulting may have caused down-dropping in the anorthositic series hanging wall that created the anorthositic inclusion block (Fig. 75-C).

Single-phase petrogenesis of the basal contact zone (Fig. 76) begins with emplacement of a crystal-laden magmatic slurry with various autoliths and xenoliths as sill lobes displace the anorthositic series hanging wall. Heat from injecting magmas induces partial melting of the granitoid GRB footwall (Fig. 76, 1). As these buoyant, siliceous partial melts rise into the overlying magma, the magma becomes silica-saturated, facilitating the crystallization of orthopyroxene to produce the BAN unit, and inducing sulfide saturation, which produces semi-massive and massive Ni-Fe-rich sulfide at the base of the deposit (Fig. 76-1). Contemporaneously, buoyant, volatile-rich fluids rise through the crystal-slurry, producing an evolved liquid, or upper differentiate of the BH unit above the crystal-slurry (Fig. 76-2). Continuous magmatic injections keep flow moving from east to west, causing a shear or drag force between the more viscous crystal-slurry (BH) and less viscous upper differentiate (PEG), which causes the upper parts of the crystal-slurry (BH) to be pushed or pulled along creating bifurcations of the

crystal-slurry up into the progressively forming U3 (Fig. 76-3). The sharp contacts at the top of the U3 unit are caused by a strong contrast in density between the U3 and PEG, while the gradational bottom U3/BH contact is due to much less of a contrast in density. Crystal segregation in the upper part of the basal contact zone is driven by both density and flow, as larger, less dense plagioclase crystals progressively rise, while smaller, denser olivine crystals progressively sink (Gray and Thornton, 2005), These flow and density processes are largely responsible for creating the olivine-rich U3 and plagioclase-rich PEG. Large-scale, deposit-wide magma flow (east to west) is observed in the upper part of the deposit by a general decrease in olivine, and an increase in plagioclase to the west (5.6.1).

Sulfide immiscibility in the metal-rich crystal-slurry is induced by assimilation of sulfur-rich Animikie Group country rocks prior to emplacement, which is enhanced by continuous partial melting and upward infiltration of GRB footwall rocks and progressive cooling of the initial magmas. Buoyant, volatile- and chlorine-rich (Severson, 1994) fluids carry metals upward, dropping them at the top of the crystal-slurry (BH), creating finer-grained sulfides at the top of the deposit in the U3 (Fig. 76, 5). Within the crystal-slurry (BH), sulfides clump together, but are unable to sink through the crystal-laden BH unit (Fig. 76-5) due to interfacial tension between the sulfide and silicate liquids (Mungall and Su, 2005).

In a two-phase emplacement model all of the above elements of petrogenesis and metallogenesis still apply to create the BAN, BH and PEG units, however the U3 unit is

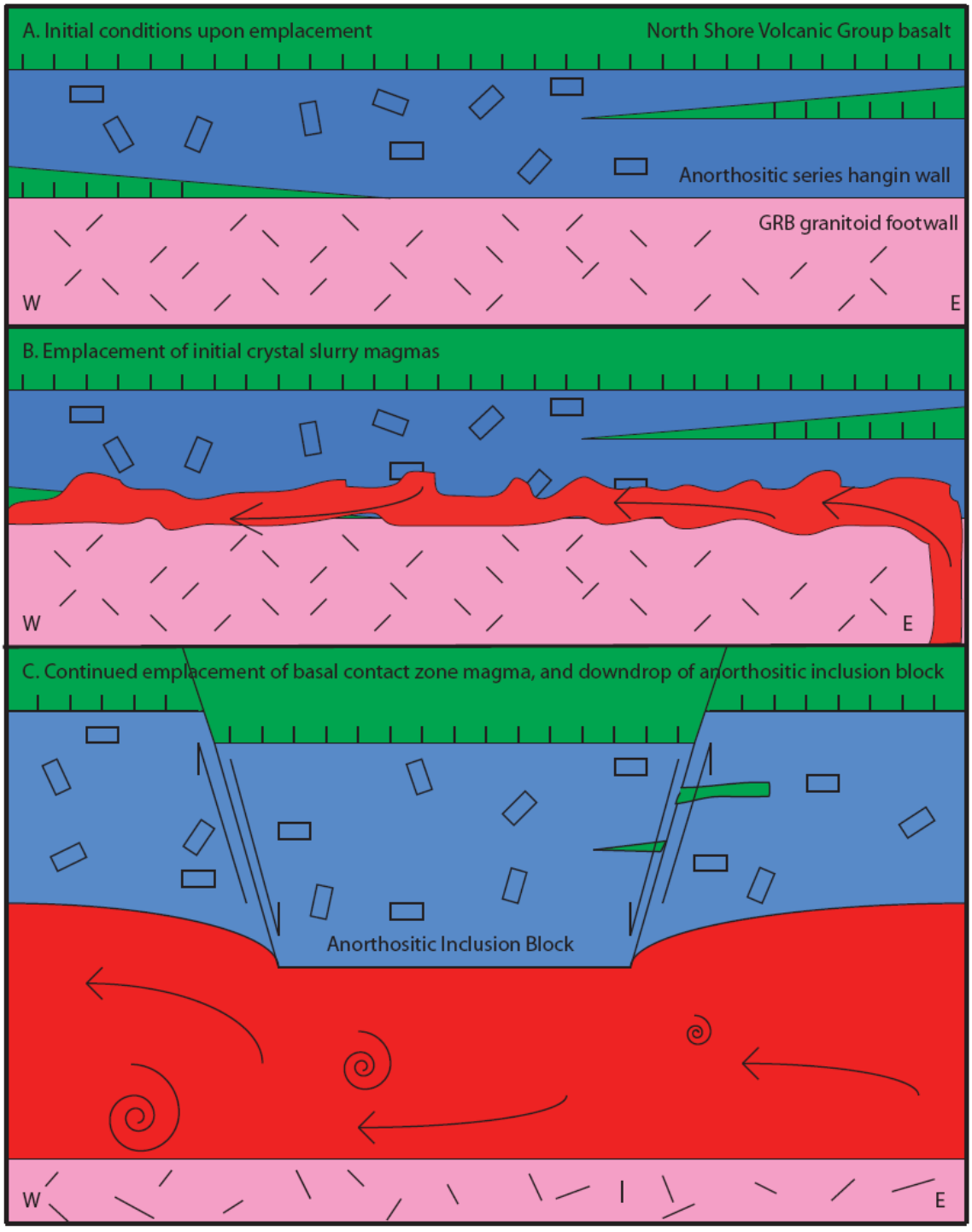


Figure 75: Early emplacement of the basal contact zone, A. initial conditions prior to basal contact zone emplacement, B. initial interfingering magmatic injections, C. down-drop of the anorthositic inclusion block with continued basal contact zone magmatism.

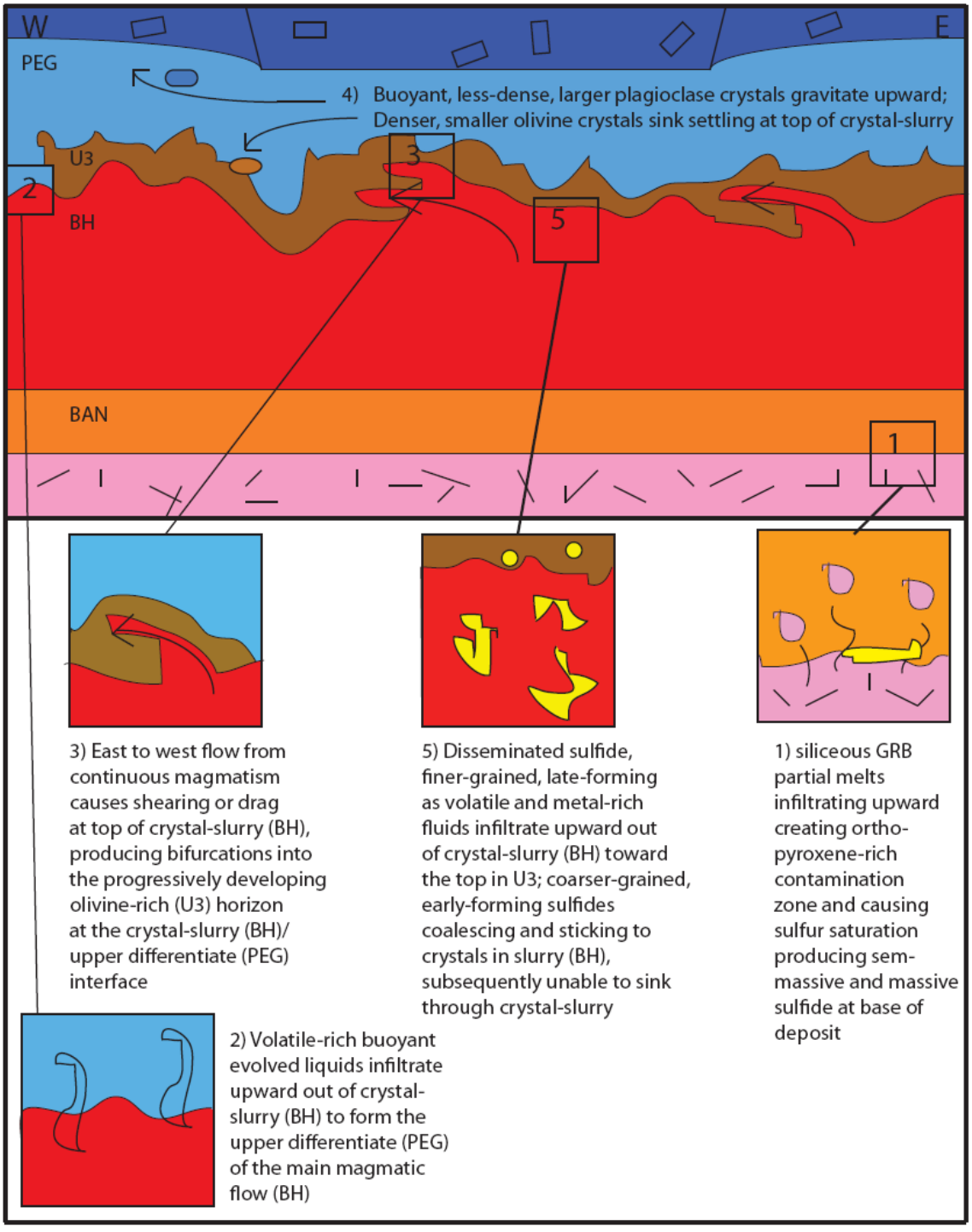


Figure 76: Single-phase petro- and metallogenesis of the basal contact zone, see text for explanation.

considered to be formed by a second late surge of primitive magma (Fig. 77). Upward and downward crystallization fronts (Marsh, 2006) propagate from the bottom and top of the basal contact zone, respectively (Fig. 77-1). These fronts leave a mushy, semi-molten center approximately at the BH/PEG interface. Continued primitive magmatism intrudes into this mushy core as it is more dense than the over-riding upper differentiate (PEG) of the underlying crystal-slurry (BH; Fig. 77-2). This magma surge interfingers downward into the upper parts of the crystal-slurry (BH), causing bifurcations of olivine-rich rocks (U3) into the BH (Fig. 77-3). This late basal contact zone injection is metal-rich, which upgrades the metal tenor at the BH/U3 interface (Fig. 77-4).

Both the single- and two-phase models are viable explanations for emplacement of the basal contact zone. The single-phase model views the U3 unit as somewhat of an afterthought, or consequence of emplacement, while the two-phase model views the U3 unit as a major (albeit secondary), episode of emplacement. Conceivably, differing sulfide mineralization styles between the BH and U3 units could provide clues concerning petrogenesis. While both the BH, and the U3 units contribute considerably to the metal budget of the basal contact zone, their mineralization styles are inherently different. Sulfides in the U3 unit are typically fine- to medium-grained, and chalcopyrite is dominant; while in the BH unit sulfides often form clumpy pegmatitic masses of chalcopyrite, talnahkite, and cubanite. This seems to indicate inherent differences at least in the emplacement environment of the two units, and it seems that when regarding metallogenesis from a physical expression standpoint (grain-size, mineralogy, texture; section 5.2.4) a two-phase model as presented here is favorable.

However, the chemostratigraphic profiles presented in section 5.3.3 regarding Cu-Ni-PGE concentrations demonstrate that distinct metal tenors cannot be linked to any specific unit. Instead, Cu-Ni-PGE grade profiles simply display a generally consistent stratigraphic variation through the entire basal contact zone. It also seems that stratigraphic variations in Cu-Ni-PGE grade profiles are laterally dependent, rather than stratigraphically dependent (i.e. beneath the anorthositic inclusion block versus beneath the upper zone), which would seem to favor a single-phase model of emplacement as presented here.

Evaluation of the single- and two-phase emplacement models for the basal contact zone presented in this study does not present a clear favorite. Possibly, both models apply, and some combination of the two may be appropriate. Given all of the chemical and physical data collected for this study (extreme heterogeneity of the BH unit, generally consistent BAN-BH-U3-PEG lithostratigraphy, major element geochemical and microprobe profiles, Cu-Ni-PGE concentration profiles, lateral chemical and physical variations), it seems evident that the general axiom for emplacement of the basal contact zone as a chaotic period consisting of an infinite number of rapid injections of an autolithic, cannibalistic, stratified, crystal-laden slurry emplaced into numerous restricted magma chambers via a network of channel-ways that eventually coalesced to form the basal contact zone may be the best explanation at this time. Possibly, more importantly, it does seem clear that there was a distinct change in emplacement styles above the basal contact marked by the interface between the PEG unit and the Main AGT unit as described below.

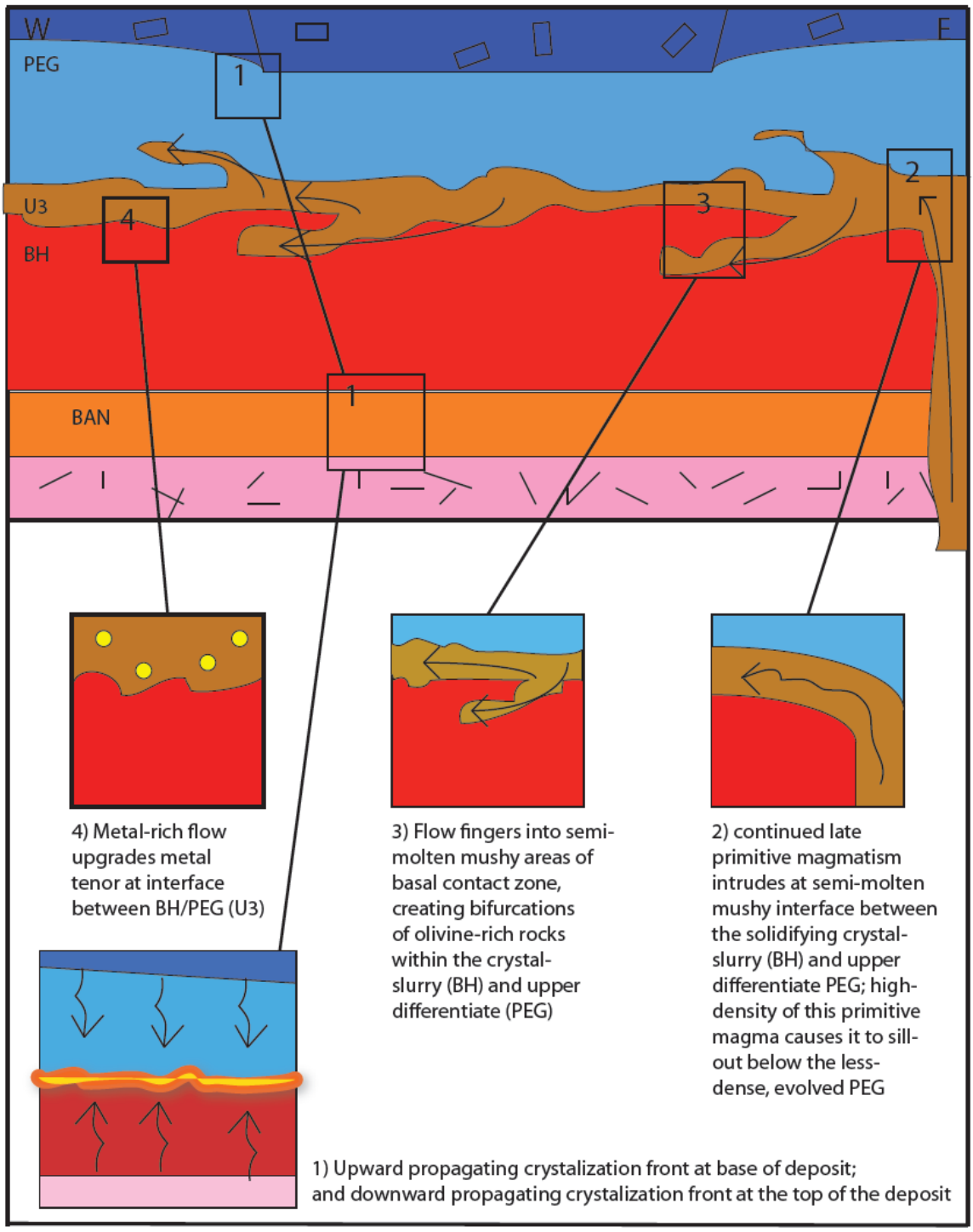


Figure 77: Two phase petro- and metallogenesis of the basal contact zone, see text for explanation.

The final step in the petrogenesis of the basal contact zone applies to both the single phase and two phase models, and involves the displacement of the anorthositic hanging wall through the emplacement of the upper zone (Fig. 78). It is evident from the

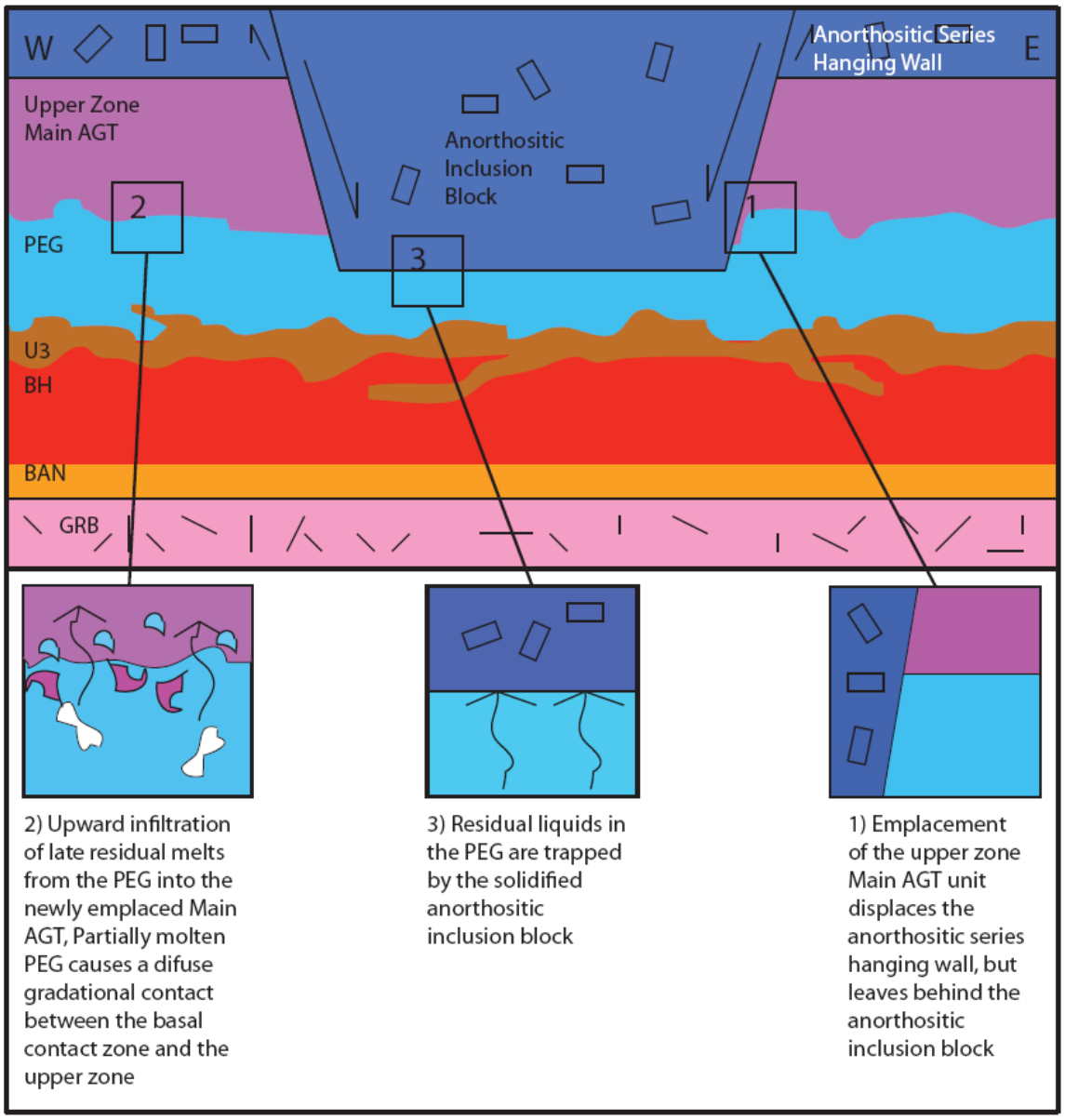


Figure 78: The final petrogenetic step in the formation of the basal contact zone, see text for explanation.

continuous stratigraphy of the basal contact zone transposing beneath both the upper zone and the anorthositic inclusion block (5.2) that the basal contact zone was largely generated while the anorthositic series composed the hanging wall in its entirety. However, substantial differences in Mg concentrations (5.3.1, 5.6.4) within the upper parts of the basal contact zone (PEG) between areas under the anorthositic inclusion block and areas under the upper zone indicate that the anorthositic series hanging wall was displaced prior to complete formation and solidification of the basal contact zone (Fig. 78-1).

Emplacement of the upper zone displaced the anorthositic series hanging wall, excluding the anorthositic inclusion block (Fig. 78-1). Emplacement of the upper zone above the basal contact zone allowed for upward infiltration of late residual magmas and/or magmatic fluids into the overlying, molten, newly forming Main AGT unit (Fig. 78-2), causing Mg enrichment in the PEG (addition through subtraction), and also producing the diffuse, very gradational contact between the PEG and Main AGT units. Conversely, below the anorthositic inclusion block late residual magmas in the PEG unit became trapped, effectively diluting the magma beneath the anorthositic inclusion block (Fig. 78, 3). Emplacement of the Main AGT unit begins a decidedly different environment for, and style of emplacement in the SKI.

### 5.7.3 Petrogenesis of the upper zone

The circumstances for emplacement and petrogenesis of the upper zone are vastly different than the restricted, dynamic environment that the basal contact zone was

emplaced into and generated from. Emplacement of the basal contact zone apparently denigrated the integrity of the hanging wall anorthositic series to the degree that subsequent magma injections were readily able to displace the hanging wall (Fig. 79, A, 1), as anorthositic inclusions become increasingly prominent upward through the stratigraphy (5.2.6). The progressive erosion of the hanging wall seemingly promoted a much calmer, more open emplacement environment for the upper zone. For reasons unknown, the anorthositic inclusion block was left behind during emplacement of the upper zone.

The magmas that created the upper zone of the SKI in the Nokomis deposit area were apparently sulfide-undersaturated, as trace to rare sulfide mineralogy extends throughout the stratigraphy of the upper zone. These magmas appear to have been emplaced episodically rather than near-continuously as in the basal contact zone. The Main AGT unit contains several thin olivine-rich to ultramafic horizons which may or may not be indicative of waning magmatism progressively becoming episodic (Fig. 79, A, 2). Above the Main AGT at least two major magmatic events are evidenced (Fig. 79, B-C). These episodes are portrayed by subtle differences in modal mineralogy between 1) the augite troctolites of the Main AGT and the anorthositic troctolites of the AT&T (Fig. 79, B, 1), and 2) the anorthositic troctolites of the AT&T and the troctolitic anorthosites of the AT(T) (Fig. 79, C, 1). The bases of both the AT&T (Fig. 79, B, 2) and AT(T) (Fig. 79, C, 2) units are marked by thin horizons of olivine-rich troctolites and ultramafic rocks. Distinct upward decreasing fractionation trends are also seen in whole-rock Mg and Ca concentration profiles of the upper zone. It is also evident

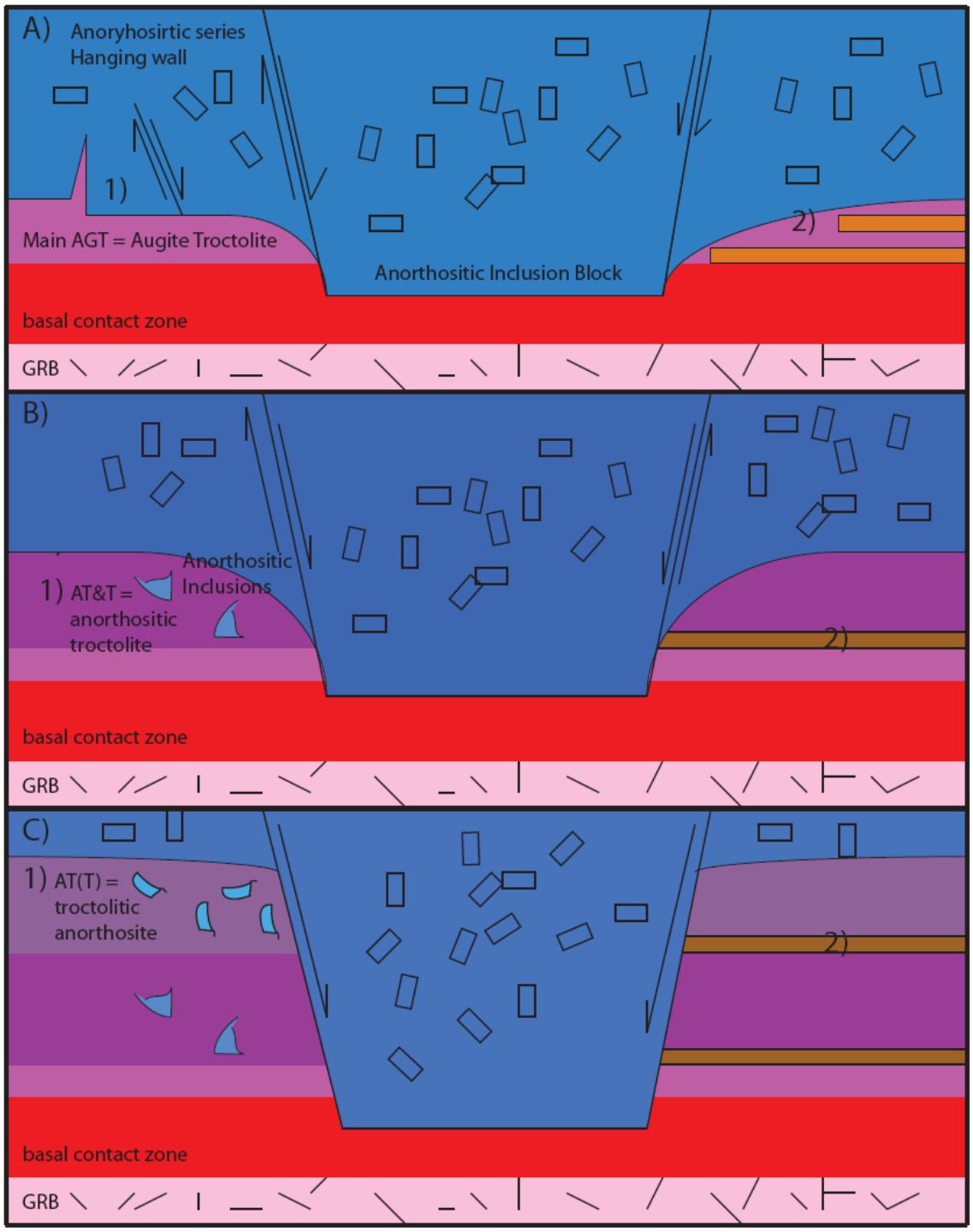


Figure 79: Petrogenesis of the upper zone, see text for explanation.

that the anorthositic inclusion block was detached from the hanging wall, as upper zone magmas of the AT(T) unit and the related G-in-T unit are present above the anorthositic inclusion block in both the field and in drill core (5.2.6). A complete petrogenetic and metallogenic model for the Nokomis deposit can be found in poster form on Plate III.

### 5.7.4 Final thoughts on the sulfide metallogeny of the SKI

Petrogenesis of the basal contact zone implicates sill-advancement through laterally and vertically propagating lobes that interfinger among and through each other. It is likely that these lobes contain different metal budgets that could be responsible for the stratigraphic variations observed in Cu, Ni, and PGE mineralization. These differing metal budgets along with sulfide fractionation could produce deposit wide vertical and lateral fluctuations in metal concentrations.

Metallogenesis of the northern SKI is directly tied to the development of magma flow channels. Repeated use of flow channels would cause high R-factors, allowing immiscible sulfide melt to scavenge metals from a very large volume of silicate magma, and would result in continuous upgrade of metal tenor in primary stream channel ways. Secondary channels and channel margins would then contain lower metal grades. The result of this should produce a maze of metal grades in plan view, with the highest grades in channel centers adjacent to much lower grades in channel margins and outside of flow channels. Upgrading of metal tenors could also be strongly connected to the height of the hanging wall cap of anorthositic series rocks. In areas where the magma chamber becomes more inflated, turbulent confined flow would be much less as magmas fill up larger areas, creating large open deposits with lower metal grades. In areas where the

anorthositic series hanging wall is not completely removed or pushed out of the way, magmas would become restricted with turbulent, confined flow ensuing. These deposits would occupy less space and have higher metal grades.

In the interest of furthering exploration, it should be stated that the dynamic nature of the SKI's basal contact zone could cause metal-tenor fluctuations to be rather unpredictable, while at the same time it is becoming clear from whole-sale drilling in the SKI by numerous exploration companies that the entire basal contact zone is mineralized to some extent. The analysis of east to west lateral flow within the basal contact zone implies higher PGE grades (Section 5.6.5) to the east, closer to the envisioned magmatic source (Nickel Lake macrodike). Largely due to accessibility and depth to footwall, the overwhelming majority of drilling in the SKI has occurred to the west, leaving the eastern extents of the intrusion largely unexplored. Given the dynamic processes invoked in the genesis of the basal contact zone, and the associated physical and chemical metallogenic processes of sulfide mineralization, it seems imperative that exploration of the SKI begins to extend eastward.

# CHAPTER SIX: CONCLUSIONS

The major objectives of this study:

1. Develop a workable unit lithostratigraphy for the Nokomis deposit area while evaluating Severson's (1994) igneous stratigraphy of the South Kawishiwi intrusion.
2. Test Peterson's (2001) open versus confined style of mineralization model for the South Kawishiwi intrusion.

were accomplished by logging and sampling (petrographic and microprobe analysis) contemporary Duluth Metals drill core, and evaluating Duluth Metals assay and whole-rock geochemistry for the deposit. Through accomplishing these primary goals, several secondary objectives were also explored including:

1. Developing a magmatic emplacement history for the SKI,
2. Examining the relationship of the sulfide-bearing basal contact zone to the sulfide-barren upper zone,
3. Examining the magmatic formational processes involved in creating the intrusion and the processes involved in concentrating metals in the northern SKI,
4. Understanding the nature of the anorthositic inclusion block within the SKI, and understanding the role played by the Anorthositic series in forming the intrusion and the included sulfide deposits.
5. Evaluating the composition of magma(s) forming the SKI, determining potential parent magma for the South Kawishiwi intrusion.

The results of this study and my conclusions pertaining to all study goals have been discussed extensively in the previous chapter (Five). The major conclusions of this study are briefly summarized below, beginning with my thoughts on the secondary objectives.

1) Emplacement of the South Kawishiwi intrusion seems to have dominantly occurred conformably from bottom to top, with the units of the basal contact zone all forming somewhat contemporaneously into restricted magma chambers or channel ways, between the Giant's Range batholith footwall and the anorthositic series hanging wall. A distinct change in emplacement dynamics seems to have occurred above the basal contact zone, giving rise to the thick largely monotonous, troctolitic units of the upper zone.
2) The sulfide-bearing basal contact zone and sulfide-barren upper zone seem to be related through a transition represented by the PEG unit, and the Main AGT unit. This transition marks a major change in magma chamber dynamics, as the restricted heterogeneous nature of the basal contact zone transitions to an open chamber, creating the homogeneous "sea of troctolite" in the upper zone.
3) An infinite number of rapid magma injections seem to have facilitated a chaotic environment that created the basal contact zone. These magmas are believed to have consisted of load carrying, autolithic, crystal mushes. Emplacement of the upper zone seems to have been largely episodic with

recharge events occurring somewhat regularly into an open magma chamber, or chambers.

4) Metals seem to have been concentrated through the development of magma flow channels that were used repeatedly and continuously, causing high R-factors between the sulfide liquid and the silicate melt, which allowed an immiscible sulfide melt to scavenge metals from a very large volume of silicate magma.

5) South Kawishiwi magmas were emplaced into anorthositic series rocks possibly by cutting channel-ways through rift-related faults in the anorthositic series and Archean GRB footwall. The anorthositic inclusion block is a remnant of the Anorthositic series rocks that once occupied the entire region. SKI magmas surrounded and engulfed the block, leaving it as a major structure to aid in concentrating metals in the Nokomis deposit, causing restricted, turbulent flow and high R-factors.

6) The maximum Fo content in olivine (71.7) was found in sample 61-3259 from the U3 unit. A parental liquid with mg# 45.5 was experimentally determined for olivine with this Fo composition. A hybrid combination of Kew-2, Kew-9, and Kew-12 (BVSP, 1981) seems the most appropriate analogue for the parental magma to the basal contact zone of the SKI.

Conclusions relating to the two major goals of the study:

Severson's (1994) lithostratigraphy of the SKI remains largely viable with consideration toward the plethora of new data available. Several minor additions and clarifications have been made for the purposes of this study.

1. I have lumped Severson's (1994) T-AGT and Upper PEG units above the anorthositic inclusion block into a single unit (G-in-T), which was found both in outcrop and drill core above the anorthositic inclusion block.
2. As alluded to by Severson (1994; Hwy 1 Corridor), the anorthositic inclusion block is a very large remnant of the anorthositic series residing within the SKI.
3. A second possible large anorthositic inclusion block or blocks in the eastern reaches of the study area (PAN unit) has been discovered, which may have also helped to concentrate metals in the Nokomis deposit.
4. For the purposes of this study the U3 unit is recognized to be consistently present above the BH unit, and to also consistently bifurcate throughout the BH unit.
5. Three major formational zones have been defined within the study area (basal contact zone, upper zone, and anorthositic inclusion block.

Testing Peterson's (2001) open versus confined mineralization model for the intrusion focused largely on deciphering evidence aimed at detecting lateral flow in the intrusion, using multiple data sets including: modal mineralogy from selected drill core, incompatible element data from assay analyses, mineral chemistry of olivine, whole-rock

and assay major element data (Mg and Ca), and copper/platinum group element assay data.

1. Modal Mineralogy of the U3 unit shows a gradual, lateral (to the west) enrichment in plagioclase relative to olivine, which can be explained as east to west flow segregation through density contrast of the U3 magma.
2. Data on incompatible elements proved to be quite complex, which may indicate that flow-induced magmatic fractionation was hindered around the anorthositic inclusion block, and that the anorthositic inclusion block may have actually trapped magmatic fluids beneath, and around it.
3. Microprobe analysis of olivine showed a general decrease in Fo contents and Ni concentrations in olivine to the west (with some inconsistencies beneath and around the anorthositic inclusion block). In an east-west flow model, we would expect these contents/concentrations to decrease to the west.
4. Mg#'s in the U3 unit from Duluth Metals whole-rock geochemical and assay analyses seem to mark what could be flow channels at the base of the intrusion, showing higher numbers in possible stream channels, with lower numbers flanking stream channels.
5. The ratio of Cu/Pd in the U3 unit is consistently much lower in the eastern reaches of the deposit than in the west, which suggests that sulfide saturated magmas flowed from east to west through the intrusion, preferentially depleting Pd from the silicate magma along the way.

The results of this study indicate that not only is Peterson's (2001) open versus confined model a viable explanation for the differences in deposit types found in the SKI, but also that magma flow channels may have been an important factor in concentrating metals in the SKI. Evaluation of data collected for this study seems to indicate that magmas creating the basal contact zone flowed in a general east to west direction, and perhaps more importantly flow seems to have been channelized around the anorthositic inclusion. Additionally, the anorthositic inclusion block seems to have acted as an impenetrable trap for fluids emanating from basal contact zone magmas, while fluids from basal contact zone magmas confined by the semi-molten upper zone seem to have been able to migrate upward out of the basal contact zone.

Data collected and evaluated to test Peterson's (2001) open versus confined model also led to the development of both single-phase and two-phase petrogenesis and metallogenesis models for the SKI in the Nokomis deposit area. Several unusual characteristics of the U3 unit (mode, texture, structure, contacts, sulfide mineralization, bifurcations) led to the development of multiple petrogenesis and metallogenesis models. These models include similar attributes concerning the genesis of the basal contact zone, upper zone, and sulfide deposits, but explain the genesis of the U3 unit as: 1) a "consequence" of the flow dynamics involved in the genesis of the basal contact zone, and 2) a late injection of metal-enriched, compositionally more forsteritic magma.

Both models seem to be viable conclusions for the genesis of the basal contact zone, and therefore neither model is preferred here over the other. Perhaps a more important conclusion recognizes that the conditions and environment of emplacement and

genesis for the basal contact zone were drastically different than the conditions of emplacement and genesis of the upper zone, and that the conditions and environment of emplacement for the basal contact zone led to significant deposits of copper, nickel, and platinum group elements and may have set the stage for emplacement of the “sea of troctolite” above.

## REFERENCES

Allen, D.J., Hinze, W.J., Dickas, A.B., Mudrey, Jr., M.G., 1997, Integrated geophysical modeling of the North American Midcontinent Rift System: New interpretations for western Lake Superior, northwestern Wisconsin, and eastern Minnesota, *in* Ojakangas, R.W., Dickas, A.B., and Green, J.C., eds., Middle Proterozoic to Cambrian Rifting, Central North America: Boulder, Colorado, Geological Society of America Special Paper 312.

Andrews, M.S., and Ripley, E.M., 1989, Mass transfer and sulfur fixation in the contact aureole of the Duluth Complex, Dunka Road Cu-Ni deposit, Minnesota. Canadian Mineralogist, V. 27, part 2, pp. 293-310.

Basaltic Volcanism Study Project (BVSP), 1981, Pre-Tertiary continental flood basalts, In Basaltic Volcanism on the Terrestrial Planets, NY, Pergamon Press, p. 30-77

Barnes, S.J., 1986. The effect of trapped liquid crystallization on cumulus mineral compositions in layered intrusions. Contributions to Mineralogy and Petrology, V. 93, pp. 524–531.

Bates, R.L., and Jackson, J.A., 1987, Glossary of Geology, 3rd edition, *ed,* Robert L. Bates, and Julia A. Jackson, Alexandria, VA, American Geological Institute, 788 p.

Bedard, J., 1994, A procedure for calculating the equilibrium distribution of trace elements among the minerals of cumulate rocks, and the concentration of trace elements in the coexisting liquids. Chemical Geology, V. 118, pp. 143-153.

Boerboom, T.J., and Zartman, R.E., 1993, Geology, geochemistry, and geochronology of the central Giants Range batholith, northeastern Minnesota, Canadian Journal of Earth Sciences, V. 30, pp. 2510-2522.

Bonnichsen, B., 1974, Copper and nickel resources in the Duluth Complex, Minnesota, Economic Geology, V. 69, No. 7, pp. 1177.

Bonnichsen, B., 1972, Southern part of the Duluth Complex: *in* Sims, P.K., and Morey, G.B., eds., Geology of Minnesota: A Centennial Volume: Minnesota Geological Survey, p. 361-387.

Bonnichsen, B., 1971, Outcrop map of southern part of Duluth Complex and associated Keweenawan rocks, St. Louis and Lake Counties, Minnesota: Minnesota Geological Survey Miscellaneous Map M-11, scale 1:125,000.

Bonnichsen, B., 1970a, Principal rock types in the southern part of the Duluth complex, Minnesota, Geological Society of America, V. 2, No. 7, pp. 498-499.

Bonnichsen, B., 1970b, Geologic investigations in southern part of Duluth complex, Minnesota Geological Survey – Information Circular, V. 8, pp. 18-19.

Bonnichsen, B., 1970c, Geologic investigations in the southern part of the Duluth complex, Minnesota Geological Survey – Information Circular, V. 7, pp. 19-20.

Bonnichsen, B., 1970d, The southern part of the Duluth complex and associated Keweenawan rocks, Minnesota, Institute on Lake Superior Geology, Meeting, V. 16, pp. 10-11.

Cannon, W.F., 1992, The Midcontinent Rift in the Lake Superior region with emphasis on its geodynamic evolution, Tectonophysics, V. 213, No. 1-2, pp. 41-48.

Cannon, W.F., Green, A.G., Hutchinson, D.R., Lee, M., Milkereit, B., Behrendt, J.C., Halls, H.C., Green, J.C., Dickas, A.B., Morey, G.B., Sutcliffe, R., Spencer, C., 1989, The North American Midcontinent Rift Beneath Lake Superior From GLIMPCE Seismic Reflection Profiling, Tectonics, v. 8, p. 305-332.

Chalokwu C.I., and Grant, N.K., 1990, Petrology of the Partridge River Intrusion, Duluth Complex, Minnesota; 1, Relationships between mineral compositions, density and trapped liquid abundance, Journal of Petrology, V. 31, No. 2, pp. 265-293.

Chalokwu, C.I., and Grant, N.K., 1987, Reequilibration of olivine with trapped liquid in The Duluth Complex, Minnesota, Geology, V. 15, pp. 71-74.

Chase, C.G., and Gilmer, T.H., 1973, Precambrian plate tectonics; the midcontinent gravity high, Earth and Planetary Science Letters, V. 21, No. 1, pp. 70-78.

Davis, D.W., and Green, J.C., 1997, Geochronology of the North American Midcontinent Rift in western Lake Superior and implications for its geodynamic evolution, Canadian Journal of Earth Sciences, V. 34, No. 4, pp. 476-488.

Dickas, A.B., and Mudrey, Jr., M.G., 1997, Segmented structure of the Middle Proterozoic Midcontinent Rift System, North America, *in* Ojakagas, R.W., Dickas, A.B., and Green, J.C., eds., Middle Proterozoic to Cambrian Rifting, Central North America: Boulder, Colorado, Geological Society of America Special Paper 312.

Duluth Metals Press Release, August 13, 2007, Duluth Metals Receives NI 43-101 Report on Copper-Nickel-PGE Nokomis Deposit and Starts Scoping Study, duluthmetals.com.

Duluth Metals Press Release, July 21, 2008, Duluth Metals Receives Ni 43-101 Report On Interim Nokomis Deposit Resource Estimate Before Commencement Of Pre-Feasibility Study, duluthmetals.com.

Eckstrand, O.R., and Hulbert, L., 2007, Magmatic nickel-copper-platinum group element deposits, in Goodfellow, W.D., ed., Mineral Deposits of Canada: A Synthesis of Major Deposit-Types, District Metallogeny, the Evolution of Geological Provinces, and Exploration Methods: Geological Association of Canada, Mineral Deposits Division, Special Publication No. 5, p. 205-222.

Foose, M.P., and Weiblen, P., 1986, The physical and petrologic setting and textural and compositional characteristics of sulfides from the South Kawishiwi Intrusion, Duluth Complex, Minnesota, USA, Special Publication of the Society for Geology Applied to Mineral Deposits, V. 4, pp. 8-24.

Foose, M.P., 1984, Logs and correlation of drill holes within the South Kawishiwi intrusion, Duluth Complex, northeastern Minnesota: U.S. Geological Survey, Open-file Report. 84-14.

Foose, M.P., and Cooper, R.W., 1978, Preliminary geologic report on the Harris Lake area, northeastern Minnesota: U.S. Geological Survey Open-File Report 78-385, 24 p., 1 pl., scale 1:12,000.

Franconia Minerals Press Release, July 9, 2008, Franconia Doubles NI 43-101 Resource Estimate On Birch Lake Copper-Nickel-PGM Resource, franconiaminerals.com.

French, B.M., 1968, Progressive contact metamorphism of the Biwabik iron-formation, Mesabi range, Minnesota, Minnesota Geological Survey – Bulletin, V. 45, pp. 103.

Ghiorso, Mark S., and Sack, Richard O., 1995, Chemical Mass Transfer in Magmatic Processes. IV. A Revised and Internally Consistent Thermodynamic Model for the Interpolation and Extrapolation of Liquid-Solid Equilibria in Magmatic Systems at Elevated Temperatures and Pressures. Contributions to Mineralogy and Petrology, V. 119, pp. 197-212.

Gray, J.M.N.T., and Thornton, A.R., 2005, A theory for particle size segregation in shallow granular free-surface flows. Proceedings of the Royal Society A, V. 461, pp. 1447-1473.

Green, J.C., 2002, Volcanic and sedimentary rocks of the Keweenawan Supergroup in northeastern Minnesota, *in* Miller, J.D., *ed,* Geology and mineral potential of the Duluth Complex and related rocks of northeastern Minnesota: Minnesota Geological Survey Report of Investigations 58, p. 106-143.

Green, J.C., 1972, North Shore Volcanic Group, Geology of Minnesota; A Centennial Volume, Minnesota Geological Survey, pp. 294-332.

Green, J.C., 1970, Lower Precambrian rocks of the Gabbro Lake quadrangle, northeastern Minnesota, Minnesota Geological Survey, Special Publication SP-13.

Green, J.C., and Miller, J.D., Jr., 2008, Bedrock geology of the Duluth quadrangle, St. Louis County, Minnesota. Minnesota Geological Survey Miscellaneous Map M-182, scale 1:24,000.

Green, J.C., and Davis, D.W., 1997, Geochronology of the North American Midcontinent Rift in western Lake Superior and implications for its geodynamic evolution, Canadian Journal of Earth Sciences, V. 34, No. 4, pp. 476-488.

Green, J.C., Phinney, W.C., and Weiblen, P.W., 1966, Gabbro Lake quadrangle, Lake County, Minnesota: Minnesota Geological Survey Miscellaneous Map M-2, scale 1:31,680.

Grout, F.F., Sharp, R.P., Schwartz, G.M., 1959, The geology of Cook County, Minnesota, Minnesota Geological Survey – Bulletin, pp. 163.

Grout, F.F., 1918, The lopolith; an igneous form exemplified by the Duluth gabbro, American Journal of Science, V. 46, No. 273, pp. 516-522.

Gunderson, J.N., and Schwartz, G.M., 1962, The geology of the metamorphosed Biwabik iron-formation, eastern Mesabi district, Minnesota: Minnesota Geological Survey Bulletin 43, 139 p.

Hauck, S.A., Severson, M.J., Zanko, L.M., Barnes, S.J., Morton, P., Alminas, H.V., Foord, E.E., Dahlberg, E.H., 1997, An overview of the geology and oxide, sulfide, and platinum-group element mineralization along the western and northern contacts of the Duluth Complex, Geological Society of America – Special Paper, V. 312, pp. 137-185.

Heaman, L.M., R.M., Easton, Hart, T.R., Hollings, P., MacDonald, C.A., Smyk, M.C., 2007, Further refinement to the timing of Mesoproterozoic magmatism, Lake Nipigon region, Ontario, Canadian Journal of Earth Sciences, V. 44, No 8, pp. 1055-1086.

Hinze, W.J., Allen, D.J., Braile, L.W., and Mariano, J., 1997, The Midcontinent Rift System: A major Proterozoic continental rift, *in* Ojakagas, R.W., Dickas, A.B., and Green, J.C., eds., Middle Proterozoic to Cambrian Rifting, Central North America: Boulder, Colorado, Geological Society of America Special Paper 312.

Hoaglund, S.A., Miller, J.D., Crowley, J.L., and Schmitz, M.D., 2010, U-Pb Zircon Geochronology of the Duluth Complex and Related Hypabyssal Intrusions: Investigating the Emplacement History of a Large Multiphase Intrusive Complex related to the 1.1 Ga Midcontinent Rift, Institute on Lake Superior Geology, Part 1 – Program and Abstracts, v. 56, p. 25-26, Type: talk. Location: International Falls, MN, Date: May 19-22, 2010.

Hutchinson, D.R., White, R.S., Cannon, W.F., Schulz, K.J., 1990, Keweenaw hot spot; geophysical evidence for a 1.1 Ga mantle plume beneath the Midcontinent Rift System, Journal of Geophysical Research, V. 95, No. B7, pp. 10,869-10,884.

Irvine, N.T., 1982, Terminology for Layered Intrusions, Journal of Petrology, V. 23, No. 2, pp. 127-162.

Irvine, N.T., Anderson, J.C.O., Brooks, K.C., 1998, Included blocks (and blocks within blocks) in the Skaergaard intrusion: Geologic relations and the origins of rhythmic modally graded layers, GSA Bulletin, V. 110, no. 11, pp. 1398-1447.

Kuhns, M.J.P., Hauck, S.A., Barnes, R.J., 1990, Origin and Occurrence of Platinum Group Elements, Gold and Silver in the South Filson Creek Copper-Nickel Mineral Deposit, Lake County, Minnesota, NRRI/GMIN-TR-89-15, 63 p.

Lee, I., and Ripley, .M., 1996, Mineralogic and oxygen isotopic studies of open system magmatic processes in the South Kawishiwi Intrusion, Spruce Road area, Duluth Complex, Minnesota, Journal of Petrology, V. 37, No. 6, pp. 1437-1461.

Lucente, M.E., and Morey, G.B., 1983, Stratigraphy and sedimentology of the Lower Proterozoic Virginia Formation, northern Minnesota: Minnesota Geological Survey Report of Investigations 28, 28 p.

Lyons, P.L., 1950, A gravity map of the United States: Tulsa Geological Society Digest, V. 18, pp. 33-43.

Marsh, B.D., 2006, Dynamics of Magma Systems, Elements, V. 2, pp. 287-292.

Martineau, M.P., 1989, Empirically derived controls on Cu-Ni mineralization; a comparison between fertile and barren gabbros in the Duluth Complex, Minnesota, USA, *in* Prendergast, M. S., and Jones, M. J., *eds*. Magmatic sulfides; the Zimbabwe volume: Inst. Min. and Metall. : London, United Kingdom, pp. 117-137

McCallum, I.S., Raedeke, L.D., and Mathez, E.A., 1980. Investigations in the Stillwater Complex: Part I. Stratigraphy and structure of the Banded zone. *Amer. J. Sci.*, 280A, 59-87.

Meuer, W.P., and Meuer, M.E.S., 2006, Using apatite to dispel the ‘‘trapped liquid’’ concept and to understand the loss of interstitial liquid by compaction in mafic cumulates: an example from the Stillwater Complex, Montana, Contributions to Mineralogy and Petrology, V. 151, pp. 157-201.

Miller, J.D., Jr., 2005, Bedrock geology of the Babbitt Southeast quadrangle, St. Louis and Lake Counties, Minnesota, Minnesota Geological Survey Miscellaneous Map M-162, scale 1:24,000.

Miller, J.D., Jr., and Severson, M.J., 2005, Bedrock geology of the Babbitt Southwest quadrangle, St. Louis County, Minnesota. Minnesota Geological Survey Miscellaneous Map M-161, scale 1:24,000.

Miller, J.D., Jr., Severson, M.J., and Foose, M.P., 2005, Bedrock geology of the Babbitt Northeast quadrangle, St. Louis and Lake Counties, Minnesota. Minnesota Geological Survey Miscellaneous Map M-160, scale 1:24,000.

Miller, J.D., Jr., Green, J.C., Severson, M.J., Chandler, V.W., Hauck, S.A., Peterson, D.M., and Wahl, T.E., 2002, Geology and mineral potential of the Duluth Complex and related rocks of northeastern Minnesota: Minnesota Geological Survey Report of Investigations 58, 207 p.

Miller, J.D., Severson, M.J., and Hauck, S.A., 2002, History of geologic mapping and mineral exploration in the Duluth Complex, *in* Miller, J.D., *ed,* Geology and mineral potential of the Duluth Complex and related rocks of northeastern Minnesota: Minnesota Geological Survey Report of Investigations 58, p. 106-143.

Miller, J.D., and Severson, M.J., 2002, Geology of the Duluth Complex, *in* Miller, J.D., *ed,* Geology and mineral potential of the Duluth Complex and related rocks of northeastern Minnesota: Minnesota Geological Survey Report of Investigations 58, p. 106-143.

Miller, J.D., Green, J.C., Severson, M.J., Chandler, V.W., and Peterson, D.M., 2001, Geologic Map of the Duluth Complex and Related Rocks, Northeastern Minnesota, Minnesota Geological Survey Miscellaneous Map M-119, 1:200,000 Scale.

Miller, J.D., and Severson, M.J., 1999, Bedrock Geology of Allen Quadrangle, Minnesota, Minnesota Geological Survey Miscellaneous Map Series, Map M-91, 1:24,000 scale.

Miller, J.D., and Chandler, V.W., 1997, Geology, petrology, and tectonic significance of the Beaver Bay Complex, northeastern Minnesota, Geological Society of America – Special Paper, V. 312, pp. 73-96.

Miller, J.D., Jr., and Ripley, E.M., 1996, Layered intrusions of the Duluth Complex, Minnesota, USA. *in* Cawthorne, R.G. (ed.), *:*Layered Intrusions: Amsterdam, Elsevier, p. 257-301.

Miller, J.D., and Vervoort, J.D., 1996, The latent magmatic stage of the Midcontinent Rift: a period of magmatic underplating and melting of the lower crust: Institute on Lake Superior Geology, 42nd Annual Meeting, Cable, Wis., Proceedings, v. 42, Programs and Abstracts, pt. 1, p. 33-35.

Miller, J.D., and Weiblen, P.W., 1990, Anorthositic rocks of the Duluth Complex; examples of rocks formed from plagioclase crystal mushes, Journal of Petrology, V. 31, No. 2, pp. 295-339.

Morey, G.B., 1996, Continental margin assemblage, *in* Sims, P.K. and Carter, L.M.H., eds., Archean and Proterozoic geology of the Lake Superior region, U.S.A., 1993: U.S. Geological Survey Professional Paper 1556, p. 30-43.

Morey, G.B., and Van Schmus, W.R., 1988, Correlation of Precambrian rocks of the Lake Superior region, United States: U.S. Geological Survey Professional Paper 1241-F, 31 p.

Morey, G.B., and Cooper, R.W., 1977, Bedrock geology of the Hoyt Lakes-Kawishiwi area, St. Louis and Lake Counties, northeastern Minnesota: Minnesota Geological Survey Open-File Report, scale 1:48,000.

Morton, P., and Hauck, S.A., 1987, PGE, Au and Ag contents of Cu-Ni sulfides found at the base of the Duluth Complex, northeastern Minnesota, Natural Resources Research Institute – Report, NRRI/GMIN-TR-87-04, 81 p.

Mungall, J.E., and Su, S.G., 2005, Interfacial tension between magmatic sulfide and silicate liquids: Constraints on kinetics of sulfide liquation and sulfide migration through silicate rocks. Earth and Planetary Science, V. 234, pp. 135–149.

Naldrett, A.J., 2004, Magmatic Sulfide Deposits Geology, Geochemistry, and Exploration, Springer-Verlag Berlin Heidelberg, New York, 727 p.

Naldrett, A.J., 1999, World-class Ni-Cu-PGE deposits; key factors in their genesis, Mineralium Deposita, V. 34, No. 3, pp.227-240

Naldrett, A.J., 1997, Key factors in the genesis of Noril'sk, Sudbury, Jinchuan, Voisey's Bay and other world-class Ni-Cu-PGE deposits: implications for exploration, Australian Journal of Earth Sciences, V. 44, p. 283-315.

Nicholson, S.W., Shirey, S.B., Schulz, K.J., Green, J.C., 1997, Rift-wide correlation of 1.1 Ga Midcontinent Rift System basalts; implications for multiple mantle sources during rift development, Canadian Journal of Earth Sciences, V. 34, No. 4, pp. 504-520.

Nicholson, S.W., and Shirey, S.B., 1990, Midcontinent rift volcanism in the Lake Superior region: Sr, Nd, and Pb isotopic evidence for a mantle plume origin: Journal of Geophysical Research, V. 95, No. 7, pp. 10851-10868.

Ojakangas, R.W., 1983, Tidal deposits in the early Proterozoic basin of the Lake Superior region; the Palms and the Pokegama formations; evidence for subtidal-shelf deposition of superior-type banded iron-formation, Geological Society of America, V. 160, pp. 49-66.

Paces, J.B., and Miller, J.D., 1993, Precise U-Pb ages of Duluth Complex and related mafic intrusions, northeastern Minnesota, U.S.A., geochronological insights to physical, petrogenetic, paleomagnetic and tectono-magmatic processes associated with the 1.1 Ga Midcontinent Rift System, Journal of Geophysical Research, V. 98, pp. 13997-14013.

Patelke, R.L., 1996, M.S. Thesis, (Advisor: P. Morton/ J. Green), The Colvin Creek Body: A Metavolcanic and Metasedimentary Mafic Inclusion in the Keweenawan Duluth Complex, Northeastern Minnesota, 232 p.

Peterson, D.M., 2009, The Nokomis Deposit, Minnesota: Integrating the true science of geology into a new exploration project to create a world-class underground mine, duluthmetals.com.

Peterson, D., 2008, Geological map of the northern South Kawishiwi intrusion and surrounding areas, Duluth Complex; St. Louis and Lake counties, northeastern Minnesota: Institute on Lake Superior Geology Proceedings, Part 1, Program and Abstracts, v. 54, p. 69-70. Type: Poster. Location: Marquette, Michigan. Date: May 6-10, 2008.

Peterson, D.M., 2007, "Where's the Nickel in the Duluth Complex? New ideas on a Voisey's Bay-type target based on recent geological mapping in the Nickel Lake Macrodike, a major feeder dike into the South Kawishiwi Intrusion," Canadian Institute of Mining and Metallurgy Thunder Bay Branch, February 15, 2007.

Peterson, D.M., 2006, Digital Base for Geologic Mapping within the Northern South Kawishiwi Intrusion: Lake and St. Louis Counties, Northeastern Minnesota, NRRI/MAP-2006/01, scale 1:20,000.

Peterson, D.M., 2002, Shaded Relief Map of the Basal Contact Surface of the South Kawishiwi Intrusion, Duluth Complex, Northeastern, Minnesota, NRRI/MAP-2002/01, scale 1:75,000.

Peterson, D.M., 2001, Development of a conceptual model of Cu-Ni-PGE mineralization in a portion of the South Kawishiwi intrusion, Duluth Complex, Minnesota: Society of Economic Geologists, Second Annual PGE Workshop, Sudbury, Ontario.

Peterson, D.M., Albers, P. B., White, C.R., 2006, Bedrock Geology Map of the Nickel Lake Macrodike and Adjacent Areas: Lake County, Northeastern Minnesota, Economic Geology Group Map Series, NRRI/MAP-2006-04 (Version 1).

Peterson, D.M., Patelke, R.L., Severson, M.J., 2004, Bedrock Geology Map and Cu-Ni Mineralization Data for the Basal Contact of the Duluth Complex West of Birch Lake, St. Louis and Lake Counties, Northeastern Minnesota, NRRI/MAP-2004/02, scale 1:10,000.

Peterson, D.M., Marma, J., Brown, P., 2002, Bedrock Geology, Sample Location, and Property Position of the West Birch Lake Area South Kawishiwi Intrusion, Duluth Complex, Lake and St. Louis Counties, Northeastern Minnesota, NRRI/MAP-2002/02, scale 1:12,000.

Peterson, D.M., and Severson, M.J., 2002, Archean and Paleoproterozoic rocks that form the footwall of the Duluth Complex, *in* Miller, J.D., *ed,* Geology and mineral potential of the Duluth Complex and related rocks of northeastern Minnesota: Minnesota Geological Survey Report of Investigations 58, p. 76-93.

Peterson, D.M., 1996, Targeting footwall copper-PGE deposits in the Duluth Complex based on Sudbury mining camp analogs: Institute on Lake Superior Geology Proceedings, Part 1, Program and Abstracts, v. 42, p. 48-49. Type: Oral. Location: Cable, Wisconsin. Date: May 15-19, 1996.

Phinney, W.C., 1972, Duluth Complex, history and nomenclature, *in* Geology of Minnesota; A Centennial Volume, Minnesota Geological Survey, St. Paul, Minnesota, pp. 333-334.

Phinney, W.C., 1972, Northwestern part of Duluth Complex, *in* Geology of Minnesota; A Centennial Volume, Minnesota Geological Survey, St. Paul, Minnesota, pp. 335-345.

Phinney, W.C., 1972, Northern prong, Duluth Complex, *in* Geology of Minnesota; A Centennial Volume, Minnesota Geological Survey, St. Paul, Minnesota, pp. 346-353.

Phinney, W.C., 1969, Geology of central part of Duluth complex, Minnesota Geological Survey – Information Circular, V. 7, pp. 18.

Phinney, W.C., 1967, Reconnaissance geologic map of part of the Kangas Bay quadrangle: Minnesota Geological Survey Open-File Map, scale 1:24,000.

Pirajno, F., 2000, Ore Deposits and Mantle Plumes, Kluwer Academic Publishers, Boston, 556 pp.

Pollard, D.D., Muller, O.H., Dockstader, D.R., 1975, The form and growth of fingered sheet intrusions, Geological Society of America, V. 86, No. 3, pp. 351-363.

Press release, June 4, 2008, Duluth metals increases Nokomis resource to 449 million tonnes indicated and 284 million tonnes inferred, www.duluthmetals.com.

Ripley, E.M., Taib, N.I.., Li, C., Moore, C.H., 2007, Chemical and mineralogical heterogeneity in the basal zone of the Partridge River Intrusion; implications for the origin of Cu-Ni sulfide mineralization in the Duluth Complex, Midcontinent Rift System, Contributions to Mineralogy and Petrology, V. 154, No. 1, pp. 35-54.

Ripley, E.M., 1986, Origin and concentration mechanisms of copper and nickel in Duluth Complex sulfide zones; a dilemma, Economic Geology, V. 81, No. 4, pp. 974-978.

Ripley, E.M., 1981, Sulfur isotopic studies of the Dunka Road Cu-Ni deposit, Duluth Complex, Minnesota, Economic Geology, V. 76, No. 3, pp. 610-620.

Ripley, E.M., and Al-Jassar, T.J., 1987, Sulfur and oxygen isotope studies of melt-country rock interaction, Babbitt Cu-Ni deposit, Duluth Complex, Minnesota, Economic Geology, V. 82, No. 1, pp. 87-107.

Roeder, P.L., and Emslie, R.F., 1970, Olivine-liquid equilibrium, Contributions to Mineralogy and Petrology, V. 29, No. 4, pp. 275-289.

Rollinson, H.R., 1993, Using geochemical data: evaluation, presentation, interpretation. Longman Group, UK, 350 p.

Sabelin, T., and Iwasaka, I., 1985, Metallurgical evaluation of chromium-bearing drill core samples from the Duluth Complex (Contract report of Minnesota Department of Natural Resources, Division of Minerals): Mineral Resources Research Center, University of Minnesota, Minneapolis, Minnesota, 58 p.

Sabelin, T., and Iwasaka, I., 1986, Evaluation of platinum group metal occurrences in Duval 15 drill core from the Duluth Complex: Internal report, Mineral Resources Research Center, University of Minnesota, Minneapolis, Minnesota, 23 p.

Sassani, D.C., 1992, Petrologic and thermodynamic investigation of the aqueous transport of platinum-group elements during alteration of mafic intrusive rocks, PhD thesis, Washington University, St. Louis.

Severson, M.J. and Miller, J.D., Jr., 2005, Bedrock geology of the Babbitt quadrangle, St. Louis County, Minnesota. Minnesota Geological Survey Miscellaneous Map M-159, scale 1:24,000.

Severson, M.J., Patelke, R.L., Hauck, S.A., and Zanko, L.M., 1996, The Babbit Copper-Nickel Deposit, Part C: Igneous Geology, Footwall Lithologies, and Cross-Sections, Natural Resources Research Institute Technical Report, NRRI/TR-94/21c, 79 p.

Severson, M.J., 1995, Geology of the Southern Portion of the Duluth Complex, Natural Resources Research Institute, NRRI/TR-95/26, 198 p.

Severson, M.J., 1994, Igneous Stratigraphy of the South Kawishiwi Intrusion, Duluth Complex, Northeastern Minnesota: NRRI/TR-93/34, December 1994, 210 p.

Severson, M.J., Patelke, R.L., Hauck, S.A., and Zanko, L.M., 1996, The Babbit copper-nickel deposit, part C: Igneous geology, footwall Lithologies, and cross-sections: Natural Resources Research Institute, Technical Report NRRI/TR-94/21c, 79 p.

Severson, M.J., and Hauck, S.A., 1990, Geology, Geochemistry, and Stratigraphy of a Portion of the Partridge River Intrusion, Natural Resources Research Institue Technical Report, NRRI/GMIN-TR-89-11, 236 p.

Shirey, S.B., 1997, Re-Os isotopic compositions of Midcontinent Rift System picrites; implications for plume-lithosphere interaction and enriched mantle sources, Canadian Journal of Earth Sciences, V. 34, No. 4, pp. 489-503.

Sims, P.K., 1965, Our Land and Mineral Resources, a Long-Range Plan for Geologic Research in Minnesota, p. iii.

Southwick, D.L., 1996, Archean and Proterozoic Geology of the Lake Superior region, U.S.A., *ed*, 1993, Sims, P.K., U.S. Geological Survey, United States, *ed*, Carter, L.M.H., U.S. Geological Survey Professional Paper, pp. 6-13.

Tharlson, E., Sweet, G., Boisjoli, T., Lentz, B., Fellows, T., Peterson, D., 2007, Geologic Map of the Nickel Lake Macrodike and Northern Bald Eagle Intrusion: Lake County Northeastern Minnesota, Precambrian Research Center Map Series, PRC/MAP-2007-01, 1:10,000.

Thy, P., Lesher, C.E., Nielsen, T.F.D., Brooks, C.K., 2006, Experimental constraints on the Skaergaard liquid line of descent, Lithos, V. 92, pp. 154-180.

Theriault, R.D., Barnes, S.J., Severson, M.J., 1997, The influence of country-rock assimilation and silicate to sulfide ratios (R factor) on the genesis of the Dunka Road Cu-Ni-platinum-group element deposit, Duluth Complex, Minnesota, Canadian Journal of Earth Sciences, V. 34, No. 4, pp. 375-389.

Thomas, M.D., and Teskey, D.J., 1994, An interpretation of gravity anomalies over the Midcontinent rift, Lake Superior, constrained by GLIMPCE seismic and aeromagnetic data, Canadian Journal of Earth Sciences, V. 31, pp. 682-697.

U.S. Geological Survey, 2008, Mineral commodity summaries 2008, U.S. Geological Survey, 199 p.

Vervoort, J.D., 2007, The magmatic evolution of the Midcontinent Rift; new geochronologic and geochemical evidence from felsic magmatism, Precambrian Research, V. 157, No. 1-4, pp.235-268.

Vervoort, J.D., and Green, J.C., 1997, Origin of evolved magmas in the Midcontinent Rift System, Northeast Minnesota; Nd-isotope evidence for melting of Archean crust, Canadian Journal of Earth Sciences, V. 34, No. 4, pp. 521-535.

Wager, L.R., Brown, G.M., and Wadsworth, W.J., 1960, Types of igneous cumulates. Journal of Petrology 1, p. 73-85.

Wager, R.L., and Brown, G.M., 1967, Layered Igneous Rocks, San Francisco, W.H. Freeman, 588 p.

Weiblen, P.W., 1965, A funnel-shaped, gabbro-troctolite intrusion in the Duluth Complex, Lake County, Minnesota, University of Minnesota at Minneapolis, Dissertation Abs., Sec. B, Sci. and Eng., V. 27, No. 4, p. 1196B.

Weiblen, P.W., and Morey, G.B., 1980, A summary of the stratigraphy, petrology, and structure of the Duluth Complex, American Journal of Science, V. 280-A, Part 1, pp. 88-133.

Weiblen, P.W., and Morey, G.B., 1976, Textural and compositional characteristics of sulfide ores from the basal contact zone of the South Kawishiwi Intrusion, Duluth Complex, northeastern Minnesota, Mining Symposium – University of Minnesota, Issue 37, pp. 22.1-22.24.

White, W.S., 1966, Tectonics of the Keweenawan basin, western Lake Superior region: U.S. Geological Survey Professional Paper 524-E, 23 p.

Woollard, J.P., 1943, Transcontinental gravitational and magnetic profile of North America and it's relation to geologic structure, Geologic Society of America Bulletin, v. 54, pp. 747-790.

Wold, R.J., and Hinze, W.J., 1982, Introduction, *in* Wold, R.J., and Hinze, W.J., eds, Geology and tectonics of the Lake Superior basin, Geological Society of America Memoir 156, pp. 1-4.

Woollard, J.P., and Joesting, H.R., 1964, Bouguer gravity anomaly map of the United States, U.S. Geological Survey, scale 1:25,000,000.

Zanko, L.M., Severson, M.J., and Ripley, E.M., 1994, Geology and mineralization of the Serpentine copper-nickel deposit: Natural Resources Research Institute, Technical Report NRRI/TR-93/52, 90 p., 3 pls.